Al-Mustansiriyah Journal of Science

ISSN 1814 - 635X

Vol. 25, No. 2, 2014

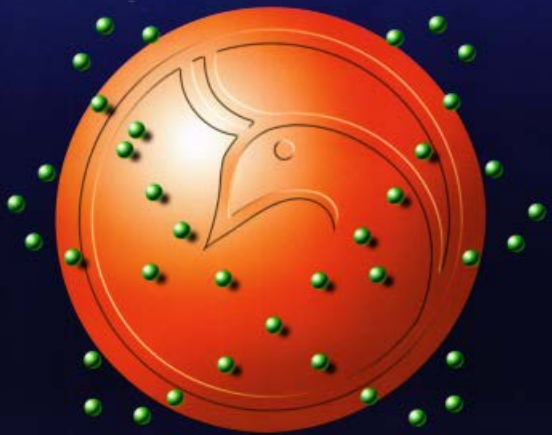

Issued by College of Science - Mustansiriyah University

Vol. 25
No. 2
2014

Al-Mustansiriyah Journal of Science

Issued by College of Science, Al-Mustansiriyah University, Baghdad, Iraq

Mobile: 07711184399
e-mail: mustjsci@yahoo.com

Instructions for Authors
Al-Mustansiriyah Journal of Science (MJS)

Manuscript text (first submission) should be double spaced on one side of high quality white A4 sheets (21.6×27.9 cm) with margins of one inch all around the page using Microsoft Word 2007 or 2010 using (doc.) type. The typing in Arabic or English must use (Times New Roman, font size of 14 pt). The sections should be arranged in the following order: Title Page, Abstract in English, Abstract in Arabic, Introduction, Materials and Methods (Experimental), Results and Discussion, Conclusion, Acknowledgment (if any), Abbreviations (if any) and list of References. The head of the sections should be capitalized, bolded and centered and font size of 16pt. **(e.g. ABSTRACT, INTRODUCTION, MATERIALS and METHODS (EXPERIMENTAL), RESULTS and DISCUSSION, CONCLUSION, ACKNOWLEDGMENTS, REFERENCES)**, and the others (sub-sections) should be in sentence case and bolded as well.

Title Page: Includes the title of the article, author's names with full names and affiliations. The affiliation should comprise the department, college, institution (University or Company), and should be typed as a footnote to the author's name. The e-mail address of the author responsible for correspondence (who is designated with an asterisk *) must be given at the first page under the name and affiliation of authors.

References: All references should be cited in using the appropriate Arabic numerals, which are enclosed in parenthesis (e.g. Polyurethane rigid foams are largely used as insulating materials for their combination of low density, low thermal conductivity and good mechanical properties [1-3].)

A list of references should be given in the end of the manuscript. References should be typed single-spaced and numbered sequentially in the order in which they are cited in the text. The number of the reference should be given between two brackets [ ].

❖ **Journal's paper**

[1]. Metallo S. J., Kane R. S., Holmlin R. E., Whitesides G. M., Journal of American chemical Society. 125, 5, 4534-4540, 2003.

❖ **Books:**

[2]. Edward M. Handbook of Adhesives and Sealants; McGraw-Hill: New York, 2000.

Tables: Tables should be created using the Table tool in MS Word using font size 9 point. Tables should be numbered with Arabic numerals and referred to by number in the Text (e.g., Table 1,2,3... etc.). Each Table should be typed with the legend above the Table.

Figures, Schemes and Diagrams should be numbered in a consecutive series of Arabic numerals in the order in which they are cited in the text (e.g., Figure 1 or Scheme 1).

CONTENTS

Synthesis and Spectroscopic Studies of Some Imines Derived From O-Tolidine and Their Conversion to New Bis-Azetidin-2-One Derivativesfrom Phenylthioacetic Acid

Mustafa Y.Jamal , Saadon A. Aowda
Chemistry department -College of Science - Babylon University
Received 16/12/2013 – Accepted 23/2/2014

الخلاصه

تم تحضير سلسله من مركبات الازتدين الرباعيه الحلقه غيرالمتجانسه (12-21) من تفاعل قواعد شف المحضره من تفاعل اورثوتوليدين مع مركبات البنزلديهايدالاروماتيه المختلفه بوجود الايثانول المطلق وبضع قطرات من حامض الخليك الثلجي والتصعيد(2-3) ساعه.ثم تم مفاعله قواعد الشف المحضره(2-11) مع حامضبنزيلثايوكلايكولك وبوجود ثلاثي اثيل امين و فسفور اوكسي كلورايد ومثيلين كلورايد في جو خامل من النتروجين وبدرجه الصفرالمئوي لينتج مشتق الازدتين-2-اون.
وقد تم متابعه وتشخيص النواتج المحضره بواسطه تقنيات كروموتغرافياالطبقهالرقيقه، الاشعه تحت الحمراء،كاربون وبروتون الرنين النووي المغناطسي، بالاضافه الى تحليل العناصر

ABSTRACT

A series of four membered ring the azetidin-2-one (11-20) have been synthesized via Schiff bases(1-10) by reaction of different aromatic aldehyde with o-Tolidine in absolute ethanol and two or three droop glacial acetic acid then reflux for (2-3)hours . Schiff bases then reacted with phenylthioacetic acid in the presence of triethylamine with phosphorusoxychloride using dry methylene dichloride under inert nitrogen atmosphere at 0 °C. to give us the corresponding azetidin-2-one. The structural of these compounds were monitored and confirmed by using (TLC), spectroscopic tools as IR , ^{1}H NMR, and Elemental analysis.

Keywords : Imines,Schiff bases,Benzidine , β-lactam , Four member ring , Staudinger reaction , Ketene

INTRODUCTION

All β-lactam antibiotics chemically possess a four-membered cyclic amide, known as azetindin-2-one or β-lactam, as showed in figure (1) which can be isolated or fused to form a bicyclic or tricyclic ring system.

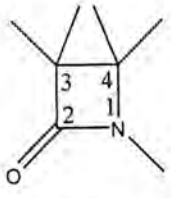

Figure-1: azetidin-2-one structure

A heterocyclic ring to which it is fused can be either saturated or unsaturated with a double bond positioned either between C-2 and C-3 of the five membered heterocycle or C-3 and C-4 of the six-membered heterocycle.The ring can be formed in several different ways, Staudinger reaction being the one most oftenly usedrecent discoveries have shown also other biological properties that have furtherincreased the significance of β-lactams as synthetic intermediates for the preparation of heterocycles of biological interest. Although they can serve as inhibitors of serine proteases[1], cholesterol acyltransferase, human

cytomegalovirus and proteasomeinhibitors [2] their antibacterial activity remains the principal mode of action [3,4].Because of good characteristics (wide spectrum, relatively low host toxicity,appropriate pharmacokinetics, synergistic effect...) β-lactam antibiotics (Figure 2) are the most used antibacterial agents in clinical practice [5,6,7,8], where they are represented with around forty compounds [9], the β-lactam compound using as anticancer agents[10,11] , A series of bicyclic N-substituted and unsubstituted b-lactams were synthesized and evaluated as targeted potential antimalarials [12].

However, a widely used method is via the [2+2] cyclocondensation of ketenes to imines, a process known as the Staudinger reaction, which have important application in pharmaceutical and synthetic chemistry[13,14,15], this reaction has been used to construct macrocyclicbisazetidinonepolyethers by the reaction of the appropriate ketene precursors with macrocyclicdiimines[16].

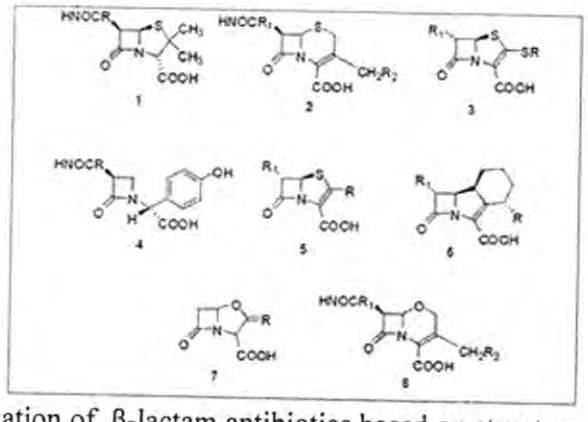

Figure-2: Classification of β-lactam antibiotics based on structure :penams (1), cephems (2), penems (3), monobactams (4), carbapenems (5), trinems (6), clavams (7), oxacephems (8)

MATERIALS AND METHODS

All melting points are uncorrected and are expressed in degree(°C), using melting point SMP3 . FT-IR spectra were recorded as KBr disks using shimadzu FT-IR 8400. ^{1}H NMR spectra were recorded using Varian VnmrJ 400 spectrometer (400 MHz)/ Izmir Institute of Technology(Turkey) and tetramethylsilane (TMS) as internal standard using DMSO-d_6 as solvent peaks showed at δ=2.5-2.4ppm .^{13}C NMR spectra were recorded using Varian VnmrJ 400 spectrometer (100 MHz)/ Izmir Institute of Technology(Turkey) and using DMSO-$d_6$and $CDCl_3$as solvent peaks showed at δ=(40-39)ppm and (77-76)ppm respectively.Elemental analysis using Leco CHNS-933 Leco corporation st.Joseph)/ Izmir Institute of Technology(Turkey) .

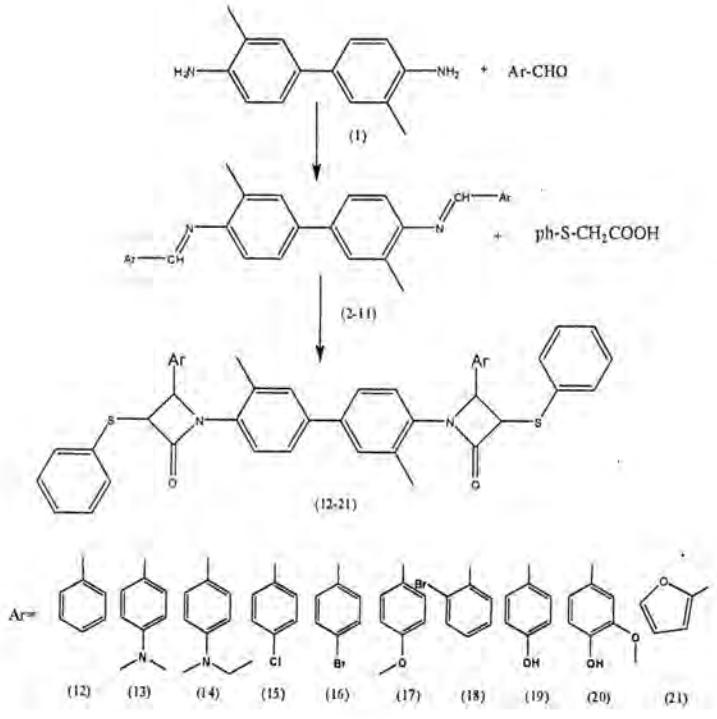

Scheme 1

(a) reflux in ethanol(2-3) h ;(b) slow addition $POCl_3$ with stirring (30-55) mint in N_2 at 0°C using dichloromethane as solvent.

Synthesis of imines derivatives (2-11):

General procedure:

A reaction mixture of o-Tolidine (1mmol, 0.42g) and differentaromatic aldehydes (2mmol) was dissolved in absolute ethanol (50 ml) with 2-3 drops of glacial acetic acid and heated in a water bath at 70- 80° C for approximately (2-3) hours. The process of the reaction completion was followed by (TLC)[(1:1) ethanol/ethyl acetate]. Filtration or evaporation of used solvent was done then the products were recrystalized from ethanol solvent.

Synthesis of N4,N4'-dibenzylidene-3,3'-dimethylbiphenyl-4,4'-diamine.(2)

benzaldehyde (4mmol, 0.40 g) ,yield=89% with m.p= 157-158 C °. FT-IRspectra in figure (3)showed adsorption bands appear in the range of(3061-3024) and(2900-2847) cm^{-1} which belong to (C-H) aromatic and aliphatic, while (C=N) appear at 1627 cm^{-1} , (C-N) appear at stretching frequency at 1126 cm^{-1} , beside that the (aromatic C=C) appear at range 1481-1575 cm^{-1} . Elemental analysis confirmed the molecular formula $C_{28}H_{24}N_2$ (calculated /found) : (C, 86.56/86.98; H, 6.23/6.66; N, 7.21/ 7.65).

Synthesis of bis(4-(dimethylamino)benzylidene)-3,3'-dimethylbiphenyl-4, 4'-diamine. (3)

N,N-dimethylaminobenzaldehyde (4mmol, 0.60 g) . Yellow-orange precipitate observed then section filtration yield=91% with m .p = 256-257 C°. FT-IRspectra showed stretching absorption bands at 3106 cm^{-1}-2906cm^{-1}referred to (C-H) aromatic and aliphatic respectively, while imines'(C=N) band appear in about 1607 cm^{-1} , (C=C) appear in the range of 1520-1587 cm^{-1}, medium intensity of band appear at 1360 cm^{-1} referred to (N-CH_3) and 1165 cm^{-1} referred to (C-N) .On the other hand the ^{1}H-NMR in DMSO-$d_6$showed,at δ=8.3ppm due to (s,2H ,2CH=N) ,δ= 6.8ppm and 7.4ppm (d,8H,Ar) due to substituted phenyl ,δ = 7.0ppm (d,2H,Ar-H) , δ = 7.2ppm and δ =7.8ppm (d,2H,Ar-H) referred to biphenyl ring ,δ = 3.1ppm (s , 12H,2(N-CH_3)$_2$) ,and at δ= 2.2ppm (s,6H , Ar-CH_3) . Elemental Analysis of the molecular formula $C_{32}H_{34}N_4$ (calculated / found) :(C, 80.98 / 81.33; H, 7.22 / 7.52; N, 11.80 /12.27).

Synthesis of bis[4-(diethylamino)benzylidene]-3,3'-dimethylbiphenyl-4, 4'-diamine (4)

N,N-diethylaminobenzaldehyde (4mmol, 0.70 g) .Yellow bold precipitate observed then section filtration yield=90% with m.p=174-175 C°.FT-IRspectrashowed stretching absorption bands at 3084 cm^{-1} and 2970 cm^{-1} refer to CH aromatic and aliphatic respectively, while imine (C=N) band appear in 1606 cm^{-1} , (C=C)aromatic appear in the range of 1587-1523 cm^{-1}, medium intensity of band appear at 1334 cm^{-1}refered to (N-CH_3) and 1172 cm^{-1} refer to (C-N).On the other hand the ^{1}H-NMR in DMSO-d_6 showed,δ=8.2ppm (s,2H ,2CH=N) , δ= 7.0-7.7ppm (dd,8H,Ar-H) due to substituted phenyl ,δ = 7.3ppm (d,2H,Ar-H) , δ=7.4ppm (d,2H,Ar-H) and 7.8ppm (d,2H,,Ar-H) referred to biphenyl ring.δ = 1.5ppm (t, 12H, 2(N(CH_3)$_2$) , at δ=3.4ppm ,(q,8H ,2N(CH_2)$_2$)and , δ=2.1ppm (s,6H, 2Ar(CH_3)), while (t,12H,4(CH_3-C)) , δ=1.04-1.29ppm. Elemental Analysis of the molecular formula $C_{36}H_{42}N_4$ (calculated / found) :(C, 81.47/81.88; H, 7.98/8.53; N, 10.56/10.77).

Synthesis of bis (4-chloro benzylidene) 3,3'dimethyl biphenyl-4,4'-diamine . (5)

p-chlorobenzaldehyde (4mmol, 0.56 g) ,yield=83% with m.p =156-157 °C. FT-IRspectrashowed stretching absorption at (3063-3020) $cm^{-1}$and (2920-2872) cm^{-1}due to (C-H aromatic and aliphatic)respectively, while imine band appear in about 1622 cm^{-1} , (C=C)aromatic appeared in the range of 1487-1591 cm^{-1}, at 1085 cm^{-1} referred to (C-N) and 875 cm^{-1} belong to (Ar-Cl).On the other hand thedata in figure(4) of ^{1}H-NMR in DMSO-d_6 showed, at δ=8.4ppm (s,2H ,2CH=N) , δ= 6.8ppm (dd,2H,Ar) and δ=7.0ppm (dd,2H,Ar-H) due to biphenyl ring. δ = 7.2ppm (m ,4H,

Ar-H) of substituted phenyl and δ =7.4ppm (m ,6H ,Ar-H) due to (4H,Ar-H) of substitutedphenyl with (2H,Ar-H) of biphenyl ,δ=2.1ppm ,(6H ,$Ar(CH_3)_2$).Elemental Analysis of the molecular formula **$C_{28}H_{22}Cl_2N_2$**(calculated / **found**):(C, 73.53/ **73.99**; H, 4.85/ **5.24;** N, 6.12/ **6.57**).

Synthesis of bis (4-bromo benzylidene) 3,3'dimethyl biphenyl-4,4'-diamine .(6)

p-bromobenzaldehyde (4mmol, 0.74 g). Direct yellow light precipitate observed .Workup of the product with percentage yield = 92% , m.p = 163-164 C° . FT-IR showed , 3057 cm^{-1}-2916 cm^{-1} referred to (C-H ,aromatic and aliphatic) respectively , at 1618 cm^{-1}due to(C=N), 1485-1560 cm^{-1} (aromatic C=C), 1182 cm^{-1} (C-N). Elemental analysis of the molecular formula $C_{28}H_{22}Br_2N_2$(calculated / found) C, 61.56 /61.89; H, 4.06/ 4.37; N, 5.13/ 5.61).

Synthesis of bis (4-methoxy benzylidene) 3,3'dimethyl biphenyl-4,4'-diamine. (7)

p-methoxybenzaldehyde (4mmol, 0.48 ml) ,under refluxing for 3 hours , direct yellowish precipitate observed . The product to give percentage yield = 76 % , m.p = 177-178 °C . FT-IR showed at 3041 cm^{-1}2839 cm^{-1} referred to (C-H ,aromatic and aliphatic) respectively , at 1626 cm^{-1}due to (C=N) ,at 1500-1600 cm^{-1} (aromatic C=C),1257cm^{-1} (C-O-C,) 1161 cm^{-1} (C-N) .On the other handthe ^{1}H-NMR in DMSO-d_6 showed,δ =7.0ppm(m ,4H,Ar) of substituted phenyl ,δ= 7.9ppm (m ,6H, Ar-H) due to (4H,Ar-H) referred to substituted phenyl and (2H,Ar-H) of biphenyl . δ= 7.3-7.4ppm (m,4H,Ar-H) due to biphenyl, δ=3.9ppm (s ,6H, CH_3O) and δ= 2.1ppm (s ,,6H, $Ar(CH_3)_2$) Elemental analysis of the molecular formula $C_{30}H_{28}N_2O_2$(calculated / found): (C, 80.33/ 80.77; H, 6.29/ 6.54; N, 6.25/6.44).

Synthesis of bis (2-bromo benzylidene) 3,3'dimethyl biphenyl-4,4'-diaminey .(8)

o-bromobenzaldehyde (4mmol, 0.72g) ,under refluxing for 2houre. slightly yellow precipitate with m.p. = 164-165 °C , yield = 85 % .FT-IR (KBr) cm^{-1} data showed weak absorption band at 3051 cm^{-1}- 2978 cm^{-1} due to(C-H, aromatic , aliphatic) respectively , 1617cm^{-1} (C=N) , 1483-1591 cm^{-1} (aromatic C=C) ,1024 cm^{-1} (C-N) , sharp peak at 762 cm^{-1} (C-Br) .On the other hand the ^{1}H-NMR in DMSO-$d_6$showed, δ=8.8ppm (s,2H,2CH=N) ,δ= 7.0ppm (d ,2H, Ar-H) and δ= 7.65ppm (d,2H,Ar) referred to four proton of biphenyl , δ= 7.3-7.5ppm (m,10H, m ,Ar-H) referred to (8H,Ar-H) of substituted phenyl with (2H,Ar-H) of biphenyl . δ = 2.2ppm (s,6H,$Ar(CH_3)_2$) . Elemental analysis of the molecular

formula $C_{28}H_{22}Br_2N_2$ (calculated /found) :(C, 61.56 /62.03; H, 4.06/ 4.55; N, 5.13/5.66.

Synthesis of bis (4-hydroxy benzylidene) 3,3'dimethyl biphenyl-4,4'-diamine.(9)

p-hydroxybenzaldehyde (4mmol, 0.50g) , yellowish orange precipitate were obtained , after filtration and drying the yield = 77 % and the m.p. = 280- 281 °C . FT-IR showed,at3444 cm^{-1} (OH ,phenolic) ,3022 cm^{-1}-2953 cm^{-1} due to (C-H) aromatic and aliphaticrespectively , 1621 cm^{-1} (C=N), , 1481- 1591 cm^{-1} (C=C , aromatic) , 1242 cm^{-1} (C–O) , and 1163 cm^{-1} (C-N) . The ^{1}H-NMR in DMSO-d_6 showed,δ= 9.8ppm (s,2H,OH) phinolic,δ= 8.8ppm (s,2H, ,2CH=N). δ= 7.0ppm (m,4H,Ar-H) and δ= 7.9ppm (m,24H ,Ar-H) referredsubstituted phenyl group . δ=7.2ppm (d,2H,ArH) δ=7.3ppm (d,2H,Ar) andδ=7.2ppm (d,2H,ArH) due to six proton of biphenyl, δ= 2.2ppm represented (s,6H,Ar$(CH_3)_2$) .·Elemental analysis of the molecular formula $C_{28}H_{24}N_2O_2$(calculated /found): C, 79.98 / 80.46; H, 5.75/ 6.09; N, 6.66 /7.11).

Synthesis of bis (4-hydroxy-3-methoxy benzylidene) 3,3'dimethyl biphenyl-4,4'-diamine .(10)

p-hydroxy-m-methoxybenzaldehyde (4mmol, 0.60g) ,a solid yellow precipitate observed after work up with section filtration yield= 78% with m.p. =199-200 C°.FT-IR (KBr) cm^{-1} spectra showedstretching absorption broad band at 3432 cm^{-1} refer to OH group ,3010 cm^{-1}-2900 cm^{-1} (CH aromatic and aliphatic) respectively, while imine band appear in about 1626 cm^{-1} , (C=C)aromatic appeared in the range of(1512-1593) cm^{-1}, medium intensity of band appear at 1274 cm^{-1} referred to (C-O) and 1122 cm^{-1} referred to(C-N). On the other hand the ^{1}H-NMR in DMSO-d_6 showed,δ=9.8ppm (s,2H ,OH) phenolic , δ= 8.5ppm (s,2H,2CH=N) ,δ = 6.8ppm (d, 2H,Ar) and δ = 6.9ppm (d,2H, ArH) due to substituted phenyl , δ = 7.4ppm (d , 2H, ArH) due to biphenyl ring. δ =7.1-7.3ppm (m ,6H ,ArH) referred to (4H,ArH) of biphenyl with (2H,ArH) due to substituted phenyl . δ= 2.2ppm (s, 6H ,Ar$(CH_3)_2$) and at δ= 4.0ppm (s, 6H ,CH_3O-Ar).On the other hand Elemental Analysis of the molecular formula $C_{30}H_{28}N_2O_4$ (calculated / found) :(C, 74.98 /75.41; H, 5.87 / 6.27; N, 5.83 /6.13).

(E)- N4,N4'-bis(furan-2-ylmethylene)-3,3'-dimethylbiphenyl-4,4'-diamine.(11)

(4mmol, 1.36 g) ,bright yellow precipitation observed with m.p.= 165-166°C and yield = 79% .FT- IR spectra showed the following bands at 3124 cm^{-1}-2980 cm^{-1} due to (C-H) aromatic and aliphatic respectively , 1629 cm^{-1} (C=N) , 1469-1558 cm^{-1}due to(C=C) aromatic .On the other

hands the ^{1}H-NMR in DMSO-d_6 showed, δ = 8.2ppm referred to (s, 2H, 2CH=N), δ= 6.6ppm (d,2H,Ar)and δ= 6.8ppm (d,2H,ArH) of furan group, δ=7.2ppm (m,4H,ArH) due to biphenyl ring,δ=7.5-7.6ppm (m, 4H,ArH) referred to (2H,Ar) of furan with (2H,ArH) of biphenyl, δ=2.1ppm (s,6H,Ar(CH_3)$_2$). Elemental analysis of the molecular formula $C_{24}H_{20}N_2O_2$ (calculated /found): C, 78.24/78 .88, H, 5.47;/ 5.94; N, 7.60;/8.03).

General method to synthesis of azetidin-2-one (12-21):

To solution of (phenylthio)acetic acid (0.5 g, 3 mmol), imine (1 mmol) and triethylamine (1 g, 6 mmol, 1.5 ml) in 80 ml dry methylene chloride was added drop wise (30-55) min under nitrogen atmosphere at 0°C, a solution of phosphorus oxychloride ($POCl_3$) (0.82 g, 0.48 ml, 3 mmol) in 20 ml of dry methylene chloride with constant stirring[17]. The reactant was stirred overnight at room temperature. The completion of reaction was monitored by (TLC). After the completion, the contents were washed successively with 1*N*HCl (30 ml), water (3x30 ml ,5% $NaHCO_3$ (30 ml) and brine (30 ml). The organic layer was separated and dried over anhydrous Na_2SO_4. The solvent was removed under reduced pressure and the crude product was purified by column chromatography using silica gel mesh (60-120)

1,1'-(3,3'-dimethylbiphenyl-4,4'-diyl)bis(4-phenyl-3-(phenylthio)azetidin-2-one) . (12)

Using imine(2), (0.388 g, 1 mmol), the product was purified by column chromatography using silica gel eluting with (8:2 hexanes /ethyl acetate). After solvent evaporation bright yellow precipitation observed with m.p.= 175-176°C , yield = 64% . FT-IR-spectra showed absorption bands appeared at the range of 3016 cm^{-1} and 2920 cm^{-1} which belong to both (C-H) aromatic and aliphatic respectively. While (C=O) appeared at 1641 cm^{-1} , beside that the (C=C aromatic) appeared at range of 1521– 1585 cm^{-1} . On the other hand the data in figure(5) of ^{1}H-NMR in DMSO-d_6 showed, at δ = 2.2ppm (s,6H,Ar(CH_3)$_2$) , δ =7.2-7.5ppm, (m,26H, Ar) due to the phenyl and biphenyl rings δ= 5.4ppm, (d,2H, C4-H), δ= 4.7ppm (d,2H, C3-H). ^{13}CNMR in DMSO-d_6 showed, at δ =18ppm due to (Ar-CH_3) , δ =52ppm and at δ =64ppm due to C3&C4 of azetidin-2-ones ring respectivelythe (C=O) of azetidin-2-ones ring appeared ,δ =167ppm, the aromatic carbons appeared at range δ =124-136ppm . Elemental analysis of the molecular formula $C_{44}H_{36}N_2O_2S_2$ (calculated /found):C, 76.71/77.23; H, 5.27/5.65; N, 4.07/4.56; S, 9.31/9.66.

1,1'-(3,3'-dimethylbiphenyl-4,4'-diyl)bis(4-(4-(dimethylamino)phenyl)-3-(phenylthio)azetidin-2-one) .(13)

Using imine(2), (0.475g), the product was purified by column chromatography using silica gel eluting with(9:1 hexanes /ethyl acetate). After solvent evaporation bright brown precipitation observed with m.p.= 183-184°C , yield = 65% . FT-IR-spectra showed absorption bands appeared at the range of 3053 cm^{-1} and 2918cm^{-1} which belong to both (C-H) aromatic and aliphatic respectively. While (C=O) appeared at 1751cm^{-1} , beside that the (C=C aromatic) appeared at range of 1481–1587 cm^{-1} .On the other hand the ^{1}H-NMR in DMSO-$d_6$showed, δ = 2.1ppm (s,6H,Ar$(CH_3)_2$) , δ = 3.0ppm (s,12H,2N$(CH_3)_2$) δ =7.1-7.5ppm, (m,24H, Ar-H) due to the substituted phenyl and biphenyl rings , δ= 5.4ppm, (d,2H, C4-H), δ= 4.6ppm (d,2H, C3-H). Elemental analysis of the molecular formula $C_{48}H_{46}N_4O_2S_2$ (calculated /found): C, 74.39/74.99; H, 5.98/6.28; N, 7.23/7.84; S, 8.27/8.65.

1,1'-(3,3'-dimethylbiphenyl-4,4'-diyl)bis(4-(4-(diethylamino)phenyl) -3-(phenylthio)azetidin-2-one).(14)

Using imine(3), (0.531 g, 1 mmol) , the product was purified by column chromatography using silica gel eluting with(9:1 hexanes /ethyl acetate). After solvent evaporation bright brown precipitation observed with m.p.=161-162°C, yield = 66% . FT-IR-spectra in showed absorption bands appeared at the range of 3055cm^{-1} and 2922 cm^{-1} which belong to both (C-H) aromatic and aliphatic respectively. While (C=O) appeared at 1735 cm^{-1} , beside that the (C=C aromatic) appeared at range of 1598–1524 cm^{-1} . On the other hand the ^{1}H-NMR in DMSO-d_6 showed, δ = 2.1ppm (s,6H,Ar$(CH_3)_2$) ,δ = 0.9ppm (q,12H,2N$(CH_3)_2$) δ = 3.6ppm (t,8H,2N$(CH_2)_2$) , δ =7.7-7.0ppm, (m,24H, Ar-H) due to the substituted phenyl and biphenyl rings , δ= 5.3ppm, (d,2H, C4-H),δ= 4.4ppm (d,2H, C3-H)Elemental analysis of the molecular formula $C_{52}H_{54}N_4O_2S_2$ (calculated /found): C, 75.14/75.67; H, 6.55/6.89; N, 6.74/7.04; S, 7.72/8.22.

1,1'-(3,3'-dimethylbiphenyl-4,4'-diyl)bis(4-(4-chlorophenyl)-3-(phenylthio)azetidin-2-one).(15)

Using imine(4) (0.457 g, 1 mmol), the product was purified by column chromatography using silica gel eluting with (8:2 hexanes /ethyl acetate). After solvent evaporation bright yellow precipitation observed with m.p.= 145-146°C , yield = 59% .FT- IR spectra showed absorption bands appeared at the range of 3050 and 2920cm^{-1} which belong to both (C-H) aromatic and aliphatic respectively. While (C=O) appeared at 1645 cm^{-1} , beside that the (C=C aromatic) appeared at range of 1585– 1487 cm^{-1} . On the other hand the ^{1}H-NMR in DMSO-d_6 showed, δ = 2.1ppm

(s,6H,Ar(CH_3)$_2$), at δ =7.2-7.5ppm, (m ,20H, Ar) and at δ =7.7-7.9ppm (m ,4H, Ar) due to biphenyl ring , δ= 5.4 ppm, (d,2H, C4-H), δ= 4.8 ppm and (d,2H, C3-H). ^{13}CNMR in $CDCl_3$showed, at δ =18ppm due to (Ar-CH_3) , δ =52ppm and δ =64ppm due to C3&C4 of azetidin-2-ones ring respectively the (C=O) of azetidin-2-ones ring appeared δ =167ppm, the aromatic carbons appeared at range 124-136ppm . Elemental analysis of the molecular formula $C_{44}H_{34}Cl_2N_2O_2S_2$ (calculated /found): C, 69.74/70.12; H, 4.52/4.87; N, 3.70/4.15; S, 8.46/8.89.

1,1'-(3,3'-dimethylbiphenyl-4,4'-diyl)bis(4-(4-bromophenyl)-3-(phenylthio)azetidin-2-one) .(16)

Usingimine(5), (0.546 g, 1 mmol) , the product was purified by column chromatography using silica gel eluting with
(8:2 hexanes /ethyl acetate). After solvent evaporation bright brown precipitation observed with m.p.=171-172°C, yield = 61% .FT-IR-spectra showed absorption bands appeared at the range of 3057 cm^{-1} and 2922 cm^{-1} which belong to both (C-H) aromatic and aliphatic respectively. While (C=O) appeared at 1761 cm^{-1} , beside that the (C=C aromatic) appeared at range of 1599– 1481
cm^{-1} . On the other hand the ^{1}H-NMR in DMSO-d_6 showed, δ = 2.1ppm (s,6H,Ar(CH_3)$_2$), δ =6.8-7.7ppm, (m ,24H, Ar), δ= 5.3ppm, (d,2H, C4-H), δ= 4.4ppm and (d,2H, C3-H)Elemental analysis of the molecular formula $C_{44}H_{34}Br_2N_2O_2S_2$(calculated /found): C, 62.42/62.89; H, 4.05/4.37; N, 3.31/3.68; S, 7.57/7.88.

1,1'-(3,3'-dimethylbiphenyl-4,4'-diyl)bis(4-(4-methoxyphenyl)-3-(phenylthio)azetidin-2-one) .(17)

Usingimine(6), (0.448 g, 1 mmol) , the product was purified by column chromatography using silica gel eluting with (9:1 hexanes /ethyl acetate). After solvent evaporation bright brown precipitation observed with m.p.=137-138°C , yield = 68% . FT-IR-spectra showed absorption bands appeared at the range of 3057 and 2955 cm^{-1} which belong to both (C-H) aromatic and aliphatic respectively. While (C=O) appeared 1755 cm^{-1} , beside that the (C=C aromatic) appeared at range of 1581– 1481 cm^{-1}, 1174 cm^{-1} peak due to(C-O) . On the other hand the ^{1}H-NMR in DMSO-d_6 showed, δ= 3.8ppm, (s,6H, OCH_3), δ= 2.1ppm, (s,6H, Ar(CH_3)$_2$) , δ= 5.7ppm and (d,2H, C4-H) δ= 4.9ppm and (d,2H, C3-H), δ= 7.0-7.5ppm (m,24H,Ar).^{13}CNMR in $CDCl_3$ showed, δ =17ppm due to (Ar-CH_3) ,δ =52ppm and at δ =61ppm due to C3&C4 of azetidin-2-ones ring respectively the , δ =55ppm due to (Ar-O-CH_3). The (C=O) of azetidin-2-ones ring appeared at δ =167ppm, the aromatic carbons appeared at range 126-136ppm , δ =159ppm due to aromatic carbon attached to oxygen of (O-CH_3) groups. Elemental analysis of the molecular formula

$C_{46}H_{40}N_2O_4S_2$ (calculated /found): C, 73.77/74.33; H, 5.38/5.85; N, 3.74/4.05; S, 8.56/8.99.

1,1'-(3,3'-dimethylbiphenyl-4,4'-diyl)bis(4-(2-bromophenyl)-3-(phenylthio)azetidin-2-one) .(18)

Usingimine(7), (0.546 g, 1 mmol), the product was purified by column chromatography using silica gel eluting with (8:2 hexanes /ethyl acetate). After solvent evaporation bright brown precipitation observed with m.p.= 169-170°C , yield = 48% . FT-IR-spectra in showed absorption bands appeared at the range of 3032 cm^{-1} and 2920 cm^{-1} which belong to both (C-H) aromatic and aliphatic respectively. While (C=O) appeared at 1750 cm^{-1}, beside that the (C=C aromatic) appeared at range of 1589– 1526 cm^{-1} . Elemental analysis of the molecular formula $C_{44}H_{34}Br_2N_2O_2S_2$ (calculated /found): C, 62.42/62.86; H, 4.05/4.47;N, 3.31/3.71; S, 7.57/8.00

1,1'-(3,3'-dimethylbiphenyl-4,4'-diyl)bis(4-(4-hydroxyphenyl)-3-(phenylthio)azetidin-2-one) .(19)

Using(8), (0.42 g, 1 mmol) , the product was purified by column chromatography using silica gel eluting with (10:1 hexanes /ethyl acetate). After solvent evaporation bright brown precipitation observed with m.p.=189-190°C, yield = 62% . FT-IR-spectra showed absorption abroad band appeared at 3333 cm^{-1} belong to(O-H) , at the range of 3055cm^{-1} and 2920 cm^{-1} showed bands belong to both (C-H) aromatic and aliphatic respectively. While (C=O) appeared at 1753 cm^{-1} , beside that the (C=C aromatic) appeared at range of 1585– 1479 cm^{-1} and at 1242 cm^{-1} band referred to (C-O) phenolic . On the other hand the ^{1}H-NMR in DMSO-d_6 showed, at δ= 2.1ppm and (s,6H, Ar$(CH_3)_2$) , δ= 5.3ppm and (d,2H, C4-H) δ= 4.2ppm and (d,2H, C3-H), δ= 9.8ppm and (s,2H, O-H) of phenol group at δ= 7.1-7.6ppm (m,24H,ArH) referred to biphenyl and substituted phenyl groups.Elemental analysis of the molecular formula $C_4H_{36}N_2O_4S_2$ (calculated /found): C, 73.31/73.77; H, 5.03/5.39; N, 3.89/4.26; S, 8.90/9.44.

1,1'-(3,3'-dimethylbiphenyl-4,4'-diyl)bis(4-(4-hydroxy-3-methoxyphenyl)-3-(phenylthio)azetidin-2-one) . (20)

Usingimine(9), (0.48 g, 1 mmol), the product was purified by column chromatography using silica gel eluting with(10:1 hexanes /ethyl acetate). After solvent evaporation bright brown precipitation observed with m.p.= 181-182°C , yield = 59% . FT-IRspectra showed absorption abroad band appeared at 3265 cm^{-1} belong to(O-H) , at the range of 3081cm^{-1} and 2918 cm^{-1} showed bands belong to both (C-H) aromatic and aliphatic respectively. While (C=O) appeared at 1643 cm^{-1} , beside

that the (C=C aromatic) appeared at range of 1585– 1481 cm^{-1}.On the other hand the ^{1}H-NMR in DMSO-d_6 showed, δ= 2.1ppm and (s,6H, $Ar(CH_3)_2$) ,δ= 2.4ppm and (s,6H, CH3-O) , δ= 5.1ppm and (d,2H, C4-H) δ= 4.4ppm and (d,2H, C3-H), δ= 9.6ppm and (s,2H, O-H) of phenol group δ= 7.2-7.5ppm (m,22H,Ar-H) referred to biphenyl and substituted phenyl groups.^{13}CNMR using $CDCl_3$in figure(6)showed, at δ =18ppm due to (Ar-CH_3) , at δ =54ppm and at δ =67ppm due to C3&C4 of azetidin-2-ones ring respectively the , δ =57ppm due to (Ar-O-CH_3). The (C=O) of azetidin-2-ones ring appeared at δ =168ppm, the aromatic carbons appeared at range 124-145ppm. Elemental analysis of the molecular formula $C_{46}H_{40}N_2O_6S_2$ (calculated /found): C, 70.75/71.22; H, 5.16/5.49; N, 3.59/3.91; S, 8.21/8.41

1,1'-(3,3'-dimethylbiphenyl-4,4'-diyl)bis(4-(furan-2-yl)-3-(phenylthio)azetidin-2-one).(21)

Usingimine(10), (0.36g, 1 mmol), the product was purified by column chromatography using silica gel eluting with (8:2hexanes /ethyl acetate). After solvent evaporation bright brown precipitation observed with m.p.=168-169°C, yield = 55% .FT- IRspectra at the range of 3051 and 2981 cm^{-1} showed bands belong to both (C-H) aromatic and aliphatic respectively. While (C=O) appeared at 1641 cm^{-1} , beside that the (C=C aromatic) appeared at range of 1583– 1520 cm^{-1} . On the other hand the ^{1}H-NMR inDMSO-d_6 showed, δ= 2.1ppm (s,6H, $Ar(CH_3)_2$), at δ =7.2-7.4ppm, (m ,22H, Ar-H) δ= 5.6ppm, (d,2H, C4-H), at δ= 4.8ppm and (d,2H, C3-H). Elemental analysis of the molecular formula $C_{40}H_{32}N_2O_4S_2$ (calculated /found): C, 71.83/72.32; H, 4.82/5.05; N, 4.19/4.48; S, 9.59/9.77.

RUSTLES AND DISCUSSION

The mixture of 1mmol of o-tolidine and 2 mmol of substituted aldehyde were heated in presence of approximately 25 ml of absolute ethanol with (2-3) drops of glacial acetic acid in water bath at 70- 80 C for approximately(2-3) hours [18].The process of reaction was followed by (TLC) ,then filtration or evaporation of the solvent then recrystalized from ethanol .

A series of different azetidin-2-one(12-21) were synthesized by the Staudinger ketene-imine [2+2] cycloaddition using phosphors compound[19][20], In this paper work we used $POCl_3$ as condensation reagent [21][22][23] as shown below Scheme(1) .

The FT-IR spectra of the different azetidin-2-one were characterized by the presence the carbonyl group (C=O) of amide carbonyl at (1757-1656)cm^{-1} and disappearance of (C=N) in(1624- 1607) cm^{-1}.The ^{1}H-NMR of β-lactam (12-21) showed at regions (8.0-7.0) ppm corresponding

to aromatic protons , and disappearance the protons of imine (2CH=N) in δ=(9.1-8.4)ppm ,at the δ=(4.3-4.8)ppm region appeared protons due to (C3-H) and at δ=(5.7-5.2) ppm referred to (C4-H) of β-lactam ring. The ^{13}C-NMR of β-lactams compounds (12-21) , at the δ=(49-54)ppm region appeared carbons due to (C3-H) , at δ=(59-65) ppm referred to carbons (C4-H) of β-lactam ring and at region δ=(20-16)ppm due to (Ar-CH_3).

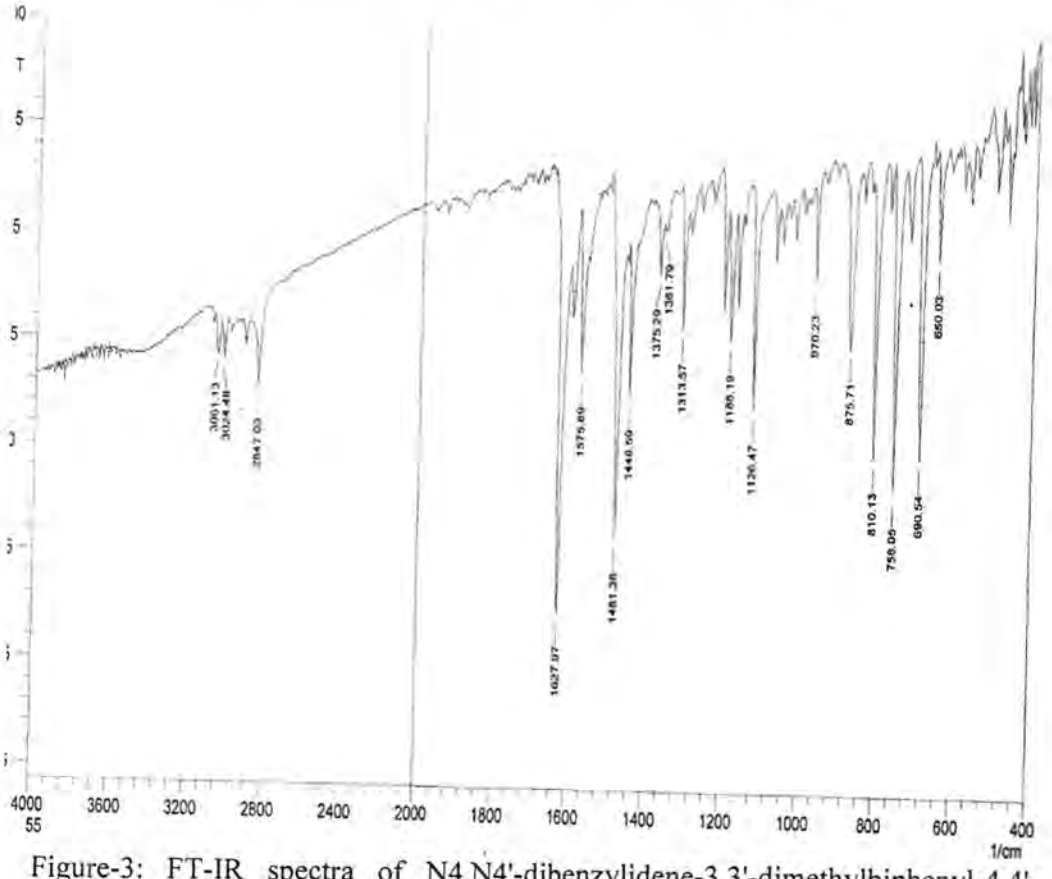

Figure-3: FT-IR spectra of N4,N4'-dibenzylidene-3,3'-dimethylbiphenyl-4,4'-diamine. (2)

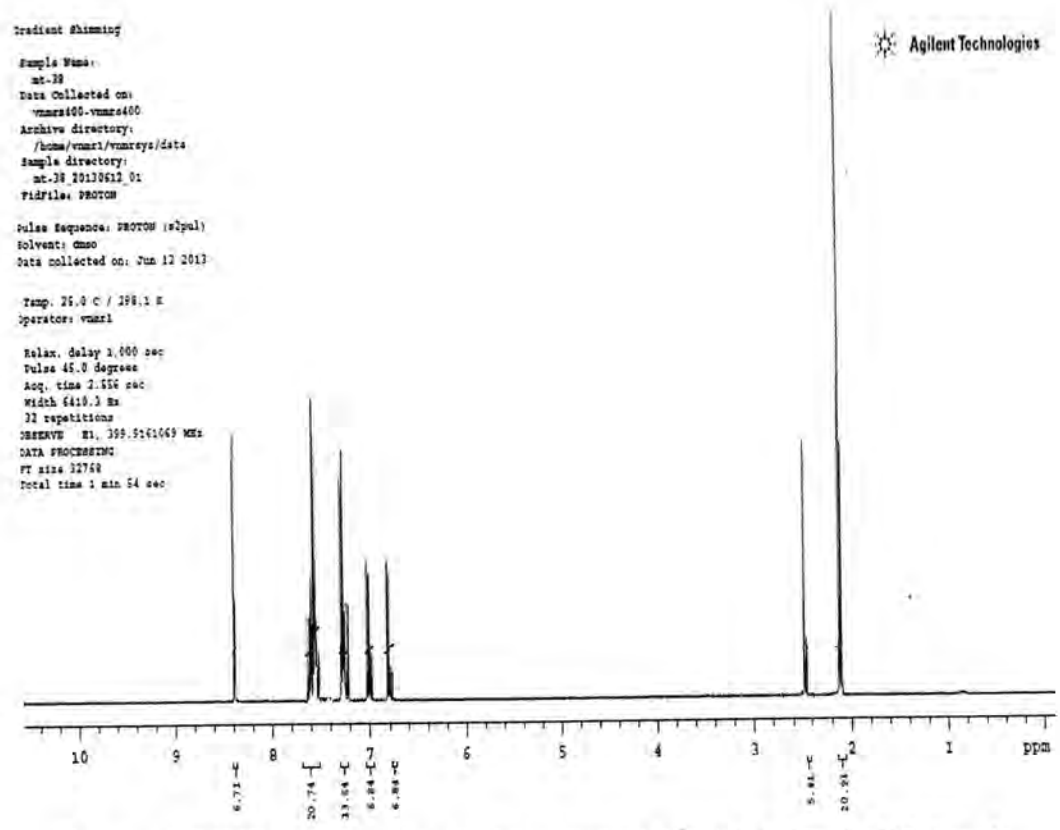

Figure-4:[1]HNMR spectra of bis (4-chloro benzylidene) 3,3'dimethyl biphenyl-4,4'-diamine . (5)

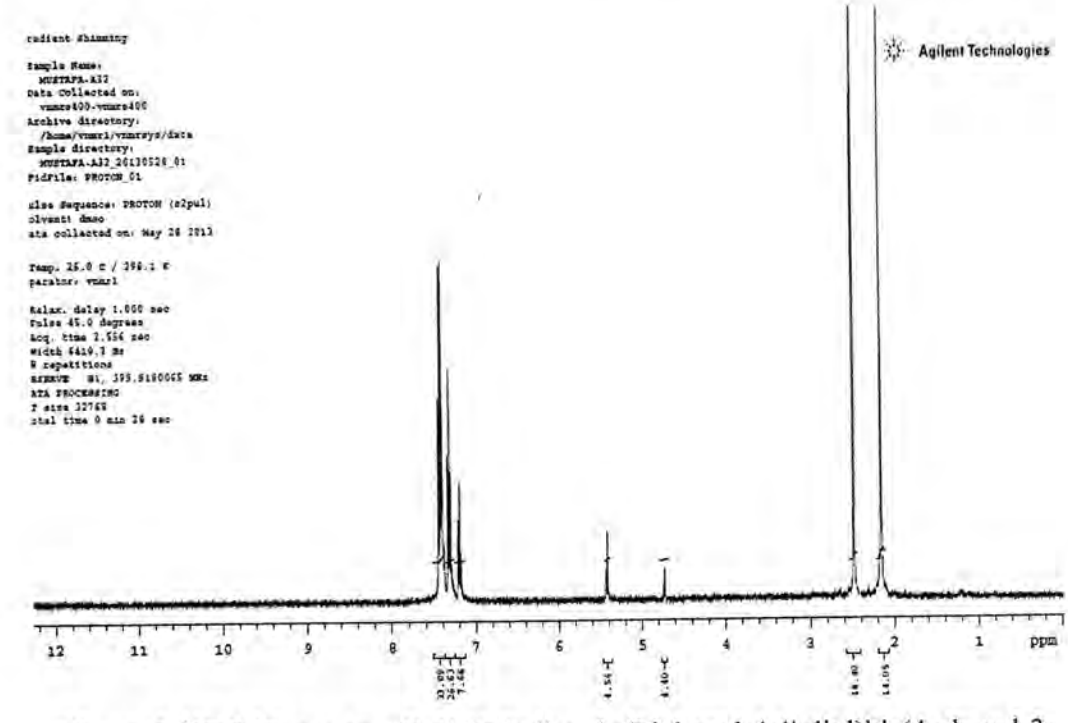

Figure-5: [1]HNMR spectra of1,1'-(3,3'-dimethylbiphenyl-4,4'-diyl)bis(4-phenyl-3-(phenylthio)azetidin-2-one) . (12)

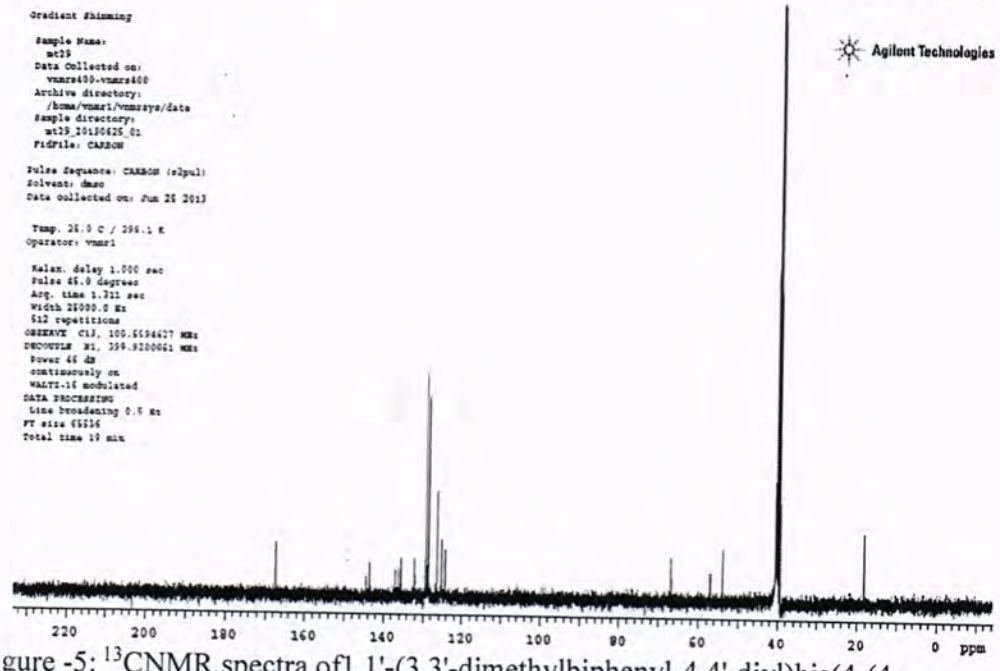

Figure -5: ^{13}CNMR spectra of1,1'-(3,3'-dimethylbiphenyl-4,4'-diyl)bis(4-(4-hydroxy-3-methoxyphenyl)-3-(phenylthio)azetidin-2-one).(20)

REFERENCES

[1] Powers J.C., AsgianJ.L., Ekici O.D. and James K.E, Irreversible Inhibitors of Serine, Cysteine, andThreonine Proteases, Chem. Rew., 102, 4639-4750 (2002).

[2] Imbach P., Lang M., García-Echeverría C., Guagnano V., Noorani M., Roesel J., Bitsch F., Rihs G.,Furet P., Novel β-lactam derivatives: Potent and selective inhibitors of the chymotrypsin-like activity of the human 20S proteasome, Bioorganic & Medicinal Chemistry Letters, 17(2), 358-362,(2007).

[3] Alcaide B., Almendros P., β-Lactams as Versatile Synthetic Intermediates for the Preparation of Heterocycles of Biological Interest, Current Medicinal Chemistry, 11, 1921-1949,(2004).

[4] Desmukh A.R.A.S., Bhawal B.M., Krishnaswamy D., Govande V.V., Shinkre B.A., Jayanthi A.,Azetidin-2-ones, Synthon for Biologically Important Compounds, Current Medicinal Chemistry, 11, 1889-1920,(2004).

[5] Modugno di E., Erbetti I., Ferrai L., Galasi G., Hammond S. M., Xerri L., In Vitro Activity of the Tribactam GV104326 against Graim- Possitive, Gram-Negative, and anaerobe Bacteria, Antimicrobal Agents and Chemotherapy, 38, 2362 – 2368(1994),

[6] Hall B. G., Barlow M., Evolution of the serine β- lactamases: past, present and future, Drug Resistance Updates,7(2), 111-123,(2002).

[7] Bulytchev A., Belletini J, R., O'Brien M., Crocker P. J., Samama J.P., Miller M. J., Mobashery S.,N- Sulfonyloxy-β-lactam Inhibitors for β-lactamases, Tetrahedron, 56, 5719 – 5728, (2000).
[8] Sader H.S., Gales A.C, Emerging strategies in infectious diseases: New Carbapenem and Trinem Antibacterial Agents, Drugs, 61, 553-564,(2001).
[9] Bassetti M., Righi E., Viscoli C., Novel β-lactam antibiotics and inhibitor combinations, Expert Opin. Investig. Drugs, 17, 285-296,(2008).
[10] Bimal K. Banik, Frederick F. Becker and Indrani Banik., Synthesis of anticancer β -lactams: mechanism of action, Bioorganic & Medicinal Chemistry ,12 ,2523–2528(2004)
[11] Bimal K. Banik, , Indrani B. and Frederick F. B.,Stereocontrolled synthesis of anticancer β -lactams via the Staudinger reaction, Bioorganic & Medicinal Chemistry 13 ,3611–3622, (2005).
[12] Manisha N., D., Thavaselvam S. P., M. S.and Kaushik M. P., synthesis and biological evaluation of novel bicyclicβ -lactams as potential antimalarials, Bioorganic & Medicinal Chemistry Letters 15 (2005) 1371–1373
[13] Staudinger, H. Ann.,356, 51–123, (1907).
[14] Tidwell, T. T. Eur. J. Org. Chem. ,563–568,(2006).
[15] Jiao, L.; Zhang, Q. F.; Liang, Y.; Zhang, S. W.; Xu, J. X. J. Org. Chem., 71, 815–818,(2006).
[16] Arumugam, N.; Raghunathan, R. Tetrahedron Lett., 47, 8855–8857, (2006).
[17] AL-Tamemay, S.M., Synthesis and Characterization Of Some New Heterocyclic
[18] Compounds Such As: Oxadiazole and Azetidine-2-One Derivatives, Iraqi National Journal of Chemistry, 44,571-581,(2011).
[19] Brian S., Antony J., Peter W., Austin R.,"Vogel's " 5th ed. Johan and Wiley ,Inc. New York , (**1989**).
[20] Krishnaswamy D., Govanda, V.V., Gumaste,V.K., Bhawal, B.M. and Deshmukh, A.R.S., Trphosgene: a verstile reagent for the synthesis of azetidin-2-one, tetrahedrone 58 ,22215-22225, (2002).
[21] Alcaide B., Almendros P., Vicentea A. R.and M. Pilar Ruiz, Free radical synthesis of benzofused tricyclic b-lactams by intramolecular cyclization of 2-azetidinone-tethered haloarenes, Tetrahedron 61 , 2767–2778, (2005).
[22] Bhalla A., Madan S., Venugopalany P. and Shamsher S. B., C-3 b-lactam carbocation equivalents: versatile synthons for C-3 substituted b-lactams, Tetrahedron 62 (2006) 5054–5063.

[23] Bhalla A., Madan S., Venugopalany P. and Shamsher S. B., Facile stereoselective synthesis of cis- and trans-3-alkoxyazetidin-2-ones, Tetrahedron 62 (2006) 8291–8302

[24] Bari S. S., Bhalla A., Reshma G. H., Facile synthesis of novel bicyclic b-lactams: analogues of C-fused penicillintype ring systems, Tetrahedron Letters 54 (2013) 483–486.

Isolation and Identification of Bacterial Burn Wound Infection and Their Sensitivity to Antibiotics

Lazim H. Al-Taie[1], Sawsan Hassan[2], Kasim Sh. Al-Mayah[3], Saba Talib[4]
[1]Department of microbiology , college of medicine , Al-Nahrain university
[2,4]Department of microbiology , college of science , Al-Mustansiriya university
[3]Research center , college of medicine , Al-Nahrain university
Received 1/9/2011 – Accepted 26/5/2014

الخلاصة

هدفت الدراسة الى التحري عن الملوثات البكتيرية للحروق ونمط المقاومة لدى البكتريا المسببه لاخماج الجروح للمضادات الحيويه الشائعة الاستعمال.

جمعت 100 مسحة من المصابين بالحروق في اربع مستشفيات في بغداد . تم زرع المسحات على اوساط زرعيه مختلفة ثم اجري للعزلات المنقاة الاختبارات الكيموحيوية لتحديد انواع العزلات البكتيرية، كما تم التحري عن حساسية العزلات اتجاه 11 مضاداً حيوياً .

بلغ العدد الكلي للمسحات الموجبه 89 مسحة وكانت بكتريا *pseudomonas aeruginosa* بأعلى نسبة [%31.46] تلتها *Klebsiella spp.* [%22.47] فبكتريا *Staphylococcus aureus* [%20.22] ، *Escherichia coli*, [%15.73] *Proteus spp.* [%10.11]. اظهرت معظم العزلات مقاومة عالية للمضادين الحيويين *Trimethoprim* و *Cephalothin* فيما كانت حساسة لكل من Nalidixic acid و Amikacin وعلى الرغم من التطور الهائل في مجال الرعاية الصحية الا انه لازالت الاخماج البكتيرية تمثل مشكلة خطيرة لمرضى الحروق ، ولا سيما ان العديد من الملوثات البكتيرية للاخماج قد طورت اساليبها المختلفة لمقاومة معظم المضادات الحيوية .

ABSTRACT The study aimed to determine the bacteriological profile and the resistance pattern of burn wound bacteria to the most common antibiotics . A total of 100 burn wound swabs were collected from burn patients from 4 hospitals in Baghdad province. After the swabs had been cultured on different media, conventional biochemical tests to identify bacterial isolates and antimicrobial sensitivity to the most common antibiotics were performed.

The total positive swabs for bacterial isolation was 89 , of which , *Pseudomonas aeruginosa* was the most commonest pathogen [31.46%] followed by *Klebsiella spp.* [22.47%] , *Staphylococcus aureus* [20.22%] , *Escherichia coli* [15.73%] and *Proteus spp.* [10.11%] . Most isolates showed high resistance to cephalothin and trimethoprim , and high susceptibility to nalidixic acid and amikacin. Despite the rapid improvement in medical care , wound burn infection still represent a serious problem for burn patients, with many bacteria developed different degrees of resistance to most known antibiotics .**Key words** : burn wounds, *Pseudomonas*, *Staphylococcus, Klebsiella*, antibiotics, susceptibility

INTRODUCTION

Burns are one of the most common and devastating forms of trauma [1] . Despite advance in the use of topical and parentral antimicrobial therapy , and the practice of early tangencial excision , bacterial infection remains a major problem in the management of burn victims[2]. In patients with severe burns over more than 40% of the total body surface area (TBSA) , 75% of all deaths are currently related to sepsis from burn wound infection or other infection complications and/or inhalation injury[3,4,5,6] . The rate of nosocomial infections are higher in burn patients due to various factors like nature of the burn injury itself, invasive diagnostic and therapeutic procedures, and prolonged intensive

care unit stay [7] . In addition, cross-infection results between different burn patients due to overcrowding in burn wards [8].

Although burn wound surfaces are sterile immediately following thermal injury, these wounds eventually become colonized with microorganisms [9]. Microorganisms colonizing burn wounds originate from the patient's endogenous skin and gastrointestinal and respiratory flora [10,11] . Some microorganisms may also be transferred to a patient's skin surface via contact with contaminated external environmental surfaces, water, fomite, air, and the solid hands of health care workers [12]. *Streptococcus pyogenes* was the most frequently recognized cause of burn wound sepsis in the early part of the last century . Over the years , however, *S. aureus* and *P. aeruginosa* have become the most frequent isolated organism in most burn units [13,14].

Emerging antimicrobial resistance trends in burn wound bacterial pathogens represent a serious therapeutic challenge for clinicians caring for burn patients [10,15] . Keeping in mind that infective agents and their susceptibility to antibiotic vary from time to time, it is desirable to carry out periodic reviews of the bacterial flora of the burn wounds .

The aim of this study was to assess the current bacterial profile of burn wounds and their antibiogram in some Baghdad hospitals.

MATERIALS AND METHODS

A total of 100 burn patients[52 males and 48 females , mean age 21.8±12.07 years , range 4 months to 70 years] admitted to burn unit in four hospitals : Al-Kindy teaching hospital, Al-Karkh general hospital, Al-Yarmouk teaching hospital, and Al-Karama hospital/Baghdad [25 patients from each hospital] were used for this study during the period from October 2003 to January 2004 . Mean total surface burned area was 15% [range 12- 83%] .

Wound swabs were taken from each patient . At direct patient contact , a protective gown and disposable gloves were used . The specimens were transported in sterile, leak-proof container to the laboratory . All specimens were inoculated on 5% blood agar and MacConkey agar plate and incubated overnight at 37Ċ aerobically . Bacterial pathogens were identified by conventional biochemical methods according to the standard microbiological technique [16] .

Antimicrobial susceptibility was performed on Mueller-Hinton agar by the standard disk diffusion method recommended by the Clinical and Laboratory Standard Institute[CLSI][17] .

The antibiotics tested were : amikacin, ampicillin, cefotaxim, cephalothin, Chloramphenicol, ciprofloxacin, erythromycin, gentamicin, naladixic acid, tobramycin, and trimethoprim. Antibiogram of bacterial isolates were done according to Kirby Bauer method [18] .

RESULTS AND DISCUSSION

Bacterial isolates were found in 89 [89%] samples and only 11 wound swabs were negative for bacterial culture . *P. aeruginosa* were the commonest pathogen isolates [31.46%] followed by *Klebsiella spp.* [22.47%[, *S. aureus* [20.22%] , *E. coli* [15.73%], and *Proteus spp.* (10.11%) (Table 1). Thermal destruction of the skin barrier and concomitant depression of local and systemic host cellular and humoral immune responses are pivotal factors contributing to infectious complications in patients with severe burns [19].

The results showed that the most common bacteria in burn wounds is *P. aeruginosa*. This finding is in accordance with previous studies which considered this bacteria as the commonest cause of burn wound infection[14,20,21] . However , other reports revealed that *Staph. aureus* was the most prevalent single organism colonizing burn wounds [22,23,24]

P. aeruginosa is part of a large group of free-living bacteria and has the ability to resist the effect of many disinfectants . The source of infection with this bacteria is from the patient's endogenous gastrointestinal flora and /or an environment . Despite burn wound infection with this bacteria can take place anywhere , nosocomial infection is more frequent than any other places for many reasons , among which contamination , presence of multidrug resistant bacteria and crowding . Since as early as 1967 , it was found that disinfectants used in many hospitals had contamination with *P. aeruginosa* [25].Furthermore , certain subjects in hospitals such as sink-traps, floor, cloths, and mops were frequently contaminated with this bacteria . On the other hand, when similar areas were examined in domestic homes , *P. aeruginosa* was rarely isolated [26].

Within the infected wound, *P. aeruginosa* produces a number of cell-associated (adhesins, aliginate, pili, flagella, and lipopolysaccharide) and extracellular (elastase, exoenzyme S, exotoxin A, hemolysins, Iron-binding proteins, leukocidins, and proteases) virulence factors that mediate a number of processes , including adhesion, nutrient acquisition, immune system evasion, leukocyte killing, tissue destruction, and blood stream invasion [27].These factors enable this bacteria to survive in burn wounds and transmit from patient to other within the burn unit .

Klebsiella spp was found as one of major pathogen that infect burn wound [14,28] . the virulence factors the bacteria possessed enable it to invade the wound easily and resist the immune response of the body . the most important virulence factors are cell wall receptors, capsular polysaccharide, and endotoxin. First, the presence of cell wall receptors enables *Klebsiella* to attach to the host cell, thereby altering the bacterial surface so that phagocytosis by polymorphonuclear leukocytes and

macrophages is impaired and invasion of the non-phagocytic host cell is facilitated. Second, invasion of the host cell is also facilitated by the large polysaccharide capsule surrounding the bacterial cell; in addition this capsule acts as a barrier and protects the bacteria from phagocytosis. Third, this bacteria produces an endotoxin that appears to be independent of factors that determine receptors and capsular characteristics[29]. An eighteen isolates of *Staphylococcus aeureus* which represents 22.2% of all isolates were found to be coagulase positive .Generally, *Staph. aureus* have a diverse array of virulence factors that facilitate adherence to host tissue, immune system evasion, and destruction of host cell and tissue, the most important of which is coagulase and hemolysin[30] . Burn wound infection with gram negative bacteria represented 77.52% , while gram positive bacteria accounts for only 22.47% . These results are in accordance with many previous studies(14,28) . Prior to the discovery of antibiotic , gram positive bacteria (especially streptococci and *Staph. aureus*) was the most frequent cause of life-threatening burns . The use of broad-spectrum antibiotics led to the emergence of gram negative bacteria as a predominant organism causing invasive burn wound infections [31]. It is because this fluctuation in bacterial profile, a periodic assessment of burn wound infection must be assessed.

Table- 2 shows the antimicrobial susceptibility pattern of the isolates . The study revealed that all isolates had resistance to trimethoprim and cephalothion [100%] . *P. aeruginosa* was unsusceptible to almost all antimicrobials . Among other gram negative bacilli , susceptibility percentage varied from 0% to cefotaxime , ampicillin to 100% to amikacin, chloramphenicol and nalidixic acid . However , *E . coli* showed high resistance to chloramphenicol, and moderate susceptibility to nalidixic acid (55.56%). *S. aureus.* isolates were highly susceptible to amikacin and gentamicin (77.78% for both)and but not to cefotaxime [22.2%]. Risk factors for acquisition of an antibiotic-resistant organism include receipt of antibiotics prior to the development of infection, extended duration of hospitalization, previous hospitalization, invasive procedures, comatose state, and advancing age[32[. Microorganisms transmitted from the hospital environment tend to be more resistant to antimicrobial agents than those originating from patient's normal flora[33].

Multidrug-resistant bacteria have frequently been reported as a cause of nosocomial outbreaks of infection in burn units or as a colonizers of the wounds of burn patients [14] Based on National Nosocomial Infection Surveillance System (NNIS) criteria , all the burn patients are required to follow the distribution of bacterial species among burn isolates. The high percentage of multidrug resistant isolates is probably due to excessive and indiscriminate use oF broad-spectrum antibiotics

.These multi drug resistant strain establish themselves in the hospital environment in areas like sinks , taps , railing, mattress , toilets and thereby spread from patient to another .This is especially obvious in *P. aeruginosa* which showed high resistance to the all used antibiotics and this is attributable to a concerted action of multidrug efflux pumps with chromosomally-encoded antibiotic resistance genes (e.g. *mexAB-oprM*, *mexXY*) and the low permeability of the bacterial cellular envelopes. Besides intrinsic resistance, *P. aeruginosa* easily develop acquired resistance either by mutation in chromosomally-encoded genes, or by the horizontal gene transfer of antibiotic resistance determinants [34]. Therefore , routine microbiological surveillance and careful in vitro testing prior to antibiotic use may help in the prevention and treatment of multidrug resistant pathogen in burn infection .

Table-1: Types of bacteria isolated from burn wounds

Type of bacteria	Number of isolates	Percentage %
Pseudomonas aeruginosa	28	31.46
Klebsiella spp.	20	22.47
Staphylococcus aureus	18	20.22
E. coli	14	15.37
Proteus spp.	9	10.11
Total	89	100

Table-2 :Antimicrobial susceptibility pattern(%) of the isolates

Antibiotic	**Concentration Disk(µg/L)**	Organisms (inhibition zone mm)				
		P. aeuroginosa	*Klebsiella spp*	*Staph. aureus*	*E. coli*	*Proteus spp*
Amikacin (AN)	30	44.4	55.56	77.78	100	100
Ampicillin (AMP)	10	ND	0	ND	0	44.4
Cefotaxime (CTX)	30	0	11.1	22.2	11.1	0
Cephalothin (KF)	30	0	0	0	0	0
Chloramphenicol(C)	30	22.2	66.67	66.67	0	100
Ciprofloxacin (CIP)	5	22.2	77.78	55.56	44.4	88.89
Erythromycin (E)	15	ND	ND	55.56	ND	ND
Gentamycin (G)	10	0	0	77.78	22.2	33.3
Nalidixic acid (NA)	30	ND	100	ND	55.56	100
Tobramycin (TM)	10	11.1	22.2	66.67	44.4	55.56
Trimethoprim (W)	1.25	0	0	0	0	0

ND : not done

REFERENCES

[1] Church, D. ; Elsayed, S. ; Reid, O. ; Winston, B. and Lindsay, R., Burn wound infection . Clin. Microbiol. Rev. **19**:403-434 (2006).

[2] De Macedo, J. L. S. and Santos, J. B., Bacterial and fungal colonization of burn wounds . Mem. Inst. Oswaldo Cruz. **100**:535-539 (2005).

[3] Atiyeh, B. S. ; Gunn, S. W. ; and Hayek , S. N., State of the art in burn treatment. World J. Surg. **29**:131-148, (2002).

[4] Bang, R. L.; Sharma, P. N. ;Sanyal, S. C. and Al Najjadah, I. Septicaemia after burn injury: a comparative study. Burns **28**:746-751, (2002).

[5] Fitzwater, J.; Purdue, G. F. ; Hunt, J. L. and O'keefe,G. E. The risk factors and time course of sepsis and organ dysfunction after burn trauma. J. Trauma **54**:959-966, (2003).

[6] Barrow, R. E. ; Spies, M. ; Barrow,L. N. and Herndon, D. N., Influence of demographics and inhalation injury on burn mortality in children. Burns **30**:72-77, (2004).

[7] Pruitt, B. A. ; McManus, A. T. ; Kim, S. H. and Goodwin, C. W., Burn wound infection : Current status . World J. Surg. **22**:135-145 (1998).

[8] Gupta, M. ; Gupta, O. K. ; Yaduvansh, R. K. and Upadhyahy, J., Burn epidemiology : the pink city scene . Burn **19**:47-51 (1993).

[9] Wysocki, A. B. Evaluating and managing open skin wounds: colonization versus infection. Am. Assoc. Critical-Care Nurse. **13**:382-397, (2002).

[10] Erol, S.; Altoparlak,U. ; Akcay,M. N.; Celebi, F. and Parlak, M., Changes of microbial flora and wound colonization in burned patients. Burns **30**:357-361, (2004).

[11] Barret, J. P., and Herndon, D. N., Modulation of inflammatory and catabolic responses in severely burned children by early burn wound excision in the first 24 hours. Arch. Surg. **138**:127-132, (2003).

[12] Weber, J. M.; Sheridan, R. L.; Pasternack, M. S. and Tompkins, R. G., Nosocomial infections in pediatric patients with burns. Am. J. Infect. Control **25**:195-201, (1997).

[13] Nasser, S. ; Mabrouk, A. and Maher, A., Colonization of burn wounds in Ain Shams University burn unit . Burns **29**:229-233 (2003).

[14] Agnihorti, N. ; Gupta, V. and Joshi, R. M., Aerobic isolates from burn wound infections and their antibiograms : a five-year study . Burns **30**:241-243 (2004).

[15] Murphy, K. D.; Lee,J. O. and Herndon, D. N., Current pharmacotherapy for the treatment of severe burns. Expert Opin. Pharmacother. **4**:369-384, (2003).

[16] Forbes, B. A. ; Sahm, D. F. and Weissfeld, A. S., Bailly and Scott's Diagnostic Microbiology . 11th ed. Mosby . An Affiliate of Eleseier Science, (2002).

[17] Clinical and laboratory Standard Institute, Performance standards for antimicrobial disk susceptibility test. NCCLS documents M100 S15 . Wayne, PA, USA, (2005).

[18] Bauer, A. W.; Kirby, W. M.; Sherris, J. C. and Turck, M., Antibiotic susceptibility testing by standardized single disk method . Am. J. Clin. Pathol. **45**:493-497 (1966).

[19] Griswold, J. A. (1993) White blood cell response to burn injury. Semin. Nephrol. **13**:409-415.

[20] Revathi, G.; Shannon, K. P. ; Stapleton, P. D. ; Jain, B. K. and French, G. L., An outbreak of extended-spectrum, beta-lactamase-producing Salmonella senftenberg in a burns ward. J. Hosp. Infect. **40**:295-302, (1998).

[21] Shahid, M. and Malik, A., Resistance due to aminoglycoside modifying enzymes in *Pseudomonas aeuroginosa* isolates from burns patients . Ind. J. Med. Res. **122**:324-329 (2005).

[22] Taylor, G. D. ; Kibsey, P. ; Kirkland, T. ; Burroghs, E. and Tredget, E., Predominance of *Staphylococcus* organism in infections occurring in a burn intensive care unit . Burns **18**:332-335 (1992).

[23] Vindebse, H. and Bjerknes, R., Microbial colonization of large wounds. Burns **21**:575-579 (1995).

[24] Komolafe, O. O. ; James, J. ; Kalogolera, L. and Makoka, M., Bacteriology of burns at Queen Elizabeth Central Hospital, Blantyre, Malawi . Burns **29**:235-238 (2003).

[25] Burden, D. W. and Whitby, J. L., Contamination of hospital disinfectant with *Pseudomonas* species . Brit. Med. J. **2**:153-155 (1967).

[26] Whitby, J. L. and Rampling, A., *Pseudomonas aeuroginosa* in domestic and hospital environments . Lancet **1**:15-17 (1972).

[27] Tredget, E. E.; Shankowsky, H. A.; Rennie, R.; Burrell, R. E. and Logsetty, S., *Pseudomonas* infections in the thermally injured patient. Burns **30**:3-26, (2004).

[28] Rasool,S.A; Ahmed ,A.,Khan ,S and Wahab ,A., Plasmid borne antibiotics resistance factors among indigenous Klebsiella .Pak.J. Bot,35(2): 243 -248, (2003).

[29] Highsmith , A. K. and Jarvis, W. R.m *Klebsiella pneumoniae*: selected virulence factors that contribute to pathogenicity. Infect. Control **6**:75-7, (1985).

[30] Foster, T.J., The Staphylococcus *aureus* "superbug"J.Clin.Investig.144:1693-1696, (2004).

[31] Altoparlak, U.; Erol, S.; Akcay, M. N.; Celebi, F. and Kadanali, A., The time-related changes of antimicrobial resistance patterns and predominant bacterial profiles of burn wounds and body flora of burned patients. Burns **30**:660-664, (2004).

[32] Clark, N. M.; Patterson, J. and Lynch, J. P., Antimicrobial resistance among gram-negative organisms in the intensive care unit. Curr. Opin. Crit. Care **9**:413-423, (2003).

[33] Fuchs, P. C.; Kopp, J.; Hafner, H.; Kleiner, U. and Pallua, N., Methicillin resistant staphylococcus aureus : retrospective analysis of an outbreak in the burn centre Aachen. Burns **28**:575-578, (2002).

[34] Poole, K., Efflux-mediated multiresistance in Gram-negative bacteria. Clinical microbiology and infection : the official publication of the European Society of Clinical Microbiology and Infectious Diseases **10** (1): 12–26, (2004).

Survey for *Pediculus Humanus Capitis* De Geer (Pediculidae: Phthiraptera: Insecta) Among Primary Schools Children in Erbil City

Karwan S. N. Al-Marjan[1] and Fouad H. Kamil[2]
[1]Department of Pharmacy, Medical Technical Institute, Hawler Poly Technique University, Erbil
[2]Department of Medical Laboratory Technical, Medical Technical Institute, Hawler Polytechnique University, Erbil
Received 24/10/2012 – Accepted 19/11/2013

الخلاصة

اخذ ما مجموع 3100 نموذج لأطفال المدارس الابتدائية بعمر 6-12 سنة من 31 مدرسة في محافظة اربيل (إقليم كردستان العراق) خلال الفترة ما بين شهر كانون الثاني وشهر نيسان من العام 2012 بصورة عشوائية. وتم فحصهم) باستخدام مشط القمل. *Pediculus humanus capitis* للكشف عن الإصابة بالطفيليات الخارجية (تبين من النتائج وجود 628 حالة إصابة بالطفيلي *Pediculus humanus capitis* أي بنسبة 20-25 % ، كما أوضحت النتائج وجود ترابط معنوي بين نسبة الإصابة ومستوى الثقافي للعائلة. تباينت نسبة الإصابة بين الجنسين حيث كان نسبة الإصابة عند الإناث 28.47% وعند الذكور 13.13%، علما أن نسبة الإصابة كانت عكسية مع العمر حيث الإصابة عند الصغار كانت أكثر.

ABSTRACT

School children were randomly selected from 31 primary schools in Erbil city (Kurdistan region-Iraq) and examined for ectoparasite, *Pediculus humanus capitis* using lice comb. This study performed between January 2012 to the end of April 2012, conducted on 3100 children aged between 6-12 years. The results of study reveals the existence of 628 cases (20.25%) of infestation with *Pediculus humanus capitis*. A significant association between the prevalence of infestation with education level of parents was demonstrated and different rates of infestation were recorded between females (28.47%) and males (13.13 %). Infestation rates increase by the decrease of the host age.

Keyword: *Peduculus humanus capitis*, head lice ectoparasite, Erbil.

INTRODUCTION

Pediculus humanus capitis, is a worldwide in distribution, especially among primary schools children, deaf and blind persons [1]. *Pediculus humanus*, especially *P. humanus capitis*, is still a crucial public health problem however, it is a low priority issue in public health [2]. In Europe, high rates can be found in almost all countries, from France to Germany, from Spain to Greece, from the Balkans to the United Kingdom and Poland [3]. Based of data which were collected by Ozlem *et al.*, [4] from 1982 till 2009, the infestation rate by *Pedeculus humanus capitis* in Turkey were increased among primary and secondary schools students and teachers. In Iran during the years 2002-2003 the prevalence of head louse infestation in primary school students was increased and make a large problem in Iranshahr city [5] and this rate was decreased in 2009 among such sector in Fars province [6] then gradually infestation rate were increased again in 2012 among primary schools in Sanandaj city, Kurdistan Province, Iran [7].

In Iraq low prevalence of infestation were recorded in 2003 among the primary schools children in Basra [8], while high rate of skin infestation especially by pediculosis were recorded in 2007 among such sector in Baghdad city [9]. In Iraqi Kurdistan region there are no previous report on head lice infestation, but high rate of infestation were demonstrated among peoples during Kurdish group migration to the neighbor countries, Iran and Turkey in 1991. *Pediculus humanus capitis* causes a disease known as pediculosis capitis, leads to intense itching and scratching of the scalp. Red marks resulting from irritation caused by the saliva of the louse, the itch scratch cycle can lead to secondary infection with impetigo and pyoderma swelling of the local lymph nodes and fever are rare [2]. This research aimed to study the prevalence of *P. humanus capitis* parasite in primary school children in Erbil city and tried to prevent head lice infestation.

MATERIAL AND METHODS

During the period from January till the end of April 2012, a total of 3100 primary school children were examined for the head lice, *Pediculus humanus capitis* infestation from 31 primary schools in Erbil city, Kurdistan region, Iraq.

Samples of the parasite (egg, nymph and adult) were derived and collected from the hair shaft of students by using lice comb to fall the parasite from the hair especially the adult and nymph [5]. Examined students were grouped according to their gender (sex) and age.

RESULTS and DISCUSSION

Parasite: *Pediculus humanus capitis* de geer.

Host: Human

Site of infection: Head scalp.

Prevalence: 20.25%

In the present study the recorded rate (20.25%) was lower than that (40.9%) previously reported in Baghdad, Iraq [9] and that previously recorded in Turkey (54%) [4], while approximately near than that which was recorded among schools children in Fars Province (20%), Southern Iran during winter [6].

Approximately similar rates (28.8% and 20.3%) also were reported among blind and deaf pupils in Saudi Arabia respectively [10].

As a result shown in table (1), it was concluded that the head lice were common among populations with poor hygiene and lower economic level in Erbil city especially in Mam Zawa (51%) and Salahaddin (44%) primary schools because such families living in a shanty houses, lack of in-house bathroom and lower levels of income and socioeconomic status which are all associated with head lice infestation.

Table-1: The prevalence of head lice infestation in different Erbil quarters.

Erbil quarters	No. of schools	No. of infected students	Prevalence of infestation (%)
Awlama	3	35	11.6
Shoresh	2	18	9
Tayrawa	4	83	20.75
Nusaran	1	0	0
Mantikawa	3	33	11
Azadi	3	17	5.66
Bakhtyari	2	25	12.5
Eskan	3	27	9
Mam Zawa	3	153	51
Aree	2	53	26.5
Sarwaran	2	8	4
Salahaddin	3	132	44
Kuran	2	44	22

Lice are a moderately contagious infestation of humans; direct person-to-person means head-to-head contact with hair of an infested person is responsible for most louse infestations and this make the high infestation among the children in more density populated schools especially in both quarters schools, Mam Zawa and Salahaddin. The prevalence of infestation in Nusaran was 0% due to small population density and high education level of parents.

Table (2), showed the distribution of the parasite stages on the human head and degree of infestation. The parasite infestation varied in location, it is more found in back of the head near the neck, both lateral sides of the head, head center and head front respectively in all stages (egg, nymph and adult).

Table-2 :The distribution of the parasites stages on the human head and degree of infestation.

Stage of parasite	Head front	Head center	Both lateral side of the head	Back of the head near the neck
Adult	+	++	+++	High infestation
Larva	+	++	+++	High infestation
Nits	+	++	+++	High infestation

(+) means 3-6 parasite in all stages on a special aeria on the head.

Our study results in table (3), prevalence of infestation is vary between males (13.13%) and females (28.47) since, were presented a higher infestation recorded among female due to high hair density which make the hair more greasy (oily), in addition to dark habitat and high humidity for the parasite. Also tie the hair with high humidity is more common

among the females comparison to males this is also reported by [7] and [11]. Back of the head with high infestation due to high hair density, darkness area, more greasy and moisten site.

Table-3: Prevalence of head lice infestation in primary schools by sex and age, Erbil city.

Gender	Ages	Age (average)	No. of examined students	No. of Infested students	Prevalence of infestation (%)	Prevalence (%) for male and female
Males	6-7 9-10 11-12	6.5 9.5 11.5	718 442 500	103 60 55	14.34 13.57 11	13.13
Females	6-7 9-10 11-12	6.5 9.5 11.5	575 378 487	189 112 109	32.86 29.6 22.38	28.47

So, depending on the risk factors which mentioned above, the head lice live in dark, moisten and oily head area and this leads to parasite distribution on the different sites on head.

Other Erbil quarters schools show the infestation by the parasite, in order to high personal hygiene and economic level but the causes of infestation were related to colder climates, where head scarves is not changed regularly, and bathing is infrequent.

In addition to that, there is other factor that leads to increase the prevalence of infestation in such quarters for example the mode of parasite transmission which is very simple because the parasite have direct life cycle, do not required the intermediate host [12].

The present study was done during the winter and spring seasons and the recorded prevalence agree with that which were previously reported by [6] during the same seasons.

In wormer climate, summer and autumn the rate of pediculosis were increased gradually because temperature elevation leads to increase the efficiency of adult stages of the parasite to lay the nits (eggs) every day [12] and this rate was decrease in both winter and spring respectively in compression with the wormer seasons.

In the present study a significant differences were demonstrated between the incidence of infestation and different student's ages. The prevalence of head lice infestation was higher in population of 6-7 years old (22.58%) group in compression with students ages of 9-12 years old.

The younger students sharing common comb because head lice infestation may be transmitted by sharing infested instruments including hats, scarves, sweaters, sharing common pillows, etc. in addition to infrequent bathing among younger student especially in winter season

(during January and February). The mentioned factors lead to increase the incidence of infestation among such sector and these factors also were reported by [7].

Acknowledgments

The authors acknowledge the assistance of Mr. Dlshad and Mr. Halkawt for their kind help of organizing the fieldwork.

REFRENCES

[1] Hunter, J. A. and Barker S. C.; Susceptibility of head lice (*Pediculus humanus capitis*) to pediculicides in Australia. Parasitol. Res., *90: 476–478.2003.*

[2] Takano-Lee, M.; John, D. E.; Bradley, A. M. and John, M. C. ; Transmission potential of the human head louse, *Pediculus capitis* (Anoplura: Pediculidae). International J. of Dermatology ,*5 (44): 811–816 .2005.*

[3] Sidoti, E. ; Bonura, F.; Paolini, G. and Tringali, G.;. A survey on knowledge and perceptions regarding head lice on a sample of teachers and students in primary schools of north and south of Italy. J. prev. med. hyg. , *50: 141-151.2009.*

[4] Ozlem, O.; Onur, H.; and Melike, Y. (2010). The Prevalence and Management of *Pediculus humanus capitis* in Turkey ;: A Critical Perspective in Terms of Public Health. Public Health Nursing, Nursing Dep., Kocaeli School of Health, Kocaeli Univ., Kocaeli, Turkey. and Kocaeli Univ. Medical Faculty, Kocaeli, Turkey. *24 (3):163-166. 1982-*2009.

[5] Salemi, J. A.; Shayeghi1, N.; Zeraati, H.; Akbarzadeh, K.; Basseri H.; Ebrahimi1, B. and Rafinejad, J. ; Some Aspects of Head Lice Infestation in Iranshahr Area (Southeast of Iran). Iranian J. Publ. Health. *32 (3): 60-63.2003.*

[6] Davarpanah, A. M.; Mehrabani, D.; Khademolhosseini, F.; Mokhtari, A.; Bakhtiari, H. and Neirami, R.; The prevalence of *Pediculus capitis* among School Children in Fars Province, Southern Iran. Tehran Univ. of Medical Sciences Publication. Iranian J. Parasitol.,*4 (2): 48-53.2009.*

[7] Shemshad, V. A.; Shemshad, K.; Sayyadi, M.; Biglarian, A.;Vahabi, B. ;Sayyad, S. ;Shemshad, M. and Rafinejad, J.; *Tropical Biomedicine. 29 (2): 207–211.2012*

[8] Al-Rubaiy, K. K.; Habib, O. S, and Ebrahim S.; Pattern of skin diseases among primary school children in Basrah, southern Iraq. Medical J. of Basrah Univ., *1–2:40–2.2004.*

[9] Khalifa, K. A.; Al-Hadithi, T. S.; Al-Lami, F. H. and Al-Diwan, J. K. ; Prevalence of skin disorders among primary-school children in

Baghdad governorate, Iraq. Health mead east J., *16 (2): 209-213.2007.*

[10] Abolfotouh, M. A. and Bahamadan, K. ; Skin diseases among blind and deaf male students in southwestern Saudi Arabia. Annals of Saudi medicine. *20:161–9.2000.*

[11] Moradi, A. R.; Zahirnia , A. H.; Alipour, A. M. and Eskandari, Z. ;J. of Res. in Health Scie., *9 (1): 48-51.2009*

[12] Sonnberg, S.; Fabíola, A. ; Oliveira; Iana, L.; Araújo, de Me.; Matheus, M. S.; Heiko B.; and Jorg H. . Ex Vivo Development of Eggs from Head Lice (*Pediculus humanus capitis*). The Open Dermatology J., *4, 82-89.2010*

Study for infection rates of Epstein – Barr virus in thyroiditis patients

Abbas Arrak Abbas al-Tamimi[1] and Rushdi Saadi Fadhel
Biology dept., college of science, Al-Mustansiriyah university
Iraqi center for cancer researches and medical genetics / Al-Mustansiriyah university
Received 7/9/2013 – Accepted 12/8/2013

الخلاصة

يعد التهاب الغدة الدرقية في الانسان من الامراض الشائعة ويصنف الى انواع مختلفة حسب نوع العامل المسبب والحالة السريرية والمناعية. تم دراسة دور فايرس Epstein – Barr (EBV) كعامل محتمل للاصابة بالتهاب الغدة الدرقية كون هذا الفايرس يعود لمجموعة Herpesviridae المعروفة بعلاقتها كمسببات لبعض انواع الاورام والاصابات الكامنة. تم التحري في هذه الدراسة عن وجود الاصابة بفايرس EB في اربعة عشر مريض مصابين بالتهاب الغدة الدرقية (من خلال التغير في مستويات هرمونات T3, T4, TSH) وذلك بالكشف عن وجود الاجسام المضادة لبعض مستضدات الفايرس (VCA-IgM, VCA-IgG, EBNA-1 IgG) في عينات الدم الماخوذة من المصابين ومقارنتها مع ثلاثة وثلاثين عينة دم عشوائية ماخوذة من اشخاص ذوو مستويات طبيعية لهرمونات T3, T4, TSH كمجموعة سيطرة. اظهرت الدراسةوجود حالتي اصابة قديمة (14%) بفايرس EB في مرضى التهاب الغدة الدرقية بالمقارنة مع ست حالات موجبة (18%) للاصابة بالفايرس في مجموعة السيطرة بينما كان معدل الاصابة في مجموعتي الاختبار والسيطرة هي 17%.

اظهرت الدراسة عدم وجود فروقات معنوية بين الاشخاص المصابين بالتهاب الغدة الدرقية وغير المصابين وقد يعود ذلك لعدم ظهور اجسام مضادة للمستضد الفايروسي EBNA في بعض المصابين. بناء عليه فان الحاجة الى استخدام عينات نسيجية ماخوذة من الغدة الدرقية واستخدام فحوص اكثر دقة مثل فحص تفاعل انزيم البلمرة PCR ضرورية لتقييم الدور الفعلي لفايرس EB في احداث الاصابة بالتهاب الغدة الدرقية.

ABSTRACT

Human thyroditis is a common inflammatory group of disorders and categorized to different types according to the etiological agents and clinical and immunological status.

In this study, Epstein – Barr virus had been investigated as a possible causative agent of thyroditis since this virus is related to Herpesviridae group there members are known as causative agents of tumors and latent infections.

We investigate of presence of EBV infection in fourteen thyroditis patients (as confirmed by the abnormality in their T3, T4, TSH levels) by detection antibodies against some viral antigens (VCA-IgM, VCA- IgG, EBNA-1 IgG) in patients serum samples matched against thirty three random samples taken from healthy individuals with normal T3, T4, TSH levels as control group.

This study showed the presence of two (14%) EBV past infection in thyroditis patients compared to six (18%) positive cases in control group while the infection rate in the whole cases was 17%. The study showed nonsignificant differences between thyroiditis patients and healthy control which may be attributed to the fail of anti-EBNA antibodies developments in certain patients. Thus, the need for thyroid tissue biopsy and advanced technique such as PCR is necessary to assess the definite role of EBV in the pathogenesis of thyroditis.

INTRODUCTION

Thyroiditis is adisease characterized mostly by thyroid inflammation and include a diverse group of disorders vary in severity between acute illness with severe thyroid pain like subacute thyroiditis and infectious thyroiditis, and conditions in which there is no clinically obvious inflammation manifested primarily by thyroid dysfunction or goiter [1, 2]. These disorders categorized in several ways according to their pathology, or their clinical features, or their known or suspected etiology.

Viral infections are frequently implicated as a major environmental factor involved in subacute thyroiditis and autoimmune thyroid diseases [3].
Subacute thyroiditis is a self-limited inflammatory disorder of the thyroid gland mostly prevalent in females. Clinically the disease has several characteristics typical of viral infections including a typical viral prodrome with myalgias, malaise and fatigue. Recurrent subacute thyroiditis has been reported [2].
The onset of subacute thyroiditis is genetically influenced and it appears that subacute thyroiditis might occur through a susceptibility to viral infection in genetically predisposed individuals since HLA-B35 has been reported to be correlated with chronic active hepatitis, hepatitis B [4], rapid progression of AIDS [5] and T lymphocyte responses against human parvovirus B19 [6]
Virus-like particles were first demonstrated in a patient suffering from subacute thyroiditis thought to be related to influenza B or mumps virus[7, 8].In another study, a cytopathic virus was isolated by co culturing patient samples with susceptible cell lines [9]. The agent was later classified as a paramyxovirus [10].
Subacute thyroiditis has occurred in epidemic form as patients with subacute thyroiditis diagnosed during a mumps epidemic were found to have circulating anti-mumps antibodies even without clinical evidence of mumps [11]. High titers of mumps antibodies have been found in some patients with subacute thyroiditis, and occasionally parotitis or orchitis, usual in mumps, were associated with thyroiditis [12] and some patients with subacute thyroiditis diagnosed during a mumps epidemic, the mumps virus was cultured from thyroid tissue obtained at biopsy [11]. Enteroviruses like coxsackie and adenovirus have also been suspected [13].
Herpesviridae are a large family of DNA viruses that share a common structure and a common characteristic which is latent and re-occurring infections and can cause lytic infections. Elevated titers of antibodies against different herpes virus antigens have been reported in some immunodeficient and systemic autoimmune disorders [14].
Epstein-Barr virus (EBV) is a ubiquitous herpesvirus that is the causative agent of acute infectious mononucleosis and is associated with nasopharyngeal carcinoma, Burkett's lymphoma, Hodgkin and non-Hodgkin lymphomas, other lymphoproliferative disorders in immunodeficient individuals, and gastric carcinoma [15].
The pathogenic role of Epstein-Barr virus in different thyroiditis conditions was controversial. Primary thyroid lymphomas were found in 23 patients in the Hong Kong Chinese population and secondary lymphomas were found in 9 patients. EBV messenger RNAs were detected in one primary and one secondary thyroid lymphoma [16]. In

another study, thirty cases with thyroid lymphoma and 28 with chronic lymphocytic thyroiditis were studied for presence or absence of EBV genome in the lesions, using the polymerase chain reaction (PCR) and the in-situ hybridization method. EBV genomes were detected by PCR in one chronic lymphocytic thyroiditis and two thyroid lymphoma. In-situ hybridization revealed positive signals in the nucleus of lymphoma cells, which also expressed latent membrane protein-1 [17]. EBV- encoded small RNA was detected in three out of thirty two cases of malignant lymphoma of the thyroid by in-situ hybridization and immunohistochemistry in another study [18]. These findings indicate that EBV implication in thyroid lymphoma is possible but not common.

The aim of this study was to investigate the frequency of Epstein - Barr virus infection in patients with uncategorized hypothyroidism to assess the role of EBV in establishing thyroditis disease.

MATERIALS AND METHODS

Fourteen patients (ages between 37 to 70 years) with hypothyroidism, as confirmed with low T3, T4,and/or high TSH levels using ELISA kit (T4, T3, TSH AccuLite CLIA Rev 3, Monobind Inc.), were tested in this study for the presence of Epstein – Barr virus infection markers (VCA-IgM, VCA- IgG, EBNA-1 IgG) using ELISA kit (Diagnostic automation, CORTEZ diagnostics Inc.) against thirty three persons (ages between 12 to 70 years) with normal T3, T4, and TSH levels as control.

Interpretation of the results was as follows: Samples with positive VCA-IgM test considered current EBV infection, VCA-IgG and/ or EBNA-1IgG positive considered past infection. The frequency of EBV infection was calculated for thyroditis patients and control. Results subjected for statistical analysis using spss software (version17).

RESULTS AND DISCUSSION

Identifying etiological infections in human disease is difficult. Besides the fact that organ tissue is not always available for direct study, the interpretation of virological data must be cautious. The presence of antibodies directed towards a virus does not prove that this pathogen is responsible for the disease, especially when the agent is common in the general population. On the other hand, the absence of viral markers at the onset of the disease does not refute the viral hypothesis. Indeed the triggering infection can take place many years previously [3].

This study revealed that ten out of fourteen thyroiditis patients were females (70%) as shown in table (1). This percentage is concordant with the fact that thyroiditis is more common in females than males [19]. The age of thyroditis patients ranges between thirty seven to seventy years as this disease mostly triggered in adults [19]. It is noteworthy to mention that thyroditis cases in this study are not classified to the specific types of

the disease since the classification requires specific tests and specialists in this type of diseases.

Table- 1: Thyroiditis patients and control cases distributed on age and sex parameters.

subject	No.	Ages (yrs)	sex		EBV marker positive
			male	female	
Patients	14	37 - 70	4	10	2
control	33	12 - 70	11	22	6

The study showed that two out of fourteen (14%) thyroiditis patients have been infected with EBV (past infections, since both samples showed VCA-IgM negative and VCA-IgG and EBNA-1 IgG positive) whereas six out of thirty three (18%) of control samples were positively reacted for EBV markers (one current infection and five past infections) as shown in table- 2.

Table- 2: Thyroiditis patients and control cases distributed by EBV markers.

subject	VCA-IgM	VCA-IgG	EBNA-1-IgG
patient		+	+
		+	+
control		+	+
	+		
		+	+
			+
			+
			+

EBV infections are thought to be worldwide distributed and the virus is thought to infect people at younger ages in developing countries whereas it mostly infect adults in developed ones [15]. This study revealed that the frequency of EBV infection is considerably low (the percentage of the total number of the cases was 17%) in comparison to the data recorded for general populations [15] and all the infections were found in females. one reason to explain the difference is that not all persons develop antibody to EBNA [15].

There are many studies showed an association between EBV infection and autoimmune thyroditis [20, 21] and with subacute thyroditis [22] and a Case report have implicated EBV in a 3-year-old girl suffering from infectious mononucleosis because of the presence of EBV DNA both in plasma and leukocytes [23]. However, when thyroid specimens of patients obtained by fine-needle aspiration biopsy were examined, no EBV DNA was detected [24]. However, it remains to determine whether they are responsible for thyroid diseases or whether they are just innocent bystanders.

A viral disease is the result of an interaction between a virus and the host, in which the genetic background plays a role. Therefore, it cannot be

excluded that a virus plays a role in a disease even though most infected individuals do not show any sign of disease. Further studies using tissue biopsy and more accurate tests like polymerase chain reaction are needed to clarify the relationship between EBV and thyroid diseases, in order to develop strategies for their prevention and/or treatment.

REFERENCES

1- Lazarus JH. Silent thyroiditis and subacute thyroiditis. In: The thyroid: A fundamental and clinical text, 7th, Braverman LE, Utiger RD (Eds), p.577, 1996, Lippincott-Raven, Philadelphia.
2- Pearce EN, Farwell AP, Braverman LE. Thyroiditis. N Engl J Med, 348(26):2646 (2003).
3- Rachel Desailloud and Didier Hober. Viruses and thyroiditis: an update Virol J, 6: 5 (2009).
4- Kacprzak-Bergman I, Nowakowska B. Influence of genetic factors on the susceptibility to HBV infection, its clinical pictures, and responsiveness to HBV vaccination. Arch Immunol Ther Exp (Warsz), 53:139–142 (2005) [PubMed]
5- Roger M. Influence of host genes on HIV-1 disease progression. Faseb J., 12:625–632 (1998)[PubMed]
6- Klenerman P, Tolfvenstam T, Price DA, Nixon DF, Broliden K, Oxenius A. T lymphocyte responses against human parvovirus B19: small virus, big response. Pathol Biol (Paris), 50:317–325. (2002) [PubMed]
7- Sato M. Virus-like particles in the follicular epithelium of the thyroid from a patient with subacute thyroiditis (de Quervain's) Acta Pathol Jpn., 25:499–501 (1975) [PubMed]
8- Joasoo A, Robertson P, Murray IP. Letter: Viral antibodies in thyrotoxicosis. Lancet, 2:125. (1975)[PubMed]
9- Stancek D, Stancekova-Gressnerova M, Janotka M, Hnilica P, Oravec D. Isolation and some serological and epidemiological data on the viruses recovered from patients with subacute thyroiditis de Quervain. Med Microbiol Immunol., 161:133–144. (1975)[PubMed]
10- Stancek D, Ciampor F, Mucha V, Hnilica P, Stancekova M. Morphological, cytological and biological observations on viruses isolated from patients with subacute thyroiditis de Quervain.Acta Virol., 20:183–188. (1976) [PubMed]
11- Eylan E, Zmucky RCS. Mumps virus and subacute thyroiditis. Evidence of a causal association. Lancet, 272:1062–1067. (1975) [PubMed]
12- Parmar RC, Bavdekar SB, Sahu DR, Warke S, Kamat JR. Thyroiditis as a presenting feature of mumps. Pediatr Infect D., 20:637–638. (2001) [PubMed]

13- Volpe R, Row VV, Ezrin C. Circulating viral and thyroid antibodies in subacute thyroiditis. J Clin Endocrinol Metab., 27:1275–1284. (1967) [PubMed]

14- Thomas D, Karachaliou F, Kallergi K, Vlachopapadopoulou E, et al. Herpes virus antibodies seroprevalence in children with autoimmune thyroid disease. Endocrine., Apr; 33(2):171-5. (2008).

15- Brooks G. F., Carroll K. C., Butel J. S., Morse S. A.: Jawetz, Melnick, & Adelberg's Medical Microbiology.25th ed. Chapter 33, Herpesviruses, 2007, The McGraw-Hill Companies.

16- Lam KY, Lo CY, Kwong DL, Lee J, Srivastava G. Malignant lymphoma of the thyroid. A 30-year clinicopathologic experience and an evaluation of the presence of Epstein-Barr virus. Am J Clin Pathol., 112:263–270. (1999)[PubMed]

17- Tomita Y, Ohsawa M, Kanno H, Matsuzuka F, Kuma K, Aozasa K. Sporadic activation of Epstein-Barr virus in thyroid lymphoma. Leuk Lymphoma, 19:129–134. (1995) [PubMed]

18- Takahashi K, Kashima K, Daa T, Yokoyama S, Nakayama I, Noguchi S. Contribution of Epstein-Barr virus to development of malignant lymphoma of the thyroid. Pathol Int., 45:366–374. (1995) [PubMed]

19- http://emedicine.medscape.com/article/125648-overview

20- Vrbikova J, Janatkova I, Zamrazil V, Tomiska F, Fucikova T. Epstein-Barr virus serology in patients with autoimmune thyroiditis. Exp Clin Endocrinol Diabetes, 104:89–92. (1996) [PubMed]

21- Shimon I, Pariente C, Shlomo-David J, Grossman Z, Sack J. Transient elevation of triiodothyronine caused by triiodothyronine autoantibody associated with acute Epstein-Barr-virus infection. Thyroid, 13:211–215. (2003) [PubMed]

22- Espino Montoro A, Medina Perez M, Gonzalez Martin MC, Asencio Marchante R, Lopez Chozas J. Subacute thyroiditis associated with positive antibodies to the Epstein-Barr virus. An Med Interna., 17:546–548. (2000) [PubMed]

23- Volta C, Carano N, Street ME, Bernasconi S. Atypical subacute thyroiditis caused by Epstein-Barr virus infection in a three-year-old girl. Thyroid, 15:1189–1190. (2005) [PubMed]

24- Mori K, Yoshida K, Funato T, Ishii T, Nomura T, Fukuzawa H, Sayama N, Hori H, Ito S, Sasaki T: Failure in detection of Epstein-Barr virus and cytomegalovirus in specimen obtained by fine needle aspiration biopsy of thyroid in patients with subacute thyroiditis. Tohoku J Exp Med., 186:13-17 (1998).

Isolation And Identification Of Fungi Associated With Roots Of Three Plants Species Infected With Root Knot Nematode And Evaluation Their Efficiency Of Parasitism On Eggs Of *Meloidogyne Javanica* In Wasit Province

Saja Hussain Dilfi[1], Mohammed Jubair Hanawi[2], Hadi Mahdi Aboud[3]
[1,2] Wasit University - Collage of Science - Department of Biology.
[3] Ministry of Science and Technology - Directorate of Agriculture Research - Dept. of biotechnology.
Received 16/9/2013 – Accepted 21/1/2014

الخلاصة

نفذت دراسة مختبرية لتقييم كفاءة بعض الفطريات المعزولة من تربة الرايزوسفير المحيطة بجذور بعض أنواع النباتات في محافظة واسط كعوامل مكافحة أحيائية ضد نيماتود العقد الجذرية *Meloidogyne javanica* . جميع الفطريات عزلت من تربة الرايزوسفير المحيطة بجذورالنباتات (الباميا ، الخيار والباذنجان) المصابة بنيماتود العقد الجذرية وفي ثلاث مناطق هي الأحرار ومركز المحافظة وشيخ سعد . أظهرت النتائج بأن 17 نوع من الفطريات عائدة لعشرة أجناس تم عزلها من تربة الرايزوسفير المحيطة بجذور الباميا في منطقة الأحرار ، و16 نوع عائدة لـ 11 جنس من جذور الخيار في مركز المحافظة ، و13 نوع عائدة لعشرة أجناس من جذور الباذنجان في منطقة شيخ سعد .

الفطريات التي أظهرت أعلى تكراراً في العزل هي الفطريات *Aspergillus* و *Fusarium* في منطقة الأحرار والفطريات *Cladosporium* و *Fusarium* في مركز المحافظة و الفطريات *Aspergillus* و *Fusarium* و *Trichoderma* في منطقة شيخ سعد .

الفطر *Verticellium lecanii* كان أكثر الفطريات كفاءة في التطفل على بيوض النيماتود *M.javanica* وبنسبة تطفل 83.57 % ويعد هذا التسجيل الأول لهذا الفطر على هذه النيماتود في العراق يليه في ذلك كل من الفطر *Paecilomyces lilacinus* والفطر *Trichoderma harzianum* بنسبة تطفل 69.02 % و 68.06 % على التوالي . الفطريات *Aspergillus terrus* و *Rhizopus* sp أظهرت أقل كفاءة وبنسبة تطفل 6.44% و 2 % على التوالي .

ABSTRACT

A laboratory experiment was conducted to evaluate the efficiency of some fungi that isolated from rhizosphere associated with roots of certain plants species in Wasit city, as biocontrol agents against the root-knot nematode, *Meloidogyne javanica*. All fungi isolated from rhizosphere soil around the roots of plants (okra, cucumber and eggplant) infected with root knot nematode in Al-Ahrar, Wasit center and Sheikh Saad locations respectively .The results showed that 17 species of fungi belonging to 10 genera were isolated from the rhizosphere soil of Okra roots, 16 species of fungi belonging to 11 genera were isolated from cucumber roots whereas 13 species of fungi belonging to ten genera were isolated from eggplant roots.

Genera that presented higher frequency were *Aspergillus* and *Fusarium* in Al-Ahrar area *Fusarium, Cladosporium* in Wasit center whereas *Aspergillus*, *Fusarium* and *Trichoderma* in Sheikh Saad location.

Verticellium lecanii was the most vigour fungus for eggs and the percent of parasitism was 83.57 %, and this is the first record of *V. lecanii* on *M. javanica* in Iraq, followed by the fungi *Paecilomyces lilacinus* 69.02 % and *Trichoderma harzianum* 68.06 %. *Aspergillus terrus* and *Rhizopus* sp exhibited lowest activity and the percent of parasitism were 6.44 %, 2 % respectively.

Key Words: Root knot nematode, Meloidogyne javanica, Biocontrol, Fungi, Rhizosphere

INTRODUCTION

The term Rhizosphere is defined as the soil volume adjacent to the roots and influenced by them [1], and represents an area of intense microbial activity [2], in which the organic nutrients coming from the roots favour the development of microorganisms [3].This environment is allocation for the activity of many beneficial microorganism in general and fungi especially [4].Plant-parasitic nematodes obligatorily feed on plant tissue. The root-knot nematodes (*Meloidogyne* spp.) are sedentary endoparasites and are among the most damaging agricultural pests. They cause serious damage to many crops worldwide. Their damages have exceeded $10 billion per year in the United States [5]. According to [6] more than 90 species have been described. Species such as *Meloidogyne javanica* and *Meloidogyne incognita* are among the major limiting factors in the production of field and plantation crops [7].

Due to the ban of many nematicides, the development of new and nonhazardous control methods is of vital importance. Biological control using antagonistic microorganisms, alone or in combination with other control methods in integrated pest management programs, may be a possible solution. Outlines of such control strategies have been suggested by several authors [8], [9], [10]. In recent years, fungi, one of the natural enemies of nematodes, have been proposed as biological agents to control the harmful nematodes because of their unique ability to infect and kill the nematodes [11], [12].

Fungi directly parasitize nematodes or secrete nematicidal metabolites affecting viability of one or more stages [13]. This group includes more than 150 species [14]. Root-knot nematodes feed in or on plant roots, and therefore we hypothesize that the activity of the biological control agent in the rhizosphere of the crop plants should enhance control. One can expect that rhizosphere colonization by nematode-trapping fungi will differ not only according to target plant species but also to fungal species and isolates. So we aimed in this study to isolation, identification and evaluation the nematode egg parasitism efficiency of fungi associated with rhizosphere of three plants species (Okra, Cucumber and Eggplant) infected with root knot nematode in Wasit province.

MATERIALS AND METHODS

Laboratory experiments were carried out to determine the effectiveness of some fungal species as biocontrol agents against *Meloidogyne javanica.*

Sampling collection

Soil samples were collected from three locations at Wasit province namely: Al-Ahrar, Kut Center and Sheikh Saad. Samples were randomly

collected from the rhizosphere of soil surrounding the roots of okra, cucumber and eggplant infected with root –knot nematode *Meloidogyne javanica*. Samples were subjected to sequence processes for fungi isolation, purification, culturing and identification. .

Fungal isolation:

Isolation of fungi from infected plants roots rhizosphere was done by using spread plate method [15]. In this technique, the air dried soil samples were ground with a mortar and pestle and mixed thoroughly. 25 g sub sample of rhizosphere soil were suspended in 250 ml of sterile distilled water in a bottle, which gave a dilution of 1:10. From that sample, 10 ml of suspension was transferred to a second bottle containing 90 ml of water to give a dilution of 1:100 and mixed well. This step was repeated to give up to $1:10^6$ dilutions. 1 ml of soil suspension from each of $1:10^3$ and $1:10^6$ dilutions was dispersed across PDA medium supplemented with 100 ppm Gentamycin in a 90 mm diameter Petri dish. The plates were incubated at 25 °C for 7 days in an incubator and were observed on daily basis. . The number of colonies that developed at the end of incubation was counted [16].Fungal colony which developed from each soil dilutions was purified on PDA slants and all isolated fungal species were preliminarily identified using the morphologic keys [17] [18] [19] and fungal species were characterized and identified microscopically.The frequency distribution (percent) of fungi isolated from rhizosphere was calculated using the following equation [20].

$$\text{Isolation frequency} = \frac{\text{Number of fungal colonies}}{\text{Total number of colonies}} \times 100$$

Approximately 50 egg masses, hand-picked from RKN infested roots by fine forceps, were surface sterilized in 1:5 (V/V) aqueous solution of "chlorax" (sodium hypochlorite) for 5 min. After the debris were allowed to settle from the suspension for 30 s, the eggs in suspension were pipetted onto an autoclaved 500-mesh sieve (pore size 25 µm) and washed four times with sterile distilled water (SDW) during 5 min and used directly for the assay, after removal of an aliquot for counting and estimated number by counting chamber [21].

Egg inoculum preparation

Approximately 50 egg masses, hand-picked from RKN infected roots by fine forceps, were surface sterilized with 1% NaOCl. After the debris were allowed to settle from the suspension for 30 s, the eggs in suspension were pipetted onto a sieve 25 µm and washed four times with sterile distilled water during 5 min and used directly for the assay, after removal of an aliquot for counting and estimated number by counting slide.

Fungal parasitism of eggs:

One ml of egg inoculum containing approximately 2000 eggs of *M. javanica* estimated by counting slide were placed on water agar and 0.5 mm disc of 7days (PDA) old culture of each tested fungus was placed in contact with egg . Infection of eggs was monitored microscopically after 3,7,10 days in randomly selected infected eggs using 4 x magnifications, Eggs developing fungal colonies and morphological changing in the eggs were scored as infected and the percentage of egg infection was then calculated using the following equation [22].

$$\% \text{ Percentage of eggs parasitism} = \frac{\text{Mean number of infected eggs in microscopic field}}{\text{Mean number of total eggs in microscopic field}} \times 100$$

RESULTS AND DISCUSSION

Results of isolation of fungi from Rhizosphere of roots infected with *Meloidogyne javanica* from three locations in Wasit province (Al-Ahrar , Kut center and Sheikh Saad) showed that there is 17 species of fungi belonging to 10 genera were isolated from the rhizosphere soil of Okra roots in Al-Ahrar area (table 1) . All fungi were representatives of Deuteromycota. *Aspergillus niger* occurred with much higher frequency (20.481%) and then *Aspergillus flavus, Fusarium graminirerium with* frequency 13.253% , 12.0481% respectively.while the fungi *Rhizopus sp., Rhizoctonia sp.* occurred with much lower frequency (1.204%).

The study indicated also that the testing fungi have variable potent parasitism against *M. javanica* eggs, and that the fungi *Aspergillus* sp. , *Fusarium* spp *and Cladosporium* sp were the most effective fungi against *M. javanica* eggs , while the other fungi had no or little effect against eggs , and the highest percentage of parasitism was 58.06% in the case of *Aspergillus falcatum* followed by *Fusarium graminearum* and *Cladosporium* sp. which was 25.28% , 23.89 respectively , while the lowest percentage of parasitism was 1% in the case of *Rhizopus* sp.

Table-1- Frequency distribution (percent) of fungi isolated from rhizosphere of Okra roots infected with *M. javanica* at Al-Ahrar area and its parasitic efficacy:-

No.	Fungi	Isolation frequency %*	*Eggs parasitism%
1	*Aspergillus niger*	20.481	9.30
2	*Aspergillus flavus*	13.253	17.02
3	*Fusarium graminearum*	12.048	25.28
4	*Penicillium Sp.*	9.638	17.50
5	*Cylindrocarpon Sp.*	8.433	7.30
6	*Cladosporium Sp.*	7.228	23.89
7	*Alternaria alternata*	6.024	8.21
8	*Fusarium oxysporium*	4.819	25.34
9	*Fusarium solanii*	4.819	25.29
10	*Aspergillus falcatum*	4.819	58.06
11	*Aspergillus terreus*	3.614	6.44
12	*Curvularia lunata*	2.409	8.68
13	*Fusarium Sp.*	2.409	25.38
14	*Drechslera australiensis*	1.204	8.56
15	*Aspergillus fumigatus*	1.204	17.04
16	*Rhizopus sp.*	1.204	2
17	*Rhizoctonia sp.*	1.204	7.62
L.S.D(0.05)			1.736

$$\text{* Isolation frequency} = \frac{\text{Number of fungal colonies}}{\text{Total number of colonies}} \times 100$$

* Eggs parasitism:-The mean number of twenty records each record express the number of parasitized egg in microscopic field (x40) to total number of the eggs in the field.

Results also showed that there is 16 species of fungi belonging to 11 genera were isolated from the rhizosphere soil of cucumber roots in Wasit center (table 2).Most were representatives of Deuteromycota, although members of Oomycota were also recorded. *Fusarium graminearum* occurred with much higher frequency (19.512%) and then *Cladosporium Sp., Fusarium solani with* frequency 15.853% , 12.195% respectively . while the Genera *Drechlera , Verticellium , Stachybotrys and Mycellus* occurred with much lower frequency (2.439 %) in this area .

It is evident from the table that all fungi revealed capability to parasitize egg of *Meloidogyne* but the most effective one was *Verticellium lecanii* with percent of parasitism 83.57% followed by Mycellus strella and *Fusarium oxysporium* with percent of parasitism 49.73% , 25.58% respectively .

Table -2: Frequency distribution (percent) of fungi isolated from rhizosphere of cucumber roots infected with *M. javanica* at Wasit center location and its parasitic efficacy:-

No.	Fungi	Isolation frequency %	Eggs parasitism %
1	*Fusarium graminearum*	19.512	25.35
2	*Cladosporium Sp.*	15.853	23.80
3	*Fusarium solani*	12.195	25.48
4	*Pythium Sp.*	7.317	4.97
5	*Phytophthora Sp.*	6.097	20
6	*Aspergillus niger*	4.878	18.60
7	*Pencillium Sp.*	4.878	17.50
8	*Aspergillus terreus*	4.878	18.46
9	*Aspergillus flavus*	3.658	17.03
10	*Fusarium oxysporium*	3.658	25.58
11	*Cylindrocarpon Sp.*	3.658	5.23
12	*Fusarium tricinctum*	3.658	25.38
13	*Drechslera australiensis*	2.439	8.64
14	*Verticillium lecanii*	2.439	83.57
15	*Stachybotrys sp.*	2.439	6.69
16	Mycellus strella	2.439	49.73
L.S.D(0.05)			1.737

Finally results had been revealed that there is 13 species of fungi belonging to 10 genera were isolated by direct plating and serial dilution techniques from the rhizosphere soil of eggplant roots in Sheikh Saad location (table3). Most were representatives of Deuteromycota, although members of Ascomycota were also recorded. *Fusarium Sp.*, *Aspergillus terreus* and *Trichoderma harzianum* were predominant in the rhizosphere soil of eggplant roots at Sheikh Saad location and the percentages of frequency were 29.411%, 23.529% and 17.647% respectively, while *Aspergillus flavus* , *Rhizoctonia sp.*and *Cladosporium* sp. were not common in this rhizosphere and the percentage of frequency was 1.176%.

Parasitism of *M. javanica* eggs by fungi is shown in (table 3). The results showed that the fungus *Paecilomyces lilacinus* was the more effective one in this location and the percentage of infected eggs was 69.02%, followed by the fungi *Trichoderma harzianum*, *Aspergillus falcatum* which were 68.06%, 58.02% respectively.

Table -3:Frequency distribution (percent) of fungi isolated from rhizosphere of eggplant roots infected with *M. javanica* at Sheikh Saad location and its parasitic efficacy:-

No.	Fungi	Isolation frequency %	Eggs parasitism %
1	*Fusarium Sp.*	29.411	25.37
2	*Aspergillus terreus*	23.529	18.46
3	*Trichoderma harzianum*	17.647	68.06
4	*Alternaria alternata*	8.235	8.16
5	*Aspergillus falcatum*	4.705	58.02
6	*Pencillium Sp.*	3.529	17.44
7	*Drechlera australiensis*	2.352	8.70
8	*Paecilomyces lilacinus*	2.352	69.02
9	*Botrytis sp.*	2.352	38.13
10	*Aspergillus niger*	2.352	9.16
11	*Aspergillus flavus*	1.176	17.09
12	*Rhizoctonia sp.*	1.176	7.54
13	*Cladosporium Sp.*	1.176	23.75
L.S.D.(0.05)			**1.712**

In general, the fungi that isolated from all three locations varied widely in its distribution and frequency. The fungi *Aspergillus* spp, *Fusarium* spp, *Drechlera australiensis* and *Pencillium* sp. Were isolated from all locations in Wasit city while the fungi *Trichoderma harzianum* and *Paecilomyces lilacinus* were isolated only from Sheikh Saad location and *Verticillium lecanii* from Wasit center.

The fungi also varied widely in virulence (Figures 1,2,3,) but *V. lecanii* tended to be more virulent than the other fungi isolated from all three locations in Wasit city against *M. javanica* eggs (This is the first record of *V. lecanii* on *M. javanica* in Iraq), followed by *P. lilacinus* , *T. harzianum* and *A. falcatum.*

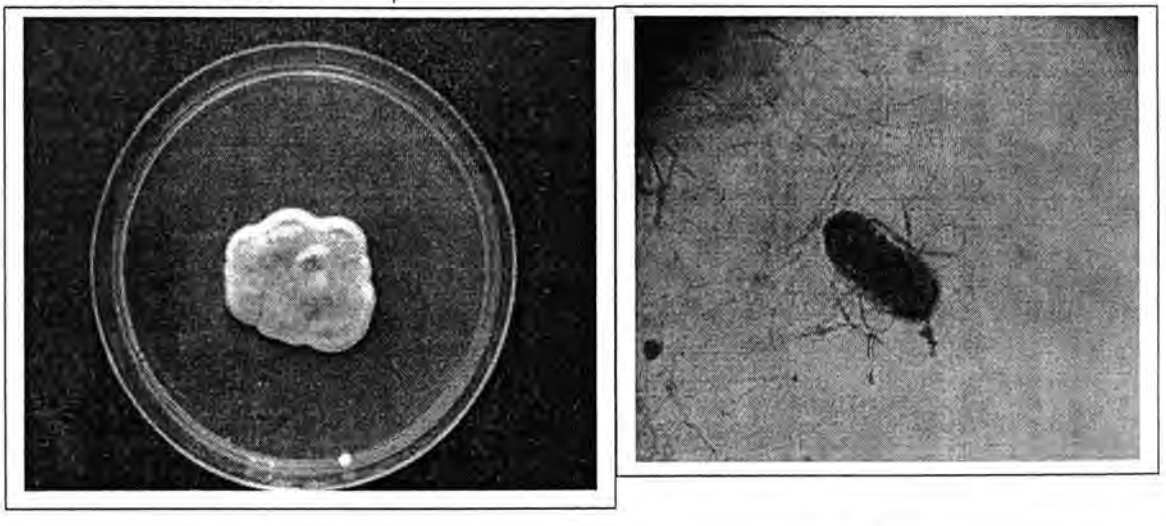

A **B**

Figure -1: *Paecilomyces lilacinus* (A) Fungal culture (B) Egg parasitism

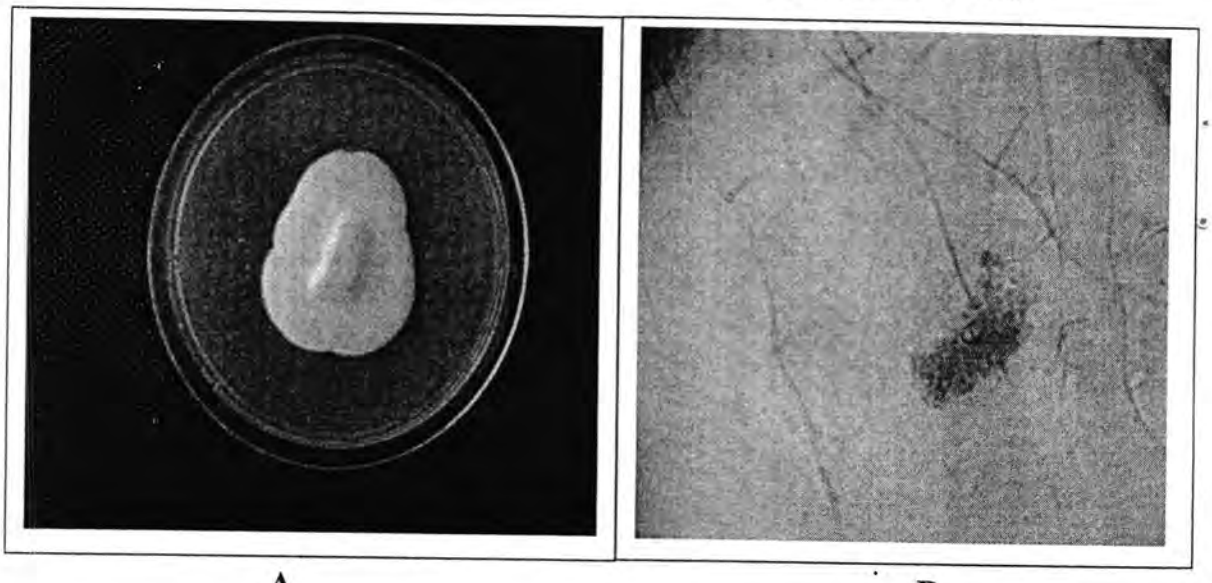

A B

Figure -2:*Verticellium lecanii* (A) Fungal culture (B) Egg parasitism

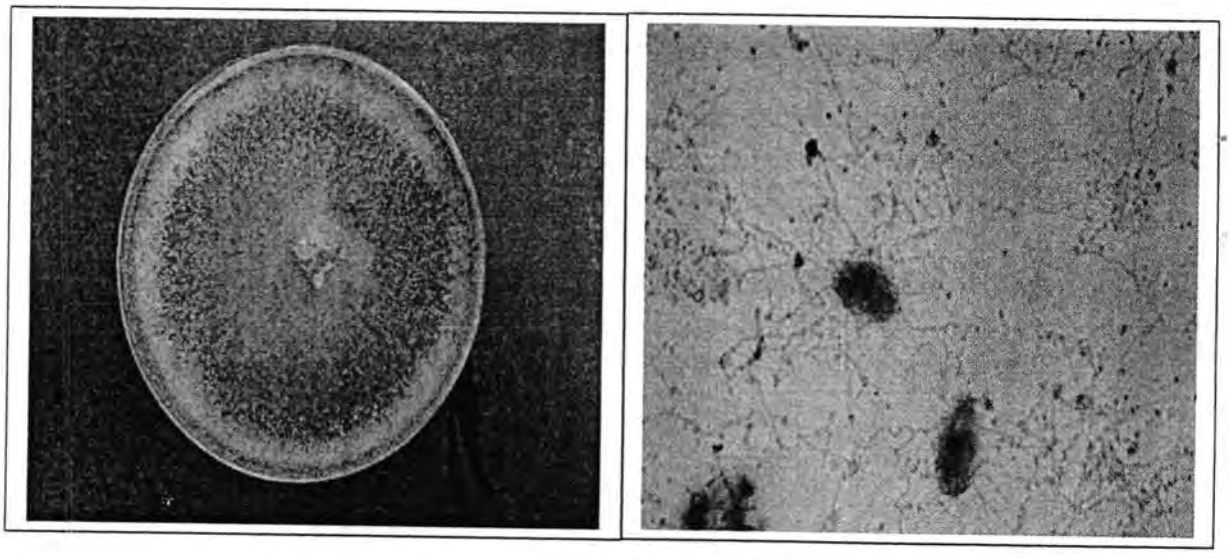

A B

Figure-3:*Trichoderma harzianum* (A)Fungal culture (B) egg parasitism

Qualitative as well as quantitative distribution of fungi in the rhizosphere is because of that the rhizosphere is a region around plant roots where simple sugars, amino acids and many other compounds are exuded by the plant and are available to the microorganisms , these components of rhizosphere variable according to the plant species , soil characters and environment , so the quantity and quality of fungi that isolated from Al-Ahrar , Kut center and Sheikh Saad areas are variable .

The relatively high frequency of *Aspergillus* spp , *Fusarium* spp , *Cladosporium* sp., *Trichoderma* sp among the other isolated fungi, indicated its high abundance near or on tested plants roots, or they are common components of the soil mycoflora.

Similar results have been reported by Oyeyiola, [23]; who refer that *genera Aspergillus*, *Penicillium*, *Rhizopus* , *Alternaria* were predominant in rhizosphere soil of Okra plants and the age of plant affect the rhizosphere components .

The result had been revealed that the testing fungi have variable potent parasitism against *M. javanica* eggs. This is mainly related to the fungi characters and mechanical force which enable fungi to penetrate egg cell wall; besides production of lytic enzymes. *Verticellium lecanii* was the most vigour fungus for eggs and the percent of parasitism was 83.5926%, followed by the fungi *Paecilomyces lilacinus* 69.0361% and *Trichoderma harzianum* 68.0272% .The efficiency of egg parasitism of *verticillium* may be related to the nematicidal action of certain enzymes [24] and toxins like Verticillin A, B and C [25] which help in weakening and dissolving the barriers of its hosts. A number of nematophagous fungi are known to have proteolytic and chitinolytic activities which cause alteration in eggs' cuticular structure, changes in egg shell permeability or cause perforations in the cuticle which allows seepage of toxic metabolites into the eggs and cause physiological disorders [24] [26]. These factors may have important role in the inhibition of egg hatch. Moreover *V. chlamydosporium* produces a subtilisin, which breaks down the outer membrane of the egg shell and exposes the chitin layer of root-knot nematode eggs [27]. Lopez-Llorca and Robertson [28] reported the secretion of a serine protease designated P-32, produced by *V. chlamydosporium* during infection of nematode eggs. Recent study indicated that Tikhonov *et al.* [29] purified and characterized chitinases from fungal-egg parasites *Verticillium chlamydosporium* and *V. suchlasporium*.

Paecilomyces lilacinus and *Trichoderma harzianum* also exhibited highly parasitic capabilities on eggs that may be due to the sufficient chitinolytic activities of these fungi. Production of chitinase and protease in these fungi has been studied and its involvement in fungal parasitism has been shown by several studies.

Cayrol *et al.* [30] reported toxin production by *P. lilacinus* against 17 species of nematodes, and this fungus can produce toxins called paecilotoxins and hydrolytic enzymes such as polysaccharidases, proteases , chitinases and leucinostatins [31] [32] [33].

The obtained results are in accordance with Khan *et al.* [32] who proof that, hatching of *M. javanica* eggs were reduced as a result of *Paecilomyces lilacinus* protease and chitinase enzymes, either

individually or in combination. They demonstrated the major changes in the egg shell structure as; lipid layer was destroyed, the chitin layer hydrolyzed and the vitelline layer had lost integrity.

The result also are in accordance with the study of Olivares-Bernabeu and Lopéz-Llorca [34] who found that the pathogenicity of egg infection by *Verticillium* sp and *paecilomyces lilacinus* was 70-100% and the severity of the penetrating hyphae/egg was 35-40%.

Similar study indicates that *Trichoderma viride* was the most effective species followed by *Aspergillus niger* and *Fusarium* sp. in parasitizing nematode eggs. Such species could cease egg embryogenesis or deplete egg content [35].

Other fungi like *Cylindrocarbon* sp, *Rhizopus* sp , *Stachybotrys* sp. *Rhizoctonia* sp.exhibited lower efficiency for parasitism of eggs , that probably because of its insufficient chitinolytic activities of these fungi.

REFERENCES

1. Metting, B. F. (1993) Soil microbial ecology. Marcel Dekker, Nova Iorque, 382P.
2. Westover, K. M.; Kennedy, A. C.; Kelley, S. E. (1997) patterns of rhizosphere microbial community structure associated with co-occuring plant species .J . Ecol., 85:863- 873.
3. Lynch, J. M. (1990) Introduction: some consequences of microbe rhizosphere for plant and soil .In :Cur , E.A.; Truelove , B. The rhizosphere Springer verlage .New York ,1986 ,p.1-10.
4. Bais, H. P.; Weir,T. L.; Perry, L.G.; Gilroy, S. and Vivanco, J. M. (2006)The role of root exudates in rhizosphere interactions with plants and other organisms. Annu.Rev. Plant Biol., 57:233-266.
5. Koenning, S. R.; Overstreet, C. and Noling, J. W. (1999) Survey of crop losses in response to phytoparasitic nematodes in the United States for 1994. J. Nem.31: 587-618.
6. Wesemael, W. M. L.; Viaene, N. and Moens, M. (2011) Root-knot nematode (*Meloidogyne spp.*) in Europe. Nematology .13, 3-16.
7. Sharon, E.; Chet, A.; Viterbo, A.; Bar-Eyal, M.; Nagan, H.; Samuels, G. J. and Spiegel, Y. (2007) Parasitism of *Trichoderma* on *Meloidogyne javanica* and role of the gelatinous matrix. EUR. J. Plant pathol.,118 : 247 -258 .
8. Kerry, B. R. (1987) Biological control. Pp. 233–263 in R. H. Brown and B. R. Kerry,eds. Principles and practice of nematode control in crops. Marrickville, Australia:Academic Press.
9. Stirling, G. R. (1988) Biological control of plant parasitic nematodes. Pp. 93–139 in G. O. Poinar, Jr.,and H.-B. Jansson, eds. Diseases of nematodes, vol. 2. Boca Raton, FL: CRC Press Inc .

10. Stirling, G. R. (1991) Biological Control of Plant Parasitic Nematode: Progress، Problems and Prospects. Wallingford,UK .CAB International.
11. Siddiqui, Z. A. and Mahmood, I. (1996) Biological control of plant parasitic nematodes by fungi: a review. Biores Technol 58:229–239.
12. Nordbring-Hertz, B., Jansson, H. B. and Tunlid, A. (2002) Nematophagous fungi. Encyclopedia of Life Science 12: 681-690.
13. Lopez-Llorca L. V. and Jansson H. B. (2006) Fungal parasites of invertebrates: multimodal biocontrol agents. In: Robson, G.D., van West, P., Gadd, G.M. (eds) Exploitation of Fungi. Cambridge University Press,Cambridge, Pp. 310–335.
14. Barron, G. L. (1977) The nematode-destroying fungi. Topics in mycobiology No. 1. Guelph, Canada: Canadian Biological Publications.
15. Pelczar, M. J., Chan E .C .S. and Krieg, N. R. (2005) Microbiology. 5th Edition, Tata Mc Graw Hill Publishing Company Ltd., New Delhi. pp. 333- 364 Robert, L. T. (1995). Soil Microbiology, John Wiley and Sons, inc., New Jersey. 398pp.
16. Roger, S and Dean, B. (2005) Management of Plant pathogenic collection, Department of Agriculture Fisheries and Forestry, Australian Government .
17. Barnett, H. L. (1960) Illustrated genera of Imperfect fungi. 2nd Ed. Burgess Pub. Company. 225pp .
18. Booth, C. (1977) The Genus *Fusarium* CMI, Kew, Survey, England.
19. Ellis, M. B. (1971) More Dematiaceus Hypomycetes. CMI, Kew, Survey, England. 507pp.
20. Dubey, R. C. and Maheshwari, D. K. (2005) Practical microbiology. S. Chand and Company Ltd., New Delhi. 352pp.
21. Den Ouden, H. (1958) A new method for culturing plants enabling observation of nematodes on growing roots. Netherlands Journal of Plant Pathology 64: 269–272.
22. Aboud, H. and Fattah, F. A. (1989) The effect of *Trichoderma* isolates plant growth parameters and Parasitism of nematode eggs. Intentional Symposium on Biological control .Antalyla-Turkey.p:59-65
23. Oyeyiola, G. P. (2009) Rhizosphere mycoflora of Okro (*Hibiscus esculentus* . Research Journal of Soil Biology.1(1): 31 -36.
24. Webb, H. M.; Ghafoor, A. and Heale, J. B. (1972) Protein and enzyme patterns in strains of *Verticillium*. Trans. Brit. Mycol., Soc. 59: 393–402 .
25. Minato, H., Matsumoto, M. and Katayama, T.(1973) Studies on the metabolites of *Verticillium* sp. structure of verticillins A, B and C.

Chem. Comm.,: 1819–25 . Metting ,B.F. Soil microbial ecology – Marcel Dekker ,Nova Iorque,1993,382 P.

26. Lopez-Llorca, L. V. (1990) Purification and properties of extracellular proteases produced by the nematophagous fungus *Verticillium suchlasporium*. Canadian J. Microbiol., 36: 530–7.
27. Segers, R.; Butt, T. M.; Kerry, B. R. and Peberdy, J. F. (1994) The nematophagous fungus *Verticillium chlamydosporium* produces a chymoelastase-like protease that hydrolyses host nematode proteins in situ. Microbiol.,140: 2715–23.
28. Lopez-Llorca, L. V. and Robertson, W. M. (1992) Immuno-cytochemical localization of a 32-k Da protease from the nematophagous fungus *Verticillium suchlasporium* in infected nematode eggs. Exp. Mycol.,16: 261–7 .
29. Tikhonov, V. E.; López-Llorca, L. V.; Salinas, J. and Jansson, H. B. (2002). Purification and characterization of chitinases from the nematophagous fungi *Verticillium chlamydosporium* and *V. suchlasporium*. Fungal Genetics and Biology 35: 67 – 78.
30. Cayrol, J.-C.; Djian, C. and Pijarowski, L. (1989) Study of the nematicidal properties of the culture filtrate of the nematophagous fungus *Paecilomyces lilacinus*. Revue de Nématologie 12:331-336.
31. Gupta, S. C.; Leathers, T. D. and Wicklow, D. T. (1993) Hydrolytic enzymes secreted by *Paecilomyces lilacinus* cultured on sclerotia of *Aspergillus flavus*. Applied Microbiology and Biotechnology 39: 99 - 103.
32. Khan, A.; Williams, K. L. and Nevalainen, H. K. M. (2004) Effects of *Paecilomyces lilacinus* protease and chitinase on the eggshell structures and hatching of *Meloidogyne javanica* juveniles. Biol. control., 31: 346-352.
33. Park, J. O.; Hargreaves, J. R.; McConville, E. J.; Stirling, G. R.; Ghisalberti , E. L. and Sivasithamparam, K. (2004) Production of leucinostatins and nematicidal activity of Australian isolates of *Paecilomyces* (Thom) Samson. Letters in Applied Microbiology 38:271-276.
34. Olivares-Bernabeu, C. and López-Llorca, L. V. (2002) Fungal egg-parasites ujhbujof plant-parasitic nematodes from Spanish soils.Rev. lberoam Mycol., 19: 104-110.
35. Ashoub, A. H.; Montasser, S. A.; Mourad, M. H. and Gamal, M. (2009) Impact of some fungi species as biocontrol agent against the root-knot nematode,*Meloidogyne incognita* . Australian Journal of Basic and Applied Sciences, 3(4): 3617-3624.

Cryo-induction of myocardial infarction in rats and its effects on Lactate dehydrogenase-1 level and histopathological changes

Mahdi Haider Hammadi[1], Noori Mohamed labiy[2], Salm Rashed Hamoodi[3]
[1,2]AL-Mustansiryia University, College of Science/Department of Biology
[3]Baghdad University/College of Medicin, Departement of Pathology
Received 7/1/2013 – Accepted 16/3/2014

الخلاصة

في الدراسة الحالية تم استخدام طريقة التبريد الشديد لحث احتشاء العضلة القلبية لدى ذكور الجرذان البيضاء البالغة باستخدام النايتروجين السائل (- 190) م° وفحص التغيرات الفسيولوجية خلال المرحلة الحادة و المزمنة من احتشاء العضلة القلبية من خلال التحري عن المؤشر الحيوي في مصل الدم(الاكتيت ديهيدروجينيز-1) وعمل مقارنة بين المؤشر الحيوي و التغيرات النسيجية المرضية في العضلة القلبية للجرذان خلال فترات زمنية مختلفة

تم استخدام 35 جرذ من الذكور البالغة وتم تقسيمهم إلى المجاميع التالية:

- مجاميع احتشاء العضلة القلبية الحاد(4 ساعات،8 ساعات و 24 ساعة)(15 جرذ).
- *مجاميع احتشاء العضلة القلبية المزمن(7 ايام،14يوم و 28يوم)(15 جرذ)*
- تم اخذ خمسة جرذ مختبري كمجموعة سيطرة (غير المصابة) ارتفع مستوى تركيز الـــ Lactate dehydrogenase-1 معنويا خلال الأربع ساعات الأولى بعد حدوث احتشاء العضلة القلبية لدى الجرذان المختبرية ، وكتسب هذا الارتفاع دلالة معنوية عالية ($p<0.01$)، ويستمر الارتفاع في التركيز لغاية 14 يوم مقارنة بالسيطرة، وكان الارتفاع معنويا جدا ($p<0.01$). أما بالنسبة إلى التغيرات النسيجية المرضية خلال المرحلة الحادة و المزمنة من مرض احتشاء العضلة القلبية لها علاقة قوية مع التغيرات الفسيولوجية في تركيز المؤشر الحيوي (Lactate dehydrogenase-1) .

تبين الدراسة وجود علاقة قوية بين مستوى تركيز المؤشر الحيوي (Lactate dehydrogenase-1) والتغيرات النسيجية المرضية خلال المرحلة الحادة والمزمنة من مرض احتشاء العضلة القلبية والذي يؤشر الدور المهم للاكتيت ديهادروجينيز-1 كعامل تنبؤي مبكر لوجود ضرر حاصل في العضلة القلبية .

ABSTRACT

Our study used cryo-injury model to induce myocardial infarction in adult male rats by using liquid nitrogen (-190 c°) and investigate the physiological changes during acute and chronic M.I through checking serum blood biomarker (Lactate dehydrogenase-1),and doing scoring between the biomarker and the histopathological changes in rats myocardium in different period time

We used a total of 35 adult male rats and divided them in to subgroups as following:

- Fifteen rats for induced acute myocardial infarction (4/hr., 8/hr. 24/hr.).
- Fifteen rats for induced chronic myocardial infarction (7/days, 14/days, 28/days).
- Five rats as a control healthy group.

Lactate dehydrogenase-1 increased significantly at 4 hours post experimental induction of myocardial infarction and persist significantly high for 14 days then decline later on.

The histopathological changes during acute and chronic M.I close related with the physiological changes in concentration of cardiac biomarker (LDH-1).

On this results showed highly significant increase in concentration levels of serum LDH-1 at 4/hr. post experimental induction of M.I this results means the importance of LDH-1 as a specific and sensitive marker of myocardial necrosis ; and The histopathological changes during acute and chronic M.I it is close related with

physiological changes occur in cardiac biomarker concentration and appear early in blood.

INTRODUCTION

Myocardial infarction (M.I) or acute myocardial infarction (A.M.I) remains a leading causes of mortality and morbidity world wide [1] acute myocardial infarction, commonly known as a heart attack, results from the interruption of blood supply to apart of the heart, causing heart cells death.

The study of certain biomarker and histopathological changes during acute and chronic myocardial infarction can be induced in experimental rats by cryo- injury model by using liquid nitrogen (- 190 c^{o})[2,3].

During the past several years, a great achievement has been made in the management of cardiovascular diseases depended on the use experimental animals, this has allowed the development of many effective treatment strategies [2].

Several biomarkers have emerge as strong predictors of risk among patients presenting with acute myocardial infarction as Lactate dehydrogenase-1 (LDH-1) which release by damaged Myocardiocytes [2].

The pathophysiology alteration during myocardial infarction occur in two stages: early changes at time of acute infarction and late changes during myocardial healing and remodeling [3].

The focuses on the role of Lactate dehydrogenase-1 as a predictive marker of myocardial necrosis and the histopathological changes during acute and chronic myocardial infarction.

MATERIAL AND METHODS

Laboratory Animals:

In the present study, 35 adult male rats (*Rattus rattus norvegicus albinos*).Weighting 250-300g.were used for induced myocardial infarction by cryo- injury method[19] and animals divided to three groups each group contain 5 rats in case of acute and chronic M.I and sacrified (4/hr., 8/hr., 24/hr.)(7/day, 14/day, 28/day) respectively, all groups compared with 5 male adult rats healthy weighting 250-300 g. as a control group. These animals were obtained from the animal house in medical research unit of college of medicine in Baghdad University; these animals were subjected to unified Laboratory circumstances in terms of light, temperature, ventilation and were given water along the duration of the study.

MYOCARDIAL INFARCTION MODEL

Myocardial infarction was induced following a standardized protocol [19].

30 adult male rats weighting 250 -300 g. were anesthetized with diethyl ether 10 mg/100 g. under aseptic condition, the rat placed a supine position on a temperature- control plate (37 c°).
Shaving the chest from hair and sterilized by antiseptic solution (Alcohol 70 %), the rat heart was exposed through a 1.5 c.m left lateral thoractomy incision.
Cryo –injury was produced with a aluminum or metal prob (0.5 c.m in diameter) cooled to – 190 c° by immersion in liquid nitrogen and was applied left ventricular (L.V) free wall for 15 second periods with a 5 second rest, this procedure was repeated two times and infarct area was visualized .
The muscle layer and skin incision were closed with 5-0 and 3-0 silk suture respectively and the animals were returned to their cages and carefully monitored for 4 hours post operatively, dressing the incision by use fucidin cream antibiotic and use benzathin pencillinG (1500 u/ ml) and procaine pencillinG (1500 u/ml) were given intra- muscularly (0.4 ml per rat) after each operation twice a day for the first 48 hours.
Animals were divided into two experimental groups:
First groups: Acute MI (4/hr., 8/hr., 24/hr.) (15 rats).
Second groups: Chronic MI (7/day, 14/day, 28/day) (15 rats).

Collection of blood samples

From each rat (acute M.I groups, chronic M.I groups and control groups) 3 ml of blood were aspirated from heart puncture by syringe 5 ml after use diethyl ether as anesthesia substance, then serum was separated by centrifugation at 3000 rpm. For 10 minutes, then collected serum was divided into (1 ml) small aliguotes and immediately frozen at (- 20) c° until used.

Determination of lactate dehydrogenase-1 (ldh-1)

LDH-1 activity was measured by colorimetric method according to the procedure provided with Randox U.K Kit

Collection of tissue samples

All the rats were sacrified for the final experiments (Acute M.I groups, chronic M.I groups and control groups) by killing the animals by diethyl ether.
The chest was opened and removed the heart, and then the tissue samples of left ventricle from the infarct zone and control groups were collected and then fixed with 10 % formalin .

Histological study

All the rats were sacrified for the final experiments (acute M.I groups, chronic M.I groups and control groups) by killing the animals by diethyl ether. The chest was opened and removed the heart, and then the tissue samples of left ventricle from the infarct zone and control groups were collected and fixed with 10% formalin. The tissue samples were

embedded in paraffin wax and cut into 5μm thick section by using rotary microtome; the sections were serially rehydrated with 100% and 70% ethanol after deparafinization with xylene. Then, staining with Harris haematoxylin and eosin stain, dehydrated in graded ethanol, cleared in xylene and mounted with Canada balsam (Wang et al., 2000).

Statistical analysis

All results were given as mean □□SD (Standard deviation) and use paired t-test. To compare between the groups, statistical analysis was performed by using SPSS statistical version 11 software package

RESULTS AND DISSCUSION

A- Statistic analysis in table (1) revealed highly increase in the levels of lactate dehydrogenase-1 of all rat study groups in acute M.I (4/hr., 8/hr and 24/hr).(862.4±135.3U/L),(1261.6±42.9U/L)and(773.8±50.9U/L)respectively compared with control group (440.6 ±42.8 U/L)

Table -1: The levels of Lactate dehydrogenase-1(LDH-1) (U/L) in rat's serum of acute M.I compared with control.

Study Groups	No.	The Concentrate Levels Of Lactate Dehydrogenase (LDH-1) (U/L)	t-test
		Mean ± SD.	
Control	5	440.6 ±42.8	
4/ hr.	5	862.4 ±135.3	6.64**
8/hr.	5	1261.6 ±42.9	30.24**
24/hr.	5	773.8 ±50.9	11.14**

** Highly significant at level $p < 0.01$

B- Table 2 show increase in the means of LDH-1 in all rats study groups in chronic M.I (7/days, 14/days and 28/days) (731.4 ±83.6 U/L), (613.4 ±71.9 U/L) and (444. ±35.0 U/L) respectively compared with control group (440.6 ±42.8 U/L).

Table -2: The concentrate levels of Lactate dehydrogenase-1(LDH-1) (U/L) in rat's serum of chronic M.I compared with control.

Study Groups	No.	The Concentrate Levels Of Lactate Dehydrogenase (LDH-1) (U/L)	
		Mean ± SD.	
Control	5	440.6 ± 42.8	
7/days	5	731.4 ± 83.6	6.92**

** Highly significant at level $p < 0.01$

14/days	5	613.4 ± 71.9	4.17**
28/days	5	444.0 ± 35.0	0.14

Histopathological study

1- **Acute M.I**: During A.M.I the rats heart muscle (myocardium) show different histopathological changes during serial period of time (4/hr, 8/hr. and 24/hr.) which can be summarized as following:

At 4/hr. the cross section of myocardium show coagulation necrosis is initiated with edema and polymorphonucleus infiltration begins.[Picture 2].

Moreover, at 8/hr. band necrosis in margins, as well as beginning of neutrophil cells infiltration. [Picture 3].

At 24/hr. cardiac muscle fibers necrotized, with loss of nuclei, striation and increased infiltration of neutrophil cells to interstitum. [Picture 4].

2- **Chronic M.I**: At the day 7 of M.I the cross section of ventricle showed the beginning of necrosis cardiac muscle fibers, and formation of fibrosis, present fibroblast cells and appear collagen fibers. [Picture 5].

Moreover, at day 14 of M.I the cardiac muscle fibers showed infiltration of monocyte cells predominant macrophage cells and present fibroblast cells.[Picture 6].

On the other hand, during day 28 of M.I the myocardium section shows get increase collagen deposition, decrease cellularity, fibrosis, and cardiac muscle fibers become hypertrophic with establish fibrotic area. [picture 7].

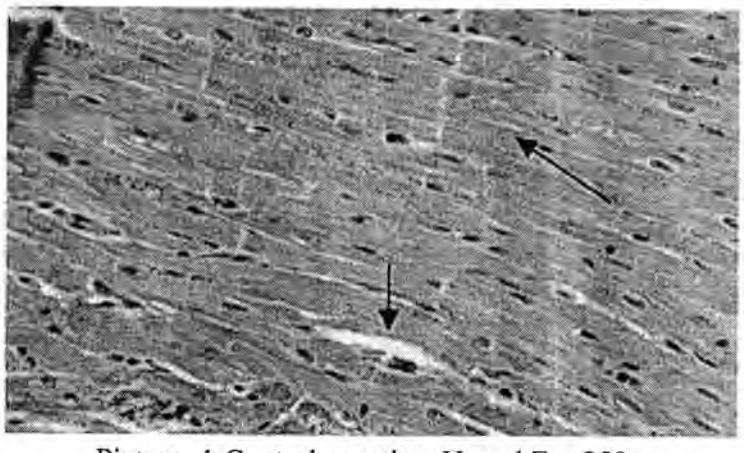

Picture -1:Control negative. H. and E. ×250.

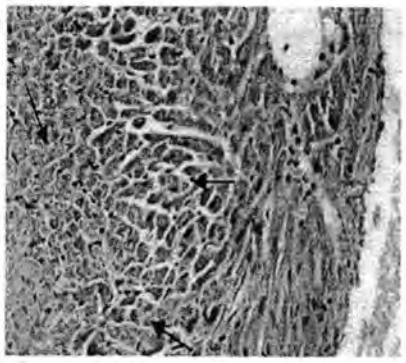

Picture-2: H and E.×250

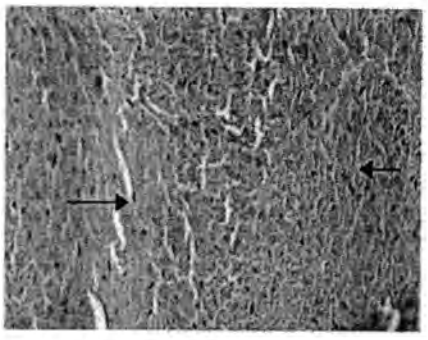

Picture-3: H and E.×250

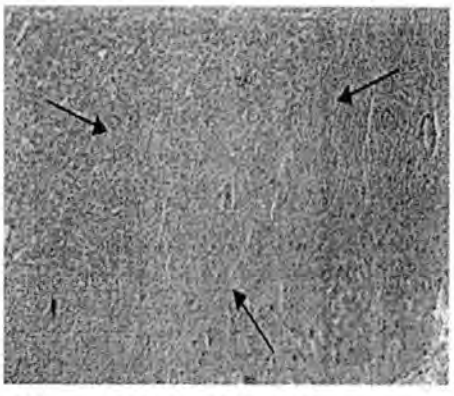

Picture-4: H and E.×100

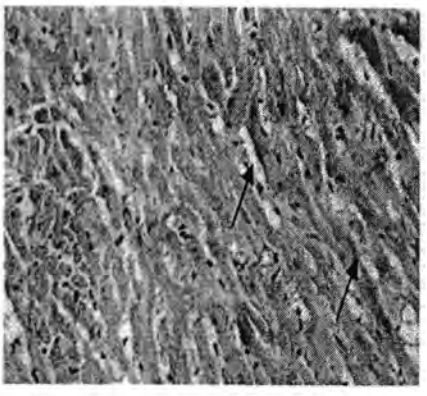

Picture-5: H and E.×250

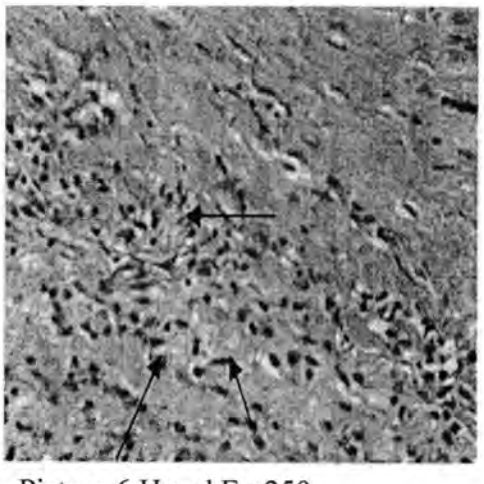

Picture-6:H and E.×250

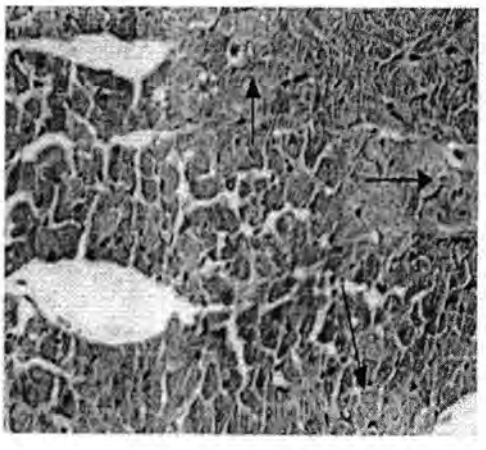

Picture-7:.H and E.×25

The present study revealed highly significant increased in concentration levels of Lactate Dehydrogenase -1 (LDH-1) during acute and chronic M.I versus control but not reach the significant degree at day 28 [table 1] [table 2].

This results is not agree with previous studies showed serum LDH-1 increase in M.I at 12- 24 hours after onset of symptoms, peaking usually

between 48 and 72 hours after onset and returning to normal after 10 to 14 days[4,5] .

L.D.H-1 and L.D.H-2 are the predominant isoenzymes in the myocardium. Ordinary, the concentration of L.D.H-1 in serum is less than that of L.D.H-2 reversal of the L.D.H 1:2 ratio in serum is used as index of A.M.I, although a similar inverted L.D ratio (LD=1>LD=2)may be seen in hemolysis and renal injury [6].

Furthermore, the major LDH isoenzyme in erythrocytes is LDH-1 so that hemolysis, either intravascular or in the collected blood specimen, may also causes the LDH flip and causes false positive results, this causes explain the elevated concentration levels of LDH-1 early in A.M.I at 4/hours and 8/hours in our experimental [6].

On the other hand, some authors showed 90% of patients with myocardial infarction the LDH.-1 was increased within 12 /hours of admission and still above normal upon admission at 6–12/days after infarction [6, 7].

Another factor that might explain the low rate of release in the initial phase and the finding of a later maximum is probably that not all cells die and disintegrate at the same moment [8, 9].

The present study revealed highly significant increased in serum levels of LDH-1 at 24/ hours after onset of M.I in rats. These results agree with many studies it shows significantly high levels of serum LDH in A.M.I at 24/hours in humans as compared to control group [4, 6, 10].

LDH-1 specific markers for M.I, but may occur only as a late event. One or more days after the infarction, and not observed at all in 15-20 % of patients [11]

HISTOPATHOLOGICAL STUDY

Various histopathological changes detected during acute myocardial infarction such as at 4 hours that showed edema, and PMN cells infiltration begins.

The edema of the myocardium may have resulted as vascular permeability increase and interstitial oncotic pressure rises because of the leak of intercellular proteins and causes myocytes altered [3, 12, 13].

This study revealed necrosis of myocardial cells with loss of nuclei and striations and increase of neutrophils cells to interstitum at 24 hours of A.M.I.

This finding agree with Jacob [14] showed that neutrophils cells activated during inflammation, these cells respond to intracellular signals. In myocardium similar signals of inflammation are generated by endothelial cells and cardiomyocytes.

Some authors mentioned neutrophils cells can interact immuno inflammatory factors to initiate myocardial injury [15, 14].

The present study shows during chronic M.I various histopathological changes in left ventricular cross section such as:

At 7 days there is persist necrosis cardiac muscle fibers, beginning formation of fibrosis, present fibroblast cells and appear collagen fibers. On the other hand, the optimal cardiac repair requires containment of the inflammation in the infracted area, extension of the inflammation in to the non infracted area could results in expansion of the neutrophil cells infiltration and worsening of the remodeling [14].

The present histological study revealed present fibroblast cells at day 7 and day 14 of M.I.

This finding agree with some reported revealed proliferation of fibroblast cells was not evident until the day 7, when spindle-shape cell with plump to elongated nuclei appeared at the edge of the necrotic muscle, all infarcts had fibroblastic proliferation along with deposition of collagen, from the seven days until formation of scar was complete [16,17].

Moreover, during day 14 of chronic M.I showed continuous cardiac muscle fibers necrosis, infiltration of monocyte predominant macrophage cells.

Irreversible injured myocytes do not regenerated, rather, the cell are remove and replaced by fibrous tissue. Macrophage cells invade the inflammed myocardium shortly after nutrophil cells infiltration and remove necrotic tissue [3].

At 28 days the myocardium section shows establish fibrotic area.

This change may be related with cytokines release such as Transforming Growth Factor (TGF-ß) is a multifunctional cytokine that control proliferation and cellular differentiation in most cell [17].

On the other hand, reduced myocardium perfusion might lead to activation of fibroblasts cells in myocardium and consequently lead to excessive collagen deposition and fibrosis [15].

CONCLUSION

This study revealed highly significant increase in concentration of serum levels of LDH-1 at AM.I and persist elevated till 14/days during chronic M.I. This result means the importance of LDH-1 as late specific marker of myocardial necrosis to detect myocardial infarction, and the histopathological changes during A.M.I and chronic M.I it is close related with physiological changes occur in cardiac biomarker concentration and appear early in blood and related with duration of infarction.

REFERENCES

1. Mallinson,T." Myocardial infarction".focus on first aid, (15):15; (2010).

2. Christenson, R. ;Morrow, D. and Apple, F. "Cardiac Troponin-I measurements with the access immuno assay system: analytical and clinical performance characteristics.clin. chem. ;44:52- 60; (2011).

3. Leonard,S. "Pathophysiology of heart disease". 4 th ed., Philadelphia, Baltimore, New York, London, 168- 184 ; (2007).
4. Haseeb, A., Abdullah ,S., Samia , H., Syed, S., Zohair, A., Adnan, A. and Abdulrahman ,A. "Serum markers of tissue damage and oxidative stress in patients with acute myocardial infarction ". Biomedical Research;24 (1):15- 20; (2013).
5. Zvi, R.; tzhak, W.; Alex, S. and Apple, F. "Lactate dehydrogenase isoenzymes in serum during recent acute myocardial infarction". Clin. Chem.;33:1419- 1420; (1987).
6. Jong, P. ;Moon, K. and Jong, W. "Proteomic biomarkers for diagnosis in acute myocardial infarction".Biomarkers;16 (1):1- 11; (2011).
7. David, E. ;Bruns, J. ;Julla, C. ; Emerson, S. ; Roger, B. ; Kenneth, E. ; Hill, J. and John, S. "Lactate Dehydrogenase isoenzyme-1: changes during the first day after acute nyocardial infarction" clin. Chem.. 27/11:1821-1823; (1981).
8. Tan, L. and Hall, A"Cardiovascular reparation and protection". UK. ;PP. 40 – 45; (1995).
9. Witteveen,M.;Hermens, W.; Lemmers, H. and Roger, B. "Cardiac biomarkers" 24 (1):15- 20; (1975) .
10. ALLAN, S. ;Yvonne, L. ;Curtis, A. ;Dana, R. ;Abendschein,E. and Jack,H. "Comparative sensitivity of cardiac troponin-I and lactate dehydrogenase isoenzymes for diagnosing acute myocardial infarction. "Clinical Chemistry, 42:11; (1996).
11. Thiagrajan,H.,Vairakkannu,V.,Bhakthavatsalam,M.,Mohammed,N., Samu,S.,and Rengarajulu,P. "Studes on biochemical markers in crtoinfarction in rats. "Royal Veterinary College, London ,27(5):311-318 ; (2006).
12. Avan, D.;Hermns, J.;Hollaar, L. and Jong, W. "Assessment of myocardial damage in patients with acute myocardial infarction by serial measurements of serum α- hydroxyl butyrate dehydrogenase levels". American Heart Journal;107:248- 260; (2006) .
13. Cotran, R. ;Kumar, v. and Robbins, S. "Pathologic basis of disease ". 5th ed. Philadeiphia ; (1994). .
14. Jakob, V" Involvement of neutrophils in the pathogensis of lethal myocardial reperfusion injury". Cardiovascular Research;61:481-497; (2004).
15. Deuk, Y. and Moo,R, "The inflammatory respons and cardiac repair after myocardial infarction".Korean Cir.J. ;39:393- 398; (2009).
16. Nathan, C. "Points of control in inflammation". Nature; 420: 846-5; (2002).
17. Michael, C.; Fishbein,M.;Derek,M. and Peter,M. "The histopathologic evalution of myocardial infarction. " Chest, 73:6; (1990).

18. Bassols A. and Massague J. "Transforming growth factor beta regulates the expression and structure of extracellular matrix chondroitin/ dermatan sulfate proteoglycans. J Biol chem.;263: 3039-45; (1988).
19. Ewout, J.; Van den, B.; Barend, M. and Curtis, A. "A novel model of cryo injury- induced myocardial infarction in the mouse: a comparison with coronary artery ligation". Am. J. phsiol. Heart circ. Physiol, 289: H 129 - H 1300; (2005).

Determination of Mercurous Ion Sepectrophotometrically using New Organic Reagent 5 – (6 -brom-2-benzo thiazolyl) azo]-4-Hydroxy Benzoic acid (6 -Br BTABA)

Yussra O. Mussa
Dept. of chemistry / college of Education university of AL-Qadisiyia .
Received 15/9/2013 – Accepted 21/1/2014

الخلاصة

تضمن البحث طريقة طيفية لتقدير أيون الزئبق(I) Hg مع الكاشف 5-((6- بروموـ2- بنزوثيازوليل) آزو)-4- هايدروكسي حامض البنزويك ليكون معقد أخضر بمتصية عظمى عند 523 نانوميتر بظروف فضلى pH=(5.5- 9.0)و تركيز الكاشف ($1x10^{-3}$) مولاري و درجة الحرارة(20-30) م° و وقت (10) دقائق. وطاوع قانون بير لامبرت بمدى تركيزي (1- 11) جزء بالمليون وبامتصاصية مولارية ($5.11x10^{3}$) لتر. مول$^{-1}$. سم$^{-1}$. وحد كشف0.02 مايكروغرام . مل$^{-1}$ وخطأ نسبي مئوي 1.23% والنسبة المئوية للاسترجاع 96.57% وحددت نسبة الفلز الى الكاشف بطريقتي النسب المولية والمتغيرات المستمرة وشخص المعقد بأطياف الأشعة ما فوق البنفسجية-المرئية والأشعة ما تحت الحمراء والتحليل الدقيق للعناصر.

ABSTRACT

Method described spectrophotometric determination of mercury metal ion Hg (I) by chelate with the reagent 5- (6-Bromo-2- benzothiazolyl) azo]-4-hydroxyBenzoic acid (6 -BrBT ABA) , to form Yellowish complex with maximum absorption at λ_{Max} 523nm at the optimum conditions, pH (5.5-9.0) , concentration reagent (1×10^{-3}M) ,temperatures (20 -30) Ċ and time (10 min) , Beer's law was obeyed in the concentration range between (1-11) $\mu g.ml^{-1}$ with molar absorptivity (5.11×10^{3}) $L.mol^{-1}.cm^{-1}$. and detection limit (D.L.) is $0.02\mu g.cm^{-1}$. the percentage relative error (E_{rel} %) 1.23, Percentage recovery (Rec%) 96.57 for assessment of the selectivity of the method , a ratio of metal to ligand was determined by using molar ratio method and continuance variation method . Also , the complex is characterized by using u.v-visible spectral , IR- spectra and elemental analysis .

INTRODUCTION

Each chromogenic system has its advantages and dis advantage with respect to sensitivity, selectivity and rapidity [1]. Formation of ternary complex by 1,10-phenanthroline-mercury(II)-Eosine[2-6] a method for determination of mercury at Nano gram level by flame less atomic absorbtion[7-9],another method base on the extraction of the ion-associated formed by a mercury (II) thiacrown cationic complex[10].Porphrine ligands are useful for simultaneous determination of metal ions in human for their toxicity because of their high molar absorptivity and high stability[11,12].Mercury as a heavy metal of high toxicity is one of the most harmful elements to human beings and other creatures [13,14].Mercury in various forms constitutes a serious environmental pollutant; hence there is the need for its detection and determination, particularly at trace levels, science mercury concentration in natural water is low, proper technique to increase its concentration cloud point extraction which is a developed environmental using protection liquid-liquid

extraction technique which bases on the cloud point phenomenon of the surfactant [15].The spectrophotometric method have gained popularity for mercury determination as advantageous in respect of simplicity and low operating costs ,for this reason a wide variety of spectrophotometric methods for the determination of mercury have been reported [16].The present paper describe the development of a simple, sensitive and selective method for the simultaneous determination of Hg(I) ion spectrophotometrically using 6-BrBTABA as chromogenic agent.

MATERIAL AND METHODS

Apparatus and chemicals

Electronic absorption spectra in the visible and ultraviolet regions were measured with UV-Visible spectrophotometer(Shimadzu-UV-1650) double beam using 0.5 cm quartz cells with absolute ethanol as solvent was used in all absorption spectra. Infrared spectra were measured by using shimadzu FTIR-8000 series , in the range between (4000 – 400) cm^{-1} using K Br discs . pH meter used for measurements were made with Philips PW 9421 . All chemicals were supplied from BDH expect of 2-amino -6- bromo benzo thaizole was prepared as described in the literature[17].

preparation and characterization of Azo Reagent (6–Br BTABA)

The thiazolylazo ligand (6-BrBTABA)(see scheme 1)[18]was prepared by dissolving (2.29 gm,0.01 mol) 2-amino-6-bromo benzothiazole in 70ml of distilled water and 10ml of concentrated hydrochloric acid . The filtered solution was cooled at 5°C.To this mixture a solution of (0.75 gm,0.01 mol) of sodium nitrate in 30 ml of distilled water was added drop wise at 0-5°C and the mixture was stirred for 40 min .This diazonium chloride solution was added drop wise in 500ml beaker containing (1.38gm,0.01 mol) of 4-hydroxy benzoic acid dissolved in 200ml anhydrous ethanol. The mixture was stirred for an additional 2 hours, in an ice-bath allowed to stand overnight and acidified with dilute hydrochloric acid until pH =6.0 was reached .The precipitate dye was filtered ,dried and recrystallized twice from ethanol then dried in the oven at 60 °C for several hours. The yield was 78% of brown powder ,melting at 188 °C .The solid ligand is stable in air at room temperature ,in soluble in water but completely soluble in most organic solvents .The preparation of this ligand is shown in scheme (1).

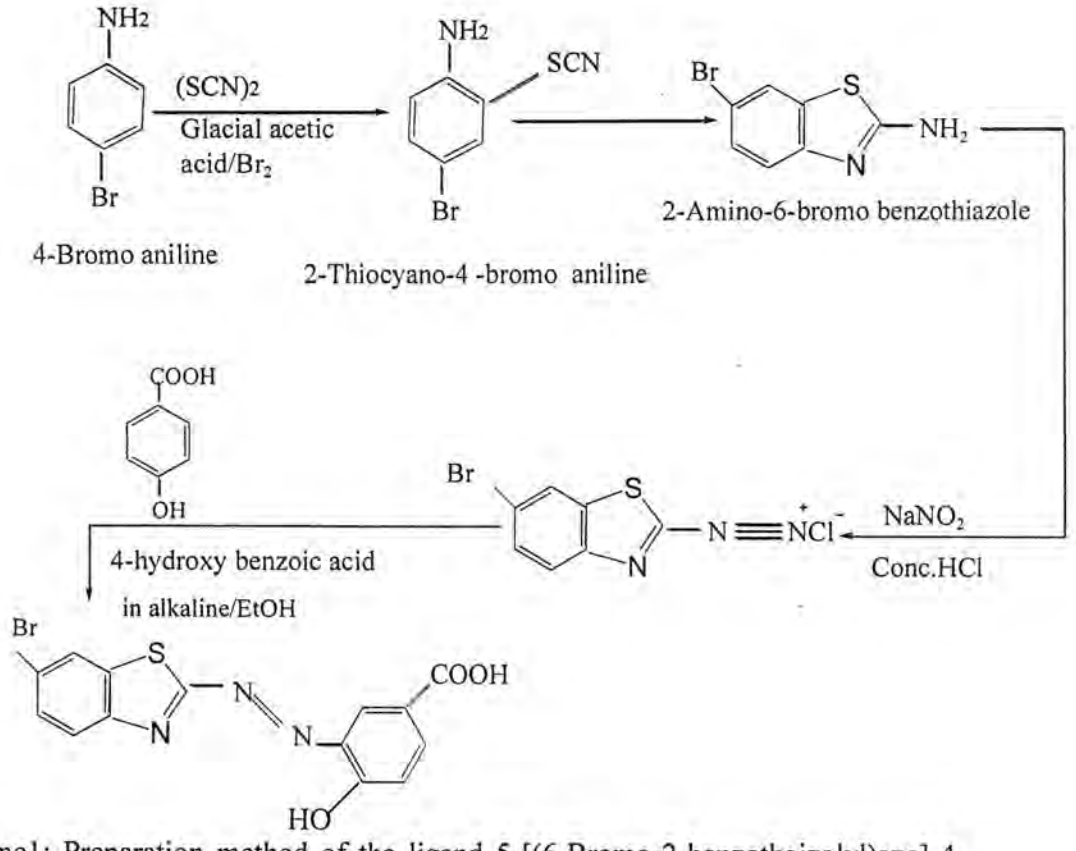

Scheme1: Preparation method of the ligand 5-[(6-Bromo-2-benzothaizolyl)azo]-4-hydroxy benzoic acid(6-BrBTABA=LH_2).

Preparation and characterization of Complexes

The metal complexes were prepared by adding (0.756gm, 0.002 mol) ligand dissolved in hot ethanol 50 ml and added drop wise with stirring stoichiometric amount of (1:1) ligand for metal ions Hg $_2Cl_2$ dissolved in 25ml hot buffer solution (ammonium acetate) at optimal pH for each metal ions. The reaction mixture was heated to 60°C for 40 min. , then left overnight . The solid produced was filtered off, washed with 15 ml ethanol to remove the remaining un reacted substances and dried in a desiccators over anhydrous
$CaCl_2$.

The prepared complexes of this ligand are stable in air at room temperature and soluble in methanol, ethanol, acetone DMF and DMSO but insoluble in water .The analytical and physical data for the prepared ligand and their metal complexes are listed in table (1).

Table-1: Analytical and physical data of the thiazolylazo ligand and it's complex .

No.	Compound	Color	m.P °C	Yield %	Molecular formula (Mol .Wt)	Found (Calc.)%			
						C	H	N	M
1	LH_2=Ligand	Brown	188	78	$C_{14}H_8N_3O_3SBr$ (378.20)	44.56 (44.46)	2.23 (2.13)	11.27 (11.11)	— —
2	[Hg(LH).H_2O]	Green	230d.	80	$C_{14}H_8N_3O_8$ S Br Cl Hg (630.24)	26.67 (26.82)	1.39 (1.42)	6.59 (6.66)	–

Standard of Hg (I) solution:

A solution of Hg (I) (1000 ppm.) was prepared by Dissolving (1.35gm) of Hg_2Cl_2 in 1000 ml of double distilled water. Working solution was prepared freshly appropriate dilution of the stock solution.

Standard solution of Reagent:

In absolute thionic solution was prepared ($1x10^{3-}$ M) from the pure reagent $C_{14}H_{8}N_3O_3SBr$ (6-BrBTABA==LH_2. M. wt. =378.125 $g.mol^{-1}$) by dissolving (0.00945gm) in 25 ml of absolute ethanol. The stock solution of reagent was stable for several months.

Buffer Solution:

0.01 M ammonium acetate (0.771) gm. was dissolved in 1 liter of distilled water. 0.2 M acetic acid to 0.2 M ammonia solution was used for pH adjustment.

General procedure:

To detection the optimum concentration of the reagent· ,different volumes from ($1x10^{-3}$ M) of ethanolic6-BrBTABA solution were added to a fixed volume 1ml from ($1x10^{-4}$ M) Hg(I) solution and measuring the absorbance at 523nm.In to a set of 10 ml calibrated flask transfer 1ml from ($1x10^{-4}$ M) Hg(I) solution and then mixed with 3ml of $1x10^{-3}$ M ethanolic 6-BrBTABA solution at pH=9.0 and measure the absorbance after(5,10,15,….,360)mints at 523nm to detect the effect of pH and temperature(10-70) Ċ .Calibration curve preparing by using a set of solutions containing 1ml from (1-11) ppm Hg(I) solution with 3ml from ($1x10^{-3}$ M) of ethanolic 6-BrBTABA solution and measuring of the absorbance for complex at 523nm,also a ratio of metal to ligand was determined by using mole ratio and continues variation methods with ($1x10^{-4}$ M) concentration for each Hg(I) and 6-BrBTABA solutions.

RESULTS AND DISCUSSION

Absorption Spectra:

The absorption spectra of the reagent (6-Br BTABA) and its complex with Hg (I) are shown in fig (1) . The wave length at maximum absorption (λ_{Max}) of the reagent was found at 425nm and (λ_{Max}) of the complex was found 523 nm. The band 425nm due to the color of the ligand and the metal complex showed a bathochromic shift 98nm.

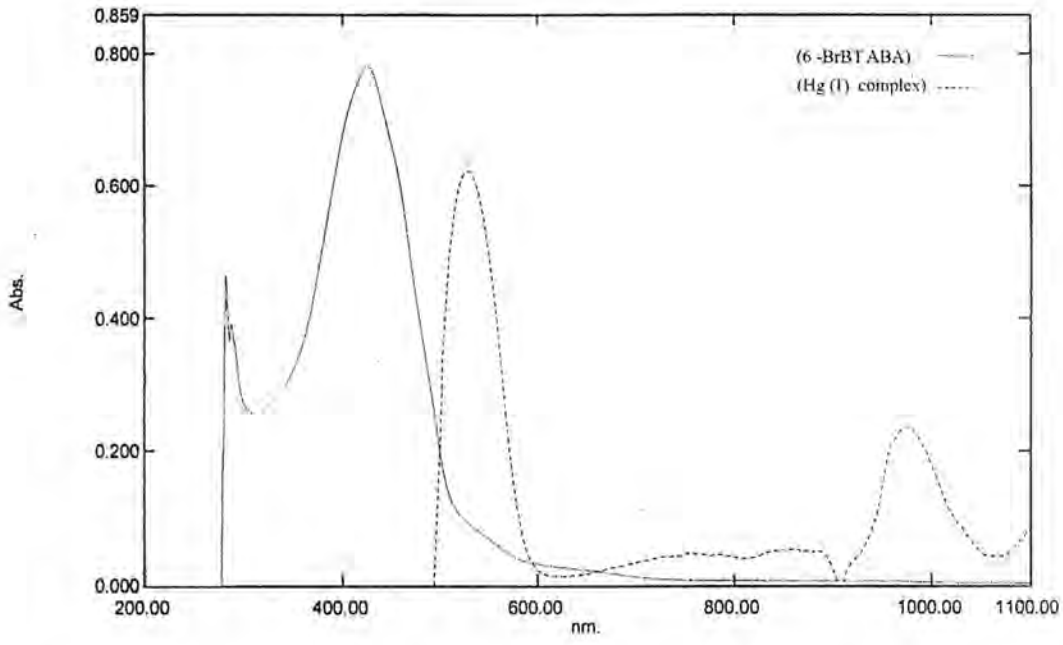

Figure-1: Absorption spectra of reagent [6-Br BTABA=LH_2] and its complex of Hg (I) complex in pH =8 in $1x10^{-3}$ M 6-BrBTABA=LH_2 , $1x10^{-4}$M Hg(I) ion .

Effect of Concentration:

Different volumes(1,2,3,4,5,6,7,8) ml from ($1x10^{-3}$ M) of reagent 6-BrBTABA=LH_2 solution were added to a fixed amount (1ml from $1x10^{-4}$M) of Hg (I) ion.3ml from the reagent was found enough to develop the color its full intensity and was considered to be optimum for the concentration range($3x10^{-3}$ M) of Hg(I) ion solution..

Effect of pH :

The effect of pH on the absorbance value of the Hg (I) complex was studied over range (5.5-9.0) as shown in fig (3). The absorbance of the Hg (I)-complex system is maximum and constant in the pH range (7.5-8.5) and a pH of 8.0 was adopted

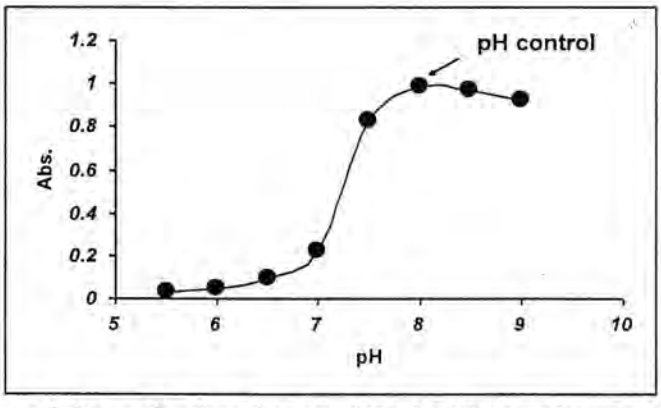

Figure-3: Effect of pH on the absorbance of the Hg(I) complex; concentration of 6-BrBTABA=LH_2=$1x10^{-3}$M ;concentration of Hg(I) $1x10^{-4}$ M at pH=8.0.

Effect of Temperature:

The effect of temperature on the absorbance of the Hg (I) complex was studied. As shown in fig (4) the study was performed at temperature range (10 – 70) Ċ and the maximum absorption was obtained at(20 – 30)Ċ. At temperature higher than 30 Ċ the Absorbance decreased with increasing temperature until it reaches 70Ċ, due to the dissociation of the Complex.

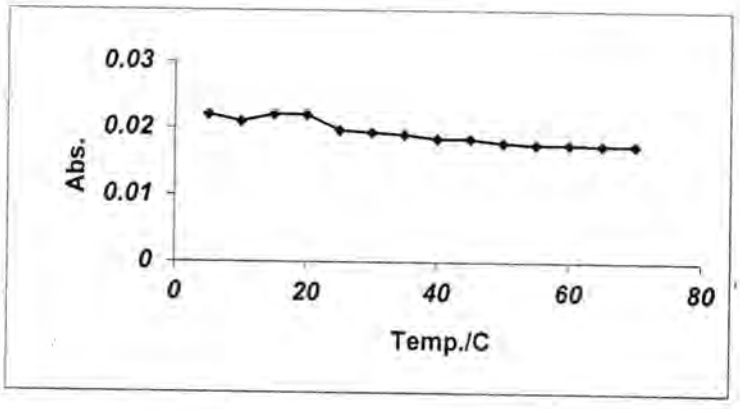

Figure-4: The effect of temperature on the absorbance of the Hg(I) complex; concentration of 6-BrBTABA=LH_2 =1x10^{-3}M ;concentration of Hg(I) 1x10^{-4} M at pH=8.0.

Effect of Time:

It was found that the absorbance of the Hg(I)-complex chromogenic system reaches a maximum value with 10 min. at room temperature and remains stable for about 24 hours .The stability of the chromogenic system with the time is shown in fig.(5).

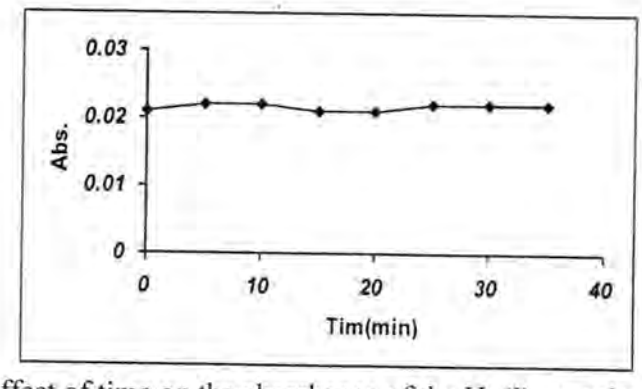

Figure-5: The effect of time on the absorbance of the Hg(I) complex; concentration of 6-BrBTABA=LH_2 =1x10^{-3}M ;concentration of Hg(I) 1x10^{-4} M at pH=8.0.

Composition of Hg (I) complex:

The composition of Hg (I) complex was determined by mole ratio method [19]fig (6) and continues variation method [20]fig (7). Both methods

6	L–$ZnSO_4.H_2O$	3375(asym)s 3298(sym) s 1618(m), 1300(m) 1246 (s)	3178 w 3062 m	1380 m 1531 m	1446 s	510 m	428 m	540 m 820 m	–	1022 s 950m 667 m
7	L–$PdCl_2$	3367 (asym) br 3311 (sym)br 1610 s 1306 s, 1249 s	3170 m 3020m	1388 m 1554 s	1444 s	540 s	462s	–	283s	–
8	L–$CdCl_2.H_2O$	3381(asym)s 3298 (sym)s 1620s, 1311m 1215 (w)	3178m 3062m	1365 m 1585 s	1446 s	540 m	425s	555 m 837 m	–	–
9	L–$SbCl_3$	3338 (asym) br 3271(sym) br 1604s 1303 s, 1230 (m)	3178 m 3055 w	1390 m 1580 m	1446 s	520 s	420s	–	–	–
10	L–$HgCl_2.H_2O$	3350 (asym) br 3282 (sym) br 1604 s 1303 s, 1238 (w)	3190 m 3043 m	1388 s 1580 m	1450m	535 m	420m	559 s 817 m	–	–
11	L-$Pb(NO_3)_2.H_2O$	3379 (asym)(s) 3298 (sym) (s) 1618 (s) 1300 (m), 1246 (s)	3178 m 3062 m	1365 w 1585 s	1446 s	530 m	405 s	550 s 820 m	–	1026 s 937 m 671 s

Ar = aromatic, a_{sym} = asymmetric, sym = symmetric, sh = shoulder
br = broad, m = meduim, s = strong, w = weak

The UV–Visible spectra of the ligand (L) and complexes

The UV–Visible spectra of the ligand (L) in EtOH solution exhibited strong absorption bands at (221nm, 45248 cm^{-1}) and (344 nm, 29069 cm^{-1}). This may attributed to the π–π^* and n–π^* transition[35]. Fig. (5).

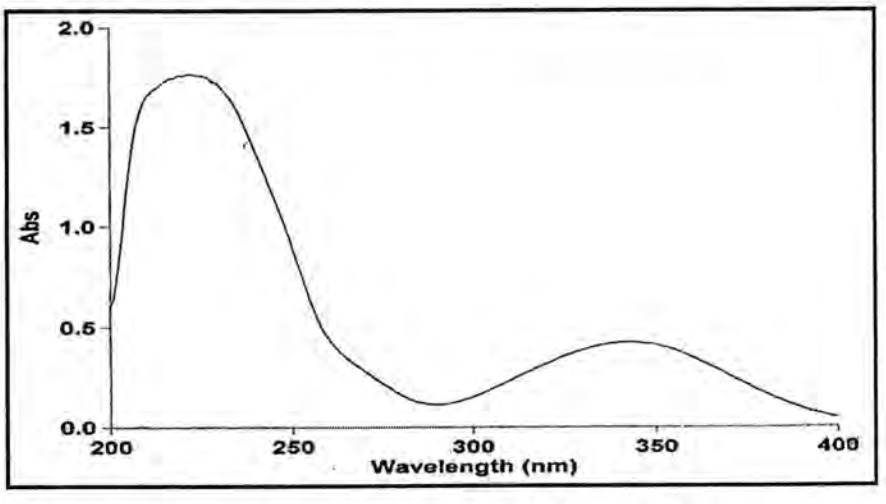

Figure-5: UV– Visible spectrum of the Ligand (L) in EtOH 10^{-3} M

The UV–Visible spectrum of Cr^{+3} complex showed one band in the region (580 nm, 17241 cm^{-1}) is due to $^4A_2g \rightarrow {}^4T_2g$[36].
The UV–Visible spectrum for Co^{+2} complex showed three bands in the region (800 nm, 12500 cm^{-1}) due to $^4T_1g \rightarrow {}^4Eg$, (651 nm, 15360 cm^{-1})

due to $^4T_1g \rightarrow {}^4A_2g$ and (553 nm, 18083 cm^{-1}) due to $^4T_1g_{(F)} \rightarrow {}^2T_1g_{(p)}$[37,38]. Fig. (6).

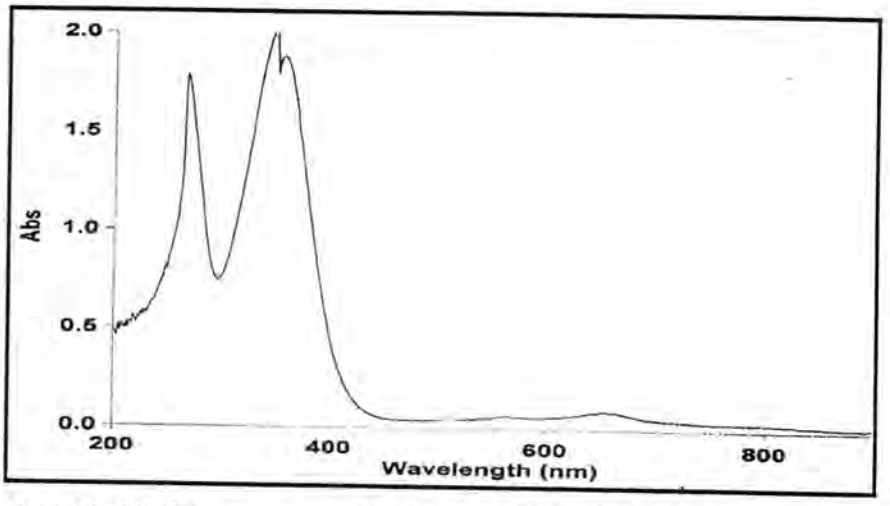

Figure-6: UV– Visible spectrum of L–$CoCl_2$. in DMSO 10^{-3} M

The ratio of 18083cm^{-1} to 12500cm^{-1} is 1.45 which fits with Tanaba–Sugano d^7 curve for E/B= 26 and $\Delta_0 / B' = 17$. $\Delta_0 = 12500\ cm^{-1}$

B' complex = 12500 / 17 = 735 cm^{-1}

B for free Co^{+2} = 971 cm^{-1}

β (nephelauxetic effect) = B' complex / B Co^{+2} = 735 / 971 = 0.756

Which indicates of d– electron delocalization on the ligand hence a significant covalent character in the complex[39].

The UV– Visible spectrum for Ni^{+2} showed one band at (828 nm, 12077 cm^{-1}) which is due to $^3A_2g \rightarrow {}^3T_1g$ .The spectrum of the Cu^{+2} complex exhibited a band at (662 nm, 15105 cm^{-1}) which is due to $^2Eg \rightarrow {}^2T_2g$.

The brown palladium complex exhibited a strong band at (420 nm, 23809 cm^{-1}) due to d– π^* transition[40].

The UV– Visible spectra of Zn^{+2} ,Cd^{+2}, Sb^{+3}, Hg^{+2} and Pb^{+2} complexes showed shifted band compared with free ligand (L) are due to charge transfer Table (3). The molar conductance of all complexes in DMSO were found to be low which suggested coordination of anion to the metal. The magnetic moments of Cr(III) complex was indicative of three unpaired electrons per Cr(III) ion suggesting consistency with their octahedral environment[41]. The magnetic monments measurements for the solid Co(II) complex is also indicative of three unpaired electrons per Co(II) ion suggesting consistency with their octahedral environment. The Co(II) complex exhibit magnetic moment values of 4.67 which are well agree with the octahedral range of (4.3– 5.2) B.M[42]. Ni(II) complex showed the magnetic moment values of 2.93 within the rang of (2.8–3.5) B.M. (octahedral range) suggesting consistency with their octahedral environment. The magnetic moments of Cu(II) complex was (1.98) B.M.

which suggests the presence of one unpaired electron with octahedral configuration[43].

Electronic spectra, Conductance in (DMSO), Magnetic moment (B.M) of the ligand and its complexes are given in Table (3).

Table-3:Electronic spectra (DMSO),Conductance in DMSO, Magnetic moment (B.M) of the ligand (L) and its complexes

NO	Compound	λ (nm) cm^{-1}	Assignment Bands	Λ s. cm^{-1} DMSO (10^{-3} M)	μ_{eff} (B.M)
1	$(L)C_{12}H_{11}N_5O_4$	45248 (221) 29069 (344)	$\pi \rightarrow \pi^*$ $\pi^* \rightarrow n$	–	–
2	L–$CrCl_3$	17241 (580)	$^4A_2g \rightarrow {}^4T_2g$	12.73	3.80
3	L–$CoCl_2.H_2O$	18083 (553) 15360 (651) 12500 (800)	$^4T_1g_{(F)} \rightarrow {}^2T_1g_{(P)}$ $^4T_1g \rightarrow {}^4A_2g$ $^4T_1g \rightarrow {}^4Eg$	7.25	4.67
4	L–$NiCl_2.H_2O$	12077 (828)	$^3A_2g \rightarrow {}^3T_1g$	5.05	2.93
5	L–$CuCl_2.H_2O$	15105 (662)	$^2Eg \rightarrow {}^2T_2g$	12.08	1.98
6	L–$ZnSO_4.H_2O$	28248 (354)	Charge– Transfer	19.84	–
7	L–$PdCl_2$	23809 (420)	$d–\pi^*$	17.79	–
8	L–$CdCl_2.H_2O$	28328 (353)	Charge– Transfer	12.73	–
9	L–$SbCl_3$	28328 (353)	Charge – Transfer	10.27	–
10	L– Hg $Cl_2.H_2O$	31446 (318)	Charge - Transfer	8.73	–
11	L–$Pb(NO_3)_2.H_2O$	28169 (355)	Charge - Transfer	5.73	–

B. M = Bohr Magneton

Study of Cr^{+3}, Co^{+2}, Ni^{+2}, Cu^{+2} and Cd^{+2} complexes formation in solution

The complexes of the ligand (L) with selected metal ions (Cr^{+3}, Co^{+2}, Ni^{+2}, Cu^{+2} and Cd^{+2}) were studied in solution using ethanol as solvent, in order to determine (M:L) ratio in the prepared complexes, following molar ratio method[44]. A series of solutions were prepared having a constant concentration (C) 10^{-3} M of the hydrated metal salts and the ligand (L). The (M:L) ratio was determined from the relation ship between the absorption of the observed light and the mole ratio (M:L) found to be (1:1).

The results of complexes formation in solution are given in(Table 4 δ 5).

Table-4: continuous variation slop for Cr^{+3} ion λ (368 nm).

L–$CrCl_3$		
V_M	V_L	Abs
1 ml	0.25	0.20
1	0.50	0.43
1	0.75	0.70
1	1	0.90
1	1.25	0.88
1	1.50	0.89
1	1.75	0.92
1	2	0.91
1	2.25	0.92
1	2.50	0.88
1	2.75	0.89
1	3	0.87
1	3.25	0.93
1	3.50	0.91
1	3.75	0.91
1	4	0.92

VM = volume of metal in ml(M)
VL = volume of ligand in ml(L).

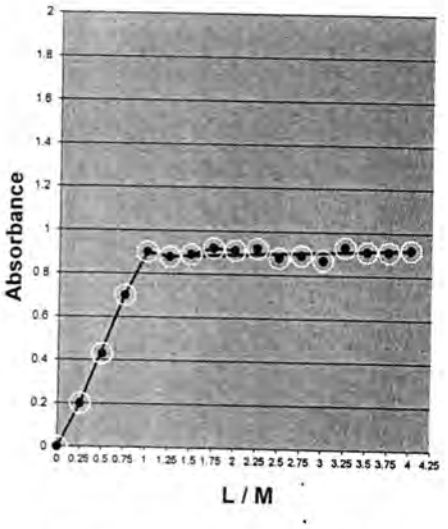

Figure-7: continuous variation slop for Cr^{+3} ion λ (368 nm)

Table-5:continuous variation slop for Ni^{+2} ion λ (348 nm).

L–$NiCl_2.H_2O$		
V_M	V_L	Abs
1 ml	0.25	0.20
1	0.50	0.39
1	0.75	0.55
1	1	0.70
1	1.25	0.73
1	1.50	0.68
1	1.75	0.69
1	2	0.73
1	2.25	0.72
1	2.50	0.71
1	2.75	0.69
1	3	0.69
1	3.25	0.74
1	3.50	0.71
1	3.75	0.72
1	4	0.71

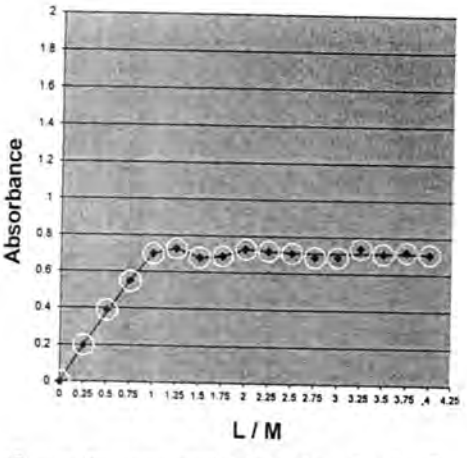

Figure-8:continuous variation slop for Ni^{+2} ion λ (348 nm)

The stability constant (Kf) was evaluated using the following equations:

$K_f = 1 - \alpha / \alpha^2 c$ .... (1)

$\alpha = Am - As / Am$ ..... (2)

(α) is the degree of the dissociation, (c) is the concentration of the complex (10^{-3} M) . (As) and (Am) are the absorbance values of the

solution were measured at (λ_{max}) of the maximum absorption .The molar absorptivity (ε_{max}) (eq .3) has been calculated using equation;

$A = \varepsilon_{max}. b. c$ ..... (3)

(A) is the average of three measurement of the absorption containing the same amount of metal ion and three fold excess of ligand, (b) is the depth of the quartz cell usually equal 1 cm.

Table-6:As, Am, K_f, ε_{max} and λ max of the Cr^{+3} , Co^{+2}, Ni^{+2}, Cu^{+2} and Cd^{+2} complexes

NO	Compound	As	Am	α	Formation constant (K_f)	Molar absorpitivity ε_{max} L. mol^{-1}. cm^{-1}	λ max (nm)
1	Cr–complex	0.90	0.93	0.051	9.462×10^5	3276	368
2	Co-complex	1.50	1.52	0.013	5.840×10^6	4702	350
3	Ni–complex	0.70	0.74	0.0540	3.244×10^5	9240	348
4	Cu–complex	1.20	1.22	0.016	3.843×10^6	2925	390
5	Cd–complex	0.60	0.63	0.047	4.314×10^5	1058	348

As =The absorbance value of the solution when the $V_M = V_L = 1$
Am = High the absorbance value of the solution.

The atomic absorption analysis was used to confirm our molar ratio calculation of [metal: ligand] (M:L) for Synthesis complex as well .The results showed a ratio M:L (1:1) for all complexes Table (1).

Biological activity study:

The biological activity of the prepared new ligand and its complexes were studied against selected types of micro organisums which include gram positive bacteria like streptococcus aureus and gram negative bacteria like E.coli in agar diffusion method, which is used (DMSO) as a solvent, and we are used these antibiotics disc which include cephalosporin as control . A gar diffusion method involves the exposure of the zone of inhibition toward the diffusion of micro organisms on agar plate . The plates were incubated for (24) hrs. at ($37c^o$), The zone of inhibition of bacterial growth around the disc was observed . (Table7).

Table-7:effect of ligand and its complexes on gram positive and gram negative bacteria

compound	Diameter of inhibition zone (mm)at concentration 1mg|ml	Diameter of inhibition zone (mm)at concentration 5mg|ml	Diameter of inhibition zone (mm)at concentration 1mg|ml	Diameter of inhibition zone (mm)at concentration 5mg|ml
	Streptococcus aureus		*E. coli*	
Cephalosporin	22.2	27.4	24.2	28.6
(L)$C_{12}H_{11}N_5O_4$	16	16.2	12.2	12.6
L–$CrCl_3$	11.2	11.4	13	13.2
L–$CoCl_2.H_2O$	14	14.4	16.2	16.4
L–$NiCl_2.H_2O$	11.6	12.2	12.4	12.6
L–$CuCl_2.H_2O$	12.4	12.6	12.0	12.2
L–$ZnSO_4.H_2O$	18.2	19	18.6	19.2
L–$PdCl_2$	18	18.4	18.6	18.9
L–$CdCl_2.H_2O$	10.2	10.6	10.8	11.2
L–$SbCl_3$	19.2	19.4	18.9	19.2
L–$HgCl_2.H_2O$	20.2	20.4	19.6	20
L–$Pb(NO_3)_2.H_2O$	12.2	12.4	11.6	11.8

CONCLUSIONS

A series of complexes of Cr^{+3}, Co^{+2}, Ni^{+2}, Cu^{+2}, Zn^{+2}, Pd^{+2}, Cd^{+2}, Sb^{+3}, Hg^{+2}, Pb^{+2}, with 2,4–dinitro–2'-amino hydrazo benzene (L) were prepared and characterized. The tridentate ligand (L) (N, N, O) is binding metal ions forming octahedral structure except with Pd^{+2} is forming trigonal bipyramidal as follows;

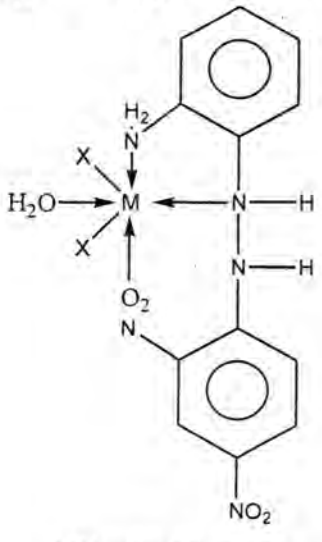

M^{+2} = Co, Ni, Cd, Hg
X = Cl^{-1}
M^{+2} = Cu, Zn
X2 = $SO4^{-2}$
M^{+2} = Pb
X = $NO3^{-1}$

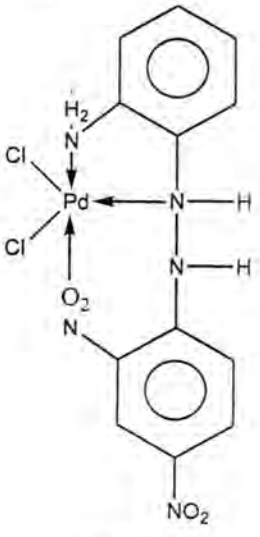

M^{+2} = Pd

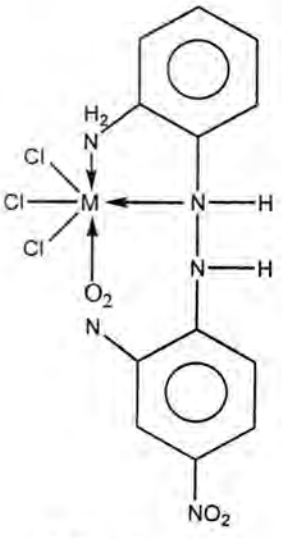

M^{+3} = Cr, Sb

Biological effects of new ligand and its complexes indicated that the new ligand and its complexes exhibited antibacterial activity against both gram positive and gram negative bacteria.

REFERENCES

[1] Sadler, P. J. and Guo, Z ., "metals in medicine",1st Ed ., 101-117, Angew, chem. Int, (1999).

[2] Sadler, P. J., "Crystal and Molecular", Inorganic. Chem.., 36, 1, 95–99, (1991).

[3] Hughes, M. N., "The Inorganic chemistry of biological procecess" ,2nd Ed., John– Wily and Sons. Ltd., New York, (1988).

[4] Fox, H. H. and Gibas, J. T., "Pyridine carboylic acid hydrazides and benzoic Acid hydrazides", J. organic chem. Easton, 17, 5, 1653–1660, (1983).

[5] Prasad, S., Agarwal, R. K., "Synthesis physico– chemical and Biological properties of complexes of cobalt (II) Derived from Hydrazones of Isonicotinic Acid Hydrazide", J. Inorg. Chem., 1,1 ,17– 26, (2008).

[6] Prasad, S., Agarwal, R. K., "Isonicotinic Acid Hydrazide and Hydrazone", J. of the Korean chem., soc, 53,1, 26– 35,(2009) .

[7] William, C.C., Lockhart, C. J., Musa, F. H., "Preparation and complexation of polydentate and macrocyclic ligands incorporating benzimidazol. X-ray Crysdtal Structure of 6, 7, 9, 10, 12, 13, 16 octahydro 23H, 25H bis–(benzimidazol [1,2–j:2,1'–0]) [1, 4, 7, 13, 10, 16 tetraoxdciazacyclo– octa– decine)), J. Chem. Soc, Dalton Trans, 1, 47, 53 – 60, (1986) .

[8] Musa, F. H., Othman, I. A.,"Synthesis of 5– phenyl–1,3,4–oxadiazo–2–thioderivatives and their reactions with some transition metal salts)), J. IBN–AL–Haitham for pure and appl, 9, 11, 85–87, (1998).

[9] Musa, F. H., AL–Bayti, H. A. and Othman, I. A., "Synthesis, characterization of chrom(III),cobalt (II), Nickel(II), Copper(II) and Palladium(II) complexes with 4,5–Diphenyl 1,2,4–rizole–2ylthio Acetic acid (TRBAC) and 4,5–Diphenyl–3–Benzyl thio 1,2,4 Triazol (TRBZ)", Iraq. J. chem., 28, 24, 507– 513, (2002).

[10] AL– Bayti, H. A.,Othman . I. A. and Musa, F. H., "Synthesis and studies of Bis – [3,4 – Diphenyl 1,2,4– Triazol– 5yl– thio] methane and its complexes with Cr(III), Co(II), Cu(II), Pd(II) and Pt(II)", Iraq . J. chem., 28, 11, 501– 505,(2002) .

[11] Musa, F. H., "preparation and characterization of Dioxadiazol and Ditriazol complexes with Divalent; Co, Ni, Cu, Zn and Hg", Iraq . J. chem., 24, 5, 239– 245,(1998).

[12] Naji, S. H., Fathel, H. A. and Musa, F. H., "Synthesis, characterization of some metal salts with 1,1` bis – (orthoaminophenylthio) – methane", J. Al – Mustansiriya . sci, 19, 12, 59– 62,(2008) .

[13] Naji, S. H., "Synthesis and spectral studies of the transition metals(Co(II), Ni(II), Cu(II), Cd(II), Hg(II), Pb(II) with aniline–2–thio methylene chloride complexes", J. AL–Mustansiriya. sci, 19, 11, 53- 56, (2008).

[14] Mohammed, H. A., Musa, F. H. and Abdullah, A.I., "Synthesis and studies of 1',2'-bis (5"- 2"thiol ethylsulphide–1,3,4–oxadiazole–2yl) Ethane and its complexes with (M(II), Cu, Ni, Co, Hg, J. Rof. Sci", 20, 9, 75– 89, (2002).

[15] Gursoy, A. N.and Otuk, T. G., "Synthesis of new hydrazides–hydrazones, thiosemicarbazides and thiazolidines as possible antimicrobials Eur", J. Med. Chem, 32, 11, 753– 759,(1997).

[16] Dodoff, N. K., Grancharov, M. O. and Spassovska, N.M, "Platinum (II) complexes of 4– methoxy and 4–chlorobenzoic Acid Hydrazides synthesis, characterization and cytotoxic effect", J. Inorg. Biochem, 60, 5, 257– 266,(1995) .

[17] Tabakova, S. and Dodoff, N., "Effect of Platinum (II) complexes of Benzoic and 3– methoxy benzoic acid Hydrazides on saccharomyces cerevisae z, Naturforsch", 50, 6, 34– 734,(1995) .

[18] Rand, D. G., Sato, D. M., signera, L. M. ,Malvezz, A. F., Leite, C. Q., Amaral, A. G., Ferreira E. I., Tavaves, L.D., "potential Tuberculostatic Agent. Topliss Application on Benzoic acid [(s–Nitrothiophen–2–yl)–Methylene]– hydrazide series", Bio .organic and Med. Chem., 10, 12, 557-560, (2002).

[19] Mamolo, M. G., Falagiani, D. V. Zamper, O. L. and E. W. Banfi, E. W., "Synthesis and antimicrobacterial activity of [5–(pyridine–2yl)–1,3,4–thiadiazole–2–ylthio] acetic acid arylidene hydrazide derivatives", Farmaco, 56 , 17, 580– 592, (2001).

[20] Rollas, S. ,Gulerman, N. N. and Erdenz, H.F., "Synthesis and antimicrobial activity of some new hydrozones of 4. flourobenzoic acid hydrazide and 3–acetyl–2,5–disubstituted–1,3,4–oxa diazolines", Farmaco, 57, 7, 171 – 174, (2002).

[21] William, D. H. and Flemin, I.N., "spectroscopic methods in organic chemistry", 1st Ed., 52, Mc Graw– Hill book company (UK) limited Amsterdam.(973).

[22] Ravich, S. R., Ran, N. S. and thangaraja, C. F., "Copper (II), Cobalt(II), Nickel(II) and Zinc(II) complexes of drived from benzyl-2,4-dinitrophenyl hydrazones with aniline", J. Chem. Soc. 116, 4, 215- 219, (2004).

[23] Abdul–Ghani, A. J. and khaleel, A. M., "Synthesis and characterization of new Schiff Bases Derived from N(1)-substituted Isatin with Dithioxamide and their Co(II), Ni(II), Cu(II), Pd(II) and Pt(IV) complexes". J. Bioinorganic chemistry and Applications, 18, 10, 22-28, (2009).

[24] Budige, G. A. and Vadde, R. A., "Synthesis, characterization and Biological Evaluation of Mononuclear Co(II), Ni(II), Cu(II), Pd(II) complexes with new N_2O_2 Schiff Bases Ligands". J. Chem. Pharm. Bull., 59, 2, 166-171, (2011).

[25] Keeton, M. N. and Lever, A.B., "Four, Five ,and Six coordinate metalcomplexes of di(2 pyridyl) disulphide and 1, 2–di (2'–pyridyl) ethane", Inorg. Chem., 10 ,5, 49–52, (1971).

[26] AL–Obadi, N. J., Abid, K. K. and AL–Naimi, Y. J., "Transition metal complexes of 2 –(thiosemicarbazino)–5–(O–hydroxyl phenyl)–1,3, 4–oxadiazole", J. Tikrit. sci, 11, 24, 164, 167, (2006).

[27] Naji, S.H., "Synthesis, spectroscopic and Biological studies of some metal complexes with 1,2 bis– (orthoaminophenyl thio) ethan", J.Al-Mustansiriya. Sci., 21, 3, 35, (2010).

[28] Naji, S.H., "Synthesis, spectroscopic and Biological studies of some metal complexes with orthoamino hydrazo benzene", J. Baghdad . Sci., 8, 2, 375, (2011).

[29] Saha, B. G. and Banerji, S. K., "Synthesis and characterization of complexes", J. Indian Chem., Soc, 1, 5, 928– 932 ,(1982) .

[30] Bahel, S.C., "Synthesis and structural studies of complexes of Zn(II),Ni(II),and Co(II) with 3– Aryloxymethyl 4–aryl–5 mercapto–1, 2, 4–triazoles", J. Indian, 1, 3 ,1127 – 1135,(1982) .

[31] Iskender, M. F., El–Sayed, L., Hefny, A. F. and Zayan, S. E., "structural studies of some metal ions", J. Inorg chem, 38 ,1 ,13 – 19,(1976) .

[32] Behei, S. C., Nath, D. N. and Srivasava, J. K., "Synthesis and structural studies of the complexes of Zn(II),Ni(II),Cu(II) and Co(II)with3– Aryloxmethyl – 4 – aryl – 5 mercapto –1,2,4 – triazoles", J. Indian chem, 1, 5, 1127 – 1135,(1982) .

[33] Greay, W.G., "Coordination chemistry reviews", 3rd. Ed., 115, Elsevier publishing company, Amsterdam (1970).

[34] Clark, R. J. and Errington, W. R., "Sulpher donor complexes", Inorg. Chem.., 5, 2, 650–660, (1980).

[35] Kadeoka, W. N., "Crystal and Molecular structure of Dichloro bis (2–pyridyl) disulphide cobalt(II)", Inorg Chem, 15, 12, 812– 820, (1976).

[36] Foresman, J.C. and Frisch, C.A., "Exploring chem., with Electronic structure methods", 2nd Ed., 101 Gaussian– Inc, pitt sub urgh,(1996)

[37] Rudolph, W. K., "Mixed chelates from thio picolinamides and β – diketones", Inorg Chem., 4, 11, 1047– 1055,(1965).

[38] El– Asmy, A. A., "Structural studies on Cd(II), Co(II) ,Cu (II) ,Ni (II) and Zn(II) complexes of 1– malonyl –bis(4-phenyl thio semicarbazide)", Transition Met. Chem, 4, 5, 12–20, (1990).

[39] Sutton, D.L., "Electronic spectra of Transition metal complexes",1st Ed., Mc Graw– Hill, London. (1969).

[40] Gajendragad, M. R. and Agarwula, U.A., "Synthesis and characterization of complexes", J. Inorg Nucl. chem., 37, 11, 29 – 35,(1975) .

[41] Figgis, B.N.and Lewis ., J. N., "Modern coordination chemistry", 3rd Ed., 304, edited by Lewis and Wilkins, R.G. Interscience, New York .(1967)

[42] Dubey, S. N. and kaushik, B. N., "Triazoles copmplexing Agent", Indian J. Chem., 24, 8, 950-959, (195).

[43] Raddy, P. M., Prasad, A. V. S. Ravinder, V., "Synthesis, Characterization of mononuclear Cr(III), Co(II), Ni(II), Cu(II) with new Schiff Base ligands", spectra chim. Acta. A., 70, 3, 704–714, (2008).

[44] Skoog, D. A., "Fundamental of Analytical chemistry", 5th Ed., 24, Wiley Inter, New York. (1988).

Preparation and Spectroscopic Study of Cr(III), Fe(III), Ni(II) and Cu(II) Complexes with New Mannich Bases Derived from 3-methyl-5-(4`-nitrophenyl)-2-(8-hydroxy quinolinol-5-yl)

Enas Mohammed Zuhair
Al-Mustansiriyah University, College of Science, Chemistry Dept.
Received 9/1/2011 – Accepted 19/11/2013

ABSTRACT

A new transition metal complexes of Cr(II), Fe(III), Ni(II) and Cu(II) have been synthesized from Mannich base (HL) derived from 3-methyl-4-(p-nitrophenyl)-2-pyrazoline and 5-amino-8-hydroxy quinolone.

The structural features were obtained from their elemental analysis, FT-IR, U.V-Vis spectroscopy, magnetic susceptibility and molar conductance activity. The data show that these complexes have composition of ML_2 for Ni(II), Cu(II) and $[ML_2(H_2O)]Cl$ for Cr(III) and Fe(III) complexes. The U.V-Vis and magnetic moments of the complexes suggest a square planer geometry for Ni(II) and Cu(II), while Cr(III) and Fe(III) were proposed as octahedral geometry.

الخلاصة

تم تحضير معقدات جديدة للفلزات الإنتقالية للكروم والحديد الثلاثية والنيكل والنحاس الثنائية مع قاعدة مانخ (HL) المشتقة من 3-مثيل-4-(بارانتروفنيل)-2-بايرازولين و 5-أمينو-8-هيدروكسي كينولين.

تم إيجاد الصيغ التركيبية المقترحة للمعقدات المحضرة إعتماداً على التحاليل الدقيقة للعناصر(C.H.N.M) والحساسية المغناطيسية للمعقدات الصلبة والأطياف الإلكترونية (U.V-Vis) وأطياف الأشعة تحت الحمراء المعززة بتحويلات فورير، إضافةً إلى قياس التوصيلية الكهربائية لمحاليل المعقدات في مذيب ثنائي مثيل سلفوكسيد.

أوضحت النتائج والقياسات الطيفية أن المعقدات تتكون من نسب مولية (1:2) (M:L) وتكون الصيغ الوضعية لمعقدي النحاس والنيكل [ML2] فيما تكون الصيغة لمعقدي الكروم والحديد [ML2(H2O)]Cl.

ومن نتائج الحساسية المغناطيسية والأطياف الإلكترونية والتحاليل الدقيقة إقترح الشكل الهندسي الثماني السطوح المنتظم لمعقدي الكروم والحديد، بينما إقترح الشكل المربع المستوي لمعقدي النيكل والنحاس الثنائيين.

INTRODUCTION

Mannich bases of 2-pyrazoline derivatives and their metal complexes have variety of applications in biological, clinical, analytical pharmacological areas [1-3]. Studies of new kind of chemotherapeutic Mannich bases are now attracting the attention of biochemists[4, 5].

The earlier work that reported the same drugs showed increased activity when administered as metal complexes rather than as organic compounds [6, 7]. A few metal (III) complexes containing 3-methyl-4-(nitrophenyl)-2-pyrazoline and other heterocyclic like quinolone have been reported [8-11].

The coordinating property of 3-substituted-2-pyrazoline ligands have been modified to give a flexible ligand system, formed by condensation with variety of reagents like aldehydes, ketons and thiosemicarbazide, formaldehyde and primary amines [12-16].

The present paper describes the synthesis of 3-methyl-5-(4`-nitrophenyl)-2-(8-hydroxy quinolinol-5-yl). Amino-methyl-2-pyrazoline (HL) by condensation of 3-methyl-5-(4`-nitrophenyl)-2-H-pyrazoline [1] with 5-

amino-8-hydroxy quinolone [2] in precence of 40% conc. formaldehyde. The present work also deals with preparation and characterization of Ni(II), Cu(II), Cr(III) and Fe(III) complexes with above mentioned new Mannich base (HL). The structure of Mannich base (HL) is shown at figure 1.

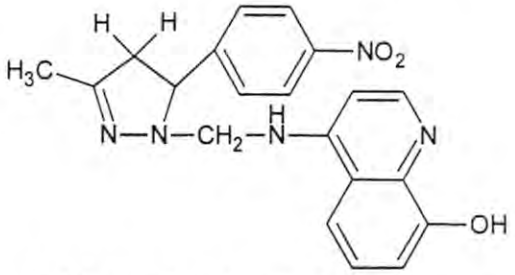

Figure-1: 3-methyl-5-(4`-nitrophenyl)-2-(8-hydroxy quinolinol-5-yl)

MATERIALS AND METHODS

All chemicals were used of Analar grade. IR spectra were recorded in KBr and CSI media on Shimadzo 8300 FT-IR spectrophotometer. U.V-Vis spectra of all complexes were measured in DMSO on Varian conc. 100%, U.V-Vis spectrophotometer. Micro analytical data were determined using an elementar vario EL at chemistry departments, King University-Jordan. Magnetic susceptibilities of the solid complexes were determined by a Gouy balance at 300°Kusing mercury (II) tetrathiocyanate, Cobaltite (II), as the calibrant. Molar conductance of the 10^{-3}M concentration of complexes solutions in DMSO were measured by using systronic Conductivity Bridge at room temperature.

Synthesis of Mannich Base (HL):

3-methyl-4-(4`nitrophenyl)-2-pyrazoline was according to method published in literature [17], as shown at scheme (1):

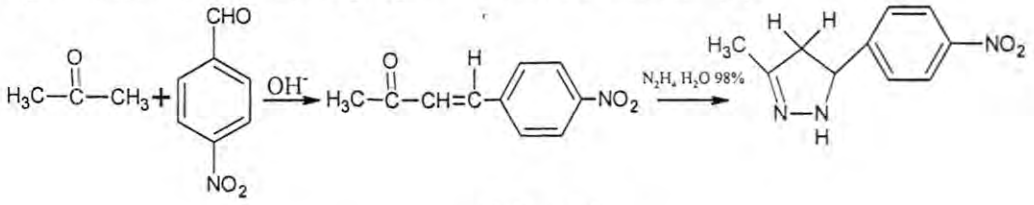

Scheme 1
Synthesis of 3-methyl-4-(4`-nitro-phenyl)-2-H-pyrazoline

The yield of the product was 85%. Found C(57.51%), H(4.51%) and N(20.01%).

Calc. C(58.21%), H(5.71%) and N(21.09%).

Preparation of 3-methyl-4-(4`nitrophenyl)-2-(8-hydroxy quinolinol-5-yl)-amino methyl-pyrazoline (HL)

A mixture of (I) compound (0.01mole, 2.02g) and formaldehyde (40%), 2.5ml) in ethanol (30ml), was stirred at room temperature with solution of 5-amino-8-quinolinol (0.01mole, 1.6g) in ethanol (12ml) for

about 1.5hrs. The solid product that separated out on standing for 2hrs, was collected by filtration, washed with ethanol and dried in desicator over $MgSO_4$ Pellets. It was recrystallized from equiquantitiz of MeOH; EtOH to yield the Mannich base (HL), having m.p. 235°C (uncorrected), scheme 2.

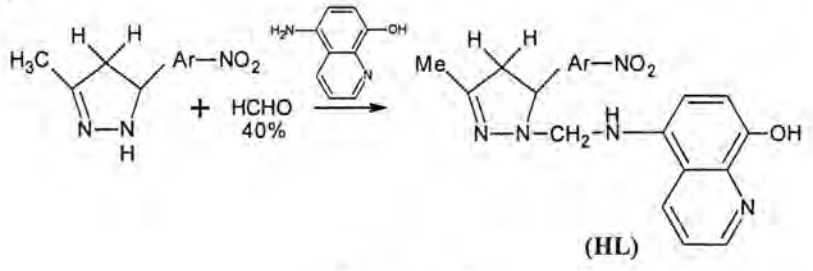

Scheme 2

Preparation of Manich Base (HL)Preparation of Metal Cr(III), Fe(III), Ni(II) and Cu(II) complexes :

Solution of metal chloride (0.001mole), $CrCl_3.6H_2O$ (0.26g), $FeCl_3.6H_2O$ (0.269g), $NiCl_2.6H_2O$ (0.237g) and $CuCl_2.2H_2O$ (0.1705g) in 15ml ethanol was refluxed with an ethanolic solution of (0.002mole, 0.752g) HL ligand for $\simeq$ 3hrs. the solution was then reduced to half on water bath. The colored solid completed precipitated, was filtered, washed several times with ethanol, water and diethylether and then dried in vacuum, scheme 3.

$$2HL + MCl_2.xH_2O \longrightarrow [ML_2] + 2HCl$$

M= Ni(II) or Cu(II)

X=6 , X=2

$$2HL + MCl_3.xH_2O \longrightarrow [ML_2(H_2O)_2]Cl + 2HCl$$

M= Cr(III) or Fe(III)

X=6 , X=6

Scheme 3: Preparation of Cr(III), Fe(III), Ni(II), Cu(II) Complexes

RESULTS AND DISCUSSION

Physical characteristics, micro analytical and magnetic susceptibility data of the complexes were given at table (1). The analytical data of all complexes correspond to the molar ratio (M:L)(1:2). Magnetic moments values of Cr(III) and Fe(III) complexes at room temperature in the range 3.05 and 2.95 BM respectively are consistent with d^3 and d^5 low spin octahedral complexes [18]. The Cr(III) and Fe(III) chelate show electronic behavior [19] in 1:1 ratio, which in well agrre with the suggested formula. On the other hand, Ni(II) and Cu(II) complexes solutions in DMSO show no appreciable conductance and this supports the hypothesis of deprotonation of Mannich Base from HL form to L^- form, so $[NiL_2]$ and $[CuL_2]$ show their neutral nature [19].

FT-IR Spectra

The FT-IR spectrum of the Mannich Base (HL), fig(1), has a medium-broad band in the range (3733-3301) cm^{-1}, which is assigned to O-H of quiniline ring [20] and N-H of methyl amino group. The breadth of this band indicates the presence of hydrogen bonds [21].

The assignments are strengthened by the disappearance of the band in metal chelates in which quinolinic protons are completely displaced by metal ions (M-O) [22]. The strong absorption in the $1635cm^{-1}$ region is assigned as the azomethine group C=N in pyrazoline and quinolone rings. In all metal complexes, $\upsilon_{C=N}$ group is shifted to lower frequency in the range $(1604\text{-}1620)cm^{-1}$, which indicate that chelation takes place through nitrogen atom of quinolone ring and oxygen atom in position (8) of quinoline. The metal complexes show new bands in the regions 393-$570cm^{-1}$ and 331-$401cm^{-1}$, which are due to formation of M-N and M-O bonds respectively [22], figures (2 &3).

Electronic Absorption Spectra :

The electronic absorption spectra of HL ligand and its Cr(III), Fe(III), Ni(II) and Cu(II) complexes were recorded at room temperature using absolute ethanol and DMSO as the solvent. The electronic spectrum of the free ligand shows, figure (6), bands at 209nm, $47846cm^{-1}$ and 307nm ($32573cm^{-1}$), which are assigned to $\pi\rightarrow\pi^*$ transitions, while the peak at 261nm ($38314cm^{-1}$) referred to change transfer band (INCT) [23]. The Cu(II) complex shows a d-d band in the region 21645-23094 cm^{-1} due to $^2B_1g\rightarrow{}^2A_1g$ and $^2B_1g\rightarrow{}^2Eg$ transitions, which supports square planar geometry [24]. Also, Ni(II) complex shows a d-d transitions in the region 21834 cm^{-1} due to $A_1g^1\rightarrow B_1g^1$ and other peak in the region $27100cm^{-1}$ due to change transfer (MLCT), which again suggests square-planar geometry [23], figures (7, 8).

The Electronic Spectrum of Cr(III) complex was shown at figure(9), indicates the transition of $A_2g^4\rightarrow T_2g^4$ and $A_2g^4\rightarrow T_1g^4$ in the regions 22222-$15290cm^{-1}$, which investigate the regular octahedral geometry around Cr(III) ion [24]. On the other hand, the term ligand of Fe(III) ion in the low spin state I^2 splits to $^6A_1g\rightarrow{}^4T_2g$ (G), this is obviously shown at figure (10), which supports the octahedral geometry around Fe(III) ion [25].

We have synthesized Cr(III), Fe(III), Ni(II) and Cu(II) complexes using the Mannich Base (HL) formed by condensation of 5-amino-8-hydroxy quinolone and 3-methyl-4-(4`-nitrophenyl)-2-H-pyrazoline (I) in presence of H_2O (40% w/v). the complexes were characterized by spectral and magnetic studies to establish the proposed four coordinated square-planar geometry around Ni(II), Cu(II) ions and six coordinated octahedral geometry Cr(III) and Fe(III) ions. It could be concluded from the elemental analysis, magnetic moments and electronic spectra data and

the proposed structure of the prepared complexes, which are shown below:

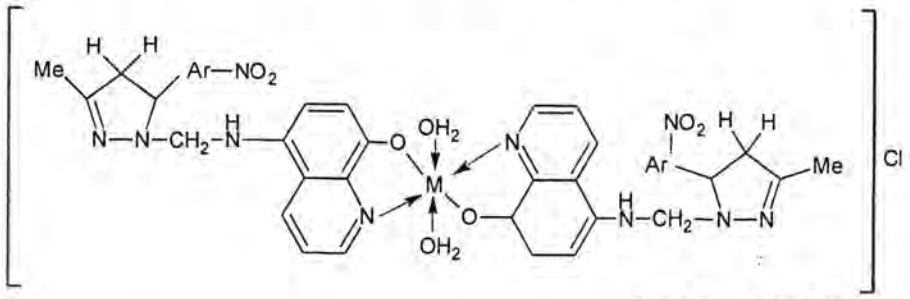

M= Cr(III) and Fe(III)

Chart (II) : Proposed Structure of Octahedral Complexes $[ML_2(H_2O)]Cl$

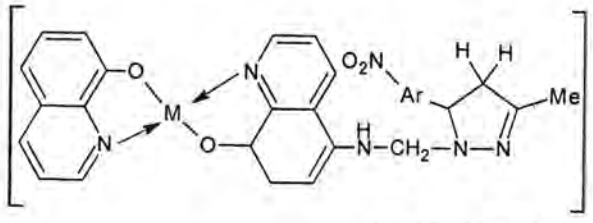

M= Ni(II) and Cu(II)

Chart (III) : Proposed Structure of Square-Planer Complexes $[ML_2]$

Table -1 : Physical Characteristics, Analytical Data and Magnetic Moments of the Prepared Compounds.

Comp.	Color /m.p.°C	Elemental Analysis (%) Found Calc.				μeff (B.M)
		M	C	H	N	
HL	Pale yellow/ 235-237	-	62.91 (63.80)	3.99 (4.78)	19.21 (18.61)	-
$[CrL_2(H_2O)_2]Cl$	Green / 315[d]	7.21 (6.51)	57.81 (58.42)	4.51 (4.62)	18.00 (17.04)	3.05
$[FeL_2(H_2O)_2]Cl$	Brown / 350[d]	6.99 (6.82)	58.01 (58.25)	4.11 (4.61)	17.21 (16.99)	2.95
$[NiL_2]$	Orange / 358[d]	7.51 (6.99)	58.90 (59.31)	3.81 (4.30)	16.41 (17.91)	Di
$[CuL_2]$	Red / 362[d]	6.25 (7.47)	55.77 (55.50)	3.75 (4.23)	17.01 (16.48)	1.73

Table -2 : The Characteristic Infrared Spectral Data of the Ligand (HL) and its Metal Complexes

Comp.	υNH, υOH	υC=N, $υNO_2$	υC-H, $δCH_2$	(O-H) rock	υM-N, υM-O
HL	3301(m), 3733	1635(s) 1458(s)	2985-2877(m), 763(w)	586.2	-
CrL	3355(m) 3448($υH_2O$)	1604(s) 1450(s)	2947(m) 732(rock)	617	570(w), 416 1542*
FeL	3425-3268	1612(S) 1473(s)	2939-2761	559(m)	331-555(w) 1562(s)
NiL	3425-3317(br)	1620(s) 1458(s)	2985-2877 (709)	632(w)	401(m) 524(w)
CuL	3324(br)	1612(s) 1442(s)	2977-2884 (735)		524(w) 393(w)

br=broad, m=medium, s=strong.

* Rocking of water molecular in Cr^{III} and Fe^{III} complexes

Table -3 : Electronic Spectral Data λ_{max}(nm) and Molar Conductance Λ_m in DMSO Solutions of the Prepared Complexes

Comp.	λ_{max} cm^{-1}	Assignment	Λ_m*(ohm^{-1} (m^2 mol^{-1}))	Geometry
HL	209 261 (16201)* 307 (1830)*	$\pi\rightarrow\pi^*$ $n\rightarrow\pi^*$	-	-
CrL	220 450 654	$\pi\rightarrow\pi^*$ $A_2g^4\rightarrow T_2g^4$	92	Regular Octahedral
FeL	205 271 (25900) 425	$\pi\rightarrow\pi^*$ C.T (MLCT) d-d	87	Octahedral
NiL_2	213 364 458	$\pi\rightarrow\pi^*$ $^1A_1g^1\rightarrow{}^1A_2g^1$ $^1A_1g^1\rightarrow{}^1B_1g^1$	22	Square Planar
CuL_2	276 217 433 462	M→L C.T $\pi\rightarrow\pi^*$ $^2B_1g\rightarrow{}^2A_1g$ $^2B_1g\rightarrow{}^2Eg$	-	Square Planner

*=molar extinction coefficients in $L.mol^{-1}.cm^{-1}$ units
** = Λ determined in DMSO solvent.

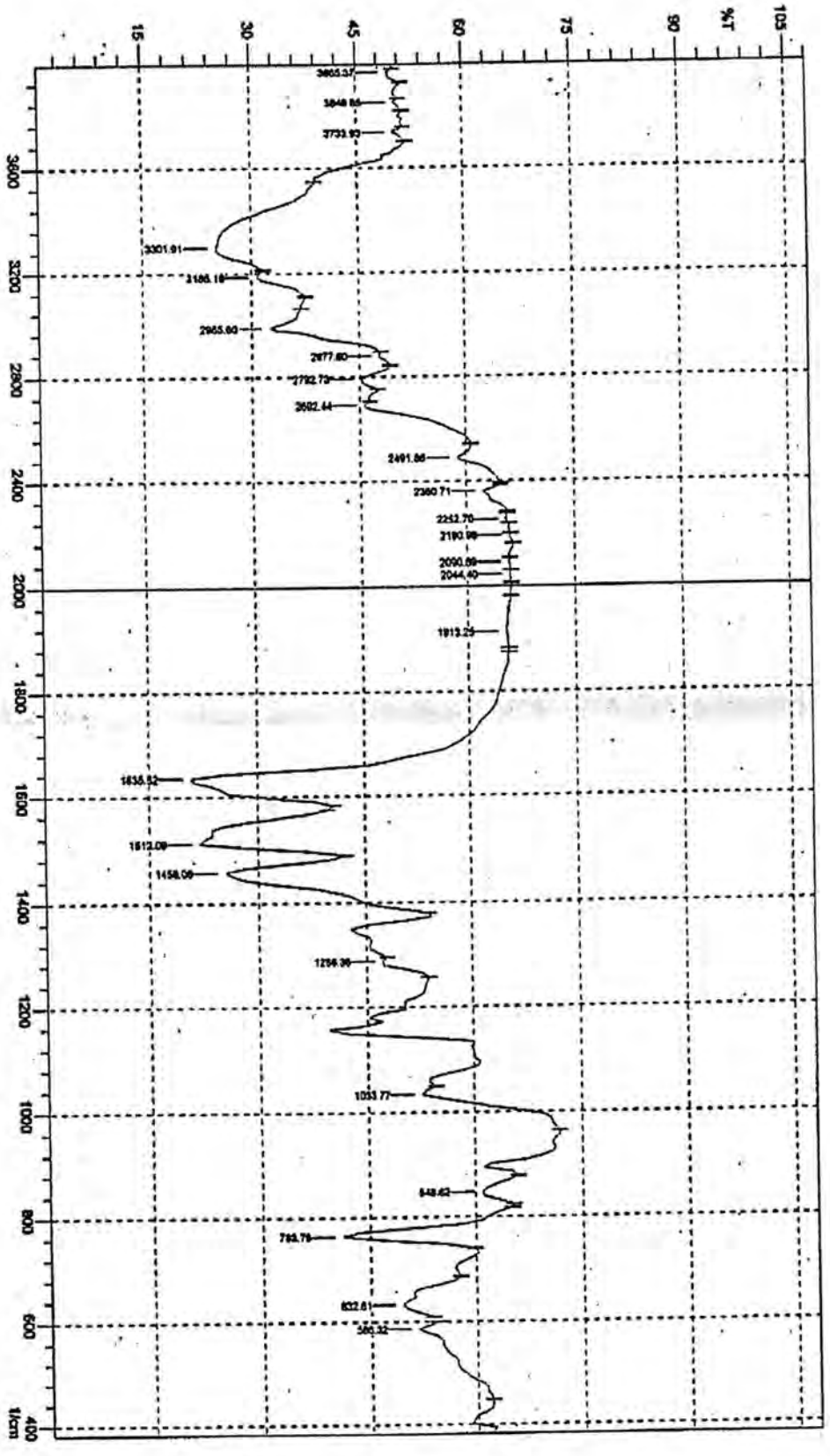

Figure -1: The FT-IR Spectrum of (HL)

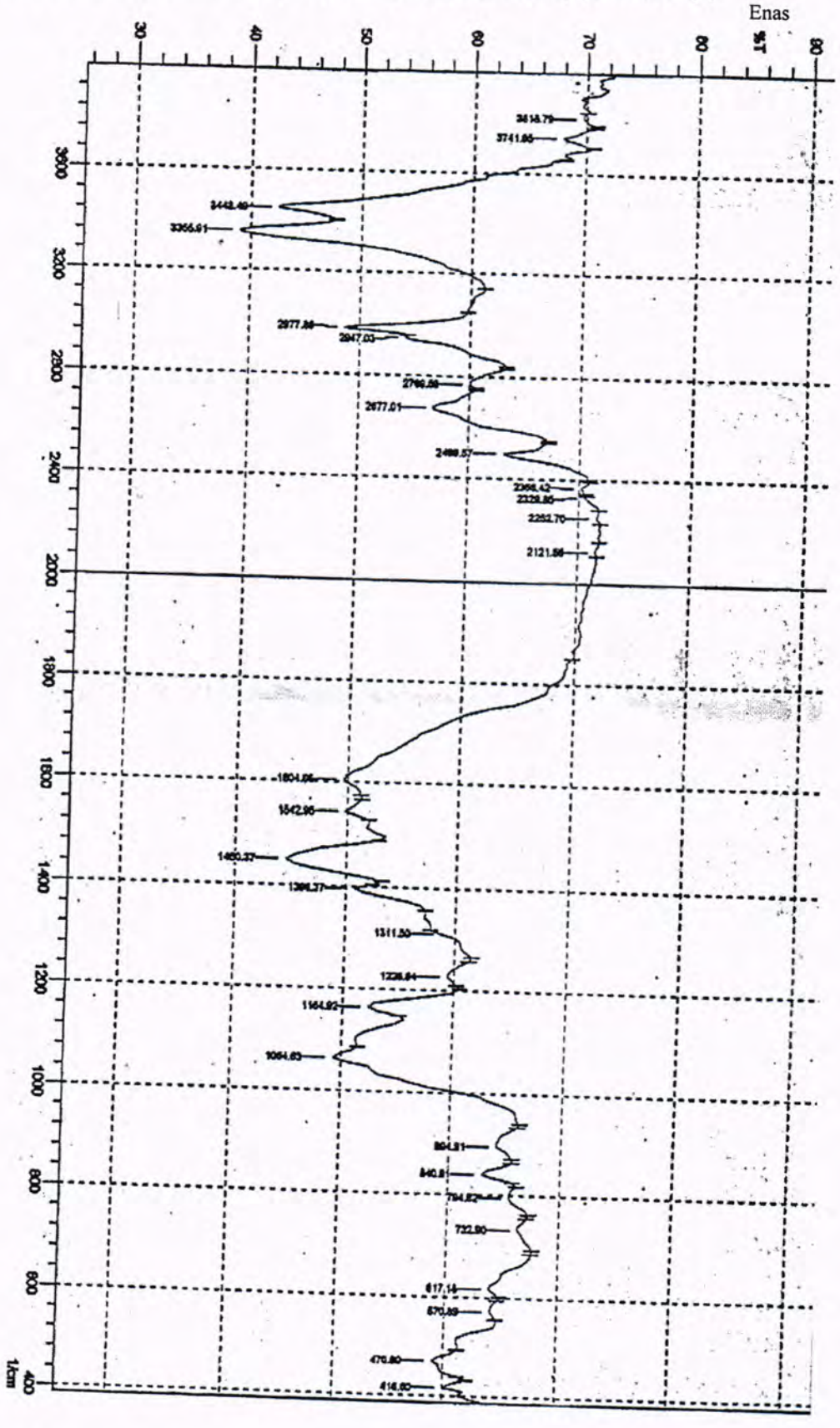

Figure -2 : The FT-IR Spectrum of [CrL]

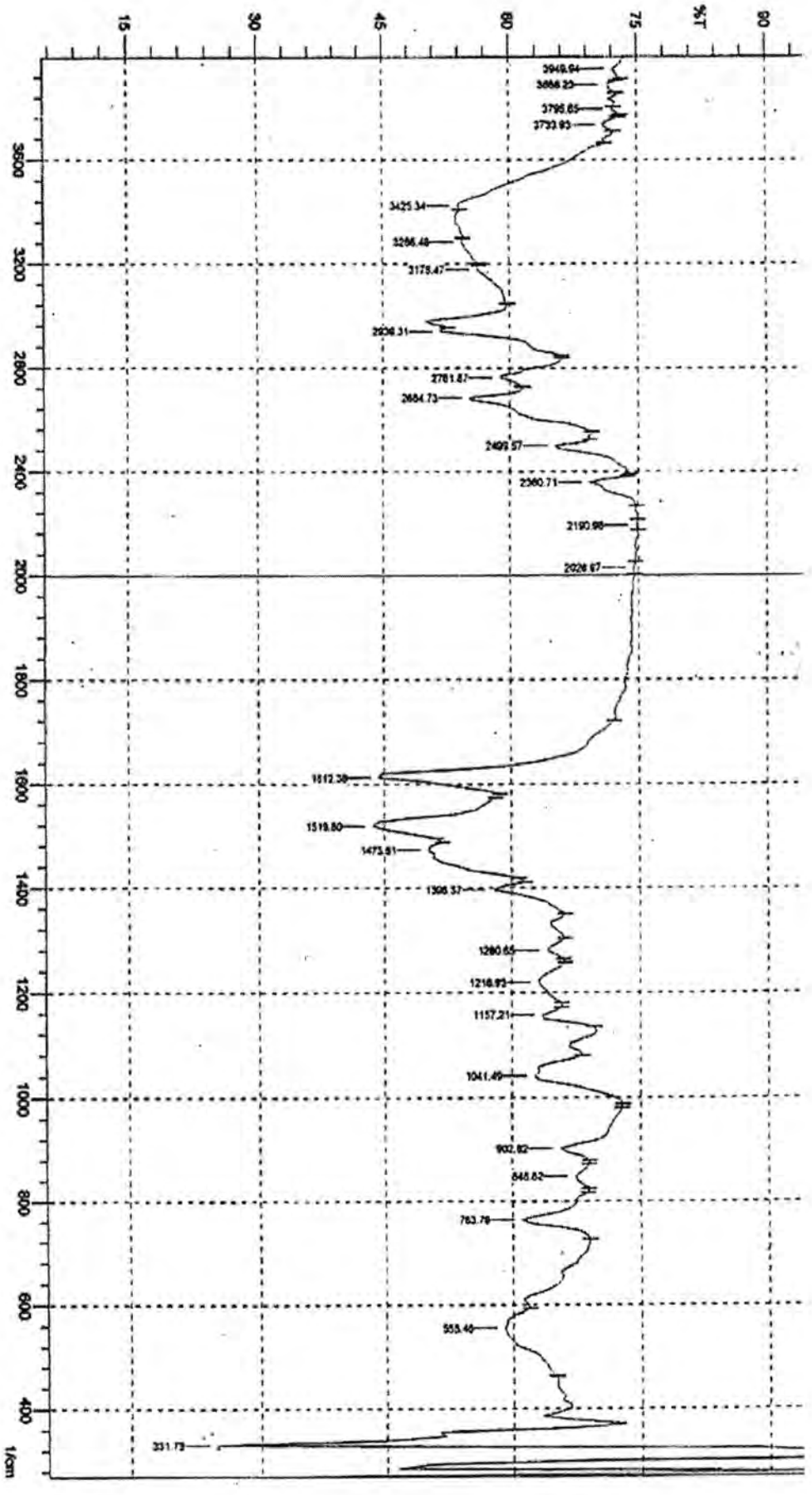

Figure -3 : FT-IR Spectrum of [FeL]

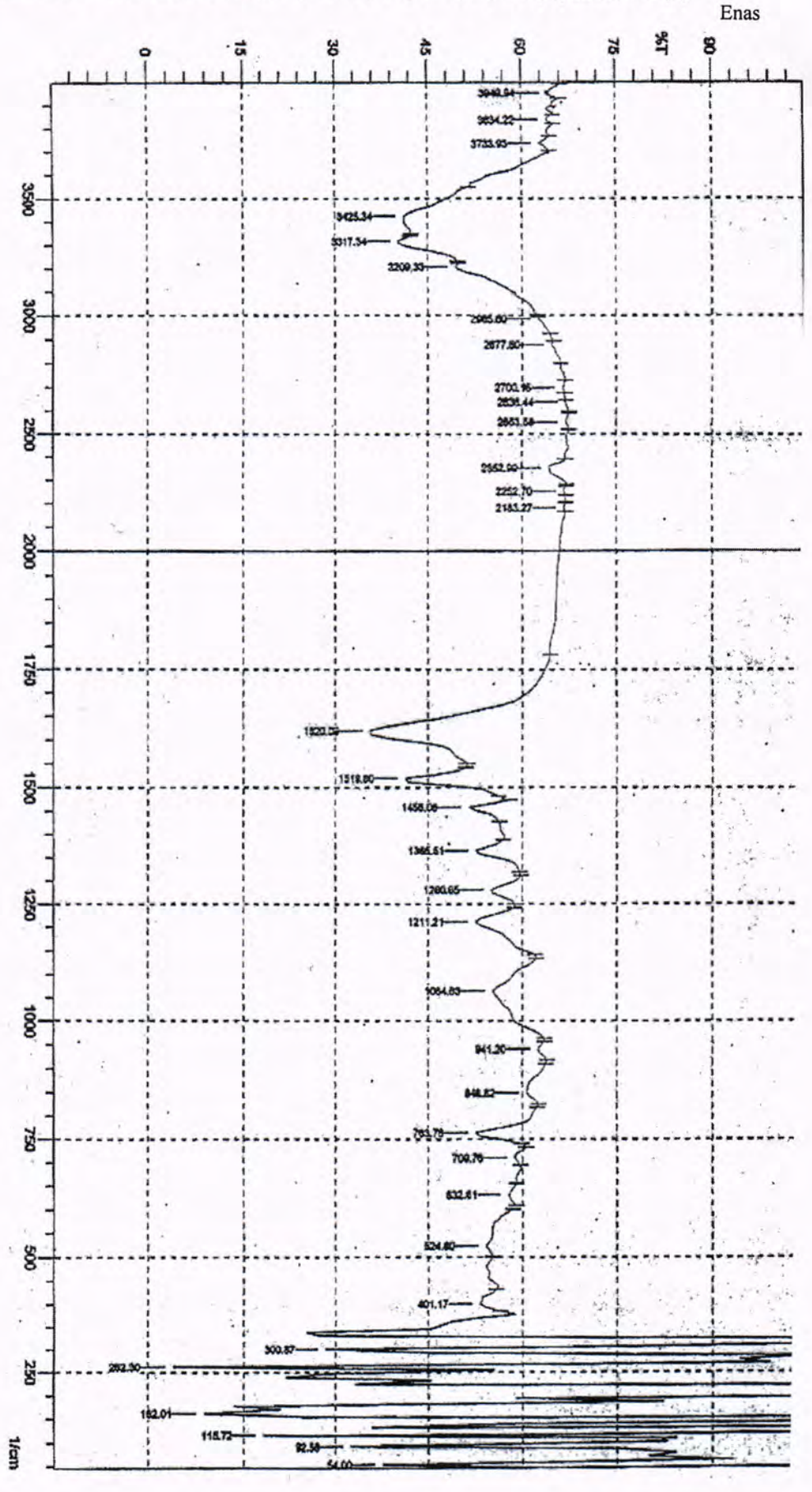

Figure -4 : FT-IR Spectrum of [NiL]

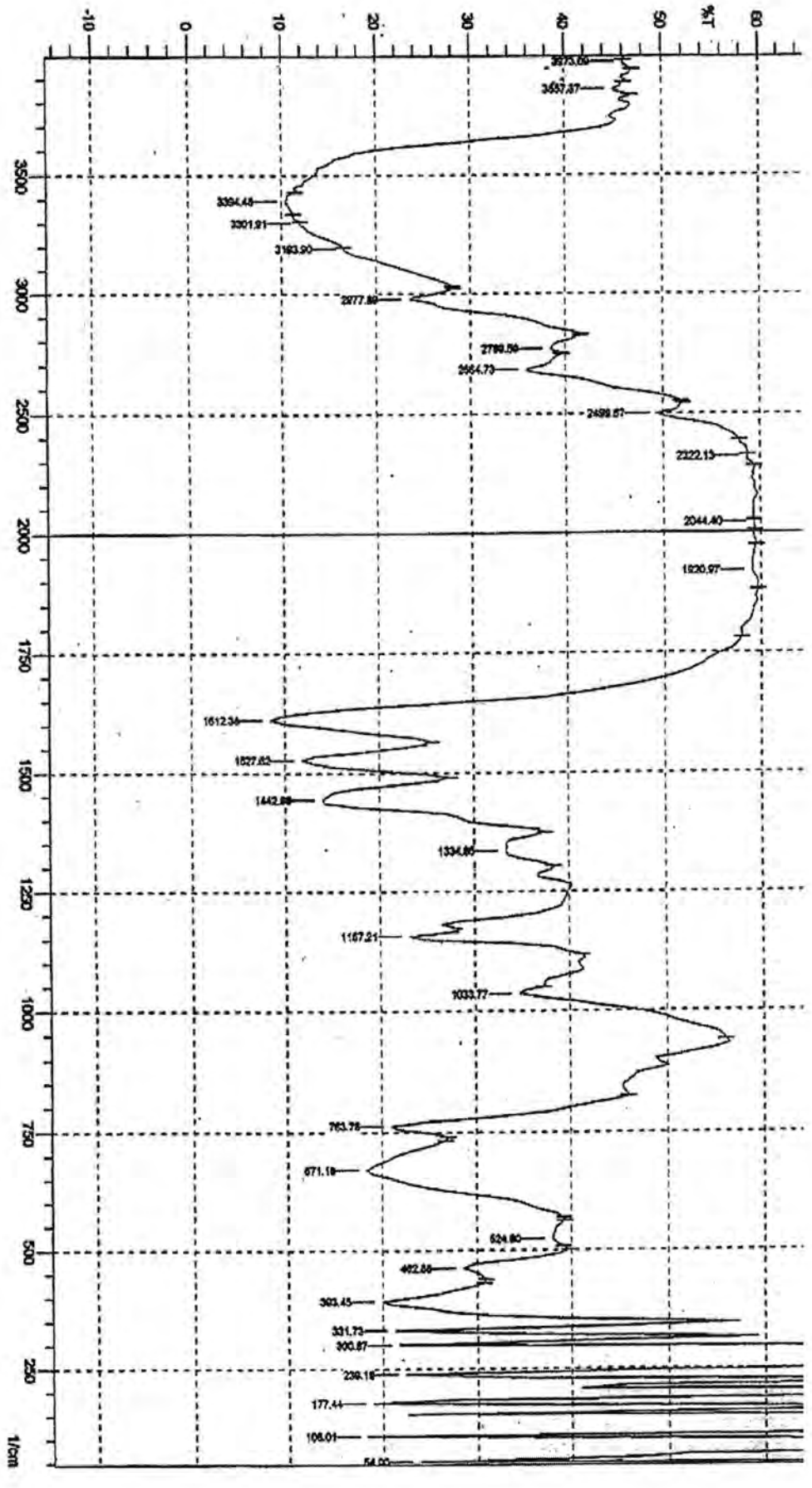

Figure -5 : FT-IR Spectrum of [CuL]

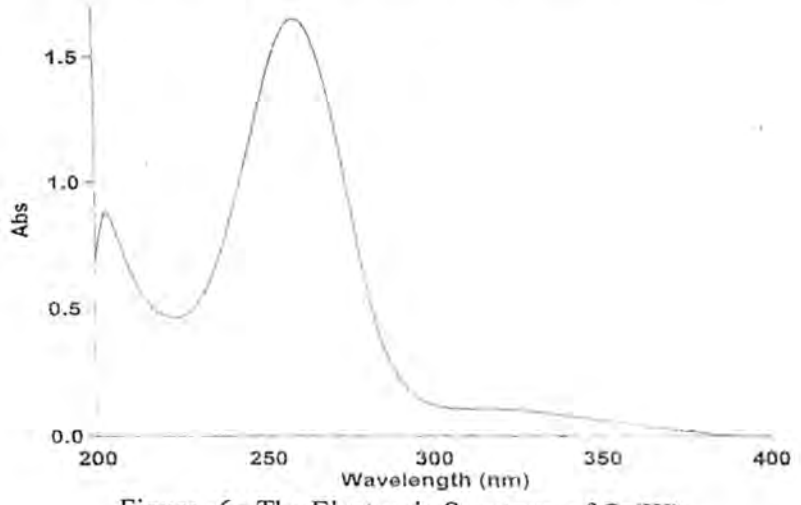

Figure -6 : The Electronic Spectrum of Cr(III)

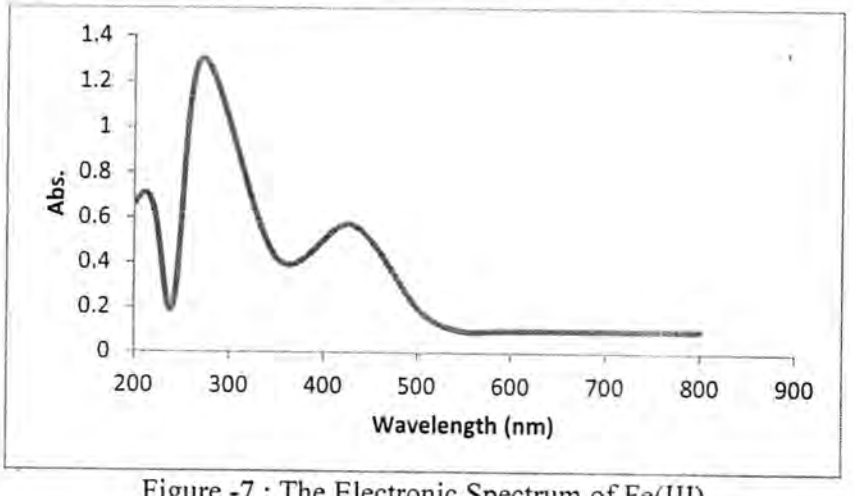

Figure -7 : The Electronic Spectrum of Fe(III)

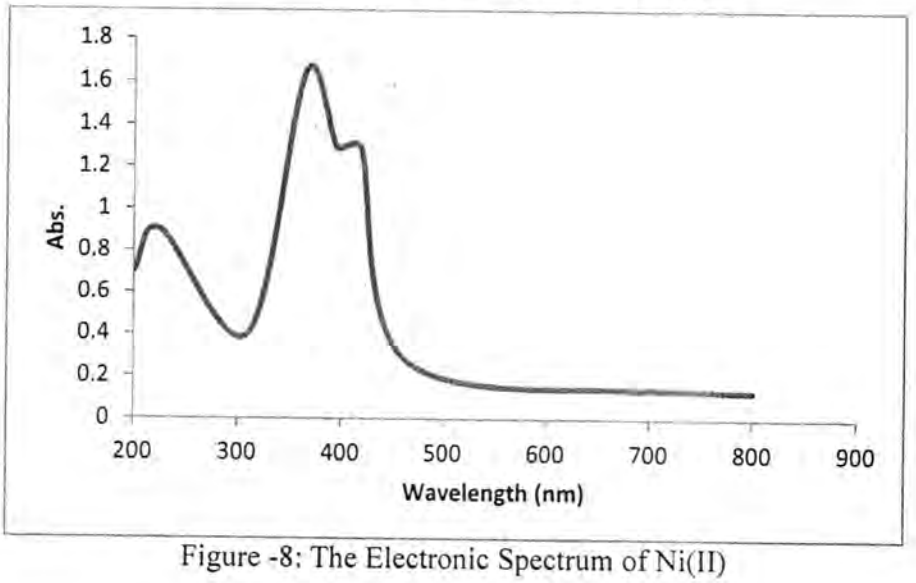

Figure -8: The Electronic Spectrum of Ni(II)

REFERENCES

[1] Rehse K. and Mullaer U., " New NO-Donors with Antithrombotic and Vasodilating Activities, Part 13: Pyrazol-4-one 1,2-Dioxides and 4-Hydroxyiminopyrazole 1,2-Dioxides", Arch Pharm. (Weinhiem), 328, 765, (1995).

[2] Kuznetsov M. I., Dement ev A. I. and Zhorink VV, ") Ab Initio Study of Structure, Protonation and omplex formation of novel pyrazolone-5 derivatives", J Mol Struct (THE OCHEM), 571, 45, (2001).

[3] Dimmock J. R., Vashishtha S. C. and Stabks J. P., J Med Chem., 35, 241-248, (2000).

[4] Liu Guong Fei, Lui Lang, Hu Xin, Jiu Dian-Ze and Yu Kia-Bei, "Synthesis,crystal structure and biological activity of diacetylferrocene-S-methyldithiocarbazate Schiff-base", Chinese J Struct Chem, 25(10), 1233-1237, (2006).

[5] Karodawado M. J. and Rona A. K., "Synthesis, Crystal Structural Characterization and Biological Properties of Thiosemicarbazones of Schiff Bases Derived from 4-Acyl-2-pyrazoline-5-one", Synth React Inorg Met Org. Chem., 33(8), 1483-1504, (2003).

[6] Kumar S., Bawa S. and Rajiv K., "Enantioselective Epoxidation of Unfunctionalized Olefins Catalyzed by Chiral Salen-mn (III) Catalyst by Axially Coordination Grafted on Novel Types of Layer Crystalline ZnPS-PVPA", J Med Chem., 4, 154-163, (2009).

[7] Abid M., Azam A., "Synthesis and antiamoebic Activities of 1-N-Substituted Cyclized Pyrazoline Analogue, of thiosemicarbazones". Bioorg. Med. Chem., 13, 2213-2220, (2005).

[8] Budakoti A., Bhat A. R., Athar F., Azam A., "Synthesis and Evaluation of 3-(3-bromo phenyl)-5-phenyl-1-(tiazolo[4,5-b] quinoxaline-2-yl)-2-pyrazoline Derivatives", Eur. J. Med. Chem., (2008).

[9] Joaquain B., Koen C., Raquel G., Stephen H. and Persoons A., "Spectroscopic Properties of Inorganic and Organometallic Compounds", J. Luis and Sexenu, J. Inorg. Chem. Acta., 8, 1925, (1998).

[10] Reiners C. S., "Use of cox-2 inhibitors for preventing immunodeficiency", Chem. Uns. Zei, 2:110, (2001).

[11] Anwander R., "Top Organomethalic Chem. Speinger Verlay", Berlin, Hers-delbery, New York, (1999).

[12] Patel B. N., Patel P. S. and Patel V. G., "Synthesis, characterization and antimicrobial activity of metal chelates of 2-(8-Quinolinol-5-yl)-amino methyl-3(4-methyl phenyl)-5-(phenyl)-pyrazoline", Pharm Chemical J., 2(1), 295-300, (2010).

[13] Patel P.S., Soha R. A., Trivedi D. K. and Vyas P. T., "Application of MATHCAD for Hydrological Analysis Using Kostikov's Method", Asian Journal of Chemical and Environmental Research, 2(2-1), 6, (2009).

[14] Anil B. and Mardi N., "Studies in Influence of Dielectric Constants on Complex Equilibria between Substituted Pyrazolines and Lanthanide Metal Ions Ph Metrically", J. Am. Chem. Soc., 3(2), 212-216, (2008).

[15] Sondawale P. J. and Narwode M. L., "Effect of Dielectric Constants of Ethanol-Water and Acetone-Water Mixtures on Proton-Ligand and Metal-Ligand Stability Constants of Cu(II)-o-Aminobenzene Sulphonic Acid Complexes", Asian J. Chem., 9(3), 749, (1997).

[16] Taylor E. C. and Morrison R. W., J. Org. Chem., 32, 2379, (2005).

[17] Crawly L. S. and Franshawe W. J., "Neighboring group participation in cyclodehydration A regiospecific · isoxazole synthesis", J. Heterocyclic Chem., 14, 531, (1977).

[18] Raman N., Muthuray V., Ravi Chandran S. and Kulandaismay A., "Synthesis, characterisation and electrochemical behaviour of Cu(II), Co(II), Ni(II) and Zn(II) complexes derived from acetylacetone and p-anisidine and their antimicrobial activity", Proc. Indian J. Chem., 3(115), 161-167, (2003).

[19] Duta R. L. and Syamal A., , "Elements of Magretochemistry", 2nd Ed., New Delhi, Elsevier, (1992).

[20] Rsilverstein M., Basseler C. G. and Moril T. E., "Spectroscopic Indentification of Organic Compounds", John Wiley, New York, (1981).

[21] Nekamato K., "Infrared and Raman Spectroscopy of Inorganic and Coordination Compounds", London Interscien Co., (1978).

[22] West D. X. and Mc. Donald L. A., "Cu(II) complexes of N-isopropyl-2-picolinamine N-oxide", J. Inorg. Nucl. Chem., 43, 1507, (1981).

[23] Lever A. B. P., "Inorganic Spectroscopy of Inorganic Compounds", Elseiver Publishing Comp. London, (1968).

[24] Sarojin T. and Ramachandraih A., "Synthesis and characterization of copper(II), cobalt(II), nickel(II), iron(II) and oxovanadium(IV) chelates of a new pair of Schiff base ligands derived from 1, 3-bis(aminomethyl)cyclohexane", J. Indian Chem., 35A, 940, (1996).

[25] Mishra S. and Chatu Vedi N., "Solvent Extraction of U(VI) & Mo (VI) from aqueous HCl Media by organophosphinic, phosphonic acids and their binary mixtures", J. Indian Chem., 10, 7, (1994).

Synthesis, Characterization and Anti-bacterial Activities of Some New β-Lactam Thiadiazole Derivatives

Abdul-Jabar Khalaf Atia[1], Fouad Mohamed Said[2] and Aoras Ameen Kadhim[3]
[1,2] Department of Chemistry ,College of Science, Al-Mustansiriya University, Baghdad, Iraq
[3] Department of Medical Chemistry, College of Medicine, University of Wassit, Wassit, Iraq.
Received 28/10/2013 – Accepted 23/2/2014

الخلاصة

كجزء من متطلبات البحث تم تحضير ودراسة الفعالية البايولوجية لعدد من المركبات الجديدة ومن ضمنها تحضير المركبات: 3-bromo-4-aryl-1-[5-(methylthio -or- methylsulfonyl)-1,3,4-thiadiazol-2-yl]azetidin-2-one[D_{10}-D_{15}] من المركبات: 5-[(Arylidene)amino]-2-(methylthio)-1,3,4-thiadiazol [D_4-D_6] 5-[(Arylidene) amino]-2-(methylsulfonyl)-1,3,4-thiadiazol [D_7-D_9] باستخدام 5-Amino-1,3,4-thiadiazole-2-thiol كمادة اولية في التخليق. تمت دراسة الفعالية البايولوجية لبعض المركبات المحضرة ضد اربعة انواع من البكتريا والمتضمنة (Staphylococcus aureus, Bacillus subtilis) gram-positive, (E. coli, Pseudomonas) gram-negative كما شخصت المركبات المحضرة باستخدام تقنية التحليل الدقيق للعناصر والتحاليل الطيفية المتضمنة (H^1-NMR, IR and UV. Visible).

ABSTRACT

As a part of systematic investigation of synthesis and biological activity of several new 3-bromo-4-aryl-1-[5-(methylthio -or- methylsulfonyl)-1,3,4-thiadiazol-2-yl]azetidin-2-one [D_{10}-D_{15}] have been synthesized from 5-[(Arylidene)amino]-2-(methylthio)-1,3,4-thiadiazol [D_4-D_6] and 5-[(Arylidene) amino]-2-(methylsulfonyl)-1,3,4-thiadiazol [D_7-D_9] using 5-Amino-1,3,4-thiadiazole-2-thiol as the starting material. Some of the synthesized products were evaluated for their antibacterial activity against gram-positive (*Staphylococcus aureus, Bacillus subtilis*) and gram-negative (*E. coli, Pseudomonas*) bacteria. The structure of all the compounds was confirmed by using physical methods such as ^{1}H-NMR, IR, UV. visible and elemental analysis.

INTRODUCTION

β-lactam drugs are most widely prescribed antibiotics used in medicine. 2-azetidinone derivative possess wide therapeutic activity like antifungal, anticonvulsant, antitumour, antiviral, cholesterol absorption inhibitior and enzyme inhibition activities.[1,2] Also β-Lactam antibiotics (e.g. ampicillin, amoxicillin) are traditionally used for the treatment of common bacterial infections in both humans and food-producing animals. β-Lactam residues in foods can result in the development of new strains of bacteria resistant to these antibiotics and in allevgic reactions.[3]

1,3,4-thiadiazole derivatives posses interesting biological activity due to strong aromaticity of the ring system which give it stability and generally, a lack of toxicity for higher vertebrates, including humans when diverse functional group that interact with biological receptor are

attached to aromatic ring.[4] Considering the above facts, the goal of the present study was to synthesize some β-lactams derivatives which combine substituted 1,3,4-thiadiazoles in order to develop hybrid molecules with potential of enhanced biological activity.

MATERIALS AND METHODS

All melting points are uncorrected and were determined by open end capillary tube method in Gallen Kamp MFB-600-Melting Point apparatus melting point apparatus. The FTIR spectra were recorded on a Shimadzu FT-IR 8400s spectrophotometer using KBr discs. ^{1}H-NMR spectra were recorded on Burker DMX- 500 NMR SPECTROPHOTOMETER on a 300 MHz, with TMS as internal standard and DMSOd6 as a solvent . UV spectrophotometer using UV-1650PC spectrophotometer and absolute ethanol as solvent. The physical data of all the synthesized compounds is presented in Table 1.

Synthesis of 5-[(Arylidene)amino]-1,3,4-thiadiazole-2-thiol [D_1-D_3] [5]:

A mixture of compound 5-Amino-1,3,4-thiadiazole-2-thiol (1.33 gm, 0.01 mole), aromatic aldehyde (0.01 mole) and NaOH (0.4 gm) in ethanol was refluxed for 4 h. The solvent was concentrated under reduced pressure, poured into water (100 mL) and neutralized with dilute HCl (1 mL, 25%). The precipitate was filtered off and recrystallized from ethanol: water mixtuer (3:7) to give compounds [D_1-D_3]. The physical properties were listed in table [1].

Synthesis of 5-[(Arylidene)amino]-2-(methylthio)-1,3,4-thiadiazol [D_4-D_6] [6]:

Compound [D_1-D_3] (0.01 mole) was suspended in distilled water (20ml), then triethylamine (1.01gm, 0.01 mole) was added and stirred for 10 minute at room temperature, and then brought the mixture to 0°C in ice bath and CH_3I (1.41gm, 0.01 mole) was added drop wise with vigorous stirring, then stirring was continued for 3 hr., the powder product [D_4-D_6] was isolated by filtration and recrystallized from ethanol. The physical properties were listed in table [1].

Synthesis of 5-[(Arylidene)amino]-2-(methylsulfonyl)-1,3,4-thiadiazol [D_7-D_9] [7]:

Compound [D_4-D_6] (0.001mole) was dissolved in ethanol (30ml), H_2O_2 (32%) (0.068 gm, 0.002mole) was added with continues stirring at room temperature for 2 hrs., then the excess of solvent was evaporated to give compounds [D_7-D_9], and recrystallized from ether. The physical properties were listed in table [1].

Synthesis of 3-bromo-4-aryl-1-[5-(methylthio -or- methyl sulfonyl)-1,3,4-thiadiazol-2-yl]azetidin-2-one[D_{10}-D_{15}][8]:

mixture of bromoacetic acid (0.74gm , 0.0053mole), imine [D_4-D_6] (0.0035mole) and triethylamine (1.074 gm , 0.01mole) in dry dichloro-

methane 40 ml at 0°C under inert gas (N_2 gas) , a solution of $SOCl_2$ (0.63gm , 0.0053mole) in dry dichloromethane 20 ml was added as drop wise . The mixture was stirred overnight at room temperature. Thereafter ,the mixture were washed successively with 1N HCl 30ml,water (3×30ml) ,5% $NaHCO_3$ 30ml. The organic layer was separated and dried over anhydrous sodium sulphate (Na_2SO_4).The solvent was removed under reduced pressure and the crude product was recrystallized from water furnished pure β-lactam [D_{10}-D_{15}]. The physical properties were listed in table [1].

Antibacterial Activity Tests

The compounds were investigated against gram-positive (Staphylococcus aureus, Bacillus subtilis) and gram-negative (E. coli, Pseudomonas). The antibacterial activity tests were performed according to agar diffusion method [9] using gentamicin (CN), Tetracycline (TE) and amoxicillin (*AX*) as the reference compounds. The sterile cotton swabs were separately dipped into each of the adjusted organism cultures and excess inoculum was removed by pressing and rotating the swab firmly several times against the wall of the tube above the level of the liquid.

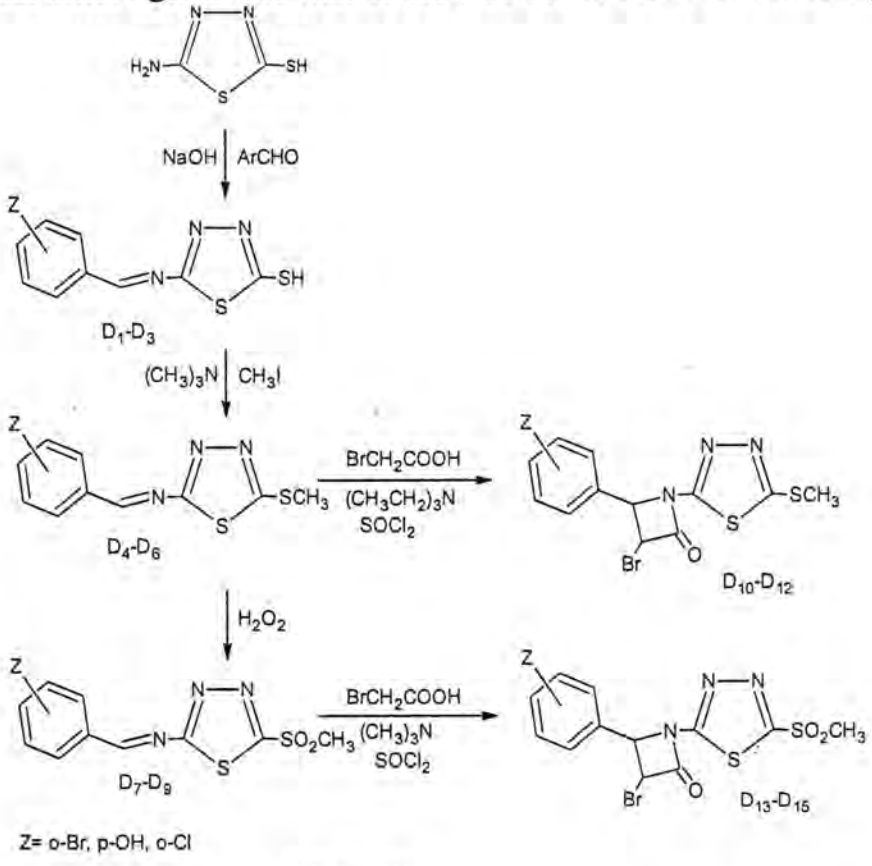

Scheme (1)

The swab was streaked all over the surface of the nutrient agar in three dimensions at an angle of 60° to obtain an even distribution of the

inoculum. The plates were then left to dry at room temperature for few minutes. Disks impregnated with DMSO solutions of the compounds under study (75, 125, 250 and 500 μg/disk) were placed on the surface of precultured agar. The plates were then incubated for 24 h at 37°C and inhibitory zones were recorded.

RESULTS AND DISCUSSION

The synthesis of 3-bromo-4-aryl-1-[5-(methylthio -or- methyl sulfonyl)-1,3,4-thiadiazol-2-yl]azetidin-2-one [D_{10}-D_{15}] was achieved through the synthetic routes outlined in scheme 1. The 5-Amino-1,3,4-thiadiazole-2-thiol, after treatment with three different aromatic aldehydes in alkali media (sodium hydroxide in ethanol) were converted to schiff's bases [D_1-D_3]. After treatment with methyl iodide, the [D_1-D_3] intermediary were converted into the 5-[(Arylidene)amino]-2-(methylthio)-1,3,4-thiadiazol [D_4-D_6]. The last compounds were then oxidized by using hydrogenperoxide to produce 5-[(Arylidene)amino]-2-(methylsulfonyl)-1,3,4-thiadiazol [D_7-D_9]. The compounds [D_4-D_9] on treatment with bromoacetic acid in the presence of thionyl chloride and triethyl amine afforded 3-bromo-4-aryl-1-[5-(methylthio -or-methylsulfonyl)-1,3,4-thiadiazol-2-yl]azetidin-2-one [D_{10}-D_{15}]
Structures of all products were confirmed by analytical and spectral methods. The IR spectra of compounds [D_1-D_3] showed disappearing of (N–H) band for ($-NH_2$) group and the (C=N) stretching band at (1616-1670 cm^{-1}) in addition to stretching band at 3261 for tautomerism (S–H) with (N–H) grope. The ^{1}H-NMR of compound [D_2] showed δ 4.68 (s, 1H, NH), δ 6.92-7.77 (d-d, 4H, Ar–H), δ 9.78 (s, 1H, –N=CH) and δ10.58 (s, 1H, OH). UV spectrum of compounds [D_1-D_3] showed intense maxima at (253 nm) and (352 nm) refering to $\pi\rightarrow\pi^*$ and $n\rightarrow\pi^*$ electronic transition respectively. While the compounds [D_4-D_6] showed disappearing of (N–H) band for (>NH) group in the ring structure. UV spectrum of compounds [D_4-D_6] mostly showed intense maxima at (254 nm) and (368 nm) refering to $\pi\rightarrow\pi^*$ and $n\rightarrow\pi^*$ electronic transition respectively.

The IR spectra of the compounds [D_7-D_9] showed the strong stretching band of (S=O) at (1357-1309 cm^{-1}) for asymetric stretch and (1199-1155) for symetric stretch. The ^{1}H-NMR of compound [D_8] showed δ 2.75 (s, 3H, CH_3), δ 6.91-7.89 (d-d, 4H, Ar–H), δ 8.72 (s, 1H, –N=CH) and δ10.60 (s, 1H, OH). UV spectrum of these compounds showed intense maxima at (242 nm) and (368 nm) due to $\pi\rightarrow\pi^*$ and $n\rightarrow\pi^*$ electronic transitions. In addition a comparison of the found composition of C.H.N. analysis with the calculated values confirmed the structure and purity of the synthesized compounds [D_5]

Also the compounds [D_{10}-D_{15}] were showed (C=O) stretching band at (1702-1735 cm^{-1}). The ^{1}H-NMR of compound [D_{12}] showed δ 2.50 (s, 3H, CH_3), δ 3.68 (d, 1H, N–CH), δ 3.82 (d, 1H, Br–CH), and δ 7.33-7.64 (m, 4H, Ar–H). farther more the ^{1}H-NMR of compound [D_{13}] showed δ 3.76 (s, 3H, CH_3), δ 4.17 (d, 1H, N–CH), δ 4.41 (d, 1H, Br–CH), and δ 7.00-7.19 (m, 4H, Ar–H). UV spectrum of these derivatives showed intense maxima at (236 nm) and (313 nm) which belonged to $\pi \rightarrow \pi^*$ and $n \rightarrow \pi^*$ transitions. Spectral data were listed in (table 2). The mechanism of the reaction is believed to be as follows:

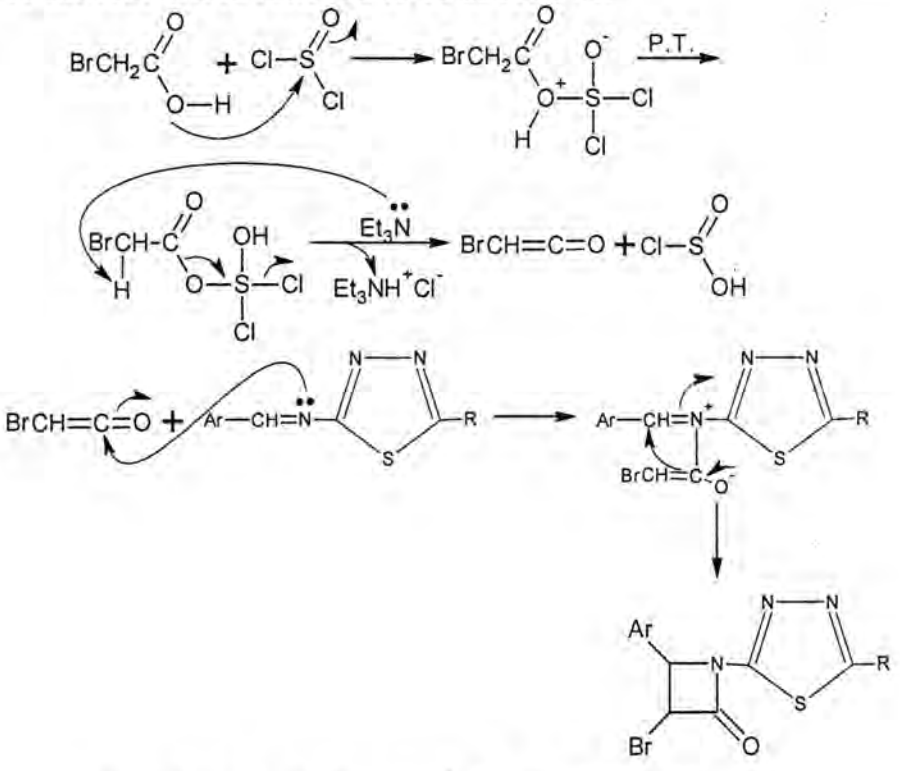

Ar=o-Br-C_6H_4-, p-HO-C_6H_4-, o-Cl-C_6H_4- R= -SCH_3, -SO_2CH_3

Biological screening: antimicrobial activity tests

The antibacterial activities of compounds [D_7-D_{15}] were tested against the micro-organisms. After incubation, the diameters of inhibition zones around the wells were measured, to the nearest mm, in three different directions using a ruler and the average diameter was recorded and compared to that of the control. From the data presented in Table 3 it is clear that compounds [D_{13}-D_{15}] were good to moderate activity against all species, while [D_{11}-D_{12}] exhibit low activity against all species but the other compounds [D_7-D_{10}] were found to be moderately active to the microorganisms.

Table-1: Physical properties of compounds [$D_1 - D_{15}$]

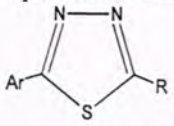

Comp. No	Ar	R	M.P (C °)	Yield %	Colour	Purification solvent
D_1	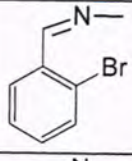	-SH	180-182	66	Yellow	EtOH:H_2O (3:7)
D_2	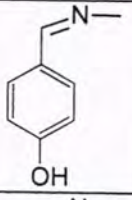	-SH	190-192	79	Orange	EtOH:H_2O (3:7)
D_3	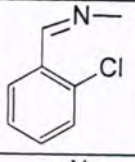	-SH	210-212	60	Yellow	EtOH:H_2O (3:7)
D_4	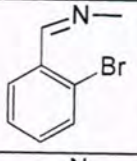	$-SCH_3$	142-144	66	Brown	EtOH
D_5	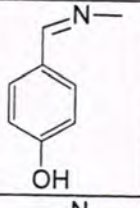	$-SCH_3$	176-178	74	Peach	EtOH
D_6	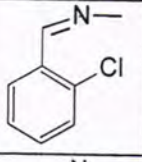	$-SCH_3$	183-185	69	Brown	EtOH
D_7	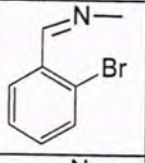	$-SO_2CH_3$	80-82	65	Maroon	Ether
D_8	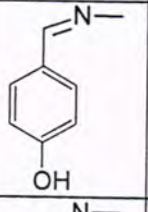	$-SO_2CH_3$	180d	67	Yellow	Ether
D_9	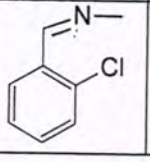	$-SO_2CH_3$	100-102	61	Black	Ether

D_{10}	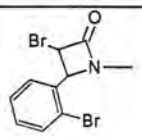	$-SCH_3$	129-131	69	Maroon	H_2O
D_{11}	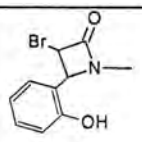	$-SCH_3$	153-155	70	Dark brown	H_2O
D_{12}	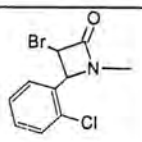	$-SCH_3$	169-171	67	Dark gray	H_2O
D_{13}	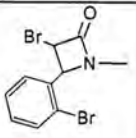	$-SO_2CH_3$	72-74	62	Coffee	H_2O
D_{14}	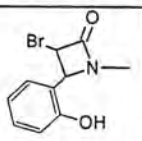	$-SO_2CH_3$	160-162	72	Deep peach	H_2O
D_{15}	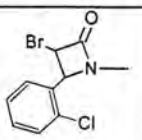	$-SO_2CH_3$	96-98	59	Yellow	H_2O

Table-2: IR , UV, and ^{1}H-NMR spectral data for compounds [$D_1 - D_{15}$]

No. of Comp	U.V\ λmax ($CHCl_3$)	Characteristic IR bands Cm-1							H^1-NMR\ ppm (DMSO\ 300 MHz)
		OH	NH	C–H ar.	C–H alp.	C=N	C=C	Other	
D_1	352, 241	–	3256	3064	2991	1616, 1572	1519	–	–
D_2	349, 253	3210	3167	3047	2970	1670, 1597	1514	–	δ 4.68 (s, 1H, NH) δ 6.92-7.77 (d-d, 4H, Ar–H) δ 9.78 (s, 1H, –N=CH) δ10.58 (s, 1H, OH)
D_3	319, 249	–	3261	3065	2993	1629, 1560	1502	–	–
D_4	320, 254	–	–	3046	2994, 2938	1625, 1585	1480	–	–
D_5	368, 246	3411	–	3075	2895, 2804	1601, 1572	1516	–	–
D_6	321, 246	–	–	3064	2927, 2858	1659, 1594	1509	–	–
D_7	354, 257	–	–	3090	2990, 2928	1681, 1630	1502	1342, 1157 Asym. &Sym. (SO_2)	–
D_8	300, 242	3417	–	3072	2965, 2885	1652, 1591	1515	1309, 1159 Asym. &Sym. (SO_2)	δ 2.75 (s, 3H, CH_3) δ 6.91-7.89 (d-d, 4H, Ar–H) δ 8.72 (s, 1H, –N=CH) δ10.60 (s, 1H, OH)
D_9	368, 254	–	–	3062	2981, 2878	1653, 1597	1506	1357, 1159 Asym. &Sym. (SO_2)	–
D_{10}	285, 236	–	–	3071	2926, 2866	1631, 1564	1469	1702 (C=O)	–
D_{11}	272, 248	3387	–	3097	2983, 2945	1654, 1599	1541	1719 (C=O)	–
D_{12}	286, 257	–	–	3068	2924, 2856	1678, 1598	1471	1735 (C=O)	δ 2.50 (s, 3H, CH_3) δ 3.68 (d, 1H, N–CH) δ 3.82 (d, 1H, Br–CH) δ 7.33-7.64 (m, 4H, Ar–H)
D_{13}	296, 251	–	–	3079	2955, 2896	1684, 1587	1513	1719 (C=O) 1350, 1155 Asym. &Sym. SO_2)	δ 3.76 (s, 3H, CH_3) δ 4.17 (d, 1H, N–CH) δ 4.41 (d, 1H, Br–CH) δ 7.00-7.19 (m, 4H, Ar–H)
D_{14}	313,260	3408	–	3057	2926, 2852	1585	1512	1705 (C=O) 1344, 1199 Asym. &Sym. SO_2)	–
D_{15}	290, 243	–	–	3065	2927, 2858	1692	1506	1721 (C=O) 1329, 1155 Asym. &Sym. (SO_2)	–

Table-3: Result of antimicrobial activity tests (agar diffusion method) of compounds [$D_7 - D_{15}$]

Comp. No.	Susceptible microorganisms															
	Gram positive species								Gram negative species							
	S.aureu				B. sub				E.coli				Pseudomonas			
	500	250	125	75	500	250	125	75	500	250	125	75	500	250	125	75
D_7	+	+	±	-	++	+	+	-	-	-	-	-	-	-	-	-
D_8	+	-	-	-	++	++	+	-	±	-	-	-	±	±	-	-
D_9	++	+	+	+	+	+	-	-	++	±	-	-	++	+	±	-
D_{10}	+	±	-	-	+	±	-	-	+	-	-	-	+	-	-	-
D_{11}	-	-	-	-	±	-	-	-	+	+	-	-	-	-	-	-
D_{12}	-	-	-	-	-	-	-	-	±	-	-	-	-	-	-	-
D_{13}	++	+	+	+	+	±	±	-	+++	++	+	+	+	+	-	-
D_{14}	++	++	++	++	+	+	±	±	++	++	+	-	++	++	+	+
D_{15}	++	+	+	±	++	+	-	-	++	+	±	-	++	±	±	-
AX25	-				-				-				-			
TE10	-				-				-				-			
CN10	++				++				++				++			

+++= zone size >21 mm; ++=zone size 21-15mm; += zone size 14-8mm; ±= zone size 7-5mm; -=not sesitive

REFERENCES

1- Dua, R. and Srivastava, S.K.; Synthesis, Characterization and Antimicrobil Activity of 2-(2'-Substituted-Benzylidene-Hydrazino-Acetyl) – Mercapto-5-Methyl- 1, 3, 4-Thiadiazoles and 2 -[2'- {4 - Substituted-Aryl- 3- Chloro-2- Oxo-Azetidine}-Acetyl-Aminomercapto]-5-Methyl-1,3,4-Thiadiazoles; International Journal of Pharma and Bio Sciences; V1(2), 1-7, 2010.

2- Arora, R.; Venugopalan, P. and Bari, S.S.; Synthesis of novel spiro-β-lactams; J. Chem. Sci.; 122 (2), 125-135, 2010.

3- Elkanzi, N.A.A.; Synthesis of Some New Isolated/Spiro β-Lactam and Thiazolidinone Incorporating Fused Thieno Pyrimidine Derivatives; OSR Journal of Applied Chemistry; 1, 01-12, 2012.

4- Senthil, K. G.; Prakash, D. and Mani T.; Thiadiazoles: Progress Report on Biological Activities; Der Pharma Chemica; 3 (2), 330-341 2011.

5- Azzouz, A.S.P.; Ali, R.T.; Synthesis of Schiff Bases Derived From Benzaldehyde and Salicylaldehyde With Some Amino Acids by a New Develop Method; National Journal of Chemistry; 37,158-168, 2010.

6- Mahdi, M. F.; Mohammed, M. H. and Jassim, A. A.; Design, Synthesis and Preliminary Pharmacological Evaluation of New Non-Steroidal Anti-Inflammatory Agents Having a 4-(Methylsulfonyl) Aniline Pharmacophore; Molecules; 17, 1751-1763, 2012.

7- Ameen, H. A. and Qasir, A. J.; Synthesis and Preliminary Antimicrobial Study of 2-Amino-5-Mercapto-1,3,4-Thiadiazole Derivatives; Iraqi J Pharm Sci; 21 (1), 98-104,2012.

8- Magtoof, M. Sh. and Hassan, Z. S.; Synthesis and Characterization Of Some 3-Phenylthio/3-Phenoxyazetidine-2- One: Application of Two Dimensional NMR HMQC 1H-13C, Cosy 1H–1H And Mass Spectroscopy; National Journal of Chemistry, 41, 90-105, 2011.

9- Sanjeev, K. and Kotresh, O.; Synthesis and Biological Activity of Some Novel 4-(5-Mercapto-1,3,4-thiadiazol-2-yl)-2-phenyl-5-[2-phenylvinyl]-2,4-dihydro-3*H*-1,2,4-triazol-3-one; E-Journal of Chemistry; 7 (2), 545-550, 2010.

Synthesis and Characterization of the Ligand Derived from 2-MercaptoBenzoxazole and It's Complexes with Some Transition Metals Ions

Najat jawad Al-Obaidi[1], Redha I.Al-Bayati[2] and Hayder Obaid Jamel[3]
[1,2] College of Science -Al- Mustansiriya University
[3] College of Education - Al-Qadisyia University
Received 23/9/2013 – Accepted 21/1/2014

الخلاصة

حضرت سلسلة معقدات جديدة لليكاند 5-(بنزواوكسازول-2- ايل امينو) -4،3،1- ثايادايازول -2- ثايول من تفاعل الليكاند مع أملاح الفلزات الأيونية (المنغنيز، الكوبلت، النحاس ، الزنك والكاديوم) الثنائية التكافؤ في مذيب الايثانول .الليكاند الجديد حضر من تفاعل 5-امينو-1،3،4 - ثايادايازول-2- ثايول مع 2- مركبتربنزواوكسازول في مذيب 4،1-داي اوكسان . تركيب الليكاند ومعقداته اثبت من خلال القياسات الطيفية(الأشعة تحت الحمراء ، الأشعة المرئية – فوق البنفسجية ، طيف الرنين النووي المغناطيسي) التوصيلية المولارية ، درجات الانصهار والامتصاص الذري، قياسات الحساسية المغناطيسية والتحليل الدقيق للعناصر. بينت النسبة المولية ان نسبة (فلز :ليكاند) كانت (2:1) لمعقدات المنغنيز، الكوبلت، النحاس و(1:1) بالنسبة لمعقدات الزنك والكاديوم . أثبتت هذه القياسات ان لمعقدات المنغنيز، الكوبلت والنحاس أشكال ثمانية السطوح وأشكال رباعية السطوح لمعقدات الزنك والكاديوم .

ABSTRACT

A new series complexes of the ligand 5-(Benzoxazol-2-ylamino)-1,3,4-thiadiazole-2-thiol (L) have been synthesized by the reaction of the ligand (L) with metals chlorides of Mn(II) , Co(II) , Cu(II) , Zn(II) and Cd(II) in ethanol as a solvent. The ligand 5-(Benzooxazol-2-ylamino)-1,3,4-thiadiazole-2-thiol (L) was prepared from the reaction 5-amino -1,3,4-thiadiazole -2- thiol with 2-Mercaptobenzoxazole in 1,4-dioxane as solvent . The structures of the ligand and its complexes were confirmed by IR , ^{1}H-NMR and UV- Vis. spectra , molar conductivity , melting points elemental analyses(CHN) , atomic absorption and magnetic susceptibility measurements. The synthesized complexes were prepared in (1:2) ratio correspond to Mn(II), Co(II), Cu(II) complexes while in case Zn(II) and Cd(II) complexes is (1:1) ratio (M : L) . These measurements suggested octahedral geometry for the Mn(II) ,Co(II) and Cu(II) complexes and tetrahedral geometry for the Zn(II) and Cd(II) complexes .

INTRODUCTION

Benzoxazoles are an aromatic organic compounds having benzene fused oxazole ring structure with a molecular formula C_7H_5NO, with IUPAC name 1-Oxa-3-aza-1H-indene, Insoluble in water and melting point 27-30^0 C [1,2] .

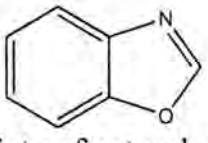

Benzoxazoles are found in a variety of natural products and are important targets in drug discovery[3,4]. Also, they have a number of optical applications such as photoluminescents , whitening agents and in dye lasers[5] and are used as organic brightening agents and organic plastic scintillators [6]. Furthermore , the benzoxazole units are used not only for optical application, but also for other important uses such as intermediates for organic syntheses and therapeutic materials[7]. On the

other hand, benzoxazole moiety is found in various pharmaceuticals displaying a broad spectrum of biological activity including anti-inflammatory[8] , antifungal[9] , anti-HIV-1[10] , anticonvulsant[11] , antiviral[12] and anticancer agents[13] . In addition , some benzoxazole derivatives are used as ligands to prepare many complexes with transition metals ions[14]. The complexes of benzoxazole have been widely applied for use in chemistry and medicine[15] .

MATERIALS AND METHODS

All chemicals were supplied from Al-Drich , Fluka and BDH . Infrared spectra have been recorded in the range (400-4000cm^{-1}) using KBr disk for the ligands and its complexes by using (Shimadzu FT-IR 8400S spectrophotometer).The UV- Vis. spectra have been recorded in the range of (200-1000) nm using (ShimadzuU.V-165PCS spectrophotometer).
^{1}H-NMR spectra were recorded on Fourier Transform Varian spectrometer, operating at 300 MHz with tetramethylsilane as internal standard in d_6-DMSO.
The metal content was determined by using Shimadzu corporation model 6809. Elemental analysis were recorded on instrument type EA-034mt. Molar conductivity measurements were obtained by using electrolytic conductivity measuring set model MC-1-MarkV in DMF solvent in concentration (10^{-3} M) at 25 °C . Magnetic susceptibility measurements were obtained at room temperature applying method using Balance Magnetic Susceptibility Model MSB-MKI.

Preparation of The Ligand 5-(Benzoxazol-2-ylamino)-1,3,4-thiadiazole-2-thiol (L) :

To a solution of 5-Amino-2-thio-1,3,4-thiadiazole (0.02mole, 1.33gm) in1,4-dioxane (25ml), a solution 2-Mercaptobenzoxazole (0.02mole , 1.5 gm) in1,4-dioxane(25ml) was added. The mixture was refluxed for 12 hours. The volume of solvent was reduced under vacuum to the half of the original volume. On cooling a pale brown precipitate was obtained which was left for overnight , filtered off and washed with 1,4- dioxane and recrystallized from absolute ethanol to form pale brown crystal (yield 72%), (m.p : 236-238°C) .

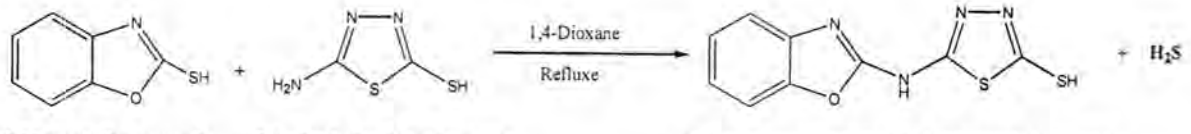

2-Mercapto Benzooxazole 5-Amino-2-thio-1,3,4-thiadiazole 5-(Benzoxazol-2-ylamino)-1,3,4-thiadiazole-2-thiol (L)

Scheme 1 : Synthesis of the ligand 5-(Benzooxazol-2-ylamino)-1,3,4-thiadiazole-2-thiol (L)

Synthesis of the Complexes(L)

The ligand (L) (0.002mol , 0.5gm) was dissolved in 20 mL ethanol in a 100 ml round-bottom flask . A solution of (0.001mol , 0.24gm , 0.24gm , 0.17gm) of the hydrated metal chloride Mn(II), Co(II) and Cu(II) respectively in 20 ml ethanol was added dropwise with continuous stirring at room temperature. Reflux for 2hr . The rustling precipitates were filtered off, washed with ethanol , dried and recrystallized from ethanol and dried .

The Zn(II) and Cd(II) complexes were prepared in same the preparation method of Mn(II), Co(II) and Cu(II) complexes expect the ratio metal to ligand was used as (1:1) ratio and (0.001mol , 0.17gm and 0.22gm) weights of the hydrated metal chloride Zn(II) and Cd(II) .

RESULTS AND DISCUSSION

The new ligand 5-(Benzoxazol-2-ylamino)-1,3,4-thiadiazole-2-thiol (L) was synthesized from the reaction 5-amino -1,3,4-thiadiazole -2- thiol with 2-mercapto benzoxazole in 1,4-dioxane as solvent, this reaction occurs by the following mechanism[16] :

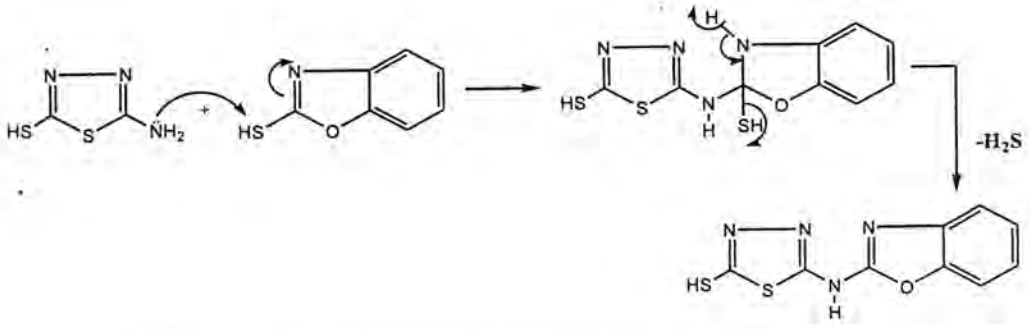

Scheme 2: The mechanism of synthesis of the ligand (L)

The complexes have been prepared from reaction the ligand (L) with metal chlorides hydrate in ethanol solvent . The physical properties and elemental analysis are shown in Table(1). The molar ratio method showed that the metal to ligand ratio is (1:2) (metal to ligand) in case Mn(II) , Co(II) and Cu(II) complexes while in case Zn(II) and Cd(II) complexes is (1:1) .

^{1}H-NMR spectrum of The Ligand(L)

The ^{1}H-NMR spectrum of the ligand , Figure (1), showed four signals , the first two signals at (d, 2H , 7.00-7.03ppm) and (d, 2H , 7.23-7.25ppm) due to aromatic protons . The other two signals at (S , 1H , 6.82ppm) and (S , 1H , 12.96ppm) which, due to protons of (N-H) and (S-H)groups , respectively [17,18] .

The Infrared Spectra

The spectrum of the ligand (L), figure(1), showed three bands at (1606, 1622 and 3255) cm^{-1} due to υ(C=N) of thiadiazole ring , υ(C=N) of benzoxazole ring and υ(N-H) group , respectively , the shoulder band at (2576) cm^{-1}assigned to υ(S–H) group . The bands at (1365) , (1280) , (1134) , (1049) , (1504, 1473,1450) and (3070)cm^{-1} attributed to the υ(C=S), υ(C-O), υ(C-N), υ(N-N), υ(C=$C_{aromatic}$) and υ(C-H $_{aromatic}$) groups , respectively[19-23].

The ligand shows υ(N-H) at 3255 cm^{-1} which shifted to lower wave number after complexation at (3247)cm^{-1} in the Mn(II) complex and higher wave number after complexation at the range (3263-3286)cm^{-1} in the Co(II) , Cu(II) , Zn(II) and Cd(II) complexes. The band (S–H) was shifted toward higher and lower frequencies at (2541-2602) cm^{-1} .The new bands at (570 , 547 , 555, 540 , 586) , (493 , 501 , 505 , 493 , 501) and (424 , 455 , 452 , 447 , 447) cm^{-1} which assigned to υ(M–O) , υ(M–N) and υ(M–S) for Mn(II) , Co(II) , Cu(II) , Zn(II) and Cd(II) complexes respectively [23-25] .

The bands at (3348–3466)cm^{-1} are due to the υ(O–H) stretching of water and ethanol molecules [26] .

The shifted of the wave number of groups of free ligand after formation complexes and the appearance a new bands in the complexes spectral are evidence on occurrence coordination between the ligand and metals ions.

Electronic Spectra

The (Uv-Vis.) spectrum of L, figure(8) shows two peaks , the first peak at (215 , 264 nm.) which assigns to π-π* , while the other peak at (302 nm.) due to n-π* transition [27] .

The (Uv-Vis.) spectrum of Mn(II) complex , (μeff 4.43 B.M), Figure(9), showed peaks at (461 , 633 and 917) nm, these peaks attributed to $^6A_1g \rightarrow {}^4T_2g(D)$, $^6A_1g \rightarrow {}^4A_1g$ and $^6A_1g \rightarrow {}^4T_1g(G)$, respectively. These transitions refer to octahedral geometry around Mn(II) ion [28] .

The (Uv-Vis.) spectrum of Co(II) complex , (μeff 4.23 B.M) , Figure(10), exhibited peak at (422 , 567 and 656 nm) , may be due to $^4T_1g \rightarrow {}^4T_1g$ (P) , $^4T_1g \rightarrow {}^4A_2g$ (F) and $^4T_1g \rightarrow {}^4T_2g$(F) respectively. These transitions refer to octahedral geometry around Co(II) ion [29] .

The (Uv-Vis.) spectrum of Cu(II) complex , (μeff 2.56 B.M), Figure(11), exhibited peak at (714 nm) , may be due to $^2Eg \rightarrow {}^2T_2g$ transition which suggested octahedral geometry around Cu(II) ion [30] .

The (Uv-Vis.) spectrum the complexes of Zn(II) and Cd(II) (diamagnetic), Figure(12and13) do not useful in determined the geometry for these complexes . The molar ratio , molar conductance , magnetic measurements , elemental analysis and atomic absorption which

suggested tetrahedral geometry[8] . The data of (UV-Vis.)spectrum and the magnetic moments of the ligand and its complexes have been shown in Table (3) .

Molar Conductivity Measurements

The molar conductance were measured in DMF solvent and concentration 10^{-3}M at room temperature. The molar conductance values of the synthesized complexes were at the range (31.98-63.6 ohm^{-1}.cm^2.mole^{-1}) . These results suggested non-ionic electrolyte for (Co(II) , Cu(II) , Zn(II) and Cd(II) complexes , while the complexes of Mn(II) is ionic nature in the (1:1) ratio [31,32] . The spectral data of molar conductance are shown in Table(3) .

CONCLUSION

The measurements (elemental analysis , Infrared and electronic spectra , magnetic susceptibility measurements , atomic absorption spectroscopy and molar conductivity) are used to determined geometry of synthesized . These measurements were suggested octahedral for Mn(II), Co(II) and Cu(II) complexes while Zn(II) and Cd(II) complexes are tetrahedral geometry, (Figure14) .

Table-1: Elemental analysis and some physical properties of the ligand(L) and its complexes

Comp. No.	Compounds	Color	M.P (C°)	Yield %	Molecular Weight (gm/mole)	Molecular Formula	Found (Calc.)%			
							C	H	N	M
1	L	brown	236-238	80	250.30	$C_9H_6N_4OS_2$	43.64 (43.19)	2.94 (2.42)	22.26 (22.38)	- -
2	$[Mn(L)_2(H_2O)Cl]Cl$	Pale brown	256-258	72	644.46	$C_{18}H_{14}Cl_2N_8O_3S_4Mn$	34.51 (33.55)	2.56 (2.19)	18.26 (17.39)	8.28 (8.52)
3	$[Co(L)_2Cl_2]\ C_2H_5OH$	Green -Blue	243-245	74	676.51	$C_{22}H_{18}Cl_2N_8O_3S_4Co$	35.55 (35.51)	2.76 (2.68)	18.68 (16.58)	8.85 (8.71)
4	$[Cu\ (L)_2Cl_2]\ H_2O$	Pale green	249-251	79	653.07	$C_{18}H_{14}Cl_2N_8O_3S_4Cu$	34.98 (33.10)	2.39 (2.16)	17.61 (17.16)	8.33 (9.73)
5	$[Zn\ (L)Cl_2]\ H_2O$	Pale yellow	263-265	82	404.61	$C_9H_8Cl_2N_4O_2S_2Zn$	- (26.72)	- (1.99)	- (13.85)	15.51 (16.16)
6	$[Cd\ (L)Cl_2]\ H_2O$	white	298-300	71	451.63	$C_9H_8Cl_2N_4O_2S_2Cd$	25.03 (23.93)	1.21 (1.79)	12.87 (12.41)	24.11 (24.89)

Table -2: The important infrared spectral bands for the of the ligand(L) and its complexes

Comp. No.	*Compounds*	*υ(C=N)*	*υ(S–H)*	*υ(N–H)*	*υ(C=S)*	*υ(O-H)*	*υ(M–O) υ(M–N) υ(M–S)*
1	L	1606 1622	2576	3255	1365	-	-
2	$[Mn(L)_2(H_2O)Cl]Cl$	1612 1622	2541	3247	1368	3364	570 493 424
3	$[Co(L)_2Cl_2]\ C_2H_5OH$	1610 1622	2602	3263	1360	3348	547 501 455
4	$[Cu\ (L)_2Cl_2]\ H_2O$	1604 1620	2598	3284	1357	3423	555 505 452
5	$[Zn\ (L)Cl_2]\ H_2O$	1589 1620	2589	3271	1373	3466	540 493 447
6	$[Cd\ (L)Cl_2]\ H_2O$	1604 1620	2602	3286	1357	3417	586 501 447

Table- 3: Electronic spectra , magnetic moments and molar conductivity of the ligand(L) and its complexes

Com,p. No.	*compounds*	*λ (nm)*	*υ (cm⁻¹)*	*Transitions*	*μeff (B.M)*	*Molar Conductivity (ohm⁻¹.cm².mole⁻¹)*	*Geometry*
1	L	215 264 302	46512 37879 33113	π-π* π-π* n-π*	-	-	-
2	$[Mn(L)_2(H_2O)Cl]Cl$	305 461 633 917	32787 21692 15798 10905	Charge transfer $^6A_1g \rightarrow {}^4T_2g(D)$ $^6A_1g \rightarrow {}^4A_1g$ $^6A_1g \rightarrow {}^4T_1g(G)$	4.43	63.6	Octahedral
3	$[Co(L)_2Cl_2]\ C_2H_5OH$	312 422 576 656	32051 23697 17361 15244	Charge transfer $^4T_1g \rightarrow {}^4T_1g(P)$ $^4T_1g \rightarrow {}^4A_2g(F)$ $^4T_1g \rightarrow {}^4T_2g\ (F)$	4.23	31.98	Octahedral
4	$[Cu\ (L)_2Cl_2]\ H_2O$	282 714	35461 14006	Charge transfer $^2Eg \rightarrow {}^2T_2g$	1.33	38.88	Octahedral
5	$[Zn\ (L)Cl_2]\ H_2O$	292	34247	Charge transfer	Dia.	39.68	Tetrahedral
6	$[Cd\ (L)Cl_2]\ H_2O$	299	33445	Charge transfer	Dia	37.48	Tetrahedral

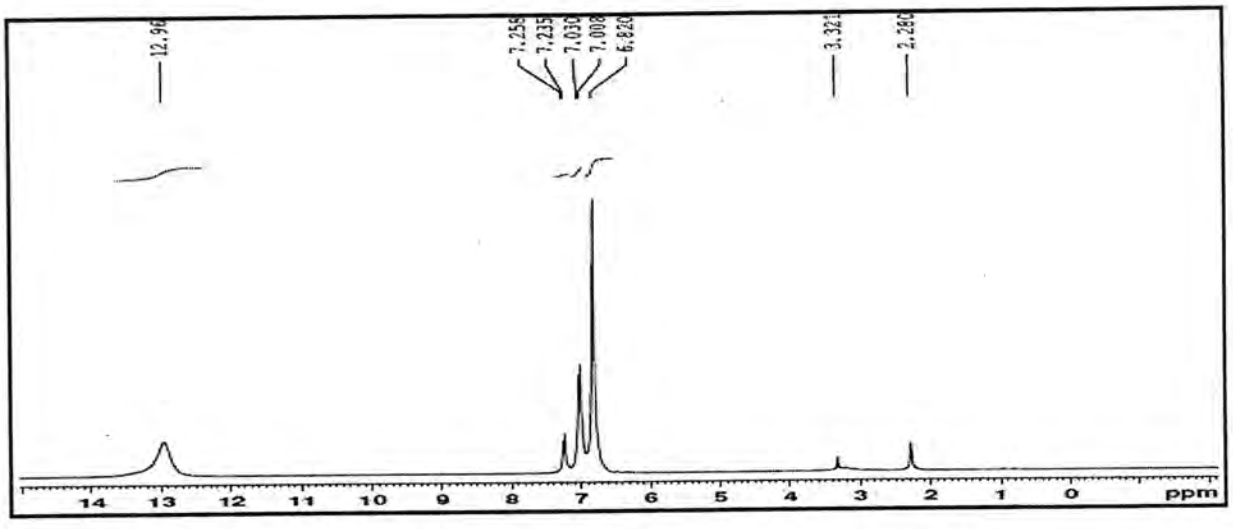

Figure- 1 : The ^{1}H-NMR spectrum of the ligand (L) .

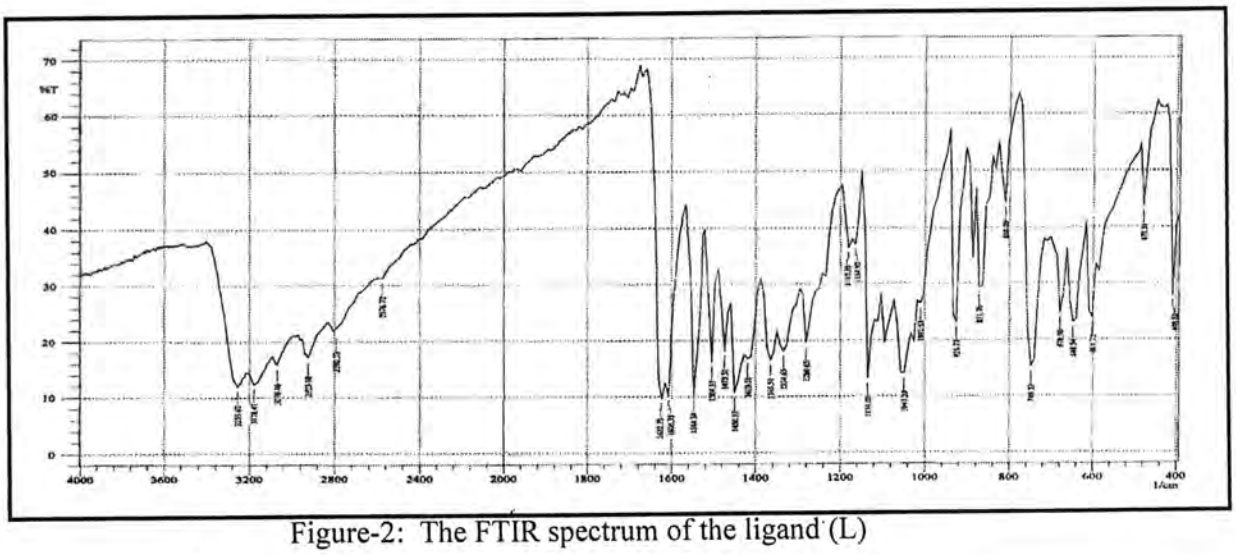

Figure-2: The FTIR spectrum of the ligand (L)

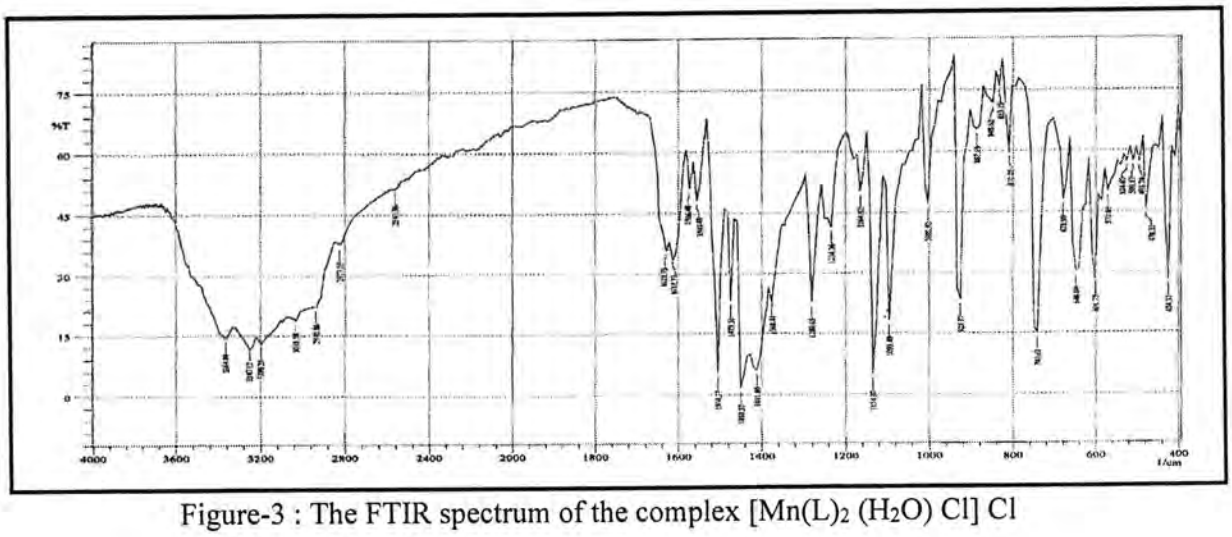

Figure-3 : The FTIR spectrum of the complex $[Mn(L)_2 (H_2O) Cl] Cl$

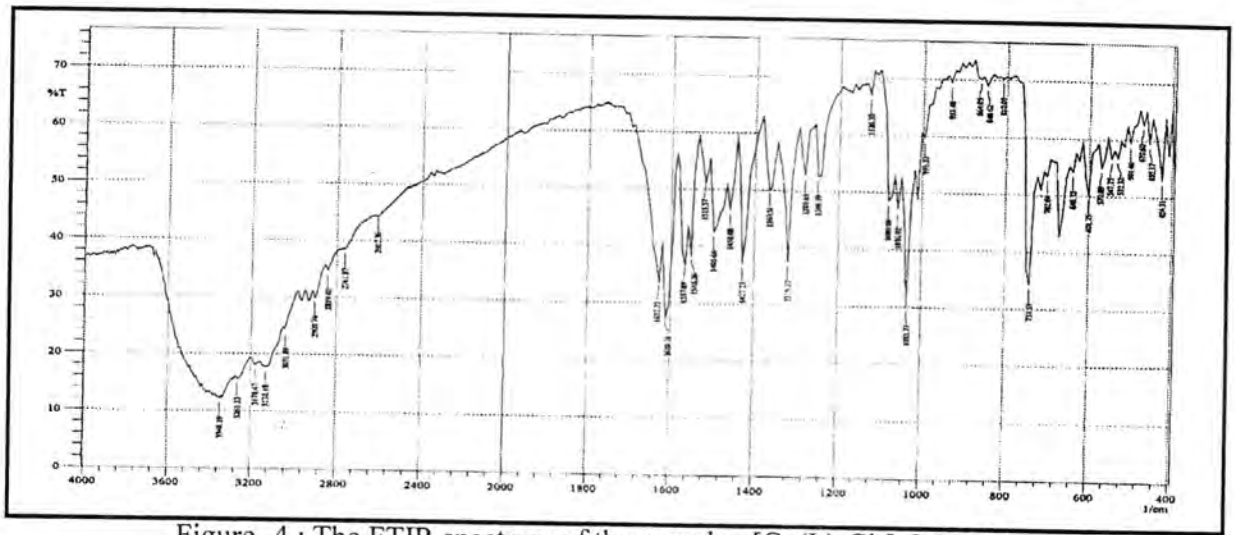

Figure -4 : The FTIR spectrum of the complex $[Co(L)_2Cl_2].C_2H_5OH$

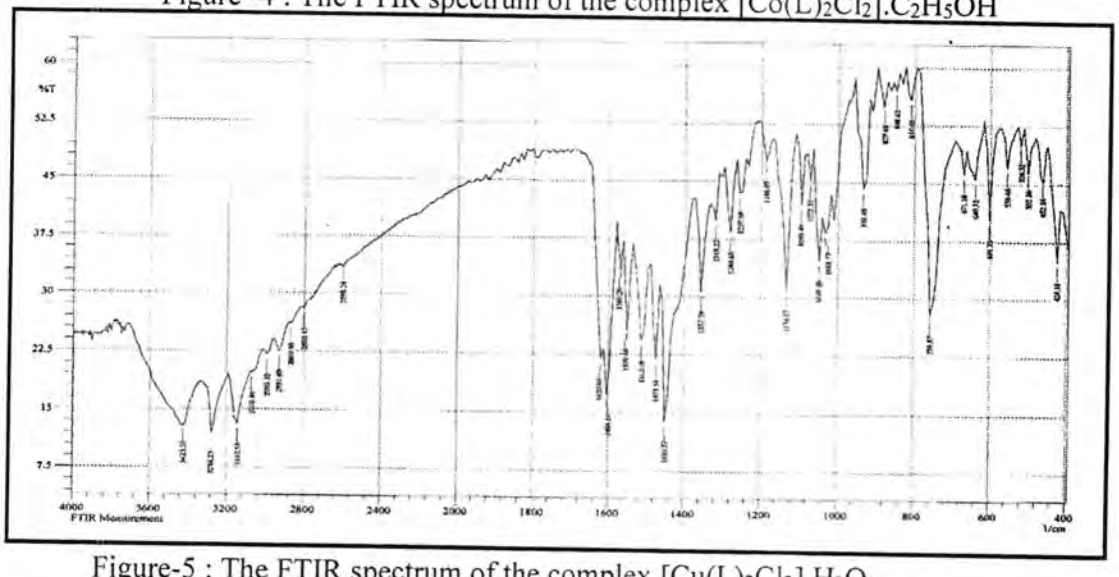

Figure-5 : The FTIR spectrum of the complex $[Cu(L)_2Cl_2].H_2O$

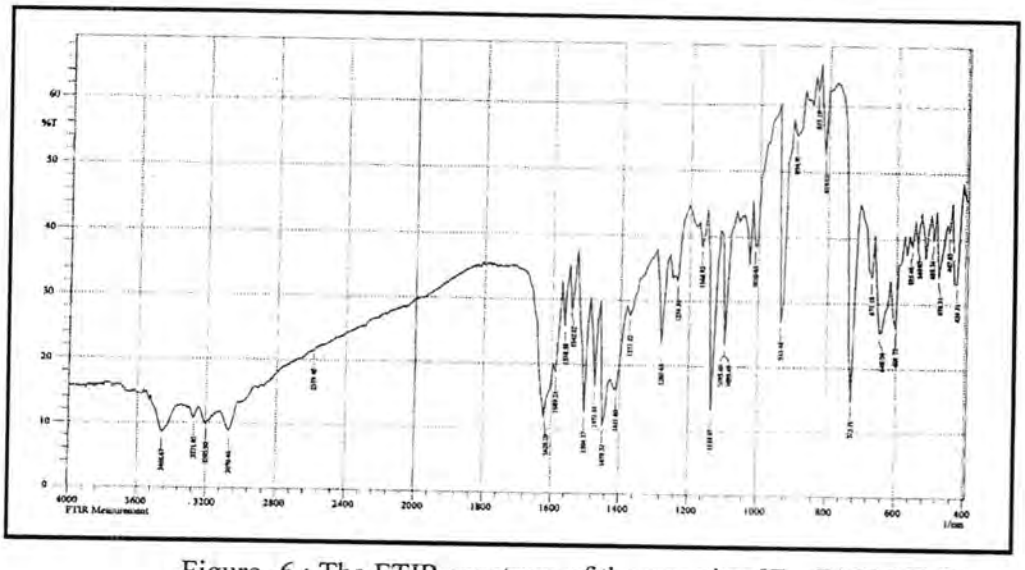

Figure -6 : The FTIR spectrum of the complex $[Zn\ (L)Cl_2].H_2O$

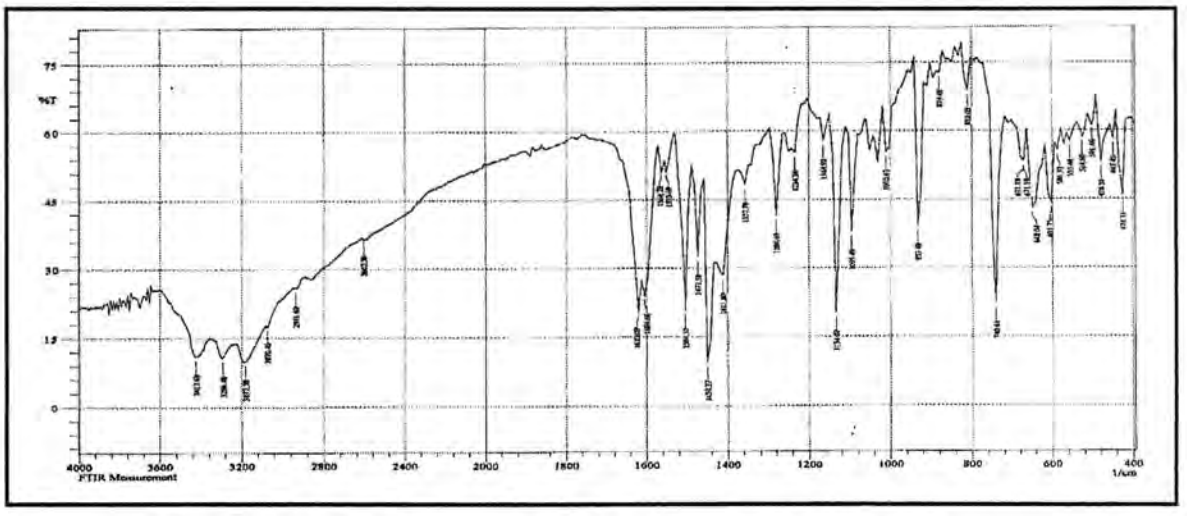

Figure-7 : The FTIR spectrum of the complex [Cd (L) Cl_2].H_2O

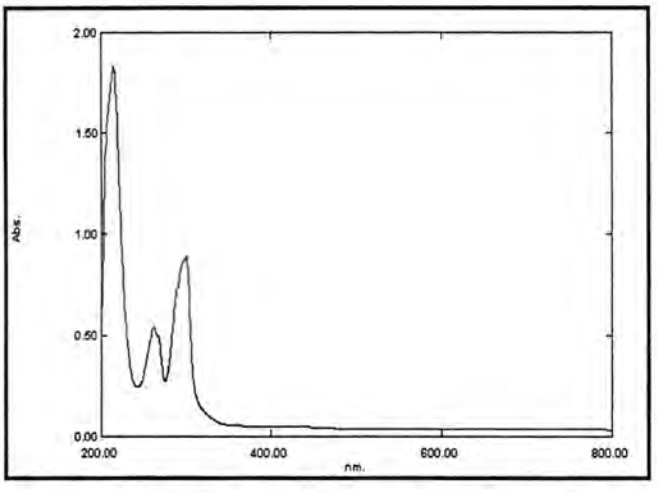

Figure -8 : Electronic spectrum of the free ligand

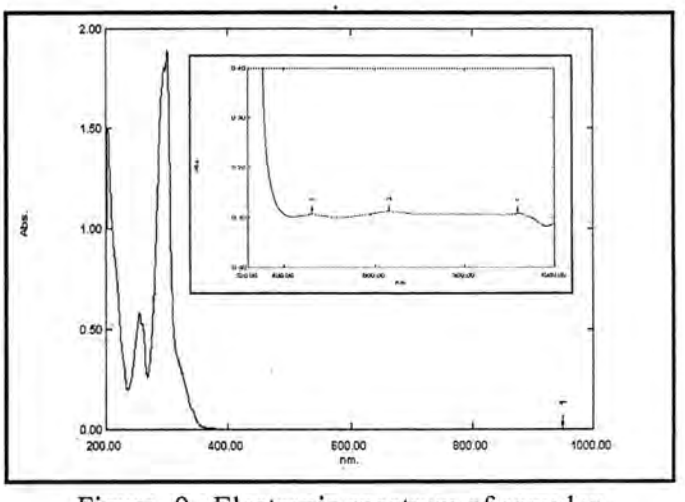

Figure- 9 : Electronic spectrum of complex [$Mn(L)_2$ (H_2O) Cl] Cl

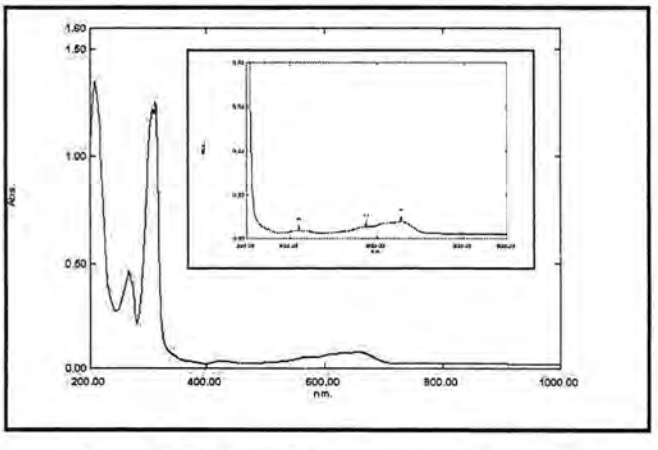

Figure-10 : Electronic spectrum of complex [$Co(L)_2Cl_2$].C_2H_5OH

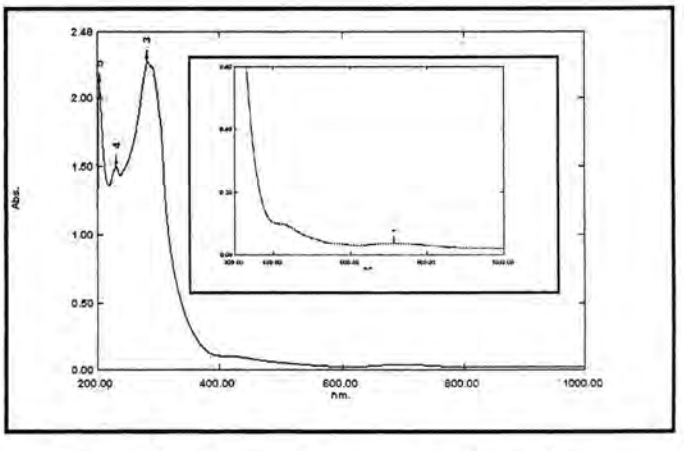

Figure-11: Electronic spectrum of complex [$Cu(L)_2Cl_2$].H_2O

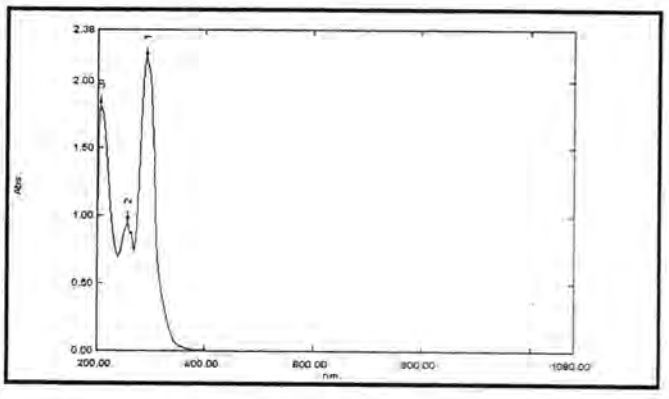

Figure-12 : Electronic spectrum of complex $[Zn\ (L)Cl_2].H_2O$

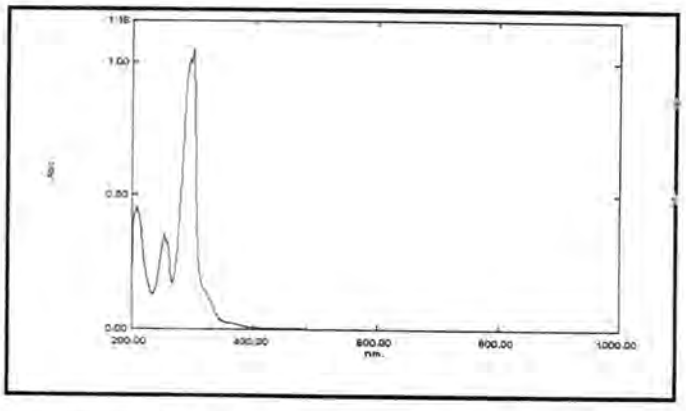

Figure-13 : Electronic spectrum of complex $[Cd(L)Cl_2].H_2O$

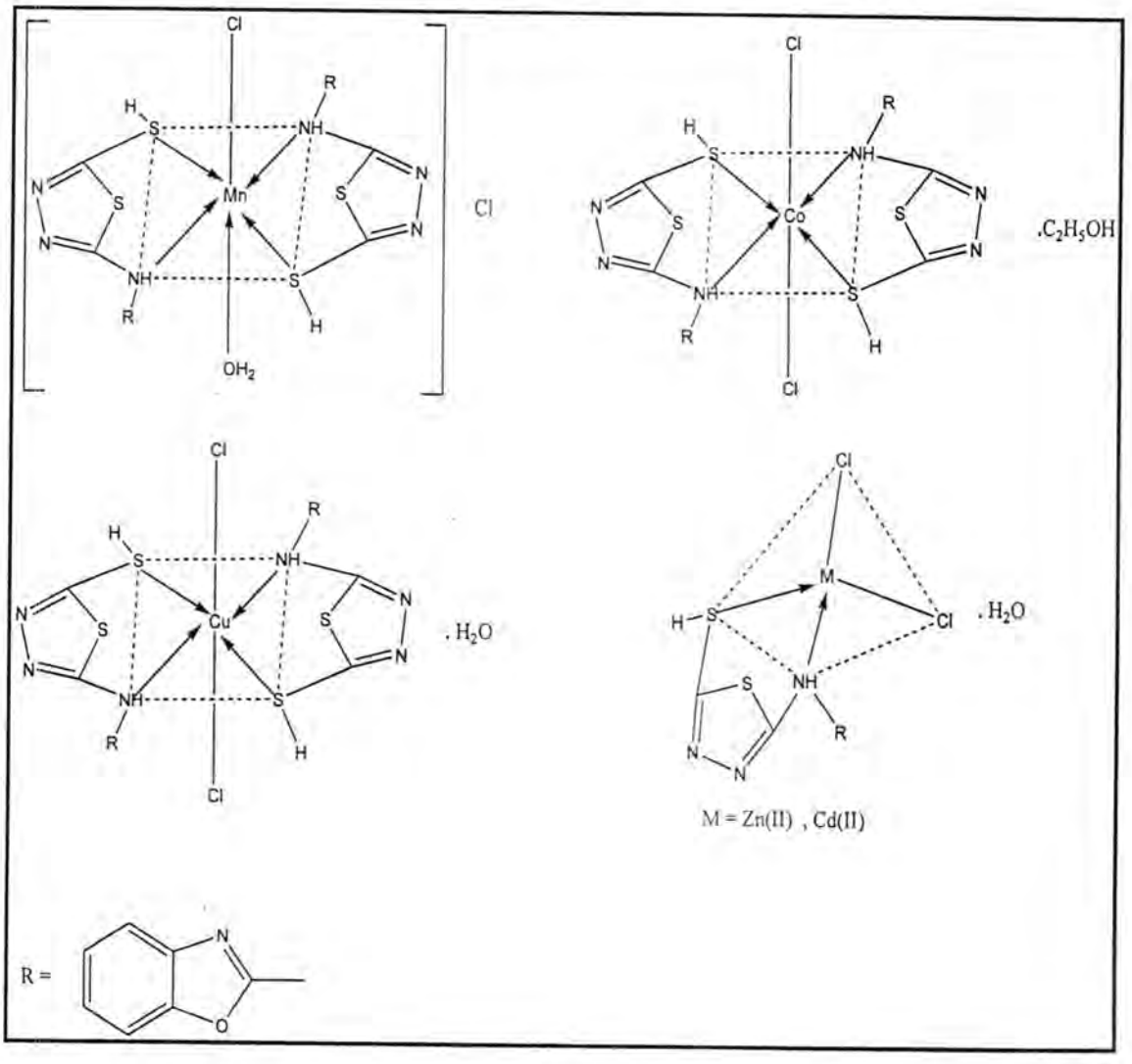

Figure-14 : The proposed chemical structure formula of the complexes

REFERENCES

[1] Shrivastava B. , Sharma V. and Lokwani P. , Benzoxazole : The Nucleus of Diverse Biological Activities , Pharmacologyonline , **1** , 236-245 (2011) .

[2] Lokwani P. , Nagori B.P., Batra N., Goyal A. , Gupta S. and Singh N. , Benzoxazole: The molecule of diverse biological activities , J. Chem. Pharm. Res., **3**, 302-311 , (2011) .

[3] Heravi M., Javanmardi N., Oskooie H., Baghernejad B., Heidari M. and Bamoharra F. , Heteropolyacid as anew , Green and Recyclable Catalyst of 2-Aryl Benzoxazole under Solvent –free Conditions , Journal of the Chinese Chemical Society , **56**, 589-593 (2009) .

[4] Ruiz H. L., Ortega H. B., Lima S. R., Santillan R., Farfan N., Phenylboronic acid catalyzed-cyanide promoted, one-pot synthesis of 2-(2-hydroxyphenyl)benzoxazole derivatives , Tetrahedron , **52** , 4308–4312 (2011) .

[5] Hangirgekar S., Phenyl-Trimethyl-Ammonium Tribromide: Facile Catalyst for the One Pot Synthesis of Substituted Benzoxazoles , Res.J.of Pharm. , Bio.and Chem. Sci. , **3**, 83-88 (2012) .

[6] Guzow K., Szabelski M., Malicka J., Karolczak J. and Wiczk W., Synthesis and Photo physical Properties of 3-[2-(pyridyl)Benzoxazole-5-yl]-L-Alanine Derivatives , Tetrahedron , **58** , 2201-2209 (2002) .

[7] Koyama E., Yang G. and Hiratani K., A novel synthesis of bis(benzoxazole) derivatives via tandem Claisen rearrangement , Tetrahedron , **41** , 8111–8116 (2000) .

[8] Praveen C., Nandakumar A., Dheenkumar P., Muralidharn D. and Perumal P., Microwave-assisted one-pot synthesis of benzothiazole and benzoxazole libraries as analgesic agents , J. Chem. Sci. , **124** , 609–624 (2012) .

[9] Oksuzoglu E., Arpaci O. T., Gulbas B. T., Eroglu H., Sen G., Alper S., Yildiz I., Diril N. , Sener E.A. and Yalcin I., A study on the genotoxic activities of some new Benzoxazoles , Med Chem Res, **16** ,1-14(2007) .

[10] Aparachivei R., Holban M., Sunel V., Popa M. and Desbrier J., Synthesis and Characterization of New Heterocyclic compounds with Potential Anti-tuberculosis Activity and their Immobilization

on Polymer Supports , Cellulose Chem. Technol. , **46** , 301-306 (2012) .

[11] Patil S. and Bhatt P., Synthesis and Characterization of Some Benzoxazole Derivatives , Der Pharmacia Sinica , **1** , 105-112 (2010) .

[12] Ampati S., Jukanti R., Sagar V., Ganta R. and Manda S., Synthesis and in vivo anti-inflammatory activity of a novel series of benzoxazole derivatives, Der Pharmacia Sinica , **1** , 157-168 (2010).

[13] Ziarani G., Badiei A., Nahad M. and Hassanzadeh M., Application of SBA-Pr-SO3H in the synthesis of benzoxazole derivatives , European Journal of Chemistry , **3** , 433-436 (2012) .

[14] Chen T., Synthesis and characterization of cyclometalated iridium (III) complexes containing benzoxazole derivatives and different ancillary ligands , Journal of Organometallic Chemistry , **693** , 3117–3130 (2008) .

[15] Malecki J., Synthesis, crystal, molecular and electronic structures of ruthenium complexes with a benzoxazole derivative ligand , Polyhedron , **31** , 159-166 (2012) .

[16] Taher N.A., M.Sc. Thesis , Synthesis of new glucose derivatives which containing various units , College of Education , University of Al-Qadisiyia : 65 ,(2012) .

[17] Oksuzoglu E., Gulbas B., Alper S., Arpaci O., Ertan T., Yildiz I., Diril N., Aki E. and Yalcin I., Some Benzoxazole and Benzimidazole as DNA topoisomerase I and II Inhibitors , Journal of Enzyme Inhibition and Medicinal Chemistry ,**23** , 37-42(2008) .

[18] Al-Shihry S. S., Synthesis and Spectral Studies of Schiff Bases of 2-amino-5-mercapto-1,3,4-thiadiazole , Scientific Journal of King Faisal University, **6** ,77-85(2005).

[19] Chufan E. E., Perdregosa J.C. and Borras J., Spectroscopic Behaviour of Metal –Drug Complexes . Infra-red Spectra of Cu(II) Complexes with 5-amino-1,3,4-thiadiazole -2-thiol(Hatm) , Vibrational Spectroscopy , **15**, 191-199(1997) .

[20] Oren I., Gulbas B., Yalcin I., Arpaci O., Sener E. and Altanlar N., Synthesis and Antimicrobial Activity of New 2-[p-Substituted –benzyl]-5- [Substituted –carbonyl –amino]Benzoxazoles , Arch. Pharm. Pharm. Med.Chem., **337** , 402-410(2004) .

[21] Siddiqui N., Sarafroz M., Alam M. M. and Ahsan W., Synthesis , Anticonvulsant and Neurotoxicity Evaluation of 5- Carbomethoxy Benzoxazole derivatives , Acta Poloniae Pharmaceutica –Drug Research , **65** , 449-455(2008) .

[22] Sugumaran M. and Hemachander R., Synthesis , Spectral Analysis and Biological Evaluation of Some Novel Flurobenzoxazole Incorporated 1,3,4-Thiadizole , International Journal Pharmaceutical science and Research , **3**, 1809-1816(2012) .

[23] Adiguzel R. , Sekerci M., Tascioglu S. and Ergin Z., Synthesis and Structural Characterization of Novel New Co(II) Complexes of Heteroatom bearing Ligands , research Journal of Pharmaceutical , Biological and Chemical Sciences , **2** , 256-267(2011) .

[24] Abd Al-Hussein M., M. Sc. Thesis ,Synthesis and study of new 1,3,4-thiadiazole derivatives and with some their transition metals complexes and identification their biological activity , Al-Mustansiriya University ,72 (2006).

[25] Al-Nahary T. T., Synthesis and characterization of metal complexes of Cr(III), Mn(II), Fe(III), Co(II), Ni(II), Cu(II), Ru(III), Rh(III) and Pd(II) with derivatives of 1,3,4 thiadiazole-2, 5-dithiol as new ligands , Journal of Saudi Chemical Society , **13**, 253– 257 (2009) .

[26] Al-Hasani R. A.M., Mannich Bases Derived From 1,3,4-Thiadiazole as Chelating Ligand For Some Transition Metal Complexes , Journal of Al-Nahrain University , **11** , 42-56 (2008) .

[27] Hamil A.M., Khalifa K.M., Al-Houni A. and El-Ajaily M.M., Synthesis , Spectroscopic Investigation and activity of Schiff Base Complexes of Cobalt (II) and Copper (II) Ions , Rasayan J. Chem. , **2** , 261-266(2009) .

[28] Spinu C., Pleniceanu M., Tigae C., Biologically Active Transition Metal Chelates with a 2-Thiophencarboxaldehyde –Derived Schiff base : Synthesis , Characterization , and antibacterial Properties , Turk. J. Chem. , **32** , 487-493(2008).

[29] Kumar H. and Chaudhary R. P., Biological Studies of a Novel Azo Based Heterocyclic Schiff Base and its Transition Metal Complexes , Der Chemica Science , **1** , 55-61(2010) .

[30] Obaleye J. A., Adediji J. F. and Adebayo M. A., Synthesis and Biological Activities on Metal Complexes of 2,5-Diamino-1,3,4-

thiadiazole Derived from Semicarbazide Hydrochloride , Molecules , **16** , 5861-5874(2011).

[31] Sonmez M., Binuclear Cu(II) Complexes of ONO Tridentate Heterocyclic Schiff base Derived from N-Aminopyrimidine with Substitutes salicylaldehyde or 2-Hydroxynaphthaldehyde , Erciyes Universitesi Fen Bilimleri Enstitusu Dergisi , **24** , 308-314(2008).

[32] Swati A., Gupta M., Karnawat R., Sharma I. and Verma P., Synthesis , spectroscopic Characterization and Antibacterial Activity of 2-[2-Hydroxyphenylazo]-1-naphthol-4-sulphonicacid and its Fe(III) ,Co(II) and Cu(II) Complexes , research Journal of Pharmaceutical , Biological and Chemical Sciences , **2** , 805-811(2011) .

Predication of Vapor Compression Refrigeration System Performance under Cyclic Loads

Johain Jawdet, Hayder Mahdi Baker, Wajdi Qassim Hussen and Doaa Zaid Khalaf
Technical –College Baghdad
Received 9/9/2013 – Accepted 23/2/2014

الخلاصة

تم اجراء الفحص التجريبي لمنظومة تبريد انضغاطية تعمل تحت تأثير حمل دوري. تم دراسة أداء المنظومة بأستخدام طريقة (RLS). اذ تم اختبار حالتين مختلفتين ، مكثف معزول حراريا و مكثف مبرد بأستمرار واستخدام مسخن حراري باحمال مختلفة 300 واط و 500 واط. طريقة (RLS) اظهرت توقعات مقبولة لأداء المنظومة. الحمل الحراي 500 واط انتج سلوك غير منتظم لتصرف المبخر في حالة التبريد وعدم التبريد بالمقارنة مع الحمل الحراري 300 واط الذي اظهر نتائج منتظمة. تاثير تبريد المكثف أدى الى المحافظة على درجة حرارة المكثف ثابتة لحالتي الحمل الحراري.

ABSTRACT

An experimental investigation to a vapor compression system working under cyclic loads was conducted. The performance was predicted also by using RLS method. Two different cases were tested, isolated condenser pool and cooled condenser pool along with two heater loads 300W and 500W. The RLS prediction method proves satisfactory in anticipating system reaction. The 500W load case resulted in an unstable cyclic evaporator behavior for both cooled and uncooled cases in contrast to 300W load that shows cyclic but stable response. The effect of condenser cooling has kept the condenser temperature almost constant for both load cases.
Keywords: Refrigeration, isolated condenser pool, RLS, cyclic load, heat pump, performance

INTRODUCTION

Refrigeration systems applications are tremendous ranges from large units used in food industry to miniature units used in electronic cooling. In general, these units were designed for their maximum load operating points, yet frequently they operate far from these design conditions due to their vast working conditions including load variations. Thus, to be able to lay out a clear control strategy, a comprehensive insight to these systems behavior under severe working conditions should be performed. Physical models are not satisfactory for such studies, yet various identification methods have been used extensively and successfully in many fields to predict existing systems performance in practical working environments. These methods enable good estimation of model order, performance parameters, and offers a good understanding of the system which otherwise may not be explained easily using physical models [1]. The identification process involves model parameters prediction in such a manner that the model output coincides with the measured data almost satisfactory. In this respect it is similar somewhat to curve fitting methods.

A general purpose microprocessor was used by Neera and Andrew [2] to identify, optimize and control the steady state vapor compression cycle (VCC) operation. Five degrees of freedom (DOFs) of the VCC are

optimized using an objective function which minimizes the rate of exergy destruction in the cycle. The use of exergy is motivated by its ability to capture the physics of both the first and second laws of thermodynamics in a single property. A case study was considered in which the optimization was applied to a commercial truck transport refrigeration system (TTRS). The results suggested that by using the optimal set points generated by the exergy-based objective function, an increase of 52.5% in coefficient of performance COP can be achieved over nominal operation. The optimization results revealed that the regulation of evaporator and condenser pressures are critical parameters in improving the efficiency of steady-state cycle operation.

Riad et al [3] presented a mathematical description for heat and mass transfer process in an air-conditioning unit with an identification to its dynamic discrete model parameters. The air conditioning unit studied was passive unit used to produce a microclimate with controlled relative humidity for crop growth chambers.

A non-traditional VCC, for electronics cooling, subjected to an imposed heat flux boundary condition on the evaporator characterized by fast time responses was studied by Juan et al [4]. This application requires different models and control algorithms than traditional VCCs with fluid-to-fluid heat exchanges. They used an experimental procedure along with an identification process to predict evaporator dynamics and handle the complications arose by the two phase flow at evaporator exit.

An Experimental verification for the effectiveness of identification methods of the Single-Phase Induction Machine (SPIM) parameters of an air conditioning compressor was conducted by Rodrigo et al [5]. The classical Recursive Least Square (RLS) algorithms are applied to improve the performance of the Field Oriented Control (FOC) and sensorless techniques used in these systems.

Enio and Filho [6] proved that using performance monitoring and identification methods is a fundamental tool to automate and to optimize refrigeration and air conditioning systems. The energy saving is reached through the optimization of the equipment performance with the use of control techniques in these systems. Many important aspects with the objective to improve the performance in each installation were incorporated, such as energy cost for residential, commercial and, mainly, industrial places using strategies and new technologies.

Recursive Least Squares Method

Recursive least squares method, adopted in this work, was used extensively to analyze unsteady signals and environments. In general, the recursive least square algorithm can be used to solve any problem requires adaptive solution methods [7]. The model parameters can be predicted by this method if sufficient sets of experimental data are available. These parameters will be updated recursively whenever a new set of

measured data are acquired. In the recursive least square algorithm, the adaptation starts with some initial state and then successive samples of the input signals are used to adapt the coefficients. The key variables y(m), x(m) and w(m)=[w_0(m), w_1(m), ..., w_{p-1}(m)] denote the heater power input, the output signal (pressure or temperature) and the coefficients vector respectively. The output can be expressed as [8]:

$\hat{x}(m) = w^T(m)\, y(m)$ ----------1

Where $\hat{x}(m)$ is an estimate of the actual output x(m). The error is defined as:

$e(m) = x(m) - \hat{x}(m) = x(m) - w^T(m)\, y(m)$ ----------2

The parameter prediction process is based on the minimization of the mean square error criterion defined by:

$\text{Min}\,(e(m)\,2) = \text{Min}\,([x(m) - w^T(m)\, y(m)]\,2)$ ----------3

The final equations can be casted in a recursive form [8]:

$w(k) = w(k-1) + Z(k)*[X_{measured} - w^T(k-1)\, y(k)]$ ----------4

$Z(k) = P(k-1)*\, y(k)*[\, y^T(k)*P(k-1)*\, y(k)+\mu]-1$ ----------5

$P(k) = [I-Z(k)*\, y^T(k)]\, P(k-1)/\,\mu$ ----------6

Where μ is the forgetting factor. The solution procedure starts with initial estimates of P and w yet assured to converge quickly.

MATERIALS AND METHODS

The experimental rig used in this work is shown in figure (1). It consisted of an existing laboratory heat pump system with two reservoirs, hot reservoir and cold reservoir, modified to suit the current work. The dimensions of the water filled reservoirs are (w=18 cm, L=18 cm, H=25 cm). The water volume in both reservoir is 5.9 lit. A copper pipe coils (tube dia. , coil dia. 15cm, 10 turns) are immersed in both reservoirs to exchange heat with the water as an evaporator and condenser. A 90 watt power, compressor (Indesit I4, 220 volts, 50 hertz) was used with a rated current of 3.5 ampere. The (1mm diameter and 2 m length) capillary tube was used as an expansion device.

An electrical panel unit (see figure 1) was used to control the heating load supplied to the vapor compression system. It is constructed from a simple heater (0-500 watt), A.C adapter, timer, and voltage regulator. Measurements are carried out using thermocouples type K for the temperature and bourdon gauges for pressure measurements. Two sets of experiments were conducted, one for 300 watt load and the other for 500 watt load. A sampling interval of 5 minutes was chosen to satisfy the predominant time constant. The experiments were carried out for each aperture position. The first data set that was used in the identification procedure is for the isolated condenser pool. The second data set that was used in the identification procedure is for the ice cooled condenser pool. Readings were recorded for the temperatures and pressures around the cycle including evaporator and condenser pressures, water temperature in condenser container, and water temperature in evaporator container.

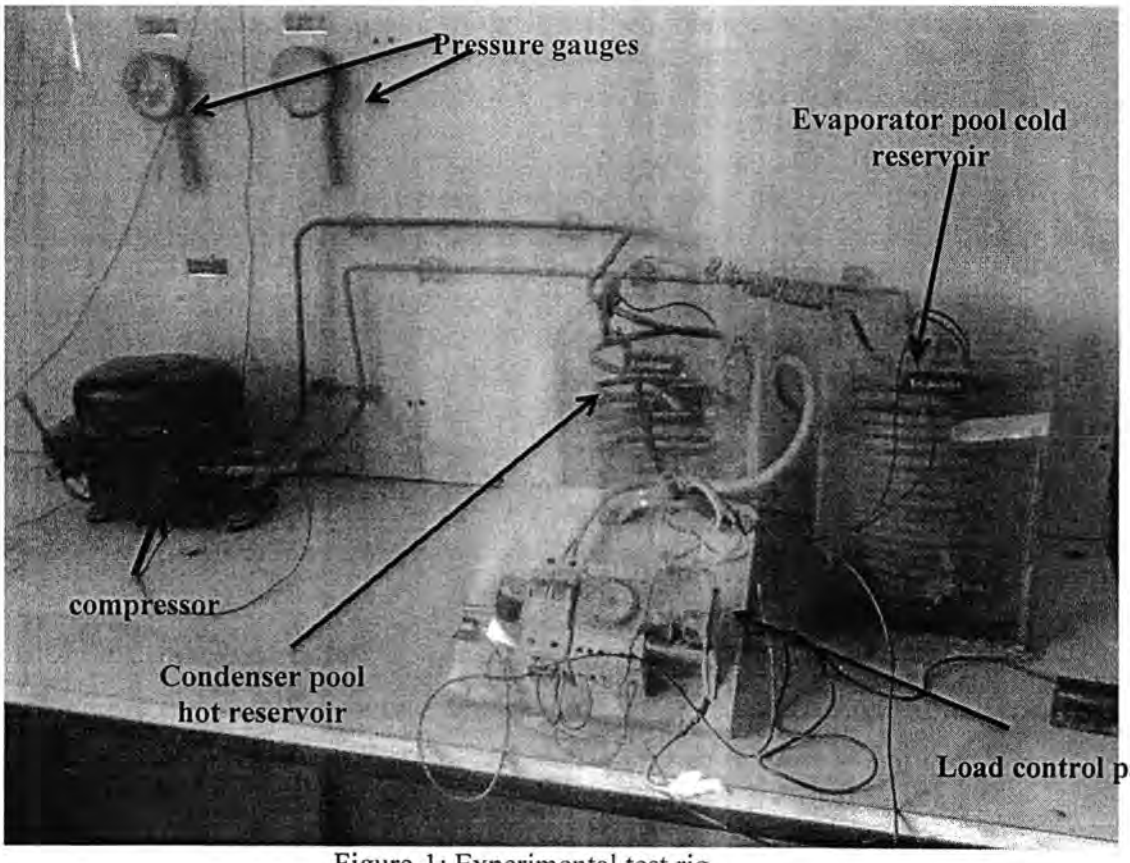

Figure-1: Experimental test rig

RESULTS AND DISCUSSIONS

Two load amplitudes (300W and 500W each of 30min period) were chosen to demonstrate the applicability of the adopted RLS method in predicting the unsteady response of heat pump to severe cyclic loads. In general, the application of the method resulted in a satisfactory success although there was a shortage in some of the measured data sets available for the RLS algorithm. The isolated pool condenser case, figure (2), shows that the RLS prediction method captured the trends of evaporator and condenser pools temperature after about 20 min. Then it follows the actual experimental data almost precisely in both phase and magnitude. The uncooled condenser temperature grows higher but shows little cyclic behavior as opposed to the evaporator. In addition, it seems that the evaporator has coped with the 300W cyclic load. The RLS method has met gathered data for the case of cooled pool condenser at about 15 minutes, figure (3), the ice kept condenser temperature almost constant with the same evaporator behvior. The results (figure 4) of the 500W uncooled condenser case show out of bond evaporator behavior with cyclic response. The cooled condenser case shown in figure (5), with a load that exceeds the maximum operating design conditions; show an unstable evaporator behavior with almost constant condenser temperature. The prediction of condenser pressure also was successful

in following the experimental data (figures 6 and 7) for both heating load cases showing that condenser pressure in both cases are almost identical with small fluctuations in the 300W load case.

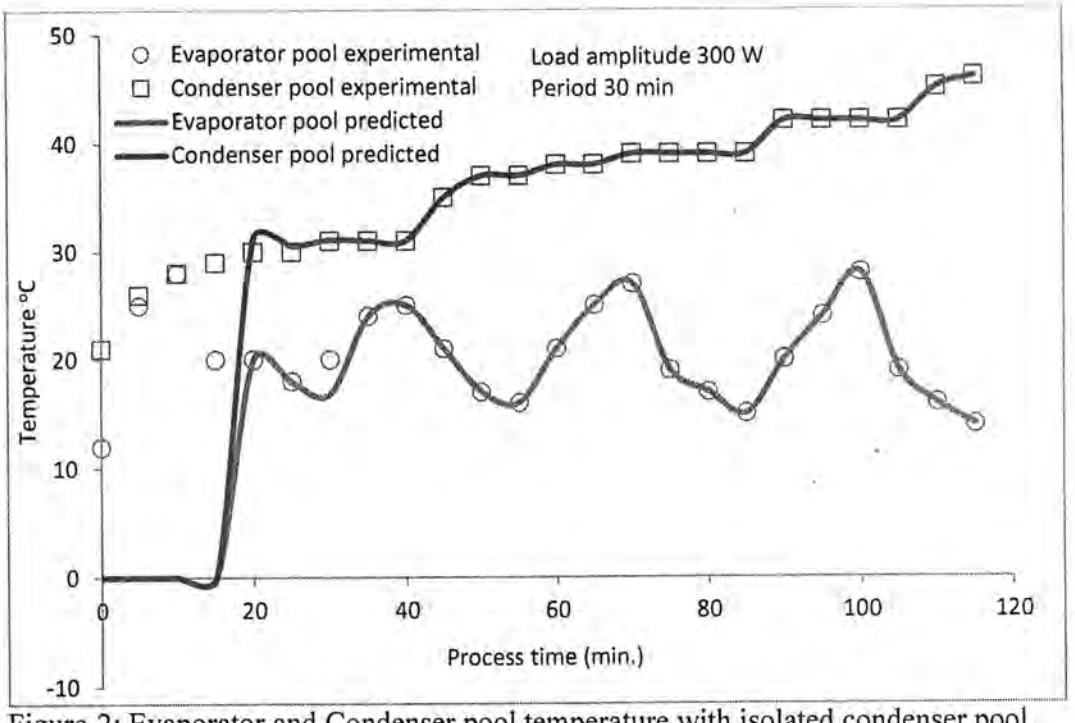

Figure-2: Evaporator and Condenser pool temperature with isolated condenser pool Under 300W load

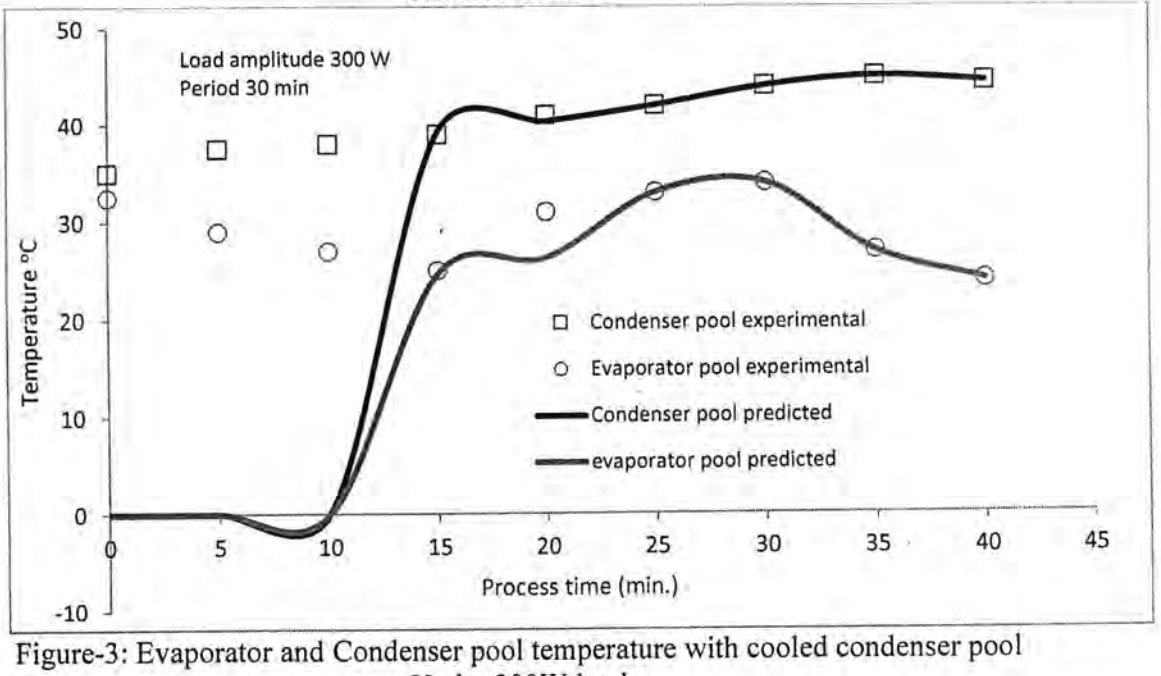

Figure-3: Evaporator and Condenser pool temperature with cooled condenser pool Under 300W load

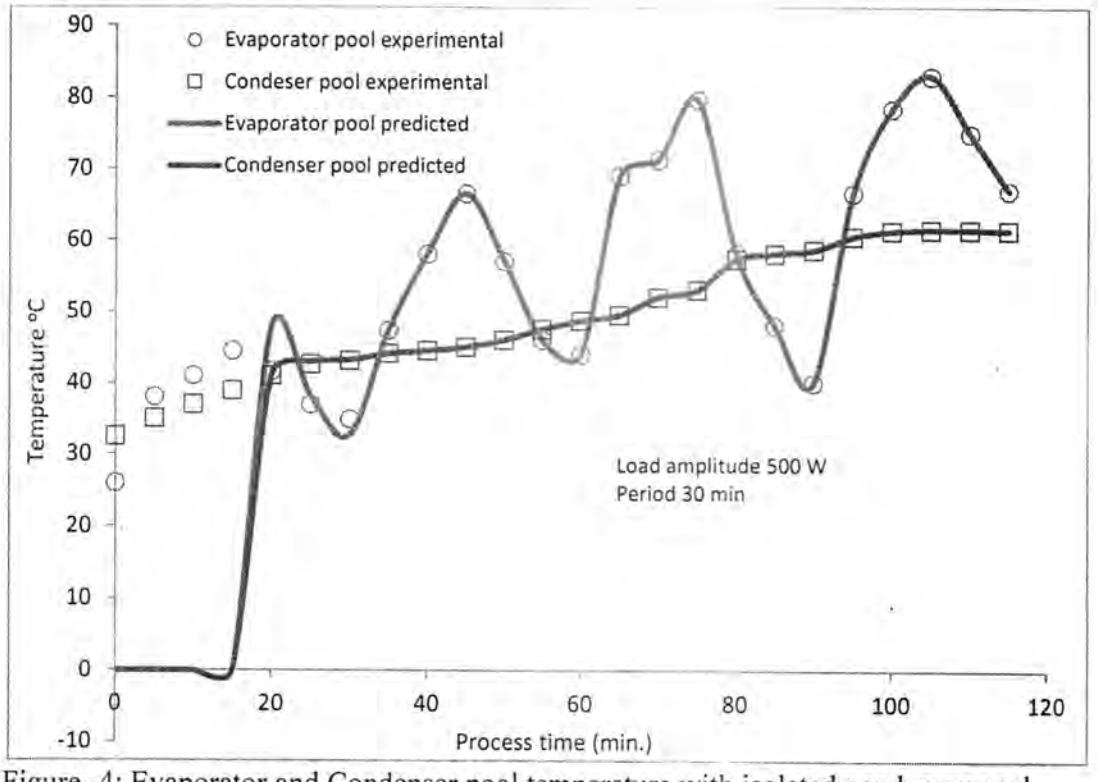

Figure -4: Evaporator and Condenser pool temperature with isolated condenser pool Under 500W load

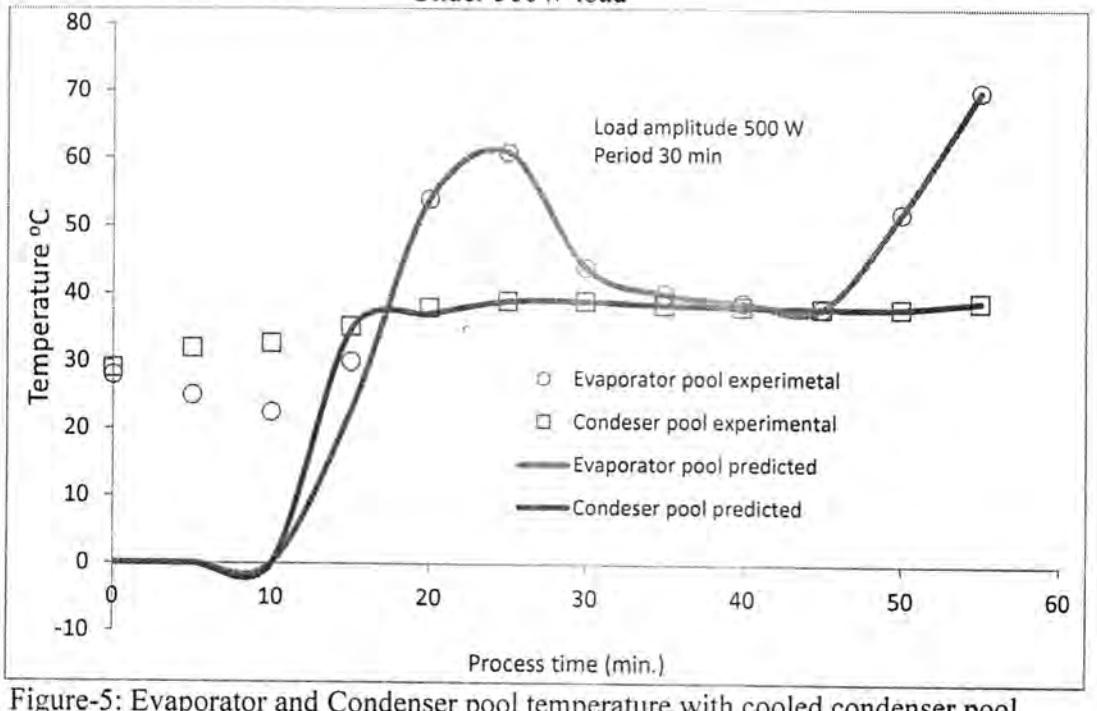

Figure-5: Evaporator and Condenser pool temperature with cooled condenser pool Under 500W load

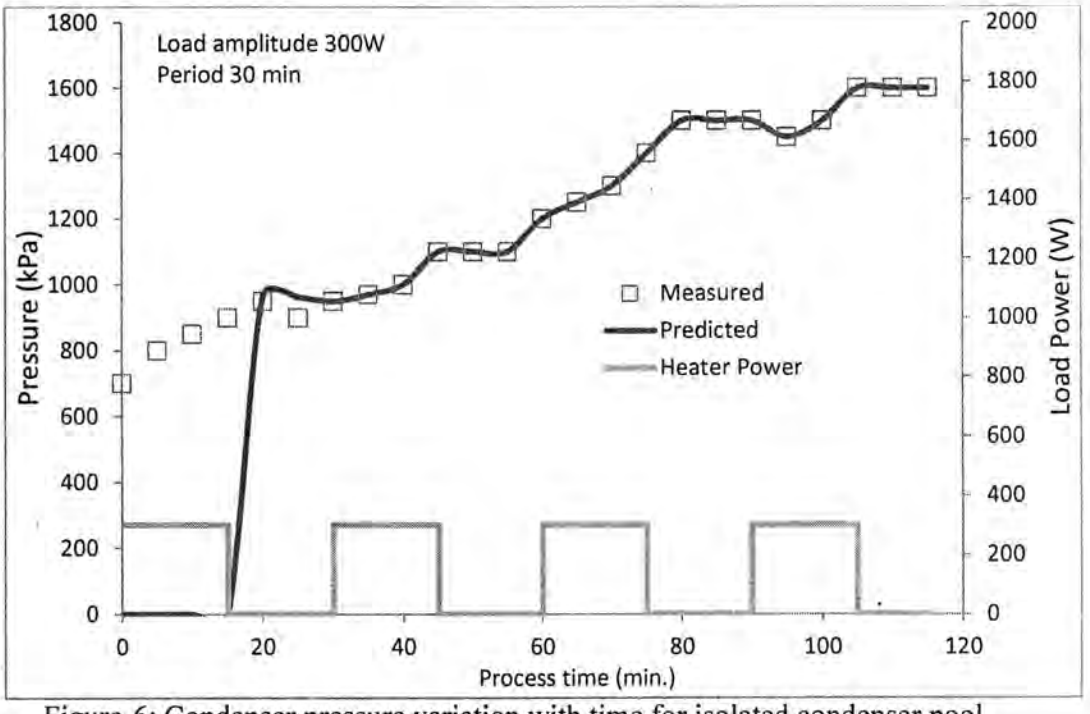

Figure-6: Condenser pressure variation with time for isolated condenser pool Under 300W Load

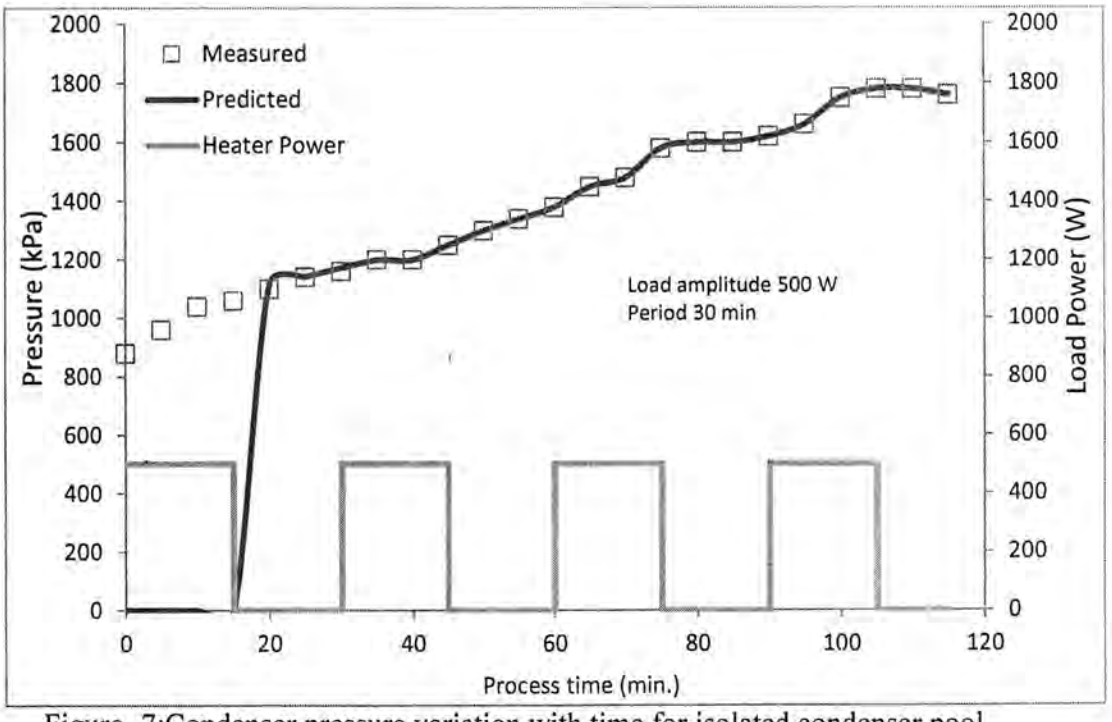

Figure -7:Condenser pressure variation with time for isolated condenser pool under 500W Load

Conclusions

The main conclusions regarding the above results are:

1. The RLS method requires an initial period before it can predict the actual behavior of the working heat pump system.

2. The evaporator is the most affected part of the cycle operating under cyclic loads.
3. The condenser temperature and pressure show an escalating trend in the isolated case.
4. The condenser show almost steady behavior in the cooled case

REFERENCES

1. Leonardo, C. Schurta; Christian, J.L. Hermesb; Alexandre, Trofino Netoa, A model-driven multivariable controller for vapor compression refrigeration systems, 2009, I. J. Ref. 32, 1672–1682.
2. Neera, Jain; Andrew G. Alleyne, Thermodynamics-Based Optimization and Control of Vapor-Compression Cycle Operation: Optimization Criteria, 2011, American Control Conference.
3. Riad Riadi, Rousseau Tawegoum, Ahmed Rachid, Gerard Chasseriaux, Modeling and Identification of a Passive Air-Conditioning Unit using the Operating Point Dependent Parameters-Structure, Computational Engineering in Systems Applications"(CESA), October 4-6, 2006, Beijing, China
4. Juan E. Catano, TieJun Zhang, Yoav Peles, Michael K. Jensen, John T. Wen, Experimental Identification of Evaporator Dynamics for Vapor Compression Refrigeration Cycle During Phase Transition, 2010, IEEE Trans. On Components and Packaging Technologies
5. Rodrigo Padilha Vieira, Rodrigo Zelir Azzolin, Cristiane Cauduro Gastaldini, Electrical Refrigeration Compressors with Single-Phase Induction Machines using RLS Algorithm, XIX International Conference on Electrical Machines - ICEM 2010, Rome.
6. Enio Pedone, Bandarra Filho, Application of Adaptive Control in a Refrigeration System to Improve Performance, ABCM, Parise , Vol. XXXIII, No. 2, April-June 2011
7. Komal, R. Borisagar; and Kulkarni, G.R., Simulation and Comparative Analysis of LMS and RLS Algorithms Using Real Time Speech Input Signal, Global Journal of Researches in Engineering, October 2010, Vol.10 Issue 5.
8. Garry, A. Einicke, Smoothing, Filtering and Prediction: Estimating the Past, Present and Future, 2012, InTech Pub., Croatia.

Edge detection in an image using Triangle Inequality Theorem

Maha A. Hameed
College of Science, Dept. of Astronomy, University of Baghdad
Received 25/4/2013 – Accepted 21/1/2014

الخلاصة

إنّ الأهميةَ الأساسيةَ لطرقِ كشفِ الحافةِ في معالجةِ الصورةِ هو كشفُ حافةِ صورةٍ بإبْقاء الملكياتِ الهيكليةِ المهمةِ في الصورةِ. في هذا البحثِ، نظريةِ عدمِ المساواة المثلثيةِ تُبنّيتْ كطريقةِ كشفِ حافةٍ باستعمال قناعِ المرشحاتَ. الخوارزميةَ المقترحةَ أُنتجتْ نوعيةَ صورةٍ جيدةٍ بالمُقارَنَة مع التي نحصَلُ عليها باستعمال الطريقةِ التقليديةِ مثل مشغلِ تفاضلِ شَحْذ صورةَ. الطريقةَ المُقتَرَحةَ أثبتَتْ بأنّها جيدُ لإبْقاء الحافةِ في بياناتِ صورةٍ.

ABSTRACT

The basic importance of edge detection methods in image processing is an image edge detection done by preserving the important structural properties in an image. In this paper, Triangle Inequality Theorem has been adopted as an edge detection method by using the filters mask. The introduced algorithm has been produced a good image quality by comparison with that which may be obtained by using the traditional method such as differentiation operator of sharpening an image. The proposed method has been proved it is good for preserving the edge in an image data.
Keywords; Edge detection, Triangle Inequality Theorem, differentiation operator

INTRODUCTION

A successful movement has been started towards the direction for processing the image by sharpening it [1]. The discontinuities in an image are immediate changes in the value of pixel which illustrate boundaries of objects in an image. The basic importance of edge detection methods in image processing is image edge detection by preserving the important structural properties in an image, while reducing the amount of data and filtering out ineffective information. So edge detection is very good in image processing [1,2]. Such as the differentiation operator on an edge which shows significant responses, this operator is used for edge detection such as using the first derivative in order to sharpening an image [2].

This paper shows the sharpening for an image using the Triangle Inequality Theorem [3,4]. In other word, in this paper, a new technique has been included the Triangle Inequality Theorem using the filters mask [1,5]. This method has been used for finding the edge in an image data. While the main objective of sharpening is to preserve fine detail in an image, therefore, in this paper, the proposed technique which advanced have focused on perceive an edge of gray-level images.

Also, a new algorithm which has been adopted to perform the edge detection procedures, the Triangle Inequality Theorem rule has been very professional in image sharpening because one can perceive high detail pixel (edge pixel). This is because many pixels which have low detail can be eliminated. The introduced algorithm has been produced good image

quality by comparison with that which may be obtained by using the differentiation operator of sharpening filter [1, 3].

First derivatives

An image is a two-dimensional signal whose intensity at any point is a function of two spatial variables [1]. Let x and y are the row and column coordinates respectively, and $f(x,y)$ the image intensity values. While an edge is a jump in intensity [1], so an edge is defined as a local variation (difference) of the image intensity $f(x,y)$. In this case, an image sharpening has been applied by using a differentiation operator on the image, therefore the filters mask are used to implement H_x and H_y in one dimension these are called Pixel Difference and they can be designed as $Hx = [1\ -1]$ and $Hy = [1\ -1]^T$. The one directional derivatives $f_x(x,y)$ and $f_y(x,y)$ are calculated as follows:

$$\nabla f_x(x,y) = f(x,y).H_x = f(x-1,y) - f(x,y) \ldots.(1)$$

$$\nabla f_y(x,y) = f(x,y).H_y = f(x,y-1) - f(x,y) \ldots.(2)$$

These can then be combined together to find the absolute magnitude of the gradient at each point [3]. The gradient magnitude is given by:

$$|\nabla f(x,y)| = \sqrt{(\nabla f_x(x,y))^2 + (\nabla f_y(x,y))^2} \ldots..(3)$$

Because this idea is derivative operator, therefore the high details for gray-level values will be high values. This will tend to produce images that have grayish edge lines.

Triangle Inequality Theorem

In a triangle the summation of lengths of any two sides is greater than the length of the third side.

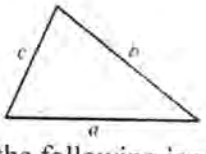

In this figure, the following inequalities hold.

$a + b > c,\ a + c > b,\ b + c > a$

Proposed algorithm

A new algorithm can be obtained by using the Triangle Inequality Theorem in order to detecting edges in an image [3,4,5]. The procedure which is used it as follows.

Step1. Initialization; Input *"T"* as threshold value then start from the pixel of value $f(2,2)$, which has the location $x=2$ and $y=2$ in an original image of size MxN, and for each pixel perform these steps;

Step2. Calculate the distance between two pixels $f(x,y)$ and $f(x-1,y)$ in x direction, and let *"Dis_x"* represents the distance between two pixels value in x direction.

Step3. If $Dis_x >= T.\ f(x,y)$, then eliminate the pixel's value $f(x,y)$ and put it equal to zero in sharpening image, because it is no edge or it has low detail value. Other wise it can be as edge value, and then continue.

Step4. Repeat the process of step 2 and 3 again on the next pixel in an original image i.e. $(f(x+1,y))$.

Step5. Repeat the process of step 2,3and 4 again on the same image but in y direction to find $K_y(x,y)$.

Step6. Calculate the gradient magnitude from equation (3) to find the edge gray level image.

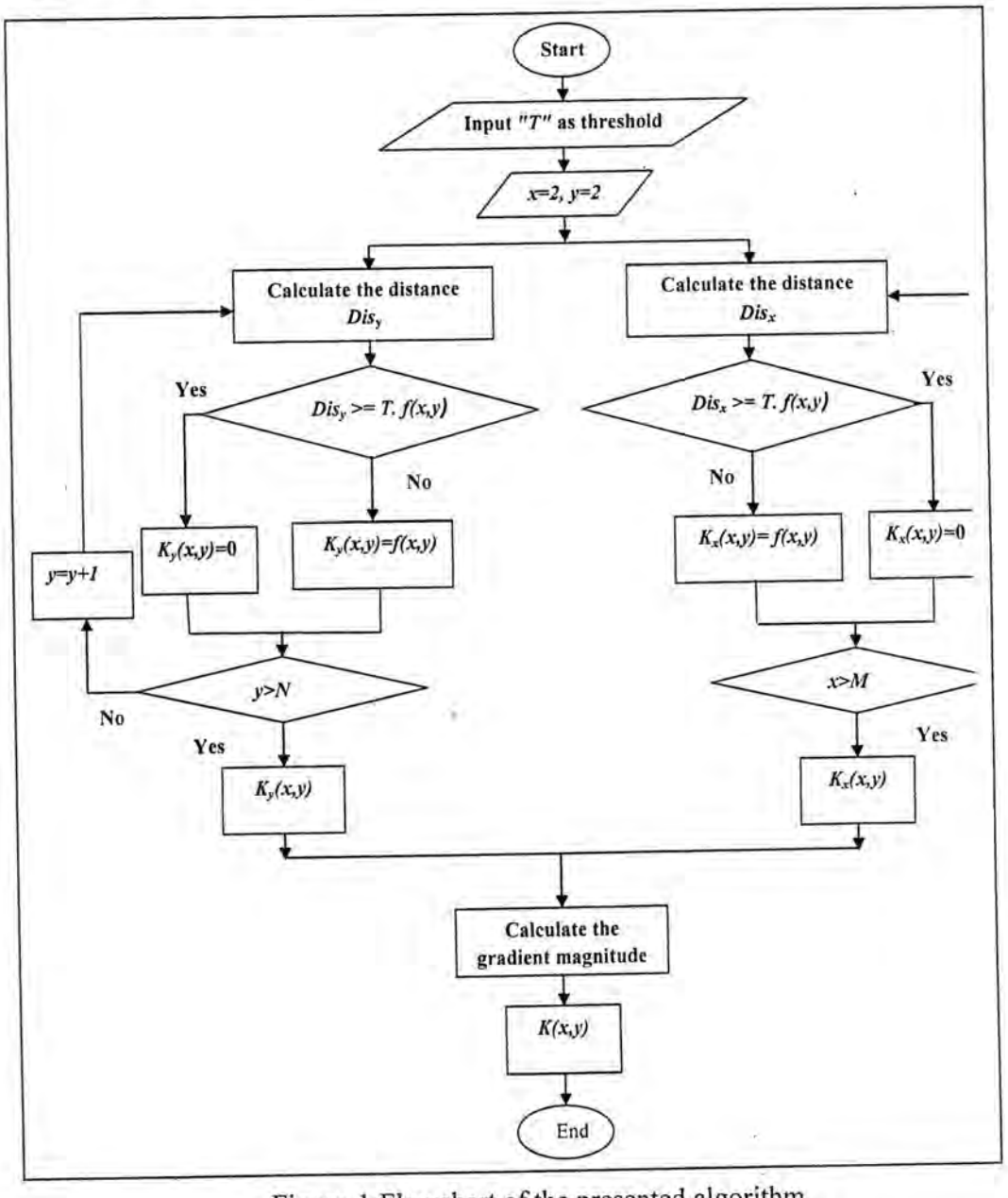

Figure-1:Flowchart of the presented algorithm.

The Triangle Inequality Theorem will be very good in edge detection because one can detect an edge pixel which has high detail.

MATERIALS AND METHODS

The purpose of this paper is to study and understand a Triangle Inequality Theorem and it is compared with sharpening filter in edge detection see the conclusions of this paper. The proposed algorithm is based on the Triangle Inequality Theorem, where this Theorem will be very efficient in image sharpening because one can detect an edge pixel which has high detail, and reduce other pixels which have low detail. In other word, this technique is simple conceptually to get edged image close to that is produced from the differentiation operator using *Pixel Difference* filters in two directional *x* and y.

Results and discussion

For image quality measurement we use objective measure (PSNR), but the subjective quality evaluation of human is the most important measurement. The introduced algorithm was produced good image quality by comparison with that which was obtained by using the differentiation operator of sharpening filter. The tested image was 256x256 pixels.

Table.1; The PSNRs obtain by applying only the differentiation operator and our proposed method. In this paper, the detecting of an edge was done according to our proposed method, on "Lena" image, for different threshold values. As expected, our proposed method lead to a good PSNR for image, by comparison with that which was obtained by using the differentiation operator which was filtered in two directional x and y.

Table-1: The MSEs and PSNRs obtain by applying only the differentiation operator and our proposed method on "Lena" image, for different threshold values.

Threshold values(T)	MSE	PSNR(dB)
0.1	12.197	27.183
0.2	8.704	29.335
0.3	6.214	31.921

Figiure-2:Original image.

Figure-3:An edge detected for "Lena" image using the differentiation operator.

a. T=0.1 **b. T=0.2** **c. T=.3**

Figure-4:An edge detected for "Lena" image using our algorithm for different threshold values.

CONCLUSION

1- Using different threshold values (T) in the presented algorithm, one can notice that many edges are preserved, where fig.4b better than fig.4a and fig.4c better than fig.4b.

2- The Triangle Inequality Theorem rule will be very good idea in edge detection because one can preserve an edge value which has high detail by depending on the threshold values.

REFERENCES

[1] E. Nadernejad, S. Sharifzadeh and H. Hassanpour, "Edge Detection Techniques: Evaluations and Comparisons", Applied Mathematical Sciences, Vol.2, No.31, Pp.1507 – 1520, 2008.

[2] Rishi R. Rakesh, Probal Chaudhuri, and C. A. Murthy, "Thresholding in Edge Detection: A Statistical Approach", IEEE Trans. on image processing, Vol.13, No.7, Pp.927-936, 2004.

[3] S.H Chen and W.M Hsieh, "Fast algorithm for VQ codebook design", IEEE proc.I, Vol. 138, No.5, 1991.

[4] S.H. Huang and S.H. Chen, "Fast encoding algorithm for VQ-based image coding", Electronics letters, Vol.26, No.19,1990.

[5] M. A. Hameed, "Fast encoding algorithm for vector quantization - based on block truncation coding technique", Iraqi Journal of Science, Vol.46, No.1, Pp.296-298, 2005.

[6] M. A. Hameed, "Edge Detection in an Image by Using the Elimination Rule", Iraqi Journal of Science, Vol.53, No.4, Pp.1017-1019, 2012.

Determination of E2/M1 Multipole Mixing Ratios of Gamma Transitions in ^{94}Sr Isotope

Ahmad Mousa Eshwakh
Physics Dept., Education college for pure sciences Ibn Al Haitham, Baghdad University
Received 27/1/2014 – Accepted 23/2/2014

الخلاصة

استخدم التنسوري الاحصائي الثابت في حسابات نسب الخلط لثنائي القطب المغناطيسي M1 ورباعي القطب الكهربائي E2 لانتقالات اشعة كاما بين مستويات الطاقة للنظير ^{94}Sr. اظهرت نتائج بحثنا هذا توافقا جيدا مع ماسبق من قيم δ العملية والنظرية، كما ان استخدام طريقة التنسوري الاحصائي الثابت اظهرت صحتها في هكذا حسابات.

ABSTRACT

In present work the constant statistical tensor (CST) method is applied to the calculi of gamma ray E2/M1 multipole mixing ratio of electromagnetic transition in ^{94}Sr isotope. The values of δ obtained for ^{94}Sr isotope are in reasonably good agreement with the previous experimental and theoretical values.

INTRODUCTION

Several calculations have attempted to explain the phenomena of nuclei in the region of neutron rich strontium isotope where they have been of great interest because of seemingly anomalous strength of the Z=38, 40 and N=56 sub shell closures in this region and because of shape that occurs at N=60, confirmed that the excited states in ^{93}Sr arise from $\upsilon d_{\frac{5}{2}}$ hole weakly coupled to a ^{94}Sr core and similarly excited states in ^{95}Sr from $\upsilon g_{\frac{7}{2}}$ particle states coupled to the ^{94}Sr core.

One of interest feature of ^{94}Sr is the excited an 3^- state. The 3^- assignment is based predominantly on the angular correlations by [1,2] for transitions in the beta-decay of ^{94}Rb.

Transitions between states with $\Delta I = 1$ and likely parity can in general have multipolarity M1, E2, M3, … where M1 is magnetic dipole, E2 is the electric quadrupole and so, assuming that only the lowest two multipolarities dominate, these transitions will be mixed E2/M1. The physical quantity, delta mixing ratio δ can be extracted from angular correlation measurement as defined by Krane and Steffan [3]. The values of δ usually used to distinction the nuclear structure and the properties of gamma-transitions from exited levels.

The constant statistical tensor (CST) depends on the coefficient of statistical tensor which is the same for all levels with the same spin value

independent upon energy and its parity. This fact used in the present work to calculate the value of δ for many transitions with undefined parities. a_2-coefficient are deduced from angular correlation experiment of [1] are used in the present calculations.

THEORETICAL CONSIDERATIONS

The multipole mixing ratios δ values have been calculated according to the following equations:

$$a_2(J_i - J_f) = \rho_2(J_i)\frac{F_2(J_fL_1L_1J_i)+2\delta F_2(J_fL_1L_2J_i)+\delta^2 F_2(J_fL_2L_2J_i)}{1+\delta} \quad \ldots(1)$$

Where:

a_2 is the coefficient determined from angular correlation experiment.

J_i and J_f are the initial and final spin states.

$\rho_2(J_i)$ statistical tensor coefficient depends on the value of J_i .

L's are the angular momentum of γ-transitions.

$L_1=1$, $L_2=L_1+1$ and $L\neq 0$

F_2 coefficients, taken from W. D. Hamilton [4].

In case of $\delta=0$, i.e pure transition, equation (1), reduced to the following form;

$$a_2(J_i - J_f) = \rho_2(J_i)F_2(J_fL_1L_1J_i) \quad \ldots(2)$$

Then

$$\rho_2(J_i) = \frac{a_2(J_i-J_f)}{F_2(J_fL_1L_1J_i)} \quad \ldots(3)$$

RESULTS AND DISCUSSION

DATA ANALYSIS AND RESULTS

Figure 1 show a part of energy levels and gamma transition in ^{94}Sr isotope. from this figure the initial and final spins of gamma transition used in present work are indicated .

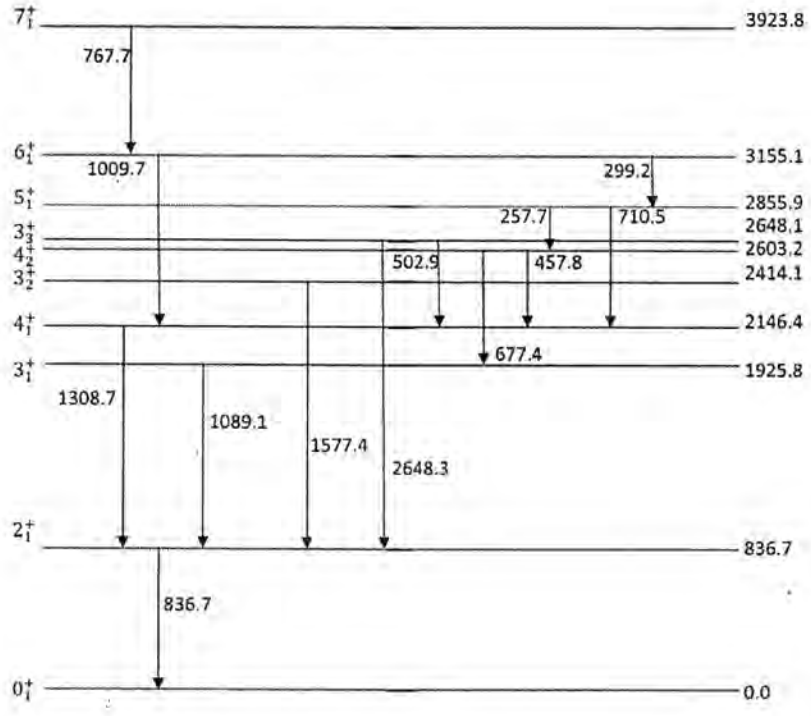

Figure -1: Gamma-transition between energy levels populated in ^{94}Sr isotope [4].

The gamma-transitions of $(3_1^+ - 2_1^+)$ of $E_\gamma = 1308.7$ keV is considered to be pure of E2 in these calculations.

$$\rho_2(3_1^+ - 2_1^+) = \frac{a_2(3_1^+ - 2_1^+)}{F_2(J_f L_1 L_1 J_i)} = \frac{a_2(3_1^+ - 2_1^+)}{0.4664}$$

The odd parity of 1926 keV level was proposed by [6] because of the dipole nature of the $3_1^+ - 2_1^+$ transition. The more sensitive measurements of [7] found that this transition is pure dipole. The level 3932 keV was assigned a J^π of 8^+ by [5,6], but the angular correlation measurements of [7] for 767.7-1308.7 keV cascade found J^π is 7^+ for this level.

$\rho_2(J_i)$ tabulated for all transitions have been calculated according to equation (3) are in table 1. The statistical tensors $\rho_2(J_i)$ which are calculated considered to be constant for all levels with the same J_i values [5]. The calculated values of $\rho_2(J_i)$ are used in equation (1) to find out the δ -values for all mixed γ-transitions.

Table -1: The values of $\rho_2(J_i)$ according to equation 3.

No.	$\rho_2(J_i) = \frac{a_2(J_i - J_f)}{F_2(J_f L_1 L_1 J_i)}$
1	$\rho_2(2_1^+ - 0_1^+) = \frac{-0.025}{-0.4183} = 0.0597$
2	$\rho_2(4_1^+ - 2_1^+) = \frac{0.101}{-0.4387} = -0.2302$
3	$\rho_2(3_1^+ - 2_1^+) = \frac{-0.085}{-0.1237} = 0.6871$
4	$\rho_2(4_2^+ - 3_1^+) = \frac{0.270}{-0.0448} = -0.0267$
5	$\rho_2(5_1^+ - 4_1^+) = \frac{0.189}{0.2944} = 0.6419$
6	$\rho_2(5_1^+ - 4_2^+) = \frac{0.236}{0.2944} = 0.8016$
7	$\rho_2(3_2^+ - 2_1^+) = \frac{-0.235}{-0.1237} = 1.8997$
8	$\rho_2(4_2^+ - 4_1^+) = \frac{-0.189}{-0.4387} = 0.4308$
9	$\rho_2(3_3^+ - 2_1^+) = \frac{0.083}{-0.1237} = -0.8501$
10	$\rho_2(3_3^+ - 4_1^+) = \frac{0.177}{0.1443} = 1.2266$
11	$\rho_2(6_1^+ - 4_1^+) = \frac{0.082}{-0.4029} = -0.2035$
12	$\rho_2(7_1^+ - 6_1^+) = \frac{-0.055}{0.2734} = -0.2011$

The d-mixing ratios of (δ)-transitions are listed in Table 2.

Table-2: δ-mixing ratios of E_γ in ^{94}Sr isotope.

$a_2(J_i - J_f) = \rho_2(J_i) \frac{F_2(J_f L_1 L_1 J_i) + 2\delta F_2(J_f L_1 L_2 J_i) + \delta^2 F_2(J_f L_2 L_2 J_i)}{1+\delta}$
$a_2(2_1^+ - 0_1^+) = 0.0597 \frac{0.4183 - 1.0952\delta - 0.2988\delta^2}{1+\delta}$
$a_2(4_1^+ - 2_1^+) = -0.2302 \frac{-0.4387 - 1.8718\delta - 0.2646\delta^2}{1+\delta}$
$a_2(3_1^+ - 2_1^+) = 0.6871 \frac{0.3464 - 1.8974\delta - 0.1237\delta^2}{1+\delta}$
$a_2(4_2^+ - 3_1^+) = -0.0267 \frac{-0.0448 - 1.1428\delta - 0.0855\delta^2}{1+\delta}$
$a_2(5_1^+ - 4_1^+) = 0.6419 \frac{0.2944 - 1.8618\delta - 0.0000\delta^2}{1+\delta}$
$a_2(5_1^+ - 4_2^+) = -0.8016 \frac{0.2944 - 1.0954\delta - 0.0170\delta^2}{1+\delta}$
$a_2(3_2^+ - 2_1^+) = 1.4761 \frac{-0.1237 - 0.9487\delta - 0.0274\delta^2}{1+\delta}$
$a_2(4_2^+ - 4_1^+) = 0.4308 \frac{-0.4387 - 0.6708\delta + 0.2646\delta^2}{1+\delta}$
$a_2(3_3^+ - 2_1^+) = 0.6709 \frac{-0.1237 - 1.1838\delta - 0.0274\delta^2}{1+\delta}$
$a_2(3_3^+ - 4_1^+) = 1.2266 \frac{0.1443 + 1.4434\delta + 0.3093\delta^2}{1+\delta}$
$a_2(6_1^+ - 4_1^+) = -0.2035 \frac{-0.4029 - 1.1396\delta - 0.3022\delta^2}{1+\delta}$
$a_2(7_1^+ - 6_1^+) = -0.2011 \frac{0.2734 - 1.8338\delta - 0.0488\delta^2}{1+\delta}$

Gamma-transitions, $J_i - J_f$ and a2-coefficients are used in this calculations are listed in Table 3. By solving the equations in Table 2 we

can calculated the values of δ-mixing ratios for gamma-transition between energy levels populated in ^{94}Sr.

Table 3 content the present values of δ for ^{94}Sr isotope with values of δ determined by other authors [1].

Table-3: The values of δ with the comparison of [1] values.

E_i(keV)	E_γ(keV)	$J_i^\pi - J_f^\pi$	a_2	δ-values	
				Present work	Ref.[1]
836.7	836.7	$2_1^+ - 0_1^+$	0.101	$-0.274^{+5.23}_{-0.533}$	0
2164.4	1308.7	$4_1^+ - 2_1^+$	0.105	$-16^{+4.085}_{-0.482}$	0
1925.8	1089.1	$3_1^+ - 2_1^+$ $3_1^+ - 4_1^+$	-0.052	$-30.337^{+5.507}_{-0.055}$	0.026(6)
2603.2	677.4	$4_2^+ - 3_1^+$	0.270	$0.057^{+0.232}_{-2.851}$	$-1.7^{+1.0}_{-0.5}$
2855.9	710.5	$5_1^+ - 4_1^+$	-0.235	$-12.646^{+3.491}_{-1.752}$	$-6.5^{+1.4}_{-2.4}$
2855.9	257.7	$5_1^+ - 4_2^+$	0.273	$5.715^{+2.390}_{-1.762}$	-----
2648.1	2648.3	$3_2^+ - 2_1^+$	-0.083	$5.314^{+2.305}_{-3.494}$	-0.015
2603.2	457.8	$4_2^+ - 4_1^+$	-0.189	$2.501^{+1.581}_{-0.012}$	$2.1^{+2.9}_{-0.7}$
2648.1	502.9	$3_3^+ - 4_1^+$	0.177	$-0.509^{+0.213}_{-3.206}$	$-4.9^{+1.4}_{-2.6}$
3155.1	1009.7	$6_1^+ - 4_1^+$	0.082	$-5.987^{+0.575}_{-2.44}$	0
392.8	767.2	$7_3^+ - 2_1^+$	-0.055	$4.080^{+2.021}_{-3.054}$	$13.5^{+21.9}_{-5.2}$

The comparisons of delta values in the table can be classified in to three classifications as follows;

1- Some of delta values in ref [1]has zero values, such as the delta of the transitions 836.7-836.7KeV, 2164.4-1308KeV and 31551-1009.7 KeV, and there is no value for transition 2855.9-257.7 Kev. In our calculations there delta values for these transitions, so we think our results more significant than the ref[1] .
2- The disagreement between the values of our calculation and ref[1] of delta for the transitions, 1925.8-1089.1 KeV, 3155.1-1009.7KeV and 3928-767.2KeV, is due to small values of a2.
3- The rest of the our results have an agreement within the error bars of delta values of ref[1].we conclude, that the values of delta is very sensitive to the values of a2.

REFERENCES

1- Christopher Goodin, Ph.D. thesis submitted to the faculty of the graduate School of Vanderbit University, (2008).

2- Al-saad.J.R.," Multipole Ratio Of Transitions N Isotopes "Oman J of Applied sciences , Vol 5,(2014)

3- Krane.K. S.,. Steffen R. M. " Determination of the E2/M1 Multipole Mixing Ratios of the Gamma Transitions in ^{110}Cd" . Phys. Rev. C2, 724 (1970)

4- Hamilton. W. D., University of Sussex, Brighton, U.K. (1975).

5- Sigbahn K., "Alpha, Beta and Gamma-rays Spectroscopy", North Holland, Amsterdam , vol 1,(1968).

6- Hamilton. J.H., Ramayya. A.V., Zhu S.J.,Alopian.G.M., Oganessian.Y.T., Cole.J. D;Rasmussen .J.O.,and Stoyes.M.A. "New Insights From Studies Of Spontaneous Fission With Large Detectors Arrays", Prog. in Part. and Nucl. Phys. (invited review), 35, 635,(1995).

7- Buchinger. F., Ramsay. E., Silverans. R., Lievens. P., Arnold. E., Neu.W., Neugart. R., Wendt. K., Ulm, G. "Nuclear ground-state spins of short-lived strontium isotopes". Zeitschrift fur physik a-hadrons and nuclei, 327(3), 361-362, (1987).

8- Stone N. J., Atomic Data and Nuclear Data sheet, (1976).

9- Urban W., Physical Rev. C2, 72, 27302, (2005).

Best Approximation Polynomial of Unbounded Multivariate Functions

Saheb AL- Saidy and Raad Falih Hassan
Department of Mathematics, College of Science, AL- Mustansiriya University.
Received 28/1/2014 – Accepted 23/2/2014

الخلاصة

الهدف من هذا البحث هو دراسة تقريبات الدوال غير مقيدة بالنسبة إلى متعددات الحدود في فضاءات الوزن وإيجاد درجة أفضل تقريب لهذه الدوال باستخدام نماذج الاستمرارية.

ABSTRACT

The aim of this paper is to study the approximations of unbounded functions with respect to the polynomials in $L_{P,\alpha}$-spaces and finding the degree of best approximation of these functions in terms of modulus of continuity.

INTRODUCTION

In 1853, the great Russian mathematician P.L. Chebyshev, while he was working on the problem of linkages and devices which translate the linear motion of a steam engine into the circular motion of a wheel, considered the following problem:

Given a continuous function f defined on a closed interval $[a,\ b]$ and a positive integer n, can we represent f by a polynomial $P(x) = \sum_{k=0}^{n} a_k\, x^k$ of degree at most n, in such a way that the maximum error at any point x in $[a, b]$ is controlled?

Chebyshev's problem is perhaps best understood by rephrasing it in modern terms.

What we have here is a problem of linear approximation in a normed linear space. Let X be a vector space, a norm on X is a nonnegative function on X satisfying $\|x\| \geq 0$ and $\|x\| = 0 \leftrightarrow x = 0$

$\|\alpha x\| = |\alpha|\|x\|$ for $\alpha \in R$ (real number).

$\|x + y\| \leq \|x\|\|y\|\ \forall\, x, y \in X$

Any norm on X induces a metric or distance function by setting dist $(x, y) = \|x - y\|$. Given a subset (or even a subspace) Y of X and a point $x \in X$, if there $y \in Y$ such that $\|x - y\| = inf_{z\in Y}\|x - z\|$ then y is called a best approximation from Y to X [1].

In (2002), S. K. Jassim and E. S. Bhaya used the direct (Jackson) theorem for the order of best nulti-approximation by algebraic polynomials also, A. H. Al-Abdulla [2] obtained some results concerning the approximation of bounded μ-measurable function in $L_P\,(\mu)$- spaces, in addition to Eman Hassan Muhammed Al-Asady [3], Hassen B. M. [4], and Hammod A. A. [5].

Approximation of a function is the problem of constructing function P, belonging to a finite dimensional linear space from a set of given data.

Usually the approximation is obtained by simplifying another more difficult function f. In this situation, p approximates f [6], [7]. Let (X,d) be a metric space and A subset of X, then for any $f \in X$, if there is $g \in A$ such that $d(f,g) \leq d(f,h)$ for every $h \in A$. then g is called a best approximation from A to f [8].

In this paper, we will study the degree of approximation of unbounded functions.

Hereunder, we listed definitions and notations need to prove our results.

Definition: (1)

Let R^n be the n-dimensional

Euclidean space equipped with the usual norm $\|.\|$ ($n \geq 1$) and G is the bounded convex domain in R^n

Let $L_{P,\alpha}(G) = \{f | f: G \to R\}$, such that

$$\|f\|_{P,\alpha,G} = \left(\int_G |f(x)w_\alpha(x)|^P dx\right)^{1/P} < \infty \quad , \ 0 < P < \infty$$

where f is an unbounded function on G and $w_\alpha(x)$ is a weight positive function.

Definition: (2)

For $0 < P \leq \infty$ and integer $\ell \geq 0, \alpha > 0$. Let $f \in L_{P,\alpha}$ be an unbounded function of several variables, $f(x), x = (x_1, \dots, x_n) \in R^n$.

An n-dimensional multi-index is an n-tuple

$m = (m_1, m_2 \dots, m_n)$ of non-negative integers. The number $|m| = m_1, m_2 \dots, m_n$ is called the order or degree of m, then

$$W_{P,\alpha}^{(\ell)}(G) = \{f | f \in L_{P,\alpha};\ D^m f \in L_{P,\alpha}\}$$

$$D^m f = \frac{\partial^{|m|} f}{\partial_{x_1}^{m_1} \dots \partial_{x_n}^{m_n}}$$

Where D^m is denotes the partial derivatives of m-th order.

Definition:(3) [9]

The k-th difference of the function f with the step $\varepsilon \geq 0$ in the direction of the unit vector e; $k \geq 0$(k is an integer) is defined by:

$$\Delta^{(K)}(\varepsilon e)f(x) = \sum_{i=0}^{k}(-1)^{k-1}\binom{i}{k} f(x + i\varepsilon e);\ \Delta^{(0)}(\varepsilon e)f(x) = f(x)$$

Where $\binom{i}{k} = \frac{i!}{k!(i-k)!}$

Definition: (4)

Let $f \in L_{P,\alpha}$ be an unbounded function and integer $\ell \geq o$, then

$$\|f\|_{W_{P,\alpha}^{(\ell)}(G)} = SUP\left\{\left\|D^{(\ell)}(e)f\right\|_{P,\alpha,G} : e \in R^n, \|e\| = 1\right\}$$

Definition: (5)

The moduli of smoothness of k-th order for the derivatives of order ℓ, $\delta \geq 0$ are

1) $\omega_k^{(\ell)}(f;\delta)_{P,\alpha} =$

$SUP_{e\in R^n,\|e\|=1} \underset{0\le\varepsilon\le\delta}{SUP} \left\|\Delta^{(k)}(\varepsilon e)D^{(\ell)}(e)f\right\|_{P,\alpha,G_{k\in e}}$

2) $\omega_k^{(\ell)}(f;\delta) = \underset{e\in R^n}{SUP} \underset{0\le\varepsilon\le\delta}{SUP} \left\|\Delta^{(k)}(\varepsilon e)D^{(\ell)}(e)f\right\|_{c(G),\alpha}$

Definition:(6) [9]

For integers $N \geq 0$ and $n \geq 1$ let $P_{N,n}$ be the set of all algebraic polynomials $g(x) = \sum c_\lambda x^\lambda$ of degree $\leq N$ respect to all n variables, where

$\lambda = (\lambda_1, \lambda_2, \dots, \lambda_n)$ is a multi-index with integer nonnegative components λ_i, $x^\lambda = {x_1}^{\lambda_1}.{x_2}^{\lambda_2} \dots {x_n}^{\lambda_n}$; C_λ are real numbers, and the sum is taken over all λ such that $|\lambda| = \lambda_1 + \lambda_2 + \cdots + \lambda_n \leq N$.

Definition: (7)

The degrees of best approximation of $f \in \mathrm{L}_{P,\alpha}(\mathrm{G})$ and $f \in \mathrm{W}_{P,\alpha}^{(s)}$ are defined by $E_N(f,G)_{P,\alpha} = \inf\{\|f-g\|_{P,\alpha,G} : g \in P_{N,n}\}$

$E_N^{(s)}(f,G)_{P,\alpha} = \inf\left\{\|f-g\|_{W_{P,\alpha}^{(s)}(G)} : g \in P_{N,n}\right\}$

$E_N^{(s)}(X)_{P,\alpha} = SUP\left\{E_N^{(s)}(f,G)_{P,\alpha} : f \in X\right\}$ where X is a set of functions.

Definition: (8)

Let f be an unbounded function $f:[a,b] \to R$, f is said to be of bounded weighting variation on $[a,b]$, if there is a constant $M > 0$ such that $\sum_{i=1}^{n}|(f.w)(x_i) - (f.w)(x_{i-1})| \leq M$

Definition: (9)

The integral modulus of order k of the function f is defined by:

$$\omega_k(f;\delta)_{P,\alpha} = SUP\left\{\int_a^{b-kh}\left|\Delta_k^h(f.w)(x)\right|dx : a \leq h \leq \delta\right\}^{1/P}, \delta\epsilon\left[0 \leq \delta \leq \frac{b-a}{K}\right]$$

Notations:

Let $Vn^{(\ell)}(M,G)$ be the set of all functions f having, for each unit vector e, a finite derivative $D^{(\ell)}(e)f$ on the nonempty intersection of each parallel to vector e straight line $\mathrm{L}\subset\mathrm{R}^n$ with the domain G the total variations of which on these intersection are bounded by the same number $M > 0$ for all vectors e[9].

Let e be any unit vector of the space R^n $(n \geq 2)$, let $\pi(e)$ be the $(n-1)$-dimensional subspace orthogonal to the vector e, let G (e) be the orthogonal projection of the bounded closed convex domain $G \subset R^n$ to the subspace $\pi(e)$, and let $\pi_{n-1}(G) = SUP\{V(G(e)) : e\}$ be the maximal value of the $(n-1)$- dimensional projection of G. let $y \in G(e)$

be an arbitrary point, let $[a(y), b(y)]$ be the segment obtained by intersection of the straight line $L \subset R^n$ passing through y and parallel to the vector e. with the domain G [9].

Proposition: (1)

Let $f \in L_{P,\alpha}(G)$ be an unbounded function, and N the set of all natural numbers, $Z_+ = NU\{0\}, \ell \in Z_+, k \in N, 1 \leq P \leq \infty$ and $f \in W_{P,\alpha}^{(\ell)}(G)$, then $\forall \delta \in (0, \infty)$ and $s = 0, \ldots\ldots\ldots, \ell$, we have

$$\omega_{\ell-s+k}^{(S)}(f;\delta)_{P,\alpha} \leq \delta^{\ell-s}\omega_k^{(\ell)}(f;\delta)_{P,\alpha}$$

Proof:

From the definition of the modulus of smoothness of order $(\ell - s + k)$, we have

$$\omega_{\ell-s+K}^{(s)}(f;\delta)_{P,\alpha} =$$

$$\sup_{e}\ \sup_{0\leq h\leq\delta}\left(\int_{G(\ell-s+K)he}\left|\Delta^{\ell-s+k}(he)D^{(s)}(e)f(x)w(x)\right|^P dx\right)^{1/P}$$

$$=$$

$$\sup_{e}\ \sup_{0\leq h\leq\delta}\left(\int_{G(\ell-s+K)he}\left|\Delta^{k}(he)\Delta^{\ell-s}D^{(s)}(e)f(x)w(x)\right|^P dx\right)^{1/P}$$

Using the Lebesgue theorem on representation of an absolutely function as the indefinite integral of its derivative.

$$\omega_{\ell-s+K}^{(s)}(f;\delta)_{P,\alpha} \leq$$

$$\sup_{e}\ \sup_{0\leq h\leq\delta}\left(\int_{G(\ell-s+K)he}\left|\Delta^{K}(he)\int_{[0,h]^{\ell-s}}D^{(\ell)}(e)f.w\left(x+\sum_{j=1}^{\ell-s}dtj\right)dt_1\ldots.dt_{\ell-s}\right|^P dx\right)^{1/P}$$

Using Minkowski's Inequality in integral form , we get

$$\omega_{\ell-s+K}^{(s)}(f;\delta)_{P,\alpha} \leq$$

$$\sup_{e}\ \sup_{0\leq h\leq\delta}\int_{[0,h]^{\ell-s}}\left(\int_{G(\ell-s+K)he}\left|\Delta^{K}(he)D^{(\ell)}(e)f.w\left(x+\sum_{j=1}^{\ell-s}tje\right)\right|^P dx\right)^{1/P}dt_1\ldots.dt_{\ell-s}$$

$$=$$

$$\sup_{e}\ \sup_{0\leq h\leq\delta}\int_{[0,h]^{\ell-s}}\left\|\Delta^{K}(he)D^{(\ell)}(e)f\right\|_{P,\alpha,G(\ell-s+K)he}dt_1\ldots.dt_{\ell-s}$$

$$=\sup_{e}\ \sup_{0\leq h\leq\delta}\left\|\Delta^{K}(he)D^{(\ell)}(e)f\right\|_{p,\alpha,G(\ell-s+k)he}$$

Since $h \leq \delta \Longrightarrow h^{\ell-s} \leq \delta^{\ell-s}$, we have

$$\omega_{\ell-s+K}^{(s)}(f;\delta)_{P,\alpha} \leq \sup_{e}\ \sup_{0\leq h\leq\delta}\left\|\Delta^{K}(he)D^{(\ell)}(e)f\right\|_{P,\alpha,G(\ell-s+k)he}$$

$$\omega_{\ell-s+K}^{(s)}(f;\delta)_{P,\alpha} \leq \delta^{\ell-s}\omega_K^{(\ell)}(f;\delta)_{P,\alpha}$$

We will list some theorems and proposition that are needed to prove our results.

Theorem (1): [10]
Any function g with bounded variation can be represented as the difference of two monotone non-decreasing functions.

Proposition (2):
Let $f \in L_{P,\alpha}$ be an unbounded function. If the function f has the bounded weighted variation $V(f,[a,b])$ on [a, b], then for any $0 \le \delta \le \frac{|[a,b]|}{2}$ we have:

$$\omega(f;\delta)_{P,\alpha} \le c(P)\begin{cases}\left(V(f,[a,b])\right)^{1/P}\delta^{1/P}(\omega(f;\delta)_{\alpha})^{1-1/p} & 1 \le P \le \infty \\ V(f,[a,b])\ \ \delta & 0 < P < 1\end{cases}$$

Proof:
Step (1) :
for $[0,1]$.
If $y = a + (b-a)x \ \ , x \in [0,1]$
$f.w(y) = V(f.w,[a,b])\psi(x), x \in [0,1]$ and $V(\psi,[0,1]) = 1$
Using definition (9), we have

$$\omega_k(f;\delta)_{P,\alpha} = SUP\ \ \left\{\int_a^{b-kh}\left|\Delta_h^k f.w(x)\right|^P dx\ \ : 0 \le h \le \delta\right\}^{1/P}$$

If $k = 1$, we get

$$\omega(f;\delta)_{P,\alpha} = SUP\ \ \left\{\int_a^{b-h}|\Delta_h f.w(y)|^p dy : 0 \le h \le \delta\right\}^{1/P}$$

$$= SUP\left\{\int_a^{b-h}|f.w(y+h) - f.w(y)|^P dy : 0 \le h \le \delta\right\}^{1/P}$$

Changing the bounds of integration
$y = b - h \Longrightarrow a + (b-a)x = b - h \Longrightarrow (b-a)x = b - h - a$
$\Longrightarrow x = \frac{b-a-h}{b-a} = \frac{(b-a)-h}{b-a} = 1 - \frac{h}{b-a}$
Since $b - a = |[a,b]|$
$x = 1 - \frac{h}{|[a,b]|}$
$y = a \Longrightarrow a + (b-a)x = a$
$\Longrightarrow (b-a)x = a - a$
$\Longrightarrow (b-a)x = 0$
$\Longrightarrow x = 0$

$$\omega_k(f;\delta)_{P,\alpha} = SUP\left\{\int_0^{1-\frac{h}{|[a,b]|}}\left|V(f.w.[a,b])\psi\left(x + \frac{h}{([a,b])}\right) - V(f.w,[a,b])\psi(x)\right|^P dx\ \ : 0 \le h \le \delta\right\}^{1/P}$$

$$= V(f.w;[a,b])|[a,b]|^{1/P}\ SUP\left\{\int_0^{1-\frac{h}{|[a,b]|}}\left|\psi\left(x+\frac{h}{[a,b]}\right)-\psi(x)\right|^P dx: 0\le h\le\delta\right\}^{1/P} =$$

$$V(f.w;[a,b])|[a,b]|^{1/P}\ \omega\left(\psi;\frac{\delta}{|[a,b]|}\right)_P$$

$$\le C(P)V(f.w;[a,b])\begin{cases}\delta^{1/P}\left(\omega\left(\psi;\frac{\delta}{|[a,b]|}\right)\right)^{1-\frac{1}{P}}, & 1\le P\le\infty\\ \delta & 0<P<1\end{cases}$$

$$= C(P)\begin{cases}\left(V(f.w;[a,b])\right)^{1/P}\delta^{1/P}\left(\omega(fw;\delta)\right)^{1-\frac{1}{P}}, & 1\le P\le\infty\\ V(f.w;[a,b])\delta & 0<P<1\end{cases}$$

$$\omega(f;\delta)_{P,\alpha} = C(P)\begin{cases}\left(V(f;[a,b])\right)_\alpha^{1/P}\delta^{1/P}(\omega(f;\delta)_\alpha)^{1-\frac{1}{P}}, & 1\le P\le\infty\\ V(f;[a,b])_\alpha\delta & 0<P<1\end{cases}$$

Step (2):

Let the function $f.w$ has a total variation $V(f.w,[0,1])=1, x\in[0,1]$

$\psi(x)=f.w(x)-f.w(0)$, using theorem (1), then

$\psi(x)=v.w(x)-u.w(x)$

Where $v.w(x)=V(\psi,[0,x])$ $u.w(x)=v.w(x)-\psi(x)$, we get

$|v.w(x)|\le V(\psi[0,1])=V(f.w,[0,1])=1$

$|u.w(x)|\le|f.w(x)-f.w(0)|+|v.w(x)|\le 2$ ...(1)

From step (1), we get

$\int_0^{1-h}|f.w(x+h)-f.w(x)|dx$

$=\int_0^{1-h}|\psi(x+h)-\psi(x)|dx$

$=\int_0^{1-h}|v.w(x+h)-u.w(x)-[v.w(x)-u.w(x)]|dx$

$=\int_0^{1-h}|v.w(x+h)-u.w(x+h)-v.w(x)-u.w(x)|dx$

$\le\int_0^{1-h}|v.w(x+h)-u.w(x+h)|dx+\int_0^{1-h}|u.w(x+h)-u.w(x)|dx$

$=\int_{1-h}^1 v.w(x)dx-\int_0^h v.w(x)dx+\int_{1-h}^1 u.w(x)\,dx-\int_0^h u.w(x)dx$

Since $.w(x)=1$ and $u.w(x)=2$

$=\int_{1-h}^1 dx-\int_0^h dx+\int_{1-h}^1 2dx-\int_0^h 2dx$

$=0$

Since $0\le h\le\delta\Rightarrow 0\le 5h\le 5\delta$ and since

$$\int_0^{1-h}|f.w(x+h)-f.w(x)|dx=0$$

$$\int_0^{1-h}|f.w(x+h)-f.w(x)|dx \le 5\delta \qquad \forall P \ge 1$$

$$\int_0^{1-h}|f.w(x+h) \quad -f.w(x)|^{1+P-1}dx \le 5\delta\left(\omega(f.w;\delta)\right)^{P-1}$$

$$\left(\int_0^{1-h}|f.w(x+h)-f.w(x)|^P dx\right)^{1/P} \le 5^{1/P}\delta^{1/P}\left(\omega(f.w;\delta)\right)^{1-\frac{1}{P}}$$

$$\omega(f;\delta)_{P,\alpha} \le 5^{1/P}\delta^{1/P}\left(\omega(f.w;\delta)\right)^{1-\frac{1}{P}} \qquad \ldots\ldots\ldots \quad (2)$$

Now let $0 < P < 1$. using the Holder's integral inequality , we get

$$\left(\int_0^{1-h}|f.w(x+h)-f.w(x)|^P\right)^{1/P} \le \int_0^{1-h}|f.w(x+h)-f.w(x)|dx$$

$$\le 5\delta \quad \text{for} \quad 0 \le h \le \delta$$

$$\left(\int_0^{1-h}|\Delta_h f.w(x)|^P dx\right)^{1/P} \le 5\delta$$

$$\omega(f;\delta)_{P,\alpha} \le 5\delta \qquad \ldots\ldots\ldots\ldots \quad (3)$$

From (2) and (3)

$$\omega(f;\delta)_{P,\alpha} = C(P)\begin{cases} 5^{1/P}\delta^{1/P}(\omega(f;\delta)_\alpha)^{1-\frac{1}{P}}, & 1 \le P \le \infty \\ 5\delta & 0 < P < 1 \end{cases}$$

Proposition (3)

Let $f \in L_{P,\alpha}(G)$ if G is a bounded convex domain in $R^n (n \ge 2)$ $\ell \in Z_+, f \in W_{P,\alpha}^{(\ell)}(G) \cap Vn^{(\ell)}(M,G)$, then:

$$\omega^{(\ell)}(f;\delta)_{P,\alpha} \le C(P)\pi_{n-1}^{1/P}(G) =$$

$$\begin{cases} M^{1/P}\delta^{1/P}\omega(f.w;\delta)^{1-\frac{1}{P}}, & 1 \le P \le \infty \\ M\delta & 0 < P < 1 \end{cases}$$

Proof:

Since $\omega_K^{(\ell)}(f;\delta)_{P,\alpha} = \underset{e}{SUP}\ \underset{0\le h\le\delta}{SUP}\left\|\Delta^K(he)D^{(\ell)}(e)f\right\|_{P,\alpha,G_{he}}$

$$= \underset{e}{SUP}\ \underset{0\le h\le\delta}{SUP}\left\{\int_{G_{he}}\left|\Delta^K(he)D^{(\ell)}(e)f.w\right|^P dx\right\}^{1/P}$$

If $K = 1$, we get

$$\omega^{(\ell)}(f;\delta)_{P,\alpha} = \underset{e}{SUP}\ \underset{0\le h\le\delta}{SUP}\left\{\int_{G_{he}}\left|\Delta^1(he)D^{(\ell)}(e)f.w(x)\right|^P dx\right\}^{1/P}$$

$$= \underset{e}{SUP}\ \underset{0\le h\le\delta}{SUP}\left\{\int_{G_{he}}\int_{a(y)}^{b(y)-he}\left|\Delta^1(he)D^{(\ell)}(e)f.w(\xi)\right|^P d\xi dx\right\}^{1/P}$$

Using the Fubini's Theorem for $0 < P < \infty$

$=$

$$\underset{e}{SUP}\ \underset{0\le h\le\delta}{SUP}V^{1/P}\left(G_{he}(e)\right)_{he}\ \underset{e}{SUP}\ \underset{0\le h\le\delta}{SUP}\left\{\int_{a(y)}^{b(y)-he}\left|\Delta^1(he)D^{(\ell)}(e)f.w(\xi)\right|^P d\xi\right\}^{1/P}$$

Using proposition (2), we get

$$\le \underset{e}{SUP}\,\pi_{n-1}^{1/P}(G)SUPSUP\left\|\Delta^{(1)}(he)D^{(\ell)}(f)\right\|_{P,\alpha,G}$$

$$\leq \sup_{e} \pi_{n-1}^{1/P}(G)\omega^{(\ell)}(f;\delta)_{P,\alpha}$$

$$\omega^{(\ell)}(f;\delta)_{P,\alpha} \leq$$

$$C(P)\pi_{n-1}^{1/P}(G)\begin{cases} M^{1/P}\delta^{1/P}\left(\omega(f.w;\delta)\right)^{1-\frac{1}{P}}, & 1 \leq P \leq \infty \\ M\delta & 0 < P < 1 \end{cases}$$

We need the following theorem of V. N. Konovalov.

Theorem: (2) V. N. Konovalov [11]

If G is a bounded domain in R^n $(n \geq 2)$ with Lipschitzain boundary, $1 \leq P \leq \infty$, ℓ and k are nonnegative integers such that $\ell + k > 0$ and for every unbounded $f \in W_P^{(\ell)}(G)$, then for each natural number $N \geq \ell + k - 1$, there exists a polynomial $g \in P_{N,n}$ such that,

$$|f - g|_{W_P^{(s)}(G)} \leq C(n,\ell,k,s,G)C\omega_{\ell-s+k}^{(s)}\left(f;\frac{1}{N}\right)_P$$

holds for $s = 0,1,2,\ldots\ldots\ldots,\ell$

Theorem (3):

If G is a bounded domain in R^n $(n \geq 2)$ with Lipschitzain boundary, $1 \leq P \leq \infty$, ℓ and k are nonnegative integers such that $\ell + k > 0$ and for every unbounded $f \in W_{P,\alpha}^{(\ell)}(G)$, then for each natural number $N \geq \ell + k - 1$, there is a polynomial P such that,

$$\|f - P\|_{W_{P,\alpha}^{(s)}(G)} \leq C(n,\ell,k,s,G)\omega_{\ell-s+K}^{(s)}\left(f;\frac{1}{N}\right)_{P,\alpha}$$

holds for $s = 0,1,2,\ldots\ldots\ldots,\ell$

Proof:

Let $g(x) = f(x)w(x)$

Thus g is a bounded function, by theorem (2) there is P^* *such that* $P^* = P.w$

and $|g - P^*|_{W_P^{(s)}(G)} \leq C\omega_{\ell-s+K}^{(s)}\left(g;\frac{1}{N}\right)_P$

Hence

$$\|f - P\|_{W_{P,\alpha}^{(s)}(G)} \leq C\omega_{\ell-s+k}^{(s)}\left(f;\frac{1}{N}\right)_{P,\alpha}$$

RESULTS AND DISCUSSION

1- Main Results

[9] proved that f is a bounded measurable function. Here we want to find some results but for any function bounded and unbounded.

Theorem (4):

For $f \in L_{P,\alpha}(G)$, let G be a bounded convex domain in R^n $(n \geq 2), \ell \in Z_+$,

$k \in N$(Natural number), $M > 0$, then for every $s = 0,1,\ldots\ldots\ldots,\ell$ and for $N \longrightarrow \infty$ we have:

$$E_N^{(s)}\left(W_{P,\alpha}^{(\ell)}(G)\cap V_n^{(\ell)}(M,G)\ \right)$$
$$\approx C\,N^{-\ell+s}SUP\left\{\omega_k^{(\ell)}\left(f;\frac{1}{N}\right)_{P,\alpha}:f\in W_{P,\alpha}^{(\ell)}(G)\cap V_n^{(\ell)}(M,G)\right\}$$

For $1\le P\le\infty$

Proof :

Put $X=W_{P,\alpha}^{(\ell)}(G)\cap V_n^{(\ell)}(M,G)$, using definition (7), we have:

$$E_N^{(S)}(X)_{P,\alpha}=SUP\ \left\{E_N^{(S)}(f,G)_{P,\alpha}\ :f\in X\right\}$$
$$=SUP_{f\in X}\ \inf\left\{\|f-g\|_{W_{P,\alpha}^{(s)}(G)}\ :g\in P_{N,n}\right\}$$

Since this norm is bounded, then there is $g_1\in P_{N,n}$ such that

$$E_N^{(S)}(X)_{P,\alpha}=SUP\ \left\{\|f-g_1\|_{W_{P,\alpha}^{(s)}(G)}:f\in X\right\}$$

Using Theorem (3) , we get

$$E_N^{(S)}(X)_{P,\alpha}\le C\ SUP\ \left\{\omega_{\ell-s+k}^{(s)}\left(f;\frac{1}{N}\right)_{P,\alpha}\ :f\in X\right\}$$

From proposition (1) , we get

$$E_N^{(S)}(X)_{P,\alpha}\le C\,SUP\ \delta^{\ell-s}\left\{\omega_k^{(s)}(f;\delta)_{P,\alpha}\ :f\in X\right\},\quad\left(\delta<\frac{1}{N}\right)$$
$$=C\,SUP\ \left(\frac{1}{N}\right)^{\ell-s}\left\{\omega_k^{(s)}(f;\delta)_{P,\alpha}\ :f\in X\right\}$$
$$=C\,N^{-\ell+s}SUP\ \left\{\omega_k^{(s)}(f;\delta)_{P,\alpha}\ :f\in X\right\},\text{ thus}$$

$$E_N^{(s)}\left(W_{P,\alpha}^{(\ell)}(G)\cap V_n^{(\ell)}(M,G)\ \right)\approx C\,N^{-\ell+s}SUP\left\{\omega_k^{(\ell)}\left(f;\frac{1}{N}\right)_{P,\alpha}:f\in W_{P,\alpha}^{(\ell)}(G)\cap V_n^{(\ell)}(M,G)\right\}$$

Theorem (5):

If G is a bounded convex domain in R^n $(n\ge 2)$ $\ell\in Z_+,k\in N,M>0,1\le P\le\infty$,f is an unbounded function and $f\in C^{(\ell)}(G)\cap V_n^{(\ell)}(M,G)$, then for all $s=0,1,\ldots\ldots\ldots,\ell$ and $N\ge\max\{1,\ell\}$, we have:

$$E_N^{(s)}(f,G)_{P,\alpha}$$
$$\le CM^{1/P}N^{-\ell-\frac{1}{P}+s}\left(\omega^{(\ell)}\left(f;\frac{1}{N}\right)_{\alpha}\right)^{1-\frac{1}{P}}$$

Where $C=C(\ell,n,k,s,P,G)$ is a constant

Proof:

Using definition (7), we get

$$E_N^{(s)}(f,G)_{P,\alpha}=\inf\left\{\|f-g\|_{W_{P,\alpha}^{(s)}(G)}\ :g\in P_{N,n}\right\}$$

Since this norm is a bounded function then there exists $g_1\in P_{N,n}$ such that

$$E_N^{(s)}(f,G)=\|f-g_1\|_{W_{P,\alpha}^{(s)}(G)}$$

From theorem (3), we get

$$E_N^{(s)}(f,G) \leq C(\ell,n,k,s,P,G)\omega_{\ell-s+k}^{(s)}\left(f;\frac{1}{N}\right)_{P,\alpha}$$

Using proposition (1)

$$E_N^{(s)}(f,G) \leq C(\ell,n,k,s,P,G)\left(\frac{1}{N}\right)^{(\ell-s)}\omega_K^{(\ell)}\left(f;\frac{1}{N}\right)_{P,\alpha}$$

By proposition (3), thus

$$E_N^{(s)}(f,G) \leq C(\ell,n,k,s,P,G)\left(\frac{1}{N}\right)^{1/P}N^{-\ell-\frac{1}{P}+s}\left(\omega^{(\ell)}\left(f;\frac{1}{N}\right)_{\alpha}\right)^{1-\frac{1}{P}}$$

CONCLUSION

i) Comparison between the moduli $\omega_{\ell-s+k}^{(s)}(f;\delta)_{P,\alpha}$ and $\omega_k^{(s)}(f;\delta)_{P,\alpha}$

ii) Comparison between $\omega(f;\delta)_{P,\alpha}$ and the variation of this function.

iii) Found the degree of best approximation of unbounded functions in terms of modulus of continuity $\omega_{\ell-s+k}^{(s)}\left(f;\frac{1}{N}\right)_{P,\alpha}$.

REFERENCES

[1] Carothers N. L., "A Short Course on approximation theory", (1998).

[2] A. H. Al-Abdulla, "On Equi Approximation of Bounded μ-Measurable Functions in $L_P(\mu)$-Space", (2005).

[3] M. Eman, "Study on the Best Approximation of Functions in the $L_P(\mu)$-Space $(0 < P < \infty)$", (2007).

[4] Hassen B. M., "Approximation of Unbounded Function", (2010).

[5] Hammod A. A., "Degree of Best Approximation in L_P Weighted Space (2012).

[6] Cheney W., Light W., "A course in approximation theory", Brooks/cole series in advanced mathematics, ITP pub (2000).

[7] Pasadas M., Rodriguez M.L, "Multivariate approximation by PDE splines", Journal of Computationl and applied mathematics, 218, 556-567, (2008).

[8] Powell M.J.D, "Approximation theory and methods", Cambridge University, (1981).

[9] Khatamov A., "On the best polynomial approximations of functions of many real variables from the sobolev space with derivatives of bounded variation", TWMS Jour. Pure Appl. Math., 2(2) :236-246, (2010).

[10] Walter Rudin "Principles of Mathematical analysis. (1964).

[11] Konovalov V. N., "Approximation of Functions of Several Variables by Polynomials Preserving the Difference-Differential Properties", Ukrain Math. Zh[Ukrainian Math.], 36(2) :154-159, (1984).

Evolutionary Operators-Based Particle Swarm Optimization (EOPSO) to Attack Classical Cryptography Methods

Ahmed Tariq Sadiq
Computer Sciences Department, University of Technology, Baghdad, Iraq
E-Mail : drahmaed_tark@yahoo.com
Received 2/2/2014 – Accepted 23/2/2014

الخلاصة

تعتبر أمثلية حشد الجزيئات من طرق الامثلية المعتمدة على المجتمع، والتي تعتبر سهلة التنفيذ والتطبيق لحل مشاكل الامثلية وبعض مشاكل من نوع NP-Complete. هذا البحث يقدم أمثلية حشد الجزيئات المطورة باستخدام عمليتين من العمليات التطويرية وهما : التضارب والطفرة، لذلك سميت الخوارزمية المقترحة بأمثلية حشد الجزيئات المعتمدة على العمليات التطويرية (EOPSO). الفائدة من العمليتين لأمثلية حشد الجزيئات هي اعطاء زخم وتنوع للمجتمع. الخوارزمية المقترحة تهاجم نوعين من التشفير التقليدي (التعويضي والابدالي). نتائج التجارب اظهرت ان نسبة استرجاع المفتاح باستخدام الخوارزمية المقترحة أفضل من الاصلية (PSO) وأفضل من خوارزميات مطورة مثل (2-op PSO) و (SAPSO).

ABSTRACT

Particle Swarm Optimization (PSO) is a population-based optimization tool, which could be implemented and applied easily to solve various function optimization problems and some NP-complete problems. This paper present a benefit developed PSO using two evolutionary operators: crossover and mutation, so it called Evolutionary Operators-based PSO (EOPSO). The benefit of these two operators in PSO is use as momentum and diversity tool in the population. EOPSO used to attack the two types of classical cryptography (substitution and transposition). Experimental results of EOPSO appear that the amount of recovered key of classical ciphers and fitness function values are best than with PSO, improved 2-opt PSO and simulated annealing PSO.

Keywords: PSO, Evolutionary Operators, Crossover, Mutation, Attack Classical Cryptography.

INTRODUCTION

Two fundamental goals in computer science are finding algorithms with provably good run times and with provably good or optimal solution quality. A heuristic is an algorithm that gives up one or both of these goals; for example, it usually finds pretty good solutions, but there is no proof the solutions could not get arbitrarily bad; or it usually runs reasonably quickly, but there is no argument that this will always be the case. Often, one can find specially crafted problem instances where the heuristic will in fact produce very bad results or run very slowly; however, these instances might never occur in practice because of their special structure. Therefore, the use of heuristics is very common in real world implementations [1].

Population-based metaheuristics share many common concepts. They could be viewed as an iterative improvement in a population of solutions. First, the population is initialized. Then, a new population of solutions is generated. Finally, this new population is integrated into the current one using some selection procedures. The search process is stopped when a given condition is satisfied (stopping criterion). Algorithms such as

evolutionary algorithms (EAs), genetic algorithms (GA), scatter search (SS), estimation of distribution algorithms (EDAs), particle swarm optimization (PSO), bee colony (BC), and artificial immune systems (AISs) belong to this class of metaheuristics [2].

In the other side, cryptanalysis can be described as the process of searching for flaws or oversights in the design of cryptosystems (or ciphers). A typical cipher takes a clear text message (known as the plaintext) and some secret keying data (known as the key), as its input and produces a scrambled (or encrypted) version of the original message (known as the ciphertext) [6]. The use of automated techniques in the cryptanalysis of cryptosystems is desirable as it removes the need for time-consuming (human) interaction with a search process. Making use of computing technology also allows the inclusion of complex analysis techniques, which can quickly be applied to a large number of potential solutions in order to weed out unworthy candidates [7].

This paper presents an attempting to use meta-heuristic techniques in the attacking of classical cipher with two type substitution and transposition. Section 2 includes the related works. Evolutionary operators types in section 3. Section 4 presents a brief overview of the classical cipher. Section 5 presents the principle of particle swarm optimization (PSO). Section 6 contains the proposed EOPSO to attacks the classical cipher. Section 7 includes the results of computational tests to evaluate the performance of the PSO and EOPSO algorithms. The conclusions are reported in section 8.

LITERATURE REVIEWS

In [20], two new variants of Particle Swarm Optimization (PSO) called AMPSO1 and AMPSO2 are proposed for global optimization problems. Both the algorithms use adaptive mutation using Beta distribution. AMPSO1 mutates the personal best position of the swarm and AMPSO2, mutates the global best swarm position. The performance of proposed algorithms is evaluated on twelve unconstrained test problems and three real life constrained problems taken from the field of Electrical Engineering. The numerical results show the competence of the proposed algorithms with respect some other contemporary techniques.

In [21], an improved algorithm for Particle Swarm Optimization (PSO) named Elite Particle Swarm Optimization with Mutation (EPSOM) is proposed in this paper. Elite particles and bad particles are distinguished from the swarm after some initial iteration steps. Bad particles are replaced with the same number of elite particles, and a new swarm is generated. To avoid losing diversity of the swarm and to decrease the risk of trapping in local optimum, mutation operation is introduced in evolution process. The results of several simulations for

different benchmark functions illustrate that EPSOM algorithm has the ability of local exploitation and global exploration. EPSOM algorithm outperforms the Linearly Decreasing Weight Particle Swarm Optimization (LDW-PSO) and Random Mutation Particle Swarm Optimization (RM-PSO) in respects of calculation accuracy and convergence.

In [22], propose an advanced PSO algorithm with mutation operator. By adding the mutation operator to the algorithm, the advanced algorithm can not only escape from the local minimum's basin of attraction of the later phase, but also maintain the characteristic of fast speed in the early convergence phase. By the contrast experiments of three multimodal test functions and an example whose problem space is non-convex set, it has been proved that the advanced PSO algorithm can improve the global convergence ability, greatly enhance the rate of convergence and overcome the shortcoming of basic PSO algorithm.

In [23], with high dimension of solution vectors, PSO also gets into trouble for finding optimal solutions. With mutation mechanism frequently used in GA into PSO algorithms, it shows improved performance for finding solution with high dimension optimization problems can be achieved compared with PSO without mutation.

In [43], MPSO have been proposed to attack the classical cryptography, the mutation operator used to enhance the performance of PSO to find the largest amount of classical cryptography keys. There are good results are obtained because mutation operator provides diversity to the PSO candidate solutions.

EVOLUTIONARY OPERATORS

Genetic algorithms have been developed by J. Holland in the 1970s (University of Michigan, USA) to understand the adaptive processes of natural systems [3]. Then, they have been applied to optimization and machine learning in the 1980s [4, 5]. GAs are a very popular class of EAs. Traditionally, GAs are associated with the use of a binary representation but nowadays one can find GAs that use other types of representations. A GA usually applies a crossover operator to two solutions that plays a major role, plus a mutation operator that randomly modifies the individual contents to promote diversity. GAs uses a probabilistic selection that is originally the proportional selection. The replacement (survivor selection) is generational, that is, the parents are replaced systematically by the offsprings. The crossover operator is based on the n-point or uniform crossover while the mutation is bit flipping [2].

The role of crossover operators is to inherit some characteristics of the two parents to generate the offsprings. As for the mutation operator, the design of crossover operators mainly depends on the representation used.

Unlike single-metaheuristics, here the search operators are always unary, this part has been independently developed in the evolutionary computation community. Some important points must be taken into account in the design or use of a crossover operator:

• Heritability: The main characteristic of the crossover operator is *heritability*. The crossover operator should inherit a genetic material from both parents. An operator is a pure recombination operator (strong heritability) if two identical individuals generate identical offsprings. Hence, the mutation and crossover operators are complementary. In this case, mutation introduces some diversification in the individuals by introducing some missing values in the current individuals of a population. A crossover operator Ox is *respectful* if the common decisions in both parents are preserved, and is *assorting* if the distance between the parents (p1,p2) and the offspring o is lower or equal to the distance between the parents [8]:

$$d(p1, o) \leq d(p1, p2) \text{ and } d(p2, o) \leq d(p1, p2), \forall o \in O(p1, p2, Ox)$$

where O(p1, p2, Ox) is the set of all possible offsprings generated by the crossover operator Ox.

• Validity: The crossover operator should produce valid solutions. This is not always possible for constrained optimization problems [2].

The crossover rate pc ($pc \in [0, 1]$) represents the proportion of parents on which a crossover operator will act. The best parameter value for pc is related to other parameters among them such as the population size, the mutation probability, and the selection procedure. The most commonly used rates are in the interval [0.45, 0.95]. Adaptive techniques for the crossover rate may also be useful. For linear representations excluding permutations, the well-known crossover operators are the 1-point crossover, its generalized form the *n*-point crossover, and the uniform crossover.

For real-valued representations, in addition to the 1-point, n-point, and the uniform crossover operators, the following two types of crossover operators are commonly used: mean-centric recombination and parent-centric recombination. In mean-centric recombination, the offsprings are generated closer to the centroid of their parents. One may use the following crossover operators [9, 10, 11, 12, 13, 14, 15]:

• Intermediate crossover.
• Geometrical crossover.
• Unimodal normal distribution crossover (UNDX).
• Simplex crossover (SPX).
• Simulated binary crossover (SBX).
• Parent-centric crossover (PCX).

Applying classical crossover operators to permutations will generate solutions that are not permutations (i.e., nonfeasible solutions). Hence,

many permutation crossover operators have been designed as, Order crossover (OX), Partially mapped crossover (PMX), maximum preservative crossover [16], cycle crossover (CX) that preserves the absolute positions of the elements [17], merge crossover [18], and position-based crossover (POS) [19].

Mutation operators are unary operators acting on a single individual. Mutations represent small changes of selected individuals of the population. The probability pm defines the probability to mutate each element (gene) of the representation. It could also affect only one gene too. In general, small values are recommended for this probability (pm $\in$ [0.001, 0.1]). Some strategies initialize the mutation probability to 1/k where k is the number of decision variables, that is, in average only one variable is mutated [2].

Some important points that must be taken into account in the design or use of a mutation operator are as follows [2]:

• **Ergodicity:** The mutation operator should allow every solution of the search space to be reached.

• **Validity:** The mutation operator should produce valid solutions. This is not always possible for constrained optimization problems.

• **Locality:** The mutation should produce a minimal change. The size of mutation is important and should be controllable. Locality is the effect on the solution (phenotype) when performing the move (perturbation) in the representation (genotype). When small changes are made in the genotype, the phenotype must reveal small changes. In this case, the mutation is said to have a strong locality. Hence, an evolutionary algorithm will carry out a meaningful search in the landscape of the problem. Weak locality is characterized by a large effect on the phenotype when a small change is made in the genotype. In the extreme case, the search will converge toward a random search in the landscape.

There are several types of mutation representation, such as [2]:

• **Mutation in binary representation:** The commonly used mutation is defined as the flip operator.

• **Mutation in discrete representation:** It consists generally in changing the value associated with an element by another value of the alphabet.

• **Mutation in permutations:** Mutation in order-based representations are generally based on the *swapping*, *inversion*, or the *insertion* operators.

CLASSICAL CIPHERS

Generally, there are two types of classical cipher methods, substitution and transposition as below.

1. Substitution Cipher

The simple substitution cipher (sometimes referred to as the monoalphabetic substitution cipher to distinguish it from the

polyalphabetic substitution cipher). Each symbol in the plaintext maps to a (usually different) symbol in the ciphertext. The processes of encryption and decryption are best described with an example, such as the one following.

For example, a simple substitution cipher key can be represented as a permutation of the plaintext alphabet. Table 1 gives a sample key. Using this representation the ith letter in the plaintext alphabet is encrypted to the i^{th} element of the key. The string "the money is in the bag" is encrypted using the key in the Table 1.

Table-1: Example Substitution Cipher

KEY	
Plaintext	ABCDEFGHIJKLMNOPQRSTUVWXYZ
Ciphertext	PQOWIEURYTLAKSJDHFGMZNXBCV
ENCRYPTION	
Plaintext	T H E M O N E Y I S I N T H E B A G
Ciphertext	M R I K J S I C Y G Y S M R I Q P U

Using the key representation in Table 1, the original message can be discovered by reversing the encryption procedure. That is, the ciphertext character at position I in the key decrypts to the i^{th} character in the plaintext alphabet. For an alphabet of 26 characters, there are 26! or greater than 4×10^{26} possible keys for a simple substitution cipher. This number is far too large to allow a brute force attack even on the fastest of today's computers. However, because of the properties of the simple substitution cipher they are relatively easy to cryptanalysis [24, 25].

2. Transposition Cipher

A transposition cipher [1], also sometimes called a permutation cipher, is one for which applying E to plaintext produces ciphertext with the same symbols as the plaintext, but rearranged in different positions. We must divide the plaintext message into message blocks. The size of the permutation is known as the period. Let us consider an example of a transposition cipher with a period of five, and a key {4, 2, 1, 5, 3}. In this case, the message is broken into blocks of five characters, and after encryption the fourth character in the block will be moved to position 1, the second remains in position 2, the first is moved to position 3, the fifth to position 4, and the third to position 5. Figure. 1 illustrates an example for this type.

Plaintext : "MYPSOALGORITHMSAREANEFFICIENT"

Encrypted using the key (32514)

M	Y	P	S	O
A	L	G	O	R
I	T	H	M	S
A	R	E	A	N

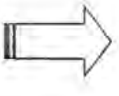

P	Y	O	M	S
G	L	R	A	O
H	T	S	I	M
E	R	N	A	A

E	F	F	I	C		F	F	C	E	I
I	E	N	T	X		N	E	X	I	T

Ciphertext: "PGHEFN YLTRFE ORSNCX MAIAEI SOMAIT"

Figure-1: An Example for Transportation Cryptography

PARTICLE SWARM OPTIMIZATION (PSO)

Particle swarm optimization (PSO) is a population based stochastic optimization technique developed by Dr. Eberhart and Dr. Kennedy in 1995 [26], inspired by social behavior of bird flocking or fish schooling and swarm theory. We have used this technique in the cryptanalysis of simple transposition ciphers.

1. The Principle

PSO shares many similarities with evolutionary computation techniques such as Genetic Algorithms (GA). The system is initialized with a population of random solutions and searches for optima by updating generations. However, unlike GA, PSO has no evolution operators such as crossover and mutation. In PSO, the potential solutions, called particles, fly through the problem space by following the current optimum particles. Compared to GA, the advantages of PSO are that PSO is easy to implement and there are few parameters to adjust. PSO has been successfully applied in many areas; function optimization, artificial neural network training and fuzzy system control. PSO simulates the behavior of bird flocking, suppose a group of birds are randomly searching food in an area, not all the birds know where the food is. The effective strategy is to follow the bird that is nearest to the food. In PSO, each single solution is a "bird" in the search space. We call it "particle". All particles have fitness values that are evaluated by the fitness function to be optimized, and have velocities, which direct the flying of the particles [26].

PSO is initialized with a group of random particles (solutions) and then searches for optima by updating generation. In each generation, each particle is updated by following two "best" values. The first one is the best solution (fitness) it has achieved so far. This value is called (pbest), another "best" value that is tracked by the particle swarm optimizer is the best value, obtained so far by any particle in the population. This best value is a global best and is called gbest. When a particle takes part of the population as its topological neighbors, the best value is a local best and is called (*l*best).

After finding the two best values, the particle updates its velocity and position with the following equations [26]:

$$V_i[t+1]=wV_i[t]+C_1*r1*(pbest_i[t]-present_i[t])+C_2*r2*(gbest_i[t]-present_i[t]) \quad (1\text{-}a)$$

$$present_i[t]=present_i[t]+V_i[t] \quad (1\text{-}b)$$

where, i =1,2,…..,*N*; *w* is the inertia weight, V[t] is the particle's velocity, present[t] is the current particle (solution), pbest and gbest are defined as stated before, r1 and r2 are two random numbers between (0,1), C_1 and C_2 are learning factors. However these values of C_1,C_2 are problem dependent. These are very essential parameters in PSO. They particles' velocities on each dimension are clamped to a maximum velocity Vmax [14].

2. Binary PSO

The original PSO is for continuous population, but is later extended by Eberhart and Kennedy [27] to the discrete valued population. In the binary PSO thus emerged, the particles are represented by binary values (0 or 1). The velocity and particle updating for binary PSO are the same as in the case of continuous one. However, the final decisions are made in terms of 0 or 1. Sigmoid function in [28] is used to restrict the decision in the range [0,1].

3. Discrete PSO

Several adaptations of the method to discrete problems, known as Discrete Particle Swarm Optimization (DPSO). Since, in words of the inventors of PSO, it is not possible to "throw to fly" particles in a discrete space [26], several Discrete Particle Swarm Optimization (DPSO) methods have been proposed.

A DPSO whose particles at each iteration are affected alternatively by its best position and the best position among its neighbors was proposed by Al-kazemi and Mohan [29]. Pampara et al. [30] solved binary problems by combining continuous PSO and Angle Modulation with only four parameters. Furthermore, several PSO variants applied to problems, where the solutions are permutations were considered in [31, 32]. The multi-valued PSO (MVPSO) proposed by Pugh and Martinoli [33] deals with variables with multiple discrete values.

Another DPSO was proposed in [34] for feature selection problems, which are problems their solutions are sets of items. A new DPSO proposed in [35, 36] does not consider any velocity since, from the lack of continuity of the movement in a discrete space, the notion of velocity loses sense; however kept the attraction of the best positions.

4. Parameters of PSO

The convergence and performance of PSO are largely dependent upon chosen parameters. *w* is termed as inertia weight [28] and is incorporated in the algorithm to control the effect of the previous velocity vector of the swarm on the new one. It facilitates the trade-off between the local and the global exploration abilities of the swarm and may result in less number of iterations of the algorithm while searching for an optimal

solution. It is experimentally found that inertia weight w in the range [0.8, 1.2] yields a better performance [37]. The velocity lies in the range [- Vmax , Vmax] where, - Vmax denotes the lower range and Vmax is the upper range of the motion of the particle. The roles of C_1 and C_2 are not so critical in the convergence of PSO, however, a suitably chosen and fine tuned value can lead to a faster convergence of the algorithm. A default value of $C_1 = C_2 = 2$ is suggested for general purpose, but somewhat better results are found with $C_1 = C_2 = 0.5$ [38]. However, the values of cognitive parameter, C_1 larger than the social parameter C_2 are preferred from the performance point of view with the constraint $C_1 + C_2 \leq 4$ [39]. The parameters r1 and r2 used to maintain the diversity of the population in equation (1-a).

EOPSO FOR ATTACKING CLASSICAL CIPHERS

PSO is rather a successful method for the continuous optimization problems; however, it is very difficult to adapt it for the discrete case; many studies have been done on it. The focus of this paper is to apply a PSO algorithm to the problem of searching through the key space of a simple transposition cipher. The type of transposition ciphers, which want to be attacked, encrypts text according to the following classical two-stage algorithm:

- A key of length N takes the form of a permutation of the integers 1 to N. The plaintext, of L characters, is written beneath the key to form a matrix N characters wide and at least L mod N characters deep.
- The text is then enciphered by reading it off in columns in the order dictated by the integers making up the key.

A. Representation of a Candidate Solution

Since 1995, Particle Swarm Optimization has been successfully applied in continuous problems, and a transposition cipher is the new field of PSO algorithm in discrete space. If the PSO algorithm is designed to tackle discrete problem, a direct correlation must be found between the particle vector and the solution representation of classical cipher.

To attack the classical ciphers using PSO we must define the position vector of a particle represents a feasible solution, that is to say, the position vector means the permutation of the solution key and specifies the order of key to be executed. The vector elements must be encoded as integer limited in $[1, N]$, and N is the key size (especially in transposition). In addition to, in substitution a key for decoding a cipher is given by an ordered list of the 26 letters of the alphabet. The order expresses the underlying substitution. Every integer in the scale appear only once in feasible solution.

B. Initial Population

Like other evolutionary algorithms, the PSO algorithm starts from an initial population. The particles are randomly generated between the maximum and the minimum operating limits of the generators.

C. Fitness Function Assessment

Fitness function values of the particles are evaluated using equation (3). These values are set as the pbest value of the particles. The fitness rating helps the transposition cryptanalysis algorithm achieve breaking by awarding scores according to the number of times two and three letter combinations (bi-and tri-grams) commonly found in English actually occur in the decrypted text. The more columns correctly put next to the other by this algorithm, the higher the fitness rating ascribed to that trail permutation. Whenever these combinations were found in decrypted text, points were awarded, the highest being given for the appearance of trigrams, as their appearance suggested that three columns have been correctly aligned. A study has been made in English text consists of more than 4500 letters, taken the 29 high frequency diagram letters and 12 high frequency trigram letters in Table 2 gives 41 combinations letters and their percentage frequency in standard English text. Were the percent calculated by :

Let frq[D_i] denotes the frequency of the bi-gram letters, where $D_i \in \{TH,HE,\ldots,HA\}$, where $1 \le i \le 29$, and frq[T_j] denotes the frequency of the trigram letters, and $T_j \in \{ARE,THE,\ldots,DTH\}$, where $1 \le j \le 12$, then, percent(bi-gram) = frq[D_i] / (L-1) and percent(tri-gram) = frq[T_j] / (L-2), (we use (L-1) and (L-2) because the diagram and trigram used with overlap), and

L: is the text length, then:

$$\textit{Total percent (bi-gram)} = \sum_{i=1}^{29} \text{frq}[D_i] / (L-1) \qquad (2\text{-}a)$$

and,

$$\textit{Total percent (tri-gram)} = \sum_{j=1}^{12} \text{frq}[T_j] / (L-2) \qquad (2\text{-}b)$$

Therefore, the total percent will represent the fitness value of the transposition cryptanalysis :

$$\textbf{\textit{Fitness}} = \sum_{i=1}^{29} \text{frq}[D_i] / (L-1) \sum_{j=1}^{12} \text{frq}[T_j] / (L-2) \qquad (3)$$

It is clear that the other non-plaintext fitness values ≤ 0.3811568, and it is important to mention that, the text fitness increased as the text length increased, and vice versa.

The most commonly used fitness function for breaking the simple substitution ciphers is based only on unigram and bigram analysis and has the form:

$$Fitness=(1-\sum_{i=1}^{26}\left\{|SF[i]-DF[i]|+\sum_{j=1}^{26}|SDF[i,j]-DDF[i,j]|\right\}/4)^8 \quad (4)$$

where, $SF[i]$ and $SDF[i, j]$ are standard frequencies of character i and the pair of symbols (i, j) in the original language, respectively, and $DF[i]$ and $DDF[i, j]$ are measured frequencies of character i and pair (i, j) in the "decrypted" text. The measured errors (i.e., the difference between standard frequencies and measured frequencies) are normalized and subtracted from 1, so that number closer to 1 represents the higher fitness. In addition, the constants 4 and 8 are used to reduce sensitivity to large errors and to amplify small differences, respectively. Some fitness functions give more weight to one of the factors (unigram or bigram) by inserting weight constants in front of the corresponding error calculation terms [1, 40, 41, 42].

Table-2: 29 Bi-Gram and 12 Tri-Gram Letters Combinations

29 Diagram Letters				12 Trigram Letters	
Diagram	Percent	Diagram	Percent	Trigram	Percent
TH	0.0250791	EA	0.0079078	ARE	0.0006778
HE	0.0237235	NG	0.0103931	THE	0.0153638
IN	0.0171713	AS	0.0112969	ING	0.0085856
AN	0.0153638	OR	0.0117488	AND	0.0085856
RE	0.0115228	TI	0.0092634	ENT	0.0042928
ED	0.0092634	IS	0.0092634	THA	0.0033891
ON	0.0108450	ET	0.0067781	NTH	0.0027113
ES	0.0131044	IT	0.0040669	WAS	0.0045188
ST	0.0151378	AR	0.0056484	HER	0.0011297
EN	0.0108450	TE	0.0070041	ETH	0.0038409
AT	0.0131044	SE	0.0079078	FOR	0.0020334
TO	0.0101672	HI	0.0063263	DTH	0.0009038
NT	0.0099413	OF	0.0074559	--------	---------
ND	0.0122006	HA	0.0079078	--------	---------
OU	0.0112969	---------	----------	---------	----------
Di-Total	Percent = 0.3246724			Tri-Total	0.0564844
Total	Percent = 0.3811568 = fitness of plaintext				

D. The Proposed Algorithm of EOPSO

The following is an algorithmic description of the attack on a classical cipher using particle swarm optimization (PSO):

1. The algorithm is given the cipher text (and its length), the key size (permutation size or period) N.
2. Initialize the algorithm parameters. They are:

a. C_1 (Self-confidence).
b. C_2 (Swarm confidence).
c. W (Inertia weight).
d. Pc (Crossover Probability).
e. Pm (Mutation Probability).
f. V_{max} (The maximum of velocity).
g. Swarm_Size (Number of particles in the swarm.)
h. Max-Iter (The maximum number of iterations).

3. Randomly generate the initial particles (keys of the cipher) to form a swarm.
4. For i=1 To Max-Iter, do
   a. Calculate the fitness function of each of the particles (keys) using equation (2 and 3).
   b. If the current position of the particle is better than the previous history, updating the particles indicated this fact.
   c. Find the best particle of the swarm. Updating the positions of the particles by using equation (1a and 1b).
   d. If no update or no regression then recombine using crossover then mutates the two best particles (depend on Pc and Pm respectively).
5. Copy the best key obtained so far in the output key variable and exit.

RESULTS AND DISCUSSION

In this paper 2 type of classical cipher have been taken, substitution and transposition. So the results will divide into these 2 types. The results of EOPSO compare with PSO, 2-op PSO and SAPSO [1, 38].

1. Experimental Results for Substitution Cipher

EOPSO algorithm was applied to cipher text created using a simple substitution cipher and the attack was run a number of times with a variety of parameter values. In general it was found that (200) iterations were usually enough to break the cipher text and the algorithm was fast enough that this took a few seconds.

The experiments shown in Figure. 2 were performed on simple substitution cipher using basic PSO and improved PSO algorithm. The fitness function used was in equation (4). As we can see, the fitness value has started from about 0.51 and come up to 0.89 in about 200 iterations using EOPSO. By using PSO, 2-op PSO and SAPSO the fitness value was less than the EOPSO. In addition, we can see a rapid increase in fitness function at the beginning and the rate of increases as we run the experiments for longer period. This is because as the fitness value increases, it becomes more and more difficult to find a better key.

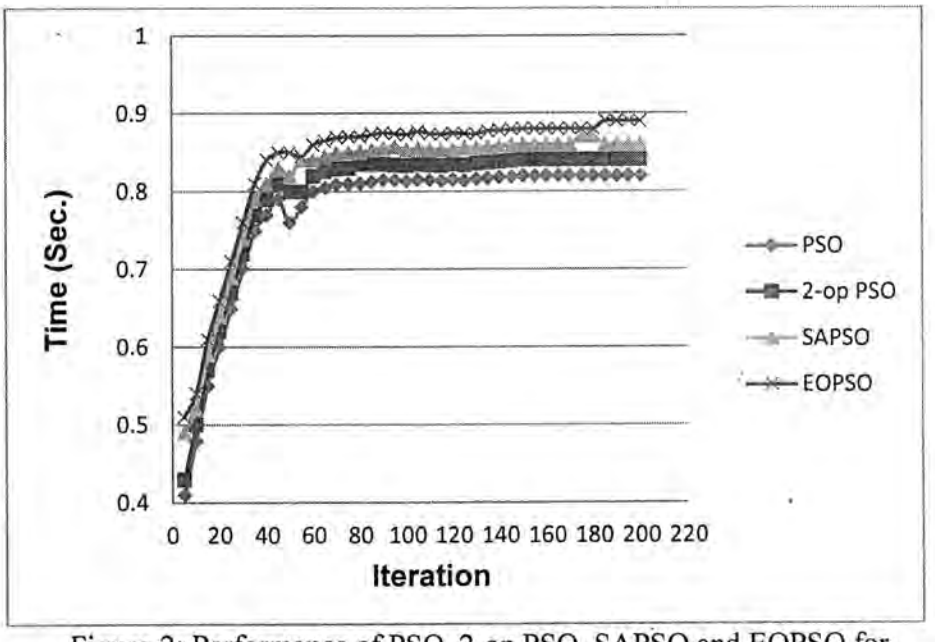

Figure-2: Performance of PSO, 2-op PSO, SAPSO and EOPSO for Substitution Attack

The best parameters value of PSO, 2-op PSO, SAPSO [1] and EOPSO to attack substitution cipher show in Table 3.

Table -3: Parameters Value of PSO, 2-op PSO, SAPSO and EOPSO to Attack Substitution Cipher

Parameter	Symbol	Value
Self-confidence	C_1	2
Swarm confidence	C_2	2
Inertia weight	W	1.2
Crossover Probability	Pc	0.65
Mutation Probability	Pm	0.05
The maximum of velocity	V_{max}	26
Number of particles in the swarm	Swarm_Size	25-50
The maximum number of iterations	Max-Iter	300

Figure. 3 illustrate the time comparison for EOPSO, PSO, 2-op PSO and SAPSO to attack substitution cipher.

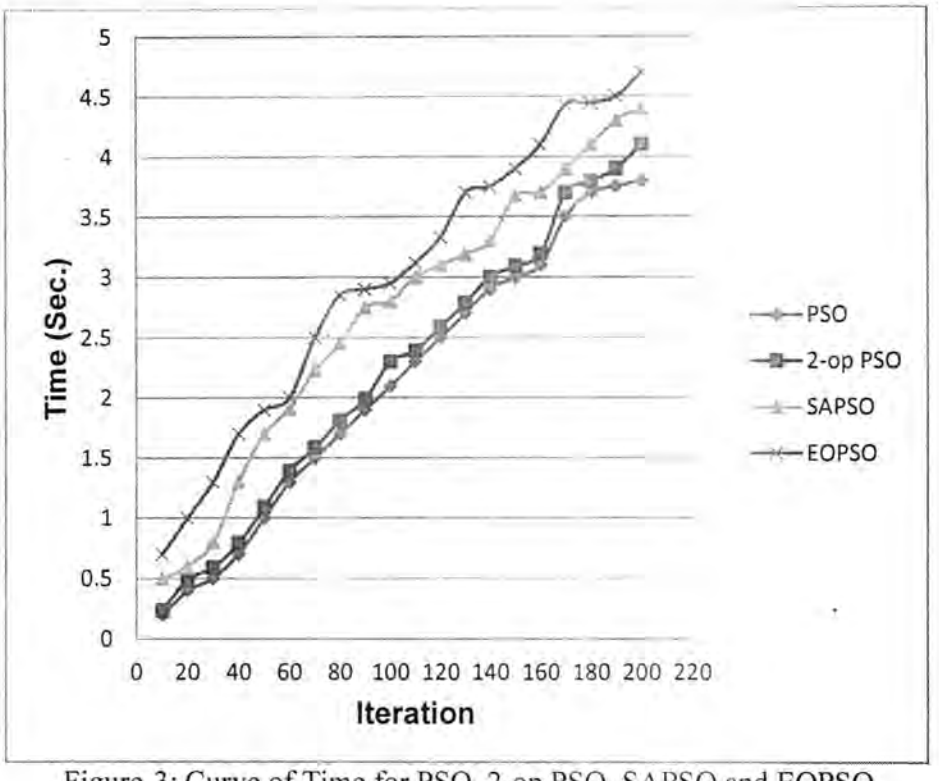

Figure-3: Curve of Time for PSO, 2-op PSO, SAPSO and EOPSO for Substitution Attack

2. Experimental Results for Transposition Cipher

The results of transposition cipher are presented in Table 4. Here the algorithm was run on different amounts of cipher text. The results in Table 2 represent the average number of key elements correctly placed for a key size of 20 with 100-1500 characters as a cipher text by using proposed EOPSO compare with PSO, 2-op PSO and SAPSO.

Table-4: The Amount of Recovered Key Versus Available Cipher Text, Transposition With Size 15 Using PSO and Improved PSO

Amount of Cipher Text	Amount of Recovered Key (PSO)	Amount of Recovered Key (2-op PSO)	Amount of Recovered Key (SAPSO)	Amount of Recovered Key (EOPSO)
100	7.75	9.75	10	10
150	10	10	11	11
250	10.50	10.75	12	12.25
400	11.25	11.25	12.5	12.5
600	12	12.25	12.75	13
800	12.75	12.75	13	13
1000	13	13.25	13.25	13.25
1250	13.25	13.25	13.5	13.5
1500	13.25	13.25	13.5	14

The amount of recovered keys using 1500 characters in known cipher text illustrate in Table 5. The table shows that the EOPSO attack was the

most powerful. For a transposition cipher of period 25 the improved PSO attack was better than basic PSO of the key elements, on the average.

Table-5: The Amount of Recovered Keys Versus Transposition Size Using 1000 Known Cipher Text Characters

Transposition Size	PSO	2-opt PSO	SAPSO	EOPSO
7	6.75	7	7	7
9	7.75	8	8	8
11	9	9	9	10
15	13	13.25	13.5	13.5
20	16.25	16.25	17	17.75
25	20	21.25	22	23

The best parameters value of PSO, 2-op PSO, SAPSO [1, 38] and EOPSO to attack transposition cipher show in Table 6.

Table-6: Parameters Value of PSO, 2-op PSO, SAPSO and EOPSO to Attack Transposition Cipher

Parameter	**Symbol**	**Value**
Self-confidence	C_1	2
Swarm confidence	C_2	2
Inertia weight	W	1.2
Crossover Probability	Pc	0.72
Mutation Probability	Pm	0.075
The maximum of velocity	V_{max}	26
Number of particles in the swarm	Swarm_Size	25-50
The maximum number of iterations	Max-Iter	550

Figure. 4 shows the performance of EOPSO compare with PSO, 2-op PSO and SAPSO. The EOPSO as compared to basic PSO, 2-op PSO and SAPSO performs better in terms of percentage of successful attacks, and we need to tune various parameters of the algorithm leading to simple program development effort.

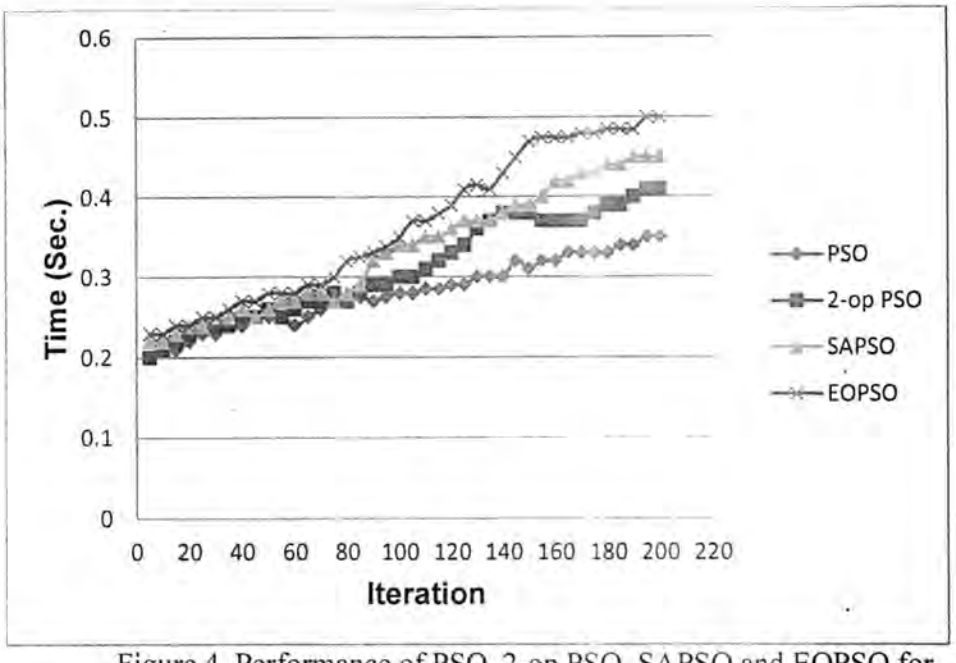

Figure.4. Performance of PSO, 2-op PSO, SAPSO and EOPSO for Transposition Attack

Figure. 5 illustrate the time comparison for EOPSO, PSO, 2-op PSO and SAPSO to attack substitution cipher.

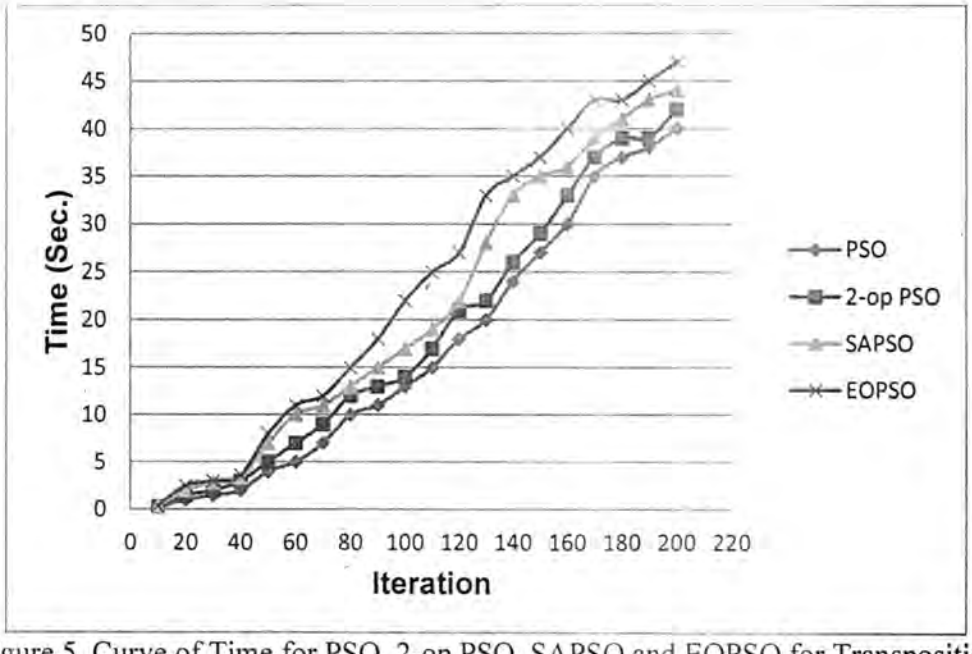

Figure.5. Curve of Time for PSO, 2-op PSO, SAPSO and EOPSO for Transposition Attack

CONCLUSIONS

The goal of this paper is to illustrate the feasibility of using EOPSO algorithm as a cryptanalysis tool and better than PSO and SAPSO. The proposed EOPSO algorithm is applied to classical ciphers (substitution

and transposition). The following points represent the important conclusions:

1- The performance (convergence) of EOPSO is better than PSO, 2-op PSO and SAPSO in both 2 types of classical ciphers (substitution and transposition).
2- The time of EOPSO is larger than PSO, 2-op PSO and SAPSO in both 2 types of classical ciphers (substitution and transposition) but the difference is small compare with increasing the performance.
3- Using the crossover operator gives a good diversity to the adjustment of PSO representation, so the convergence increases with a reasonable value.
4- Using mutation operator gives a momentum value to the adjustment of PSO parameters, so the convergence increases with small value. Also it provides population diversity, therefore it is useful to find the solutions.
5- The amount of recovered key in transposition cipher using EOPSO is larger than the other techniques (PSO, 2-op PSO and SAPSO).
6- The instability in EOPSO is less than PSO, 2-op PSO and SAPSO, so it is very useful technique in optimization problems.

REFERENCES

[1] Salih H. H., Ahmed Tariq Sadiq and Ismail K. Ali, "Attack on the Simple Substitution Ciphers Using Particle Swarm Optimization", Proceeding of 1st Conference of Software Eng., University of Technology, Baghdad, Iraq, (2009).

[2] El-Ghazali T., "Metaheuristics : From Design to Implementation", John Wiley & Sons Inc. Pub., USA, (2009).

[3] Holland J. H. "Adaptation in Natural and Artificial Systems", University of Michigan Press, Ann Arbor, MI, (1975).

[4] Goldberg D. E. "Genetic Algorithms in Search, Optimization, and Machine Learning", Addison-Wesley, (1989).

[5] De Jong K. A. "Genetic algorithms: A 10 year perspective", In International Conference on Genetic Algorithms, (1985), pp. 169–177.

[6] Mao, W., "Modern Cryptography: Theory & Practice". Upper Saddle River, NJ: Prentice Hall PTR, (2004).

[7] Giddy J. P. and Safavi-Naini R., "Automated Cryptanalysis of Transposition Ciphers". The Computer Journal, 37(5):429–436, (1994).

[8] Radcliffe N. J. and Surry P. D., "Fitness Variance of Form and Performance Prediction", In L. D. Whitley and M. D. Vose, editors, 3rd Workshop on Foundations of Genetic Algorithms, Morgan Kaufmann, (1994), pp. 51–72.

[9] Michalewicz Z., Nazhiyath G., and Michalewicz M., "A Note on Usefulness of Geometrical Crossover for Numerical Optimization Problems", In 5th Annual Conference on Evolutionary Programming, San Diego, CA. MIT Press, (1996), pp. 305–312.

[10] Ono I. and Kobayashi S., "A Real-Coded Genetic Algorithm for Functional Optimization Using Unimodal Normal Distribution Crossover", In ICGA-7, 7th International Conference on Genetic Algorithms, (1997), pp. 246–253.

[11] Tsutsui S., Yamamura M., and Higuchi T., "Multi-Parent Recombination with Simplex Crossover in Real-Coded Genetic Algorithms", In GECCO'99 Genetic and Evolutionary Computation Conference, (1999), pp. 657–664.

[12] Deb K. and Agrawal R. B., "Simulated Binary Crossover for Continuous Search Space", Complex Systems, 9:115–148, (1995).

[13] Deb K. and Joshi D., "A Computationally Efficient Evolutionary Algorithm for Real Parameter Optimization", Technical Report 003, KanGal, (2002).

[14] Davis L., "Job-shop Scheduling with Genetic Algorithms", In J. J. Grefenstette, editor, International Conference on Genetic Algorithms and Their Applications, Pittsburgh, PA, (1985), pp. 136–140.

[15] Goldberg D. E. and Lingle R., "Alleles, Loci, and the Traveling Salesman Problem", In J. J. Grefenstette, editor, 1st International Conference on Genetic Algorithms and Their Applications. Lawrence Erlbaum Associates, (1985), pp. 154–159.

[16] Muhlenbein H., Schleuter M. G., and O. Kramer, "Evolution Algorithms in Combinatorial Optimization", Parallel Computing, 7:65–85, (1988).

[17] Oliver I. M., Smith D. J., and Holland J. R. C., "A Study of Permutation Crossover Operators on the Traveling Salesman Problem", In J. J. Grefenstette, editor, 2nd International Conference on Genetic Algorithms, Hillsdale, NJ, (1987), pp. 224–230.

[18] Blanton J. L. and Wainwright R. L., "Multiple Vehicle Routing with Time and Capacity Constraints Using Genetic Algorithms", In S. Forrest, editor, 5th International Conference on Genetic Algorithms. Morgan Kaufmann, San Mateo, CA, (1993), pp. 452–459.

[19] Syswerda G., "Schedule Optimization Using Genetic Algorithms", In Handbook of Genetic Algorithms. Van Nostrand Reinhold, (1991), pp. 332–349.

[20] Pant M., Thangaraj R. and Abraham A., "Particle Swarm Optimization Using Adaptive Mutation",19th International Workshop on Database and Expert Systems Application, DEXA '08, (2008).

[21] Wei J., Guangbin L. and Dong L., "Elite Particle Swarm Optimization with mutation", 7th International Conference on System Simulation and Scientific Computing, ICSC 2008, Nov. (2008).

[22] Li N., Qin Y., Sun D. and Zou T., "Particle swarm optimization with mutation operator", Proceedings of 2004 International Conference on Machine Learning and Cybernetics, (2004).

[23] Chou P. C., "Improved Particle Swarm Optimization with Mutation", Modeling, Simulation, and Identification, Edt. H. Ma and S. Narayanan, (2009).

[24] Douglas R. Stinson., "Cryptography: Theory and Practice". CRC Press, Boca Raton, Florida, USA, (1995).

[25] Henry B. and Fred P., "Cipher Systems: The Protection of Communications", Wiley-Inter Science, London, (1982).

[26] Kennedy J. and Eberhart R., "Particle Swarm Optimization", in Proceedings of the IEEE International Conference on Neural Networks, pp. 1942-1948, (1995).

[27] Eberhart R. C. and Kennedy J., "A New Optimizer Using Particle Swarm Theory", Proc. 6th Symposium on Micro Machine and Human Science, pp. 39–43, (1995).

[28] Khanesar M. A., Teshnehlab M., and Shoorehdeli M. A, "A Novel Binary Particle Swarm Optimization", Proc. 15th Mediterranean Conference on Control and Automation, (2007).

[29]Al-Kazemi, B and Mohan C., "Multi-phase Discrete Particle Swarm Optimization". In: Fourth International Workshop on Frontiers in Evolutionary Algorithms, Kinsale, Ireland, (2002).

[30] Pampara G, Franken N and Engelbrecht A., "Combining Particle Swarm Optimization with Angle Modulation to Solve Binary Problems". In: Proceedings of the IEEE Congress on Evolutionary Computing, vol 1, pp 89-96, (2005).

[31] Onwubolu G. and Clerc M., "Optimal Operating Path for Automated Drilling Operations by a New Heuristic Approach Using Particle Swarm Optimization". International Journal of Production Research 42(3):pp.473-491, (2004).

[32] Pang W, Wang K, Zhou C and Dong L., "Fuzzy Discrete Particle Swarm Optimization for Solving Traveling Salesman Problem". In: Proceedings of the 4th International Conference on Computer and Information Technology (CIT04), IEEE Computer Society, vol 1, pp 89-96, (2004).

[33] Pugh J, and Martinoli A., "Discrete Multi-Valued Particle Swarm Optimization". In: Proceedings of IEEE Swarm Intelligence Symposium, vol 1, pp 103-110, (2006).

[34] Correa E., Freitas A., Johnson C., "A New Discrete Particle Swarm Algorithm Applied to Attribute Selection in a Bio-informatic data set". In: Proceedings of GECCO 2006, pp35-42, (2006).

[35] Martinez-Garcia F., Moreno-Perez J., "Jumping Frogs Optimization: A New Swarm Method for Discrete Optimization". Tech. Rep. DEIOC 3/2008, Dep. of Statistics, O.R. and Computing, University of La Laguna, Tenerife, Spain, (2008).

[36] Moreno-Perez J., Castro-Gutierrez J., Martinez-Garcia F., Melian B, Moreno-Vega J. and Ramos J., "Discrete Particle Swarm Optimization for the p-median Problem". In: Proceedings of the 7th Metaheuristics International Conference, Montreal, Canada, (2007).

[37] Shi Y. and Eberhart R.C., "A Modified Particle Swarm Optimizer", Proc. IEEE Conference on Evolutionary Computation, (1998).

[38] Kumar A., and Zhang D., "Palm Print Authentication Using Multiple Representation", Pattern Recognition, vol. 38; pp.1695-1704, (2005).

[39] Carlisle A. and Dozier G., "An off-the-Shelf PSO", Proc .Particle Swarm Optimization Workshop, pp. 1–6, (2001).

[40] Clark, A., "Modern Optimization Algorithms for Cryptanalysis". In Proceedings of the 1994 Second Australian and New Zealand Conference on Intelligent Information Systems, November 29 - December 2,pp. 258-262, (1994).

[41] Spillman, R., Jansses, M., and Kepner, M., "Use of Genetic Algorithm in the Cryptanalysis of Simple Substitution Ciphers", Cryptologia, vol. 17, issue 1, January 1993,pp. 31-34, (1993).

[42] Ismail K. Ali, "Intelligent Cryptanalysis Tools Using Particle Swarm Optimization", Ph. D. Thesis, Computer Sciences Department, University of Technology, Baghdad, Iraq, (2009).

[43] Sadiq A. T., "Evolutionary Operators-Based Particle Swarm Optimization (EOPSO) to Attack Classical Cryptography Methods", Journal of Advanced Computer Science and Technology Research, Vol. 2, No. 1, pp. 50-65, (2012).

Analysis of the Earth's Radiation Budget over Iraq

Iqbal Hussain Abd AlKareem
Department of Atmospheric Sciences, College of Science, Al-Mustansiriyah University
Received 6/11/2013 – Accepted 26/3/2014

الخلاصة

تعتبر موازنة طاقة الإشعاع من أهم العوامل المؤثرة في مناخ الكرة الأرضية .فعندما يصل الإشعاع الشمسي المرئي إلى سطح الأرض فان جزءا منه ينعكس باتجاه الفضاء وجزء يتشتت بصورة مباشرة نحو الفضاء كإشعاع قصير الموجة والجزء الأخر يمتص من قبل سطح الأرض وبعض المكونات الجوية وخصوصا الغيوم. وفي حالة عدم وجود الغيوم فان الامتصاص يحدث بشكل رئيسي من قبل سطح الأرض .إن الطاقة الممتصة تعمل على تسخين سطح الأرض والذي بدوره يبعث هذه الطاقة كإشعاع طويل الموجة. إن الهدف من هذا البحث هو دراسة بعض مركبات موازنة الإشعاع فوق العراق للفترة من 1983 إلى 2005. تم الحصول على بيانات المتوسطات الشهرية من وكالة الفضاء الأمريكية ناسا – مشروع أنواء الطاقة الشمسية لأربع مدن في العراق وهي الموصل وبغداد والبصرة والرطبة والتي تمثل شمال ووسط وجنوب وغرب البلاد. أظهرت النتائج أن منحني الإشعاع الشمسي عند قمة الغلاف الجوي منتظم وغير متعرج وله نفس المنحى لجميع المدن وان قيمة الإشعاع تتغير من مدينة إلى أخرى تبعا لخط عرضها. كما دلت النتائج على أن الغيوم لها تأثير واضح على الإشعاع الشمسي الساقط وخصوصا خلال أشهر الشتاء . وبينت النتائج أن الأجزاء الغربية من العراق تستلم أعلى قيمة من الإشعاع الشمسي قصير الموجة مقارنة ببقية المناطق كما هذه الأجزاء تستلم اقل قيمة من فيض الإشعاع طويل الموجة.

ABSTRACT

The global energy balance is important for Earth's climate. When visible solar radiation from the Sun reaches the Earth, some of it is reflected or scattered directly back into space as shortwave radiation and some of it is absorbed the earth surface and atmospheric constituents specially the clouds. In the absence of clouds, absorption happens mainly at the surface. The absorbed energy warms the Earth's surface, which, in turn, emits this energy at a longer wavelength. The aim of this research is to investigate some components of the Earth's radiation budget over Iraq for the period 1983 to 2005 . Monthly means data were obtained from NASA solar energy meteorology project for four selected cities in Iraq. These represent the northern, central, western, and southern parts of Iraq. Results showed that the top of the atmosphere insolation curves were smooth and have similar behavior for all cities and its value varies from one location to another depending on the latitude of the place. The results also indicated that the cloud has significant effects on solar insolation during winter season. The results illustrated that the western region of Iraq receives the highest solar radiations but receives relatively low downward longwave flux.

INTRODUCTION

The energy that drives the climate system comes from the Sun. When the Sun's energy reaches the Earth it is partially absorbed in different parts of the climate system. The absorbed energy is converted back to heat, which causes the Earth to warm up and makes it habitable. Solar radiation absorption is uneven in both space and time and this gives rise to the intricate pattern and seasonal variation of our climate [1].

The solar energy is short-wave radiation. Although the Earth also receives electromagnetic energy from the other bodies in space, it's negligible, compared with solar energy [2]. The incident solar energy

(shortwave) may be reflected and absorbed by the Earth's surface or the atmosphere. And Earth's surface and atmosphere also emit the radiation (longwave) [3] . The Earth Radiation Budget is the balance between incoming energy from the sun and the outgoing longwave (thermal) and reflected shortwave energy from the Earth. Therefore the radiation budget of the Earth governs its climate. Knowledge of the Earth's radiation budget is based on satellite measurements from which monthly mean maps of outgoing longwave radiation and reflected solar radiation are computed. Many workers have conducted research on the Earth radiation balance, among them Kushnir (2000) [4] who reported on the balance between solar radiation and Earth's radiation. Hansen et. al, (2005) [5] who discussed Earth's energy imbalance and its confirmation and implications. Trenberth et al. (2009) [6] gave an extensive review on the Earth's global energy budget. Davis and Davis (2010) [7] discussed the Earth's heat flux. The aim of this research is to investigate the Earth's radiation budget over Iraq using satellite data.

The Earth Radiation Budget

The Surface radiation budget is divided into downward shortwave radiation, reflected shortwave radiation, downward longwave radiation, upward longwave radiation, net radiation. They are dominated by cloud. The downward shortwave radiation may be reflected to the space absorbed in the atmosphere and absorbed at the ground.
The equation of the Earth's radiation budget is given by [8]:

$$(1 - A)E_{sun} = E_{atm} + (1 - A_{sfc})E_{sfc} \quad (1)$$

$$E_{atm} = \varepsilon_a \sigma T_a^4 \quad (2)$$

$$E_{sfc} = \varepsilon_o \sigma T_o^4 \quad (3)$$

where E_{sun} is the incident solar radiation (the solar constant), A is albedo of TOA (Top of atmosphere), E_{atm} is the energy of absorbed in atmosphere, E_{sfc} is downward irradiance at surface and A_{sfc} is surface albedo. σ is the Stefan Boltzmann constant , ε_a ε_o are the emissivity of the atmosphere and the earth surface respectively. T_a and T_o are the temperature of the atmosphere and the earth surface respectively. and This equation implicitly includes scattering and multiple reflectors between the surface and clouds. Usually the incident solar radiation and TOA albedo is measured by satellite measurement.(ERBE) [9]. The reflected solar radiation is the product of surface albedo and the downward solar radiation, the surface albedo should be determined. One method to estimate surface albedo is the minimum albedo technique. Because few locations are likely to be cloud-covered for an entire month,

the minimum albedo is likely to be represent the clear-sky albedo. It can be calculated from narrow band AVHRR observations [10]. The downward longwave radiation is mostly from the atmosphere. It depends on the temperature and moisture of the atmosphere. The water vapor and other gases, aerosols absorb some solar energy and emit some longwave radiation energy computation of downward longwave radiation from the atmosphere is difficult, even when the distributions of water vapor, carbon dioxide, cloudiness, and temperature are measured. Some satellite measurements like TOVS estimates downward longwave radiation. Little longwave radiation is reflected by the surface: natural surface emission is dominant. It is also difficult to measure and define the surface temperature especially vegetation surface. To combine the above four components makes the calculation of net radiation at the surface. This is not accurate because the errors in each accumulate. So it is developed the research to use some satellite measurements-NOAA, GOES etc. [11].

Methodology

The averages monthly means of daily values for solar insolation at the top of atmosphere and at the surface of Earth were analyses for four locations in Iraq representing the north (Mosul), center (Baghdad), west (Rutba), and south (Basra). The data were obtained from the NASA Solar Energy Meteorology site [12] for the period 1983 to 2005.

Table-1: Geographical location of the selected cities

City	Longitude (°E)	Latitude (°N)
Mosul	43.08	36.25
Baghdad	44.39	33.33
Rutba	40.25	33.00
Basra	47.83	30.50

RESULTS AND DISCUSSION

Figure 1 to figure 4 illustrates the results of analysis for the four cities. The results show that the behavior of all types of radiation under study are similar for all cities.

It is evident that the curves top of atmosphere solar insolation are smooth and reaching the peak values during the month of June for all cities. The effects of clouds on solar insolation is obvious since the clear sky isolation is higher that actual insolation for all months except the summer months (June, July, August) and September. The downward longwave radiation flux values are higher than those of insolation and generally values during summer months. To see the variation of the four components of radiation budget from one location to another, each component was plotted alone for the four cities. The results are shown in

figures 5 to 8. Figure 5 reflects the effect of latitude of the top of atmosphere insolation, i.e. southern city of Basra receives the highest insolation while northern city of Mosul receives lowest insolation. The cities of Baghdad and Rutba receive the same amount of insolation since they are located on the same latitude circle (33 °N). Figure 6 illustrate that Rutba receives the highest clear sky insolation followed by Mosul city. The variability in Baghdad's curve may be attributed to the attenuation of solar radiation by suspended particles. Figure 7 shows that the insolation follows similar behavior to that of clear sky insolation. Figure 8 gives the downward longwave flux for the four cities. It is seen that this components also depends of latitude but in this case the flux for Baghdad city is higher than that of Rutba. This may be attributed to the fact that the albedo of Rutba is higher that of Baghdad and therefore the desert land of Rutba absorbs lower radiation than that of Baghdad.

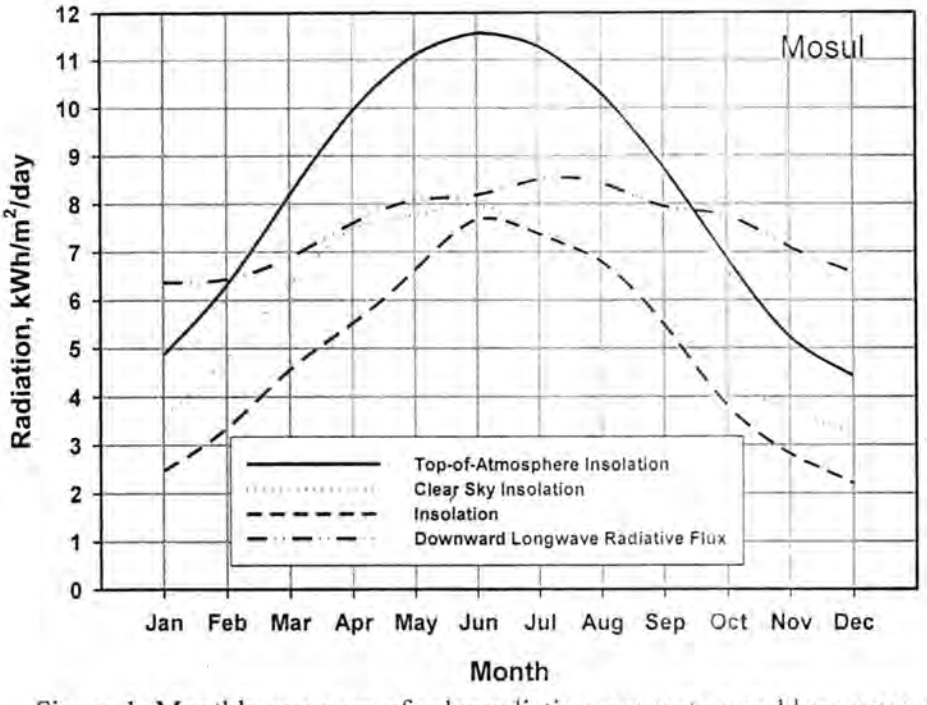

Figure-1: Monthly averages of solar radiation parameters and longwave radiative flux for Mosul for the period 1983-2005.

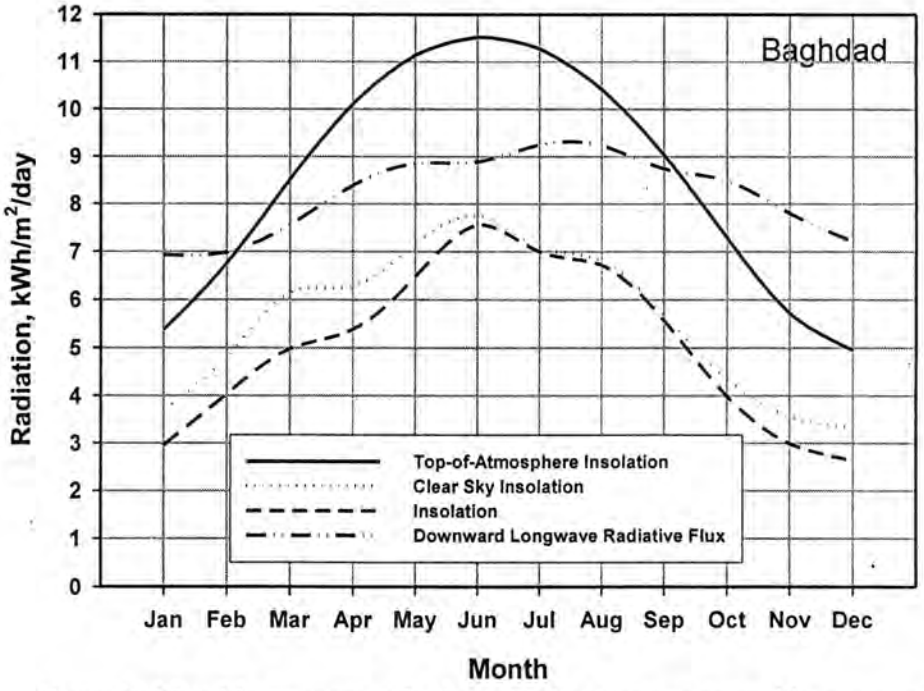

Figure-2: Monthly averages of solar radiation parameters and longwave radiative flux for Baghdad for the period 1983-2005.

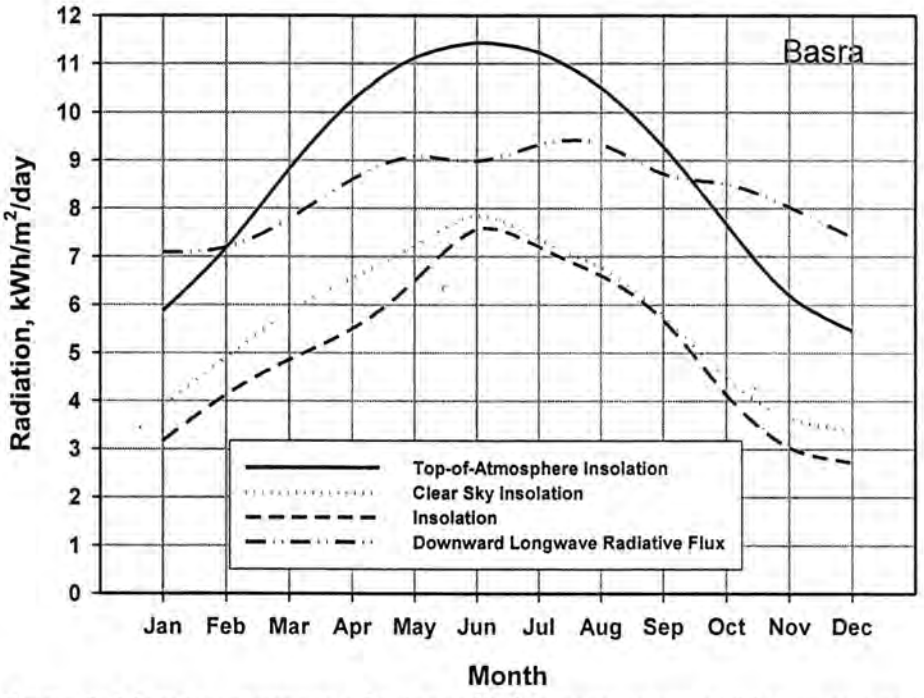

Figure-3: Monthly averages of solar radiation parameters and longwave radiative flux for Basra for the period 1983-2005.

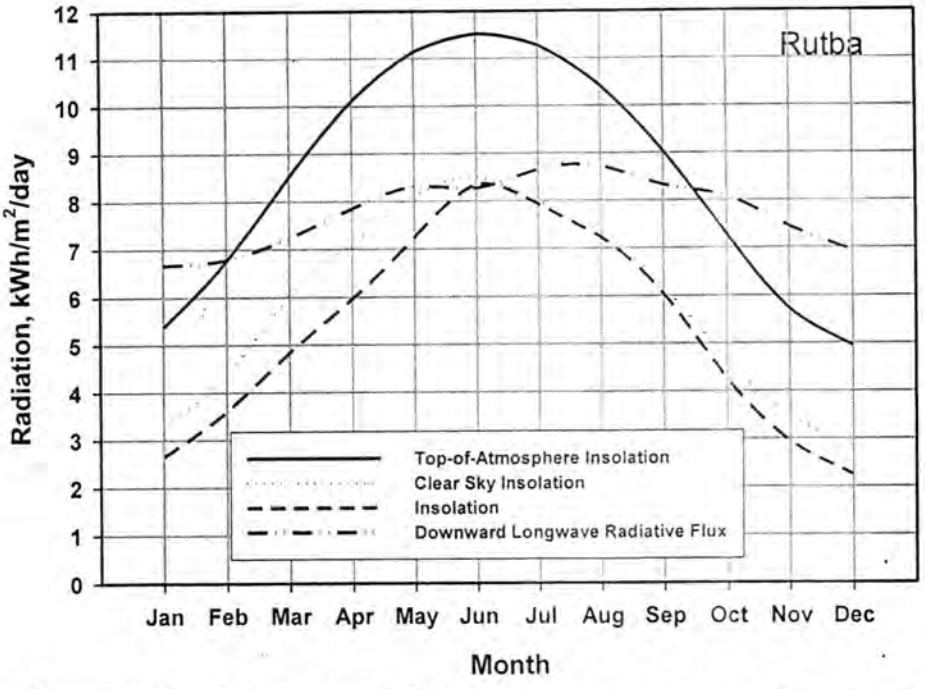

Figure-4: Monthly averages of solar radiation parameters and longwave radiative flux for Rutba for the period 1983-2005.

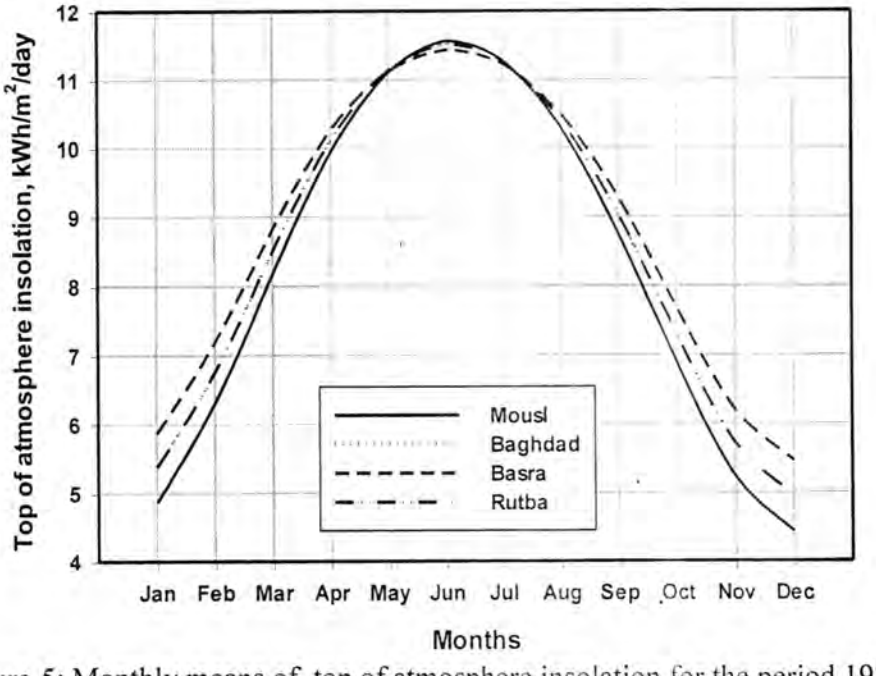

Figure-5: Monthly means of top of atmosphere insolation for the period 1983-2005

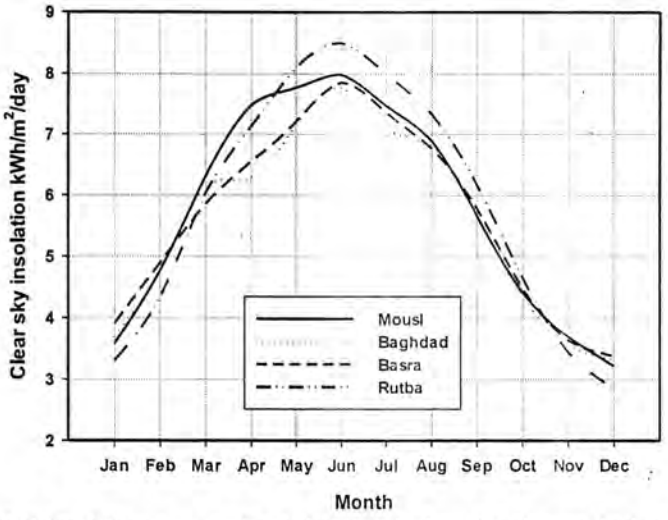

Figure- 6: Monthly means clear sky insolation for the period 1983-2005 .

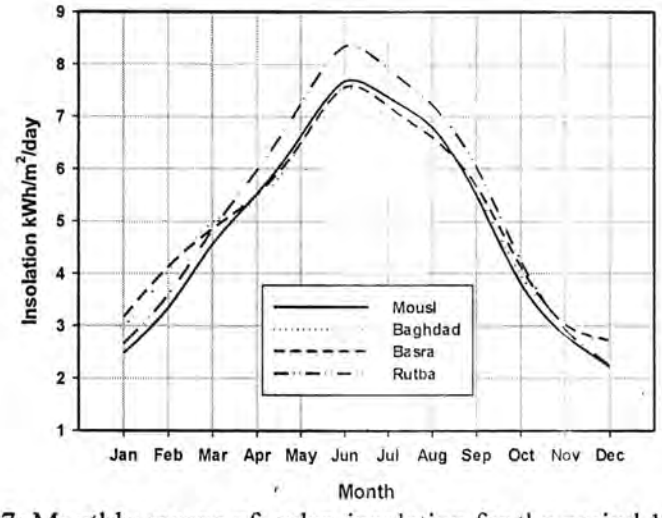

Figure- 7: Monthly means of solar insolation for the period 1983-2005 .

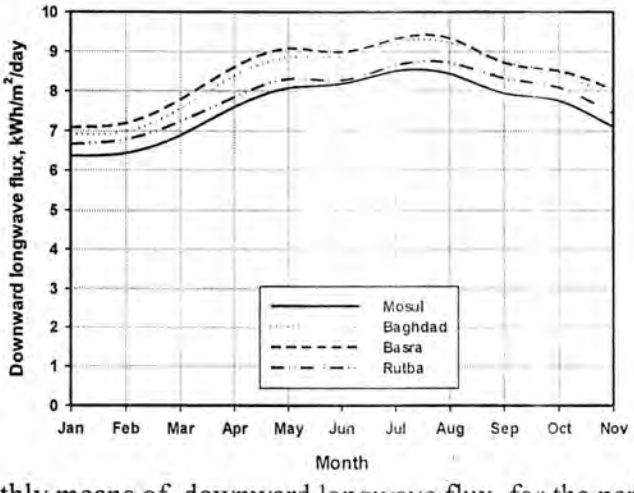

Figure- 8: Monthly means of downward longwave flux for the period 1983-2005 .

CONCLUSIONS

The main concluding remarks obtained from this research is that Earth's radiation budget over Iraq varies from one location to another depending on location (latitude), nature of land (albedo) and pollution. The results showed that the western desert city of Rutba receives the highest solar radiations but receives relatively low downward longwave flux.

REFERENCES

1. Peixoto, J., and Oort, A.. Physics of Climate. Woodbury, NY: American Institute of Physics Press (1992).
2. Marshall, J., and Plumb, R.A.. Chapter 2: The global energy balance. In Atmosphere, Ocean, and Climate Dynamics: an Introductory Text (pp. 9-22) (2008).
3. Bridgman, H. A., and Oliver J. E.. The Global Climate System: Patterns, Processes, and Teleconnections. Cambridge University Press (2006).
4. Kushnir, Y.. Solar Radiation and the Earth's Energy Balance. Published on The Climate System, complete online course material from the Department of Earth and Environmental Sciences at Columbia University (2000).
5. Hansen, J., Nazarenko, L., Ruedy, R., Sato, M., Willis, J., Del Genio, A., Koch, D., Lacis, A., Lo, K., Menon, S., Novakov, T., Perlwitz, J., Russell, G., Schmidt, G.A., and Tausnev, N.. Earth's Energy Imbalance: Confirmation and Implications. Science, (308) 1431-1435 (2005).
6. Trenberth, K., Fasullo, J., Kiehl, J.. Earth's global energy budget. Bulletin of the American Meteorological Society (2009).
7. Davies, J.H., and. Davies, D.R., "Earth's Surface heat flux," Solid Earth, 1, 5–24 (2010).
8. Lindsey, R.. Climate and Earth's Energy Budget. NASA Earth Observatory (2009).
9. The Earth Radiation Budget Experiment (ERBE). http://www.nasa.gov/centers/langley/news/factsheets/ERBE.html
10. Advanced Very High Resolution Radiometer. http://noaasis.noaa.gov/NOAASIS/ml/avhrr.html
11. National Oceanographic and Atmospheric Authorization. http://www.noaa.gov/.
12. Surface Meteorlogy and Solar Energy. http:/eosweb.larc.nasa.gov/sse.

Vol. 25
No. 2
2014

مجلة علوم المستنصرية

تصدر عن كلية العلوم الجامعة المستنصرية

Mobile: 07711184399
e-mail: mustjsci@yahoo.com

المـــحتـــويـات

مجلة علوم المستنصرية

مجلة علمية محكمة تصدر عن عمادة كلية العلوم في الجامعة المستنصرية بأختصاصات الكيمياء والفيزيا والرياضيات وعلوم الحياة وعلوم الحاسبات وعلوم الجو. تنشر المجلة البحوث العلمية التي لم يسبق نشرها في مكان آخر بعد إخضاعها للتقويم العلمي من قبل مختصين وباللغتين العربية او الانكليزية وتُصدر المجلة اربعة اعداد سنوياً على الاقل وبكلا اللغتين.

تعليمات النشر في المجلة

1. يقدم الباحث طلبا تحريريا لنشر البحث في المجلة ويكون مرفقا بثلاث نسخ من البحث مطبوعة على ورق ابيض قياس (A4, 21.6×27.9 cm) مع ترك حاشية بمسافة انج واحد لكل طرف من اطراف الصفحة ومطبوعة بأستعمال برنامج (Microsoft Word, 2007 او 2010) بصيغة (.doc) اضافة الى نسخة الكترونية لأصل البحث مخزنة على قرص (CD).
2. يرفق مع البحث ملخص باللغة الإنجليزية على ان لاتزيد كلمات الملخص عن (150) كلمة.
3. عدد صفحات البحث لاتتجاوز 10 صفحة بضمنها الاشكال والجداول على ان تكون الاحرف بقياس 14 نوع (Time New Roman) وبمسافة مزدوجة بين الاسطر. وينبغي ترتيب اجزاء البحث دون ترقم وبالخط العريض (Bold) كالاتي: صفحة **العنوان، الخلاصة باللغة العربية، الخلاصة باللغة الإنجليزية، مقدمة، المواد وطرائق العمل (الجزء العملي)، النتائج والمناقشة، الاستنتاجات وقائمة المراجع.**
4. يطبع عنوان البحث واسماء الباحثين (كاملة) وعناوينهم باللغتين العربية والانكليزية أضافة الى البريد الاليكتروني للباحث الرئيس وتطبع على ورقة منفصلة شرط ان لاتكتب اسماء الباحثين وعناوينهم في أي مكان اخر من البحث ، وتعاد كتابة عنوان البحث فقط على الصفحة الاولى من البحث.
5. ترقم الجداول والأشكال على التوالي حسب ورودها في المتن، وتزود بعناوين، ويشار إلى كل منها بالتسلسل ذاته في متن البحث.

6. يشار الى المصدر برقم يوضع بين قوسين بمستوى السطر نفسه بعد الجملة مباشرة وتوضع بين قوسين كبيرين مثلاً [1] وفي حالة وجود اكثر من مصدر وبتسلسل فيكتب من الراقم الاول الى الاخير مثلاً [1-4]. تطبع المصادر على ورقة منفصلة ، ويستعمل الاسلوب الدولي المتعارف عليه عند ذكر مختصرات اسماء المجلات.

7. يتبع الاسلوب الاتي عند كتابة قائمة المصادر على الصفحة الاخيرة كالاتي: ترقيم المصادر حسب تسلسل ورودها في البحث ، يكتب الاسم الاخير (اللقب) للباحث او الباحثين ثم مختصر الاسمين الاولين فعنوان البحث ، اسم المجلة ، المجلد ، العدد ، الصفحات الاولى والاخيرة ، سنة نشر. . وفي حالة كون المصدر كتابا يكتب بعد اسم المؤلف او المؤلفين عنوان الكتاب ، الطبعة ، الصفحات ، اسم دار النشر، الدولة واخيراً سنة النشر.

دور البوتاسيوم والسايتوكاينين في بعض مؤشرات النموالخضري والمركبات الفعالة لنبات الكزبرة المحلي (*Coriandrum sativum* L.)

بهاء الدين مكي فيروزالربيعي[1]، امل عبد سيد الجلالي [2]
[1]الجامعة المستنصرية ,كلية التربية الاساسية قسم العلوم
[2]الجامعة المستنصرية كلية التربية الاساسية قسم العلوم
تاريخ تقديم البحث 2013/12/15 - تاريخ قبول البحث 2014/1/21

ABSTRACT

The experiment was conducted at the field es of BobAlsham City in Baghdad during the growing season 2012-2013 to study the effects of cytokinin (Kin.) concentrations and level of potassium fertilizer on the morphological and to determine some of the medically active ingredients in Coriander *Coriandrum sativum* L. plant. Experiment was accomplished as acompletely Randomized Complete Block Design R.C.B.D. by using three replicates including concentrations of Cytokinin is (0.50.100,150)mg.L^{-1} and four level of potassum fertilizer at the rate of(300,150,75,0)Kg.h^{-1}., the following parametens were studied plant height , fresh weight , dry weight.$Plant^{-1}$, While the results of the High performance Liquid Chromatography (HPLC) analysis are reveald eight active compounds (Camphor, Broneal، Cis-dihydroxycarvone، Limonene,Linalool, Coumarin، Geranyl acetate، Neral) Coumarin compound showed more effective by treatment. of Cytokinin and potassium fertilizer compared to the others of active compounds .

الخلاصة

اجريت التجربة في احد حقول منطقة بوب الشام في محافظة بغداد .للموسم الزراعي 2012-2013 وذلك لمعرفة تأثير تراكيزمختلفة من السايتوكاينين و البوتاسيوم في كل من المؤشرات المظهرية وبعض المركبات الفعالة طبياً في نبات الكزبرة *Coriandrum sativum* L. نفذت التجربة بتصميم القطاعات تام التعشية Randomized Complete Block Design (RCBD) وبثلاث مكررات اذ أستخدم في التجربة أربعة تراكيز من السايتوكاينين هي (0,50,100,150)ملغم.لتر$^{-1}$واربعة مستويات من البوتاسيوم هي (0,75,150,300) كغم.هـ$^{-1}$.وتم دراسة مؤشرات النمو الآتية أرتفاع النبات،الوزن الطري والوزن الجاف والمركبات الفعالة في الزيت الطيار أظهرت النتائج زيادة معنوية في مؤشرات النمو المدروسة بزيادة تركيز السايتوكاينين ومستوى سماد البوتاسيوم أظهرت نتائج الفحص والتشخيص الكروماتوغرافي بأستعمال تقنية الـ High Performance Liquid Chromatographyتشخيص ثمانية مركبات في الزيت الطيار للكزبرة هي (Camphor, Limonene, Cis-dihydroxycarvone Broneal Linalool, Neral, Geranyl acetate, Coumarin)، وتفوقت التراكيزالعالية من السايتوكاينين في اعطاءها اعلى القيم من المركبات الفعالة وكان مركب الـ Coumarin هو الأكثرتأثراً بمعاملات الدراسة .

المقدمة

شهد العالم اهتماما بالغا بطب الأعشاب أو الطب البديل والعودة إلى الطبيعة وما تزخر به أعشابها ونباتاتها الطبية من كنوز ، وقد تزايد الطلب تجاريا على النباتات الطبية في مختلف أنحاء العالم بتزايد البحوث العلمية الهادفة عليها بسبب كثرة الأضرار الجانبية للأدوية الكيميائية المستعملة وتعاظم مخاطرها . لذا توجهت الاهتمامات إلى معالجة بعض الأمراض باستخدام النباتات الطبية نظرا لأمانها وقلة التأثيرات الجانبية ، فضلا عن توافرها وكونها اقتصادية [1].

يعد نبات الكزبرة Coriander (*Coriandrum sativum* L.) من النباتات الطبية المستعملة منذ القدم فقد عثر عليها في أحد الكهوف بفلسطين ويعود تاريخها الى عام 6000 ق . م وقد استعملها الآشوريون والمصريون القدماء والصينيون علاجاً وغذاءً منذ آلاف السنين قبل الميلاد [2] وتعود أهميتها الطبية لاحتوائها على الزيوت الطيارة التي تضم بحدود مائتي مركب [3].

تعد السايتوكاينينات مركبات كيميائية تعمل كمنظمات نمو، ويحتوي في تركيبها الأساس على حلقة البيورين Purine ring [4]، ولها أنواع كثيرة طبيعية وصناعية ، وينحصر تأثيرها في بدء نمو

وانقسام الخلايا وتأخير الشيخوخة وإطالة فترة التخزين في للخضر الورقية كما في الخس والتغلب على السكون الحراري في بذور الخس ومنع السيادة القمية وتنشيط الإنزيمات في بعض النباتات ويمكن للسايتوكاينينات التغلب على تأثير حامض الأبسيسك المثبط لفعل الجبرلين [5].

يعد البوتاسيوم هو دالة للعديد من العمليات الفسيولوجية في النبات ، لذا حظي باهتمام العديد من الباحثين والمهتمين بكيمياء التربة وخصوبتها وتغذية وفسلجة والكيمياء الحياتية للنبات. يكون البوتاسيوم 2.6% من القشرة الارضية مما يجعله سابع عنصر من العناصر الاكثر سيادة في القشرة الارضية ورابع مغذ للنبات الاكثر سيادة على اليابسة [6]. كان الاعتقاد السائد في العراق ان الترب العراقية تحتوي عال خزين عالي من البوتاسيوم [7]، لذا أهمل تضمين البوتاسيوم في التوصيات السمادية ولسنين طويلة. ونتيجة التكثيف الزراعي وتزايد وتنوع المحاصيل الزراعية في القطر وعدم التسميد بالبوتاسيوم ظهرت الحاجة لاضافة الاسمدة البوتاسية. ومن مصادر الاسمدة البوتاسية وأكثرها استخداماً في العراق هو سمادي كلوريد البوتاسيوم KCl وكبريتات البوتاسيوم (K_2SO_4). ذكر [8] ان البوتاسيوم ضروري لزيادة قدرة النبات على مقاومة التذبذب الحاد في درجات الحرارة ومقاومة الجفاف والاوبئة ، ويحافظ على ضغط الخلية وتنظيم فتح الثغور وغلقها. ونظرا لأهمية النباتات الطبية والعلاجية جاءت فكرة البحث بهدف معرفة تاثيرالاسمدة ومنظمات النمو وتداخلهما في مؤشرات النمو والحاصل والمركبات الفعالة لنبات الكزبرة .

المواد وطرائق العمل

نفذت التجربة في احد حقول منطقة بوب الشام في محافظة بغداد لموسم النمو2012 - 2013 . تم تهيئة أرض التجربة من خلال حراثتها وتنعيمها و التخلص من الادغال وقسمت ال ثلاث مكررات (ألواح)بحيث تضمن كل مكرر(16) وحدة تجريبية بمساحة (60×60)سم^2 لكل وحدة اذ تم زراعة كل منها بأربع سطور كل سطر يحتوي على أربع جور وكل جورة تحتوي (5)بذور أي بمعدل (80) بذرة في كل وحدة تجريبية صممت التجربة وفق تصميم القطاعات تام التعشية (Randomized complete Blocks Design R.C.B.D)كتجربة عاملية (4×4×3) ، تضمنت التجربة اربع مستويات من البوتاسيوم (K_2SO_4)هي (300,150,75,0)كغم.هـ$^{-1}$. فضلاً عن المستوى صفر والذي عُدّ كمعاملة سيطرة(Control). واربع تراكيز من منظم النمو السايتوكاينين وهي (150,100,50, 0) ملغم.لتر$^{-1}$ حضرت أعتمادا على قانون التخفيف من المحلول القياسي الرئيسي (Stock) الذي حضر بأذابة غرام واحد من السايتوكاينين في لتر من الماء المقطر للحصول على محلول قياسي تركيزة 1000ملغم .لتر$^{-1}$ حيث أستعمل الكاينتين (6-Furfuryl amino purine)المستورد من شركة Qualikems الهندية وحضرت التراكيز أعلاه قبل يوم من أستخدامها.

زرعت بذورالكزبرة ورويت التربة بالماء رية أولية بتاريخ 2012/11/20 وبعد الانبات و النمو تم خف النبات إلى نبات واحد لكل جورة بتاريخ 2012/12/24 مع إجراء كافة العمليات الزراعية من عملية الري حسب الحاجة وإزالة الادغال و متابعة نمو النبات حتى موعد الحصاد .ثم رش منظم النمو السايتوكاينين بتاريخ 2013/2/2 عند بلوغ النباتات الى الورقة 5-6 وبالتراكيز المحضرة سابقاً وحسب المعاملات وذلك باستخدام مرشة يدوية حجم 1لتر. وتم الرش في الصباح الباكر حيث رش النبات حتى البلل الكامل مع رش معاملة السيطرة بالماء المقطر فقط [9]. والشكل رقم (1) يوضح نمو النبات في التجربة الحقلية.

الشكل1-: يوضح نمو النبات في التجربة الحقلية

تم هضم العينات حسب طريقة [10].وتم قياس بعض الصفات المضهرية ،ارتفاع النبات في تاريخ 2013/3/10 سطح الارض ولغاية اعلى نقطة من النبات وكذلك قيس الوزن الطري مباشرة للمجموع الخضري ، تم قياس الوزن الجاف للمجموع الخضري .

وتم تشخيصها باستعمال جهاز HPLC نوع 2010LC Shizmadzu اعتماداً على نماذج قياسية تم الحصول عليها من شركة سكما للتجارة العامة Sigma International tranding اذ تم حقن الجهاز بتراكيز معلومة مقدارها 25 مايكروغرام.مليلتر$^{-1}$ لكل نموذج قياسي في ظروف الفصل الموضحة في الجدول (1) وتم قياس زمن الاحتجاز ومساحات الحزم للنماذج القياسية مقدرة بالمايكروفولت وكما موضح في الجدولين (2).

جدول -1:ظروف الفصل الكروماتوغرافي HPLC لبعض المركبات الفعالة من زيت الكزبرة

طول العمود	50X2.0mmI.D
الطور المتحرك	1.01M ammonium acetate
سرعة جريان الطور المتحرك	1.1 مليلتر.دقيقة$^{-1}$
نوع الكاشف	الاشعة فوق البنفسجية عند الطول الموجي 285
درجة حرارة الفصل	30م°

جدول-2: زمن الاحتجاز ومساحات الحزم لبعض المركبات الفعالة لزيت الكزبرة

المركبات القياسية	زمن الاحتجاز	المساحة
Camphor	1.16	33015
Limonene	1.90	52034
Cis-dihydroxycarvone	3.65	37871
Broneal	4.47	40237
Linalool	5.30	42212
Neral	6.14	53561
Geranyl acetate	7.31	46260
Coumarin	7.96	45747

بعد ذلك حضـــر محلول النموذج المطلوب بطريقة التقطير المائية اذ أخذ 5 غم بذور مطحونة وغمرت بالماء ثم غليت لان درجة الحرارة العالية تساعد على تحرر الجزيئات العطرية

من البذرة اذ تتبخر جزيئات هذه الزيوت القلقة الى المكثف الذي يحولها إلى الحالة السائلة ثم بعد ذلك يفصل الزيت عن الماء ويأخذ منه 20 مايكروليتر ويحقن في جهاز الـــــ HPLC تحت ظروف الفصل المذكورة نفسهـــا ومن ثم تم القياس الكمي للمركبات الموجودة في النماذج عن طريق مقارنة الحزم المجهولة للنماذج من مساحات الحزم المعلومة للمواد القياسية ثم حسبت تراكيز المركبات المشخصة في النموذج وفقاً المعادلة الآتية :

$$\text{تركيز المركبات في العينة} = \frac{\text{مساحة حزمة المادة الفعالة في النموذج}}{\text{مساحة حزمة المادة الفعالة في المحلول القياسي}} \times \text{تركيز المحلول القياسي}$$

[11] واجري التحليل الاحصائي حسب طريقة [12] و مقارنة المتوسطات باستعمال اقل فرق معنوي .L.S.D على مستوى احتمال 0.05.

النتائج والمناقشة

أرتفاع النبات (سم)

بينت النتائج في الجدول (3) أن معاملة نبات الكزبرة بالسايتوكاينين رش على المجموع الخضري قد أعطى زيادة معنوية في أرتفاع النبات ولكافة التراكيز المستعملة أذ أعطت التراكيز (150,100,50) ملغم.لتر$^{-1}$ معدل لأرتفاع النبات هو(59.50,61.50,58.87)سم ،على التوالي بالمقارنة مع معاملة السيطرة التي أعطت أقل معدل للارتفاع هو57.4سم ، قد تفوق التركيز100 ملغم.لتر$^{-1}$ معنويا في أرتفاع النبات مقارنة بالتراكيزالاخرى وهي (150,50.0) ملغم.لتر$^{-1}$ الذي أعطى معدل هو 61.50 سم وكذلك الحال بالنسبة لزيادة مستوى السماد البوتاسي فقد أعطت المستوى (300,150,75) كغم.هـ$^{-1}$ زيادة معنوية في أرتفاع النبات وكان معدل أرتفاع النبات في هذه التركيزات هو58.75,60.45,63.25 سم على التوالي بالمقارنة مع معاملة السيطرة التي أعطت أقل معدل لأرتفاع النبات هو 54.50 سم مع تفوق معنوي للمستوى 75 كغم.هـ$^{-1}$مقارنا بالمستويات . أما بالنسبة للتداخل بين السايتوكاينين والسماد البوتاسي فكان تأثيره معنوياً في هذة الصفة فقد أعطى التداخل بين التركيز ملغم.لتر$^{-1}$ 100سايتوكاينين ومستوى 75كغم.هـ$^{-1}$سماد أعلى معدل للارتفاع هو64.00سم بالمقارنة مع معاملة السيطرة التي أعطت اقل معدل للأرتفاع هو 49.00 سم وبنسبة زيادة مقدارها 30.61% . أن سبب الزيادة الحاصلة في أرتفاع النبات نتيجة رش السايتوكاينين يعود الى أنه يزيد من بناء الحوامض DNA,RNA [12]و يزيد من معدل طول الخلايا وعرضها لكونه يشارك في أنقسام النواة ويحفز أنقسام السايتوبلازم وبالتالي فأنة يؤثر بدرجة كبيرة في النمو الخضري من خلال تحفيزة لأنقسام الخلايا وتمايزها ، فضلا عن دورة في تكوين بعض الانزيمات منها أنزيمات البناء الضوئي ، وهذا ماأكدة [13] . ان السايتوكاينين يحفز تكاثر الخلايا من خلال دوره الفعال في تنظيم الدورة الخلوية فهو يعمل على تنظيم التعبيرالجيني عن جين CycD3 سايكلين نوع D kinases cyclin-dependent الذي هو مفتاح للدورة الخلوية .الجانب الثاني من عمل السايتوكاينين هوالتأثير في تعبير عائلة الجين Knotted (KN1)و يعمل السايتوكاينين تنظيم عمل المرستيم meristem Shoot (SAM) apical [14] . هناك دراسات مختلفة اكدت ارتباط الانظمة الثنائية المكونات في اشارات السايتوكاينين . و ادواره في دورة الخلية هو تفعيل سلسلة متعاقبة من تحركات البروتين(انزيمات بروتينية ، Proteins Kinases) وتفعيل السايكلينات المعتمدة على الكاينيز وهي (Cdc2,Cdk4,Cdk6) cyclin-dependent kinases [14] .الاضافة الخارجية للسايتوكاينينات ترفع مستوى(steady-state)الحالة الثابتة CycD3, Cdc2 (سايكلين نوع D). [15]

جـدول-3: تأثيرتركيزالسـايتوكاينين ومسـتوى السـماد البوتاسـي وتـداخلاتهما فـي أرتفـاع النبـات (سم) لنبات الكزبرة

مستوى السماد البوتاسي (كغم.هـ$^{-1}$)	تركيز السايتوكاينين ملغم.لتر$^{-1}$				معدل تأثير البوتاسيوم
	0	50	100	150	
0	49.00	54.00	60.00	55.00	54.50
75	63.00	63.50	64.00	63.50	63.25
150	59.00	59.50	62.00	61.00	60.45
300	58.60	58.50	60.00	58.50	58.75
معدل تأثيرالسايتوكاينين	57.4	58.87	61.50	59.50	.....
LSD (0.05)	تركيز السايتوكاينين =0.649 مستوى البوتاسيوم =0.649 التداخل =1.29				

2-الوزن الطري للمجموع الخضري (غم)

أظهـرت النتـائج فـي الجـدول (4) وجـود زيـادة معنويـة فـي الـوزن الطـري للمجمـوع الخضـري للنباتـات المعاملـة بالسـايتوكاينين ولجميـع التراكيـز وقـد أعطـى التركيـز 100 ملغم.لتر$^{-1}$ اعلـى معـدل اذ بلـغ 1.99غم بالمقارنـة مـع معاملـة السـيطرة التـي أعطـت معـدل 1.19غم وبنسـبة زيـادة هـي 67.22% . أظهـرت معاملـة النباتـات بالسـماد البوتاسـي زيـادة معنويـة فـي معـدل الـوزن الطـري اذ أعطـى المسـتوى 75 كغم.هـ$^{-1}$ أعلـى معـدل هـو 2.31غم بالمقارنـة مـع معاملـة السـيطرة التـي أعطـت أقـل معـدل لهـذه الصـفة هـو 1.13غم وبنسـبة زيـادة هـي 104.42% أمـا بالنسـبة للتـداخل الثنـائي بـين عـاملي الدراسـة فقـد أظهـرت النتـائج وجـود فـروق معنويـة فـي الـوزن الطـري للمجمـوع الخضـري وقـد تفـوق التـداخل بـين التركيـز 100 ملغم.لتـر$^{-1}$ سـايتوكاينين مـع المسـتوى 75 كغم.هـ$^{-1}$ بوتاسـيوم معنويـاً علـى بـاقي معـاملات التـداخل إذ أعطيـا وزن طـري هـو 2.72غـم وكـذلك نسـبة زيادة 202.22 % مقارنة مع معاملة السيطرة .

جدول-4: تأثيرتركيزالسايتوكاينين ومستوى السمادالبوتاسي وتداخلاتهما في الوزن الطري للمجموع الخضري (غم) لنبات الكزبرة

مستوى السماد البوتاسي (كغم.هـ$^{-1}$)	تركيز السايتوكاينين ملغم.لتر$^{-1}$				معدل تأثير البوتاسيوم
	0	50	100	150	
0	0.90	1.02	1.31	1.30	1.13
75	1.83	2.20	2.72	2.50	2.31
150	1.24	1.30	1.73	1.70	1.49
300	1.68	1.70	2.20	2.00	1.89
معدل تأثيرالسايتوكاينين	1.19	1.55	1.99	1.75	.....
LSD (0.05)	تركيز السايتوكاينين = 0.032 مستوى البوتاسيوم =0.033 التداخل =0.067				

3- وزن الجاف للمجموع الخضري (غم)

توضح النتائج في الجدول (5) وجود زيادة معنوية في الوزن الجاف بزيادة مستوى السايتوكاينين المستعملة رشاً ، إذ أظهر المستوى 100 ملغم.لتر$^{-1}$ تفوقاً معنوياً على باقي التراكيز

المستخدمة في هذه الصفة اذ أعطى أعلى معدل وهو 0.38غم مقارنة بمعاملة السيطرة التي بلغت 0.32غم .أظهرالمستوى المستعمل من البوتاسيوم زيادة معنوية في الوزن الجاف مع تفوق معنوي للمستوى 75 كغم.هـ$^{-1}$ بأعطائة أعلى معدل للوزن الجاف هو0.39غم مقارنة بالمستويات (300,150,0)كغم.هـ$^{-1}$سماد ، والتي اعطت (0.38,0.36,0.29) غم على التوالي. أما بالنسبة للتداخل فقد كان تأثيرة معنوياً في الوزن الجاف أذ كان أفضل تأثير للتداخل هو بين التركيز 100ملغم.لتر$^{-1}$ سايتوكاينين والمستوى البوتاسيوم 75كغم.هـ$^{-1}$ بوتاسيوم من خلال أعطائة أعلى معدل لهذه الصفة هي 0.41 غم وبنسبة زيادة 105% بالمقارنة مع معاملة السيطرة .

جدول-5: تأثيرتركيزالسايتوكاينين ومستوى السمادالبوتاسي وتداخلاتهما في الوزن الجاف (غم) لنبات الكزبرة

مستوى السماد البوتاسي (كغم.هـ$^{-1}$)	تركيز السايتوكاينين ملغم.لتر$^{-1}$				معدل تأثير البوتاسيوم
	0	50	100	150	
0	0.20	0.31	0.35	0.32	0.29
75	0.38	0.39	0.41	0.40	0.39
150	0.35	0.36	0.38	0.37	0.36
300	0.38	0.39	0.40	0.38	0.38
معدل تأثيرالسايتوكاينين	0.32	0.36	0.38	0.36	.....
LSD (0.05)	تركيز السايتوكاينين =0.003 مستوى البوتاسيوم =0.003 التداخل =0.007				

ويعزى السبب في زيادة الوزن الجاف الى دور السايتوكاينين في زيادة المجموع الجذري والذي أنعكس تأثيرة أيجابياً على نمو المجموع الخضري للنبات [16]، من خلال زيادة قابلية النبات لامتصاص المغذيات اذ زاد محتوى النبات من المغذيات ومحتوى الكلورفيل والبروتين والذي يؤدي بدورة الى زيادة كفاءة عملية البناء الضوئي في تصنيع المواد الغذائية وتراكمها في النبات مما ينعكس على زيادة المادة الجافة [17]، في حين يعزى تأثيرالبوتاسيوم الى كون يعمل على زيادة محتوى النبات من البروتين وصبغات البناء الضوئي والمغذيات ممايؤدي الى زيادة عملية البناء الضوئي مما يزيد من الكربوهيدرات المصنعة ومن ثم زيادة الوزن الجاف للنبات [18] ،[19]أما بالنسبة للزيادة المعنوية لتأثير التداخل فيرجع للتأثير المشترك لعاملي الدراسة . أن قيم الوزن الجاف تتماشى مع قيم الوزن الطري جدول (2) وحسب معاملات التجربة .

4-المركبات الفعالة في الزيت الطيار لنبات الكزبرة (مايكروغرام.مليلتر$^{-1}$)

ان النتائج المتوفرة في الجدول (6) أشارت الى أن الزيت الطيار المستخلص من بذور الكزبرة أحتوى على ثمانية مركبات فعالة تم تشخيصها بناء على توفر المركبات القياسية وظروف الفصل الكروماتوغرافي والمركبات المشخصة هي Broneal، Neral،Camphor,Linalool, Coumarin, Geranyl acetate ، Limonene ،Cis-dihydroxycarvone, وهذه المركبات قد تأثرت بمعاملات التجربة أذ أزداد تركيزها بزيادة تراكيز السايتوكاينين ومستوى البوتاسيوم بالمقارنة بمعاملة السيطرة ،وقد تفوق التركيز 100ملغم.لتر$^{-1}$مع مستوى التسميد 75كغم.هـ$^{-1}$ على بقية المعاملات بأعطائة أعلى تركيز لجميع المركبات الفعالة موضع الدراسة،وان التركيز 100ملغم.لتر$^{-1}$ سايتوكاينين اعطى أعلى القيم هي (86.31,22.41,17.92,26.12,16.30,37.21,15.61,14.62)مايكروغرام.مليلتر$^{-1}$

نما لوحظ تفوق المستوى75كغم.هـ$^{-1}$بوتاسيوم على باقي المعاملات بأعطانة أعلى القيم وبنسبة زيادة هي (28.85, 34.04,71.84, 66.55, 41.45, 15.62, 56.49, 87.06)% بالمقارنة مع معاملة السيطرة التي أعطت أقل القيم.كما أوضحت نتائج الجدول (6) تأثرتراكيز المركبات الفعالة بمعاملات التداخلات ولوحظ تفوق التداخلات بين التركيز 100ملغم.لتر$^{-1}$ سايتوكاينين والمستوى 75كغم.هـ$^{-1}$ بوتاسيوم على باقي معاملات التداخل بأعطانة أعلى القيم لتركيزالمركبات الفعالة هي (104.11,24.96,13.11,34.48,32.80,47.78,30.21,20.26) مايكروغرام.مليلتر$^{-1}$ بالمقارنة مع معاملة السيطرة التي أعطت أقل القيم لهذه المركبات وبنسبة أنخفاض هي (91.13, 71.43, 6.48, 59.25, 65.76, 84.28, 71.53, 36.96)% وكان المركب الأكثرتأثراً بمعاملات الدراسة هو مركب الـCoumarin حيث كانت قيم تراكيز هذا المركب هي أعلى القيم وتحت تأثيرجميع المعاملات بالمقارنة مع بقية المركبات الفعالة .

الأستنتاجات

أن أهم الأستنتاجات التي توصلت اليها هذة التجربة هي :-

1-أن لمعاملات الرش بالكاينتين تأثيراً أيجابياً في نمو النبات ، اذ أدت الى تحسين الصفات المظهرية والفسلجية والزهرية ومحتوى الزيت الطيار من المركبات الفعالة ، مع تفوق التركيز 100ملغم.لتر$^{-1}$بأعطانة أعلى القيم في جميع الصفات المدروسة .

2-أدت مستويات التسميد الى زيادة في الصفات المدروسة أعلاه ،وكان أفضلها عند مستوى التسميد 75 كغم.هـ$^{-1}$.

3-أظهر التداخل بين تركيز السايتوكاينين ومستوى التسميد تأثيراً معنوياً في زيادة الصفات المدروسة .

4-اظهر التحليل الكروماتوكرافي الى وجود ثمانية مركبات فعالة هي (Camphor,Linalool, Cis-dihydroxycarvone، Broneal، Neral،Coumarin, Geranyl acetate Limonene)

المصادر

[1] يحيى ، توفيق الحاج. النباتات والطب البديل. الدار العربية للعلوم مطبعة المتوسط ، بيروت ، لبنان(2003).

[2] Diederichsen, A.Coriander. Promoting the conservation and use of under utilized and neglected crops. International plant genetic resources institutes. (1996).

[3] Lamparsky, D. and I. Klimes.. Heterocyclic trace Components in the essential oil of coriander. Perfum. Flav., 13 (5), 17-25(1988).

[4] Meyer, B. S ; Anderson, D. B. ; Bohning, R. H. and Fratianne, D. G.. Introduction to plant physiology. D. Van Nostrand company 450 west 33rd Street, New York, N. Y. 10001(1973).

[5] كذلك، محمد محمد. مقدمة في زراعة الخضر. منشأة المعارف / الاسكندرية / جمهورية مصر العربية(2001).

[6] Hurbut, C. S. and C. Klein. Soil Mineralogy، Jr. manual of Minerlogy, 19th Ed.، John Wiley and Sons. New York. (1977).

[7] Al-Zubaidi, A. and Pagel, H.. Content of different potassium forms in some Iraqi soils, Iraqi J. Agric. Sci. 14:214-220(1979).

[8] Ball. J.. Don't overlook role of potassium. A news and views. For Potash and Phosphat Institute of Canda (PPIC) (2004).

[9]الخـزاعي ، أسماء عبد الأمير بدن . . مقارنـة بين التغـذية النهـارية والليلية بالنتـروجين وتأثيرها على نمووأنتاجية القمح *Triticum aestivum* L. وطريقة الري بالرش . رسـالة ماجستير ، كلية التربية للعلوم الصرفة ، جامعة الأنبار ، العراق (2008).

[10] Agiza, A. H. ; El – Hinieidy , M.L.and Ibrahim,M.E.The determination of different fractions of phosphorus . Plant and Soil Bull. Fac. Agric. Cairo. Univ., 121(1960).

[11] SAS.SAS/STAT Users Guide for Personal Computer .Relase 7.0. SAS In Stiute Inc.Cary,NC.,USA. (SAS= Satistical Analysis System) (2004).

[12] وعدو ، مي صـالح حسين . . تأثير الكاينتين والمغنسيوم على النمو والأيض في بادرات نخلة التمر (صنف روثانا) . رسالة ماجستير ، كلية العلوم ، جامعة الملك سعود (1997).

[13] وصـــــفي ، عماد الدين .. منظمات النمو والأزهار وأسـتخدامها في الزراعة . المكتبة الأكاديمية ، مصر (1995).

[14] Agostino, I. B.;Joseph, J. K.Molecular mechanisms of Cytokinin action.Department of Biological Sciences, Laboratory for MolecularBiology,Unniversity of lllinois at Chicago,IL .USA 60607 359-36 (1999).

[15] Samsonova, Z. ;Kuklova, A.; Mazura, P.;Rotkova, G. ;Novak, O.and Brzobohaty, B. Natural Variation in The Cytokinin Metabolic Network in *Arabidopsis Thaliana* .Department ofMolecular Biology and Radiobiology ,University in Brno,Zemedelska.881-886(2012).

[16] الراوي ,أثير هاشم عبد المجيد رشيد . تأثير الرش باليوريا والسايتوكاينين ومستخلص عرق السوس في الصفات المورفولوجية والفسلجية والتشريحية لنبات الخس *Lactuca sativa* L. (الصنف المحلي) . رسالةماجستير/ كلية التربية للعلوم الصرفة/جامعة الأنبار/العراق(2010).

[17] الحلبي , حـــنين عصـام صـالح. تأثير السـايتوكاينين والسـماد المركب NPK في النموالمركبات الفعالة لنبات الحبة السوداء (Nigella sativa L.). رسالة ماجستير . كلية التربية ابن الهيثم . جامعة بغداد . العراق(2012) .

[18] Borowski,E. ;S.Michalek.The Effect of foliar Potassium salts and Urea in spinach on gas Exchange,Leaf yield and quality. Department of Plant Physiology, University of Life Sciences in Lublin.62(1):155-162 (2009) .

[19] الربيعـي، بهـاء الـدين مكـي فيـروز .استخدام معادلـة الرتبـة الاولـى فـي التنبـؤ بسلوكية تحرر البوتاسيوم في ترب وسط العراق .مجلة الانبار للعلوم الزراعية كلية الزراعة ،جامعة الانبار ،العدد 1 (2013) .

تقييم تراكيب وراثية من الرز الهوائي المزروع في مشاتل مختلفة

فوزي زياد عزو، عبد الكريم حايف كاظم، عبد الجليل رحيم عبود، محمد هادي حميد، اثير عبد الخالق اسماعيل، ثامر احمد سعود
مركز تكنولوجيا البذور/وزارة العلوم والتكنولوجيا
تاريخ تقديم البحث 2013/5/20 - تاريخ قبول البحث 2013/11/19

ABSTRACT

This study was carried out in the Tuwaitha research station/Seed Technology Center/Ministry of Science and Technology to assess 61 aerobic rice genotypes obtained from International Rice Research Institute (IRRI) in Philippines. The same genotypes were planted in 7 different environments in China and India during the agricultural season 2009. Additive Main Effect and Multiplicative Interaction Analysis (AMMI) was used for early flowering and grain yield (t/ha). The results showed that 49 genotypes superior in grain yield (t/ha) and 12 genotypes was early flowering and 10 genotypes excellence in high yield and early flowering.

الخلاصة

نفذت هذه الدراسة في محطة ابحاث التويثه/مركز تكنولوجيا البذور/وزارة العلوم والتكنولوجيا لتقييم 61 تركيب وراثي من الرز الهوائي مدخل من المعهد الدولي لابحاث الرز IRRI في الفلبين وزرعت نفس التراكيب الوراثية في 7 بيئات مختلفة ضمن دولتين هي الصين والهند خلال الموسم الزراعي 2009. استخدم تحليل التأثير التجميعي الرئيس والتداخلات المتعددة AMMI لصفتي التبكير في التزهير وحاصل الحبوب (طن/هكتار). اظهرت النتائج تفوق 49 تركيب وراثي بحاصل الحبوب (طن/هكتار) وتبكير 12 تركيب وراثي في التزهير، وامتازت 10 تراكيب وراثية بالحاصل العالي والتبكير في التزهير.

المقدمة

يعد الرز الهوائي من التضريبات الحديثة للرز حيث نجح الباحثون في الفلبين واندونيسيا وكولومبيا من استنباط اصناف من الرز الهوائي من خلال التهجين بين الرز الياباني والرز الهندي في منتصف الثمانينات من القرن الماضي [1]، في حين تمكن الباحثون الصينيون من استنباط اصناف من الرز الهوائي من خلال تهجين رز المناطق المرتفعة Upland مع رز المناطق المنخفضة Lowland [2 و 3] ويتميز هذ التضريب بالحاصل العالي الذي يصل من 4 – 6 (طن/هكتار) وتحمله للجفاف، كما يمتاز بنمو الجنين في ظروف هوائية حيث اشار [4] إلى ان 10 فعاليات ايضية تحدث في فترة الانبات كانت هوائية تتضمن عمل 1136 جين، في حين كانت هناك 13 فعالية ايضية لا هوائية شملت 730 جين من اصل 110 فعالية ايضية و9596 جين، وان عمل هذه الجينات الهوائية يتوقف بعدم وجود الهواء وعكس الحالة في جينات الفعاليات الايضية اللاهوائية. إن استخدام تحليل التأثير التجميعي الرئيس والتداخلات المتعددة AMMI هو طريقة حديثة في تحليل تباين تداخل التركيب الوراثي × البيئة ويعتمد بدرجة رئيسة على تحليل المكونات الرئيسة Principle Component Analysis (PCA) وهو مشابه لتحليل الانحدار لكنه يعطي وصفاً دقيقاً للتراكيب الوراثية أكثر من الانحدار [5].

توصل [6] إلى وجود فروق معنوية بين التراكيب الوراثية والبيئات فقط اما التداخل فلم يكن له تأثير معنوي وذلك باستخدام تحليل AMMI وقد تفوق تركيبين وراثيين من الرز طويل الحبة بالحاصل وكانا اكثر استقرار وتأقلم من اصل 6 تراكيب وراثية مزروعة في 4 مواقع في الولايات المتحدة الامريكية وعلى مدى 3 سنوات. استخدم [7] نموذجين لتحليل AMMI هما AMMI 1 و AMMI 2 لدراسة تداخل 6 تراكيب وراثية من الرز مزروعة في 15 بيئة في الهند، وتبين لهم أن مكونات التباين لكلا النموذجين كانت معنوية وتميزت 3 تراكيب وراثية بتطبع عالي للبيئات المختلفة. وجد فروق معنوية بين التراكيب الوراثية، مواقع، سنوات، تراكيب وراثي × مواقع، عند مستوى احتمال 0.01 في تجربة تضمنت 47 تركيب وراثي من الرز المزروع في 5 مواقع في الولايات المتحدة الامريكية والمزوعة على مدى 3 سنوات وتمكن من تحديد 3 تراكيب وراثية

متفوقة بالحاصل [8]. تمكن [9] من تحديد التركيب الوراثي الملائم لكافة المواقع والتراكيب المتحملة للجفاف من اصل 4 تراكيب وراثية من الرز المزروع في 4 مواقع في الهند وتحت 3 مستويات للري باستخدام تحليل AMMI. وجد [10] تأثير معنوي لمحتوى الحديد في بذور الرز للتراكيب الوراثية، البيئات وتداخل التركيب الوراثي × البيئة وتم تحديد التركيب الوراثي الذي يحتوي على أعلى نسبة من الحديد وافضل موقع في دراسة شملت 10 تراكيب وراثية من الرز المزروع في 8 بيئات في اندونيسيا وعلى مدى سنين.

يهدف هذا البحث إلى تقييم تراكيب وراثية من الرز الهوائي المزروع في مشاتل مختلفة في العالم وتحديد التراكيب الوراثية المبكرة في التزهير وذات حاصل حبوبي عالي.

المواد وطرائق العمل

تمت هذه الدراسة خلال الموسم الزراعي 2009 في محطة ابحاث التويثه التابعة لمركز تكنولوجيا البذور/ وزارة العلوم والتكنولوجيا. حيث زرعت بذور 61 تراكيب وراثي من الرز الهوائي المدخل من المعهد الدولي لابحاث الرز IRRI باعتماد طريقة الزراعة الجافة بتاريخ 2009/6/14 بواقع 4 خطوط لكل تركيب وراثي وبطول 3م للخط الواحد وفق مواصفات المعهد الدولي لابحاث الرز IRRI. سمدت التجربة بالسماد المركب NP 27:27 وبكمية 200 كغم/هكتار كدفعة أولى عند الزراعة ثم سمدت التجربة بسماد اليوريا (N 46%) وبكمية 120 كغم/هكتار كدفعة ثانية في مرحلة التفرعات. نفذت نفس التجربة في 7 بيئات خارج العراق شملت دولتين هما الهند والصين وكما مبين في جدول (1) إذ بلغ عدد الوحدات التجريبية 488 وحدة.

استخدم تصميم القطاعات العشوائية الكاملة RCBD. حللت النتائج احصائياً بواسطة البرنامج الاحصائي Cropstat 7 وباستخدام ايعاز Cross site analysis لتحليل AMMI وقورنت المعدلات عند مستوى احتمال 0.05 باستخدام اختبار أقل فرق معنوي LSD.

جدول-1: المواقع قيد الدراسة مع رموزها.

Code	Location	Code	Location
A	China-Kumming	G	India-Imphal, Manipur
D	India-Mawagam, Gujarat	H	India-Rewa
E	India-Ludhiana, Punjab	K	India-Allahabad District, U. P.
F	India-Kaul, Haryana	M	Iraq-Twatha

النتائج والمناقشة

تشير النتائج في الجدول (2) إلى وجود فروق معنوية عند مستوى احتمال 0.05 لكل من التراكيب الوراثية والبيئات ومكونات التداخل الرئيسة PCA لصفتي الفترة من الزراعة إلى 50% تزهير وحاصل الحبوب (طن/هكتار)، هذه النتائج تتفق مع ما اشار إليه [6 و 8] من وجود فروق معنوية بين البيئات والتراكيب الوراثية لصفة حاصل الحبوب (طن/هكتار)، واختلف مع ما وجده [6] من عدم وجود فروق معنوية لقيم PCA لصفة حاصل الحبوب (طن/هكتار). قد يعود سبب التأثير المعنوي للتراكيب الوراثية والبيئات في هذا البحث إلى اختلاف البيئات فيما بينها واختلاف المصادر الوراثية للتراكيب.

اظهرت النتائج في جدول (3) تبكير التركيب الوراثي 32 في التزهير إذ بلغ عدد الايام من الزراعة إلى 50% تزهير (73.87) يوم، ولم يختلف معنوياً عن التراكيب الوراثية 24، 52، 7، 2، 3، 4، 10، 1، 35، 13 و 28، في حين تأخر التركيب الوراثي 58 في التزهير، إذ بلغ عدد الايام من الزراعة إلى 50% تزهير (94.50) يوم، ولم يختلف معنوياً عن التراكيب 56، 42، 53، 12، 43، 48، 47، 18، 8، 20، 31، 44، 14، 45، 21، 16، 54، 11، 41، 26، 55، 9، 59، 39، 61، 57، 38، 50، 30، 60، 34، 15، 17، 33، 22، 36، 40 و 46. بلغ أعلى

حاصل للحبوب (5.90) طن/هكتار للتركيب الوراثي 10، ولم يختلف معنوياً عن التراكيب 2، 5، 15، 4، 3، 26، 18، 16، 23، 20، 25، 35، 21، 12، 24، 33، 34، 22، 14، 36، 6، 28، 45، 13، 38، 17، 1، 29، 51، 37، 47، 53، 27، 43، 19، 46، 55، 31، 7، 11، 54، 56، 41، 8، 57، 40، 30 و 44، بينما أدنى حاصل بلغ (3.02) طن/هكتار للتركيب الوراثي 61 ولم يختلف معنوياً عن التراكيب 52، 58، 50، 42، 39، 32، 59، 60، 48، 49، 9، 44، 30، 40، 57، 8، 41، 56، 54، 11، 7، 31، 55، 46، 19، 43، 27، 53، 47، 37، 51، 29، 1، 17، 38، 13 و 45. يستدل من هذه النتائج تميز 10 تراكيب وراثية بالحاصل العالي والتبكير في التزهير ولم تختلف معنوياً فيما بينها ولكلا الصفتين وهذه التراكيب 24، 2، 7، 3، 4، 10، 1، 35، 13، 28.

جدول- 2: تحليل AMMI لصفة الفترة من الزراعة إلى 50% تزهير وحاصل حبوب (طن/هكتار) لـ 61 تركيب وراثي من الرز الهوائي والمزروع في 8 بيئات للموسم 2009.

الفترة من الزراعة إلى 50% تزهير			
Source of variance	D. F.	S. S.	M. S.
Genotypes	60	10690.3	178.17*
Location	7	35808.7	5115.52*
Genotypes x Location	420	310931.0	
PCA 1	66	11694.0	177.18*
PCA 2	64	9025.0	141.01*
PCA 3	62	4388.4	70.78*
PCA 4	60	3214.0	53.56*
Genotypes x Environment Residual	168	2609.5	
Total	487	77429.9	
حاصل الحبوب (طن/هكتار)			
Genotypes	60	228.96	3.81*
Location	7	4010.98	572.99*
Genotypes x Location	420	1531.57	
PCA 1	66	654.30	9.91*
PCA 2	64	538.30	8.41*
PCA 3	62	173.44	2.79*
PCA 4	60	86.71	1.44*
Genotypes x Environment Residual	168	78.79	
Total	487	5771.52	

*معنوي عند مستوى احتمال 0.05

جدول-3: معدل الفترة من الزراعة إلى 50% التزهير (يوم) وحاصل الحبوب (طن/هكتار) لـ 61 تركيب وراثي من الرز الهوائي والمزروع في 8 بيئات مختلفة للموسم 2009.

رمز التراكيب الوراثية	50% تزهير	الحاصل (طن/هكتار)	رمز التراكيب الوراثية	50% تزهير	الحاصل (طن/هكتار)
1	81.37	4.75	32	73.87	3.54
2	78.50	5.80	33	86.25	4.98
3	79.37	5.48	34	87.75	4.96
4	80.12	5.52	35	82.25	5.07
5	85.50	5.63	36	86.25	4.92
6	84.75	4.92	37	85.00	4.62
7	78.50	4.30	38	88.37	4.81
8	91.00	4.21	39	88.75	3.47
9	89.37	3.95	40	86.12	4.16
10	81.25	5.90	41	89.37	4.22
11	89.62	4.27	42	93.62	3.47
12	93.12	5.01	43	93.00	4.42
13	82.37	4.86	44	90.12	4.03
14	90.00	4.94	45	90.00	4.87
15	86.87	5.58	46	86.12	4.39
16	89.87	5.25	47	91.12	4.60
17	86.62	4.79	48	92.37	3.79
18	91.12	5.39	49	82.50	3.81
19	84.50	4.42	50	88.25	3.21
20	90.75	5.14	51	85.12	4.64
21	90.00	5.03	52	77.37	3.14
22	86.25	4.95	53	93.25	4.53
23	83.50	5.22	54	89.75	4.27
24	74.62	4.99	55	89.37	4.38
25	84.87	5.14	56	94.00	4.24
26	89.37	5.48	57	88.50	4.16
27	84.25	4.49	58	94.50	3.19
28	82.37	4.90	59	89.00	3.68
29	84.25	4.65	60	87.75	3.78
30	88.25	4.12	61	88.75	3.02
31	90.25	4.33			
LSD 0.05	50% تزهير = 8.58 حاصل (طن/هكتار) = 1.90				

رمز البيئات	50% تزهير	الحاصل (طن/هكتار)	رمز البيئات	50% تزهير	الحاصل (طن/هكتار)
A	89.90	0.79	G	91.26	7.21
D	74.44	5.59	H	79.32	10.02
E	78.98	4.51	K	97.41	1.66
F	83.08	4.40	M	99.50	2.26
LSD 0.05	50% تزهير = 3.13 حاصل (طن/هكتار) = 0.69				

يلاحظ من نتائج البيئات تبكير البيئة D في التزهير إذ بلغ عدد الايام من الزراعة إلى 50% تزهير (74.44) يوم، أما البيئة M فتأخرت بالتزهير إذ بلغ عدد الايام من الزراعة إلى التزهير (99.50) يوم ولم تختلف معنوياً عن البيئة K. تفوقت البيئة H في حاصل الحبوب إذ بلغ الحاصل (10.02) طن/هكتار أما ادنى حاصل بلغ (0.79) طن/هكتار للبيئة A.

استخدم معدل حاصل الحبوب (طن/هكتار) وقيم PCA1 لحاصل البيئات الثمانية والتراكيب الوراثية العشرة المتميزة بالحاصل العالي والتبكير في التزهير في رسم ثنائي الشكل (شكل 1)، ويلاحظ من الشكل تباعد البيئات عن التراكيب الوراثية واتجاهها بعيد عن مركز الشكل، بينما يلاحظ تجمع التراكيب الوراثية في الوسط وهذا يطابق لما وجده [6 و 7 و 9] من تجمع التراكيب

الوراثية للداخل والبيئات للخارج، كما يؤكد هذا الشكل على ما اشار اليه [9] من ان التراكيب الوراثية المستقرة والملائمة للبيئات الهدف تكون أعلى خط معدل الحاصل، وكلما اقتربت التراكيب من هذا المحور دل ذلك على استقرارها، وعليه فان هذه التراكيب العشرة تمتاز باستقرارها في البيئات المختلفة اضافة لتفوقها بالحاصل والتبكير في التزهير، وهذا يدعم ما اشار إليه [11] من تفوق هذه التراكيب في البيئات المختلفة عدى البيئة M.

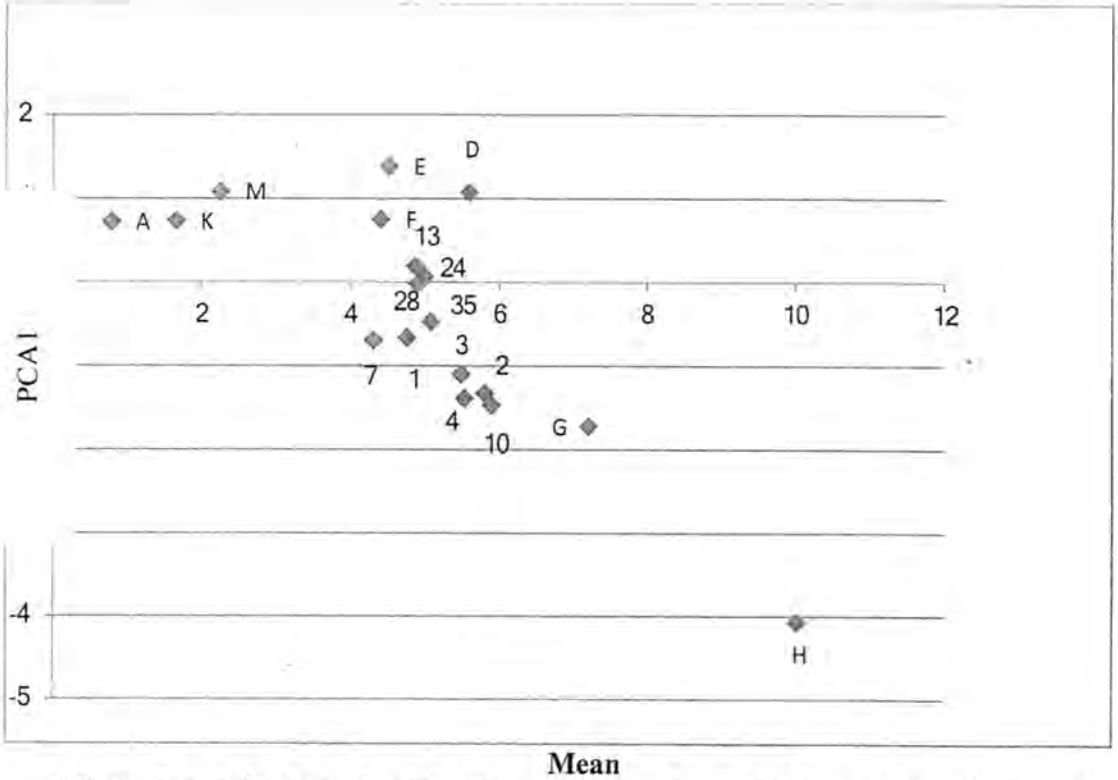

شكل-1: رسم ثنائي الشكل يبين العلاقة بين معدل حاصل الحبوب (طن/هكتار) وقيم PCA1 لـ 10 تراكيب وراثية من الرز الهوائي المبكرة في التزهير والمزروعة في 8 بيئات.

الاستنتاجات

نستنتج من هذه الدراسة تميز 10 تراكيب وراثية (24، 2، 7، 3، 4، 10، 1، 35، 13، 28) بالتبكير في التزهير والحاصل العالي واستقرارها في البيئات قيد الدراسة لذا نوصي بادخال هذه التراكيب الوراثية في برامج التربية للرز الهوائي لتحسين الاصناف المحلي من الرز.

REFERENCE

1. Bouman, B. A. M. Aerobic Rice: 10 Frequently Asked Questions. Available at [www.Ebookbrowse.com/aerobic-rice-faq-pdf-d26613507]. (2007)
2. Huaqi, W.; B. A. M. Bouman; D. Zhao; W. Changgui and P. F. Moya. Aerobic Rice in Northern China: Opportunities and Challenge. IRRI. Los Banos. Philippines. P.143 – 154. (2002)
3. Bouman, B. A. M.; R. M. Lampayan and T. P. Tuong. Water Management in Irrigated Rice: Coping with Water Scarcity. IRRI. Los Banos. Philippiners. P.54. (2007)

4. Narsai, R.; K. A. Howell; A. Carroll; A. Ivanova; A. H. Millar and J. Whelan. Defining Core Metabolic and Transcriptomic Responses to Oxygen Availability in Rice Embryos and Young Seedings. Plant Physiology, Vol.151, P.306 – 322. (2009)
5. Gauch, H. G. Statistical Analysis of Regional Yield Trails: AMMI Analysis for Factorial Designs. Elsevier. Amsterdam. P.520. (1992)
6. Samonte, S. O. PB; L. T. Wilson; A. M. McClung and J. C. Medley. Torgeting Cultivars onto Rice Crowing Environment Using AMMI and SREG GGE Biplot Analysis. Crop Science, Vol.45, P.2414 – 2424. (2005)
7. Mahalingam, L.; S. Mahendran; R. Chandra Babu and G. Atlin. AMMI Analysis for Stability of Grain Yield in Rice (*Oryza sativa* L.). International Journal of Botany, Vol.2, No.2, P.104 – 106. (2006)
8. Samonte, S. O. PB; L. T. Wilson; R. E. Tabien and A. M. McClung. Use of Gross Income as a Measure of Productivity in Rice Breeding. Canadian Journal of Plant Science, P.1015 – 1022. Available at [www.pubs.aic.ca] (2008)
9. Muthuramu, S.; S. Jebaraj and M. Gnanasekaram. AMMI Biplot Analysis for Drought Tolerance in Rice (*Oryza sativa* L.). Research journal of Agricultural Science, Vol.2, P.98 – 100. (2011)
10. Suwarto and Nasrullah. Analysis of Effect of Genotype x Environment Interaction on Rice Grains Iron Content in Indonesia Using Graphical GGE-Biplot Method. Electronic Journal of Plant Breeding, Vol.2, No.3, P.288 – 294. (2011)
11. Redona, E. D. Summary Report of the INGER Nurseries. IRRI. P.211 – 232. (2009)

الكشف عن انتاج الاغشية الحيويةBiofilmمن قبل بكتريا *Escherichia coli*ودراسة التأثيرالتثبيطي للعسل على نموها

رشا محمد ساجت العكيلي و نبأ عبد الخالق عثمان و استبرق محمد عاتي و رفل نعمان عباس
قسم علوم الحياة /كلية العلوم /الجامعة امستنصرية
تاريخ تقديم البحث 2013/4/4 - تاريخ قبول البحث 2014/2/23

ABSTRACT

Urine samples frome 70 patients with urinary tract inflammation were collected from urinary tract infection patients during the period ofJuly 2012 to November 2012. The bacterial diagnosis depending on cultural and microscopical characteristics of bacterial cell and biochemical tests were done using the API 20E system .The results diagnosis was30 isolates *Escherichia.coli*. This study aimed todetect the biofilmproductionby *E.coli* using Congo Red Agar (CRA).The results showed that 27 isolates were biofilm production and 3 isolates were non biofilm production and the inhibitory effect of honeyusing standardwell diffusion methodagainst*E. coli*.honey samples were tested using four concentrations100%andwere diluted with distilled water to get(75%, 50% and 25% w/v).The high inhibitory effect of concentration of the honey samples was (100% w/v)showed higher inhibition zone on *E.coli* isolated.Also study resistance isolates*E. Coli* toantimicrobial, The results showed that isolated *E.coli* were resistance to Ampicillinand Sensitivity to Gentamicin, Ciprofloxacin, Amoxicillin, Norfloxacin .

الخلاصة

جمعت 70 عينة ادرار من مرضى مصابين بالتهاب المجاري البولية للفترة من تموز 2012 الى كانون الاول 2012 . شخصت البكتريا اعتمادا على صفاتها الزرعية والمجهرية والفحوصات البايوكيميائية باستخدام نظام Api 20 E.وكانت نتيجة التشخيص30 عزلة *Escherichia.coli*.هدفت هذه الدراسة الكشف عن قابلية بكتريا *E.coli* على انتاجها للاغشية الحيوية biofilm باستخدام طريقة الزرع على وسط Congo Red Agar (CRA) ،اظهرت النتائج ان27 عزلة كانت منتجة للاغشية الحيوية و3 عزلات غير منتجة، وتم دراسة الدور التثبيطي للعسل على البكتيريا *E.coli* باستخدام طريقة الانتشار.تمت الدراسة بأستخدام اربعة تراكيز 100% و تخافيف من العسل مع الماء المقطر وهي 75%،50%،25% وقيست مناطق التثبيط ،و اظهر التركيز 100% مناطق تثبيط عالية لجميع العزلات البكتيرية. وتمت دراسة مقاومة عزلات*E. Coli* للمضادات الحيوية واظهرت النتائج ان العزلات كانت مقاومة لمضادAmpicillin وكانت حساسة لمضادGentamicin وCiprofloxacin وAmoxicillinوNorfloxacin.

المقدمة

الغشاء الحيوي هو تجمع الكائنات الحية الدقيقة مع إفرازاتها الخارج خلوية التي تلتصق على بعضها البعض أو على الأسطح . [2,1] هذه الخلايا الملتصقة بشكل متكرر هي جزء لا يتجزأ من أرضيةكثيفة من مواد بوليميريه خارج خلوية Extracelluar Polymeric Substance(EPS) والتي يشار إليهاأيضا باسم المخاطmucus[3]. تكون الخلايا البكتيريةالأغشية الحيوية في مجال واسع من العوامل الفسيولوجية وفي أنماط سكانية مختلفة وهذه تكون مميزة لمسارات التعبير عن التمثيل الغذائي واستجابات التوتروغيرها من الأنشطة المحددة البايولوجية جنبا إلى جنب[4]. لذا تكّون الميكروبات الأغشيةالحيوية رداً على العديد من العوامل المؤثرة والتي يكون تأثيرهاإمابصورةمتخصصة مثل التأثير على التنظيم الخلوي لمواقع ارتباط معينةأو يكون تأثيرها بصورة غير متخصصة كأن تكون على الأسطح[6,5] .هناك علاقةوثيقة بين قدرة البكتريا على تكوين الغشاء الحيويوقدرتها على إحداث المرض والتسبب بحدوث التهاب مزمن (Chronic inflammation)فالبكتريا المكونة للغشاء الحيوي لها قابلية اكبر على استعمار جسم المريض والإقامة فيه وتصبح اقل حساسية للعلاج بمضادات الحياة . وتنتج البكتريا بروتينات مرتبطة بالغشاء الحيوي في أثناءالإصابة("Biofilm – Associated Protiens"BAP)إن وجود هذه

البروتينات (BAP) يسهل تكوين الغشاء الحيوي المرتبط ببقاء الجرثومة مدةأطول في جسم المريض ويقوم الجسم المصاب بالاستجابة مناعيا لهذه البروتينات فيلاحظ وجود أجسامضادة لهذه البروتينات في مصل المريض [5] .

ذكر [8,7]أن العسل الذي هو نتاج طبيعي غير سام وغير مكلف يكون فعال في قتل الجراثيم من خلال عمله كأداة فعالة ضد مقاومة الجراثيم لمضادات الحيوية حيث يعمل كمضادات للجراثيم الموضعية وتفكيك الاغشية الحيوية التي تشكلها والسماح لمضادات الحيوية التي كانت تقاومها هذه البكتريا بالقضاء عليها. وقد استخدم[9]تراكيز مختلفة من العسل ودرس تأثيرها على*Escherichia coli* لمدة 24 ساعة ولاحظ عند تعرضها لعدة تراكيز من العسل ادى الى تثبيط نموها . درس[10] تأثير العسل على الاغشية الحيوية للزوائفالزنجارية لمدة 24 ساعة ولاحظ عند تعرضها لعدة تراكيز من العسل ادى الى انخفاض الاغشية الحيوية للزوائفالزنجارية وبالتالي القضاء عليها وبشكل نهائي وبمساعدة المضادات الحيوية التي كانت تقاومها هذه الاغشية في السابق.

المواد وطرائق العمل

جمع النماذج

جمعت 70 عينة ادرار من مرضى مصابين بالتهاب المجاري البولية Urinary tract infection (UTI)المراجعين لمستشفى بغداد التعليمي ومستشفى الكاظمية التعليمي في مدينة بغداد للفترة من تموز الى كانون الاول لسنة 2012،جمعت النماذج في اكواب معقمه.

زرع النماذج

تمت زراعة جميع العينات على اطباق حاوية وسط nutrient agar,blood agar بأستخدام swab معقمة وحضنت الاطباق بدرجة حرارة 37c° لمدة 24 ساعة .

عزل وتشخيص البكتريا

شخصت بكتريا *E.coli* مجهريا ومظهريا وبايوكيميائيا حسب[11] ،شخصت على وسط Eosin Meythlene Blue (EMB) ، وسط MacConky agar وشخصت باستخدام Api 20E kitللفحوصات البايوكيميائية وفحصت تحت المجهر بعد تصبيغها بصبغة كرام .

الكشف عن قدرة بكتريا*E.coli* على إنتاجالغشاء الحيوي Biofilm

باستخدام طريقة Congo Red Agar method (CRA)

استعملت الطريقة التي وصفها[12]للتحري عن قابلية بكتريا*E.coli*علىانتاجالغشاء الحيوي Biofilm،اخذت مستعمرة من *E.coli* بعمر 24 ساعة وزرعت على اطباق حاوية على وسطCongo Red Agar (CRA)المحضر(بأذابة 37غم منوسط نقيع القلب والدماغ السائل brain heart infusion broth (Oxoid, UK)،50 غم من السكروز sucrose،10 غم من الاكارagar No.1(Oxoid, UK)،8 غم من صبغة الكونكو CongoRed indicator(Oxoid,UK)في لتر من الماء المقطر وعقم بالموصدة بحرارة 121°م لمدة 15 دقيقة ،حضنت الاطباق بدرجة حرارة 37 °م لمدة 24 ساعة .

اختبار تاثير العسل على نمو بكتريا *E.coli* المنتجة للأغشية الحيوية Biofilm استخدام طريقة الانتشاربالحفر

The agar diffusion technique (well diffusion method)

تم بهذه الطريقة صب الوسط الزرعي مولرهنتون في أطباق بلاستيكيه معقمة وتسمى طريقة الانتشار Diffution methodولقحت بالعزلات البكتيرية و تم عمل اربعة حفر معلمة في الوسط الزرعي وأضيف إليها العسل من السوق المحلي حسب التراكيز (25 و 50 و 75 و 100) % بالاضافة الى حفرة خامسة كـ control(c) بأستخدام ماء مقطر ، واضيفت جميع تراكيز العسل في طبق واحد لكل عزلة ، وحضنت بدرجة حرارة 37°م ولمدة24 ساعة .قرأت النتائج بقياس مناطق التثبيط حول الحفر[9][13].

اختبارحساسيةبكتريا *E.coli* للمضاداتالحيوية :-

أجري اختبار حساسية المضادات الحيوية لجميع عزلات*E.coli*على وسط مولر – هنتون الصلب باعتماد طريقة Bauer and Kirbyوتسمى طريقة الانتشار Diffution method وحسب[14] ، بنقل مستعمرة بعمر 24 ساعة بواسطة swab معقمة الى (5) مليلتر من المحلول الفسيولوجي Normal saline ورجت جيدا بتحريكها بالمازج (Vortex) قورنت عكورة النمو مع عكورة محلول ثابت العكورة القياسي (0.5) .No، بعدها نقل (100) مايكروليتر من العالق البكتيري ثم نشر بوساطة مسحة قطنية (Swab) معقمة في وسط اكار مولر – هنتون وتركت الاطباق لتجف في درجة حرارة الغرفة لمدة (10 – 15) دقيقة، ومن ثم وضعت اقراص المضادات بملقط معقم الى الاطباق بواقع (4- 5) اقراص للطبق الواحد ، حضنت الاطباق بدرجة (37) م لمدة (24) ساعة . قرأت النتائج بقياس مناطق التثبيط حول الحفر[9]،واستخدم 5انواع من المضادات الحيوية وهي:-

AmpicillinA (25 µg),Amoxicillin AM (10 µg) ,GentamicinGEN (10 µg) ,,Ciprofloxacin CIP (10 µg)NorfloxacinNOR (10 µg)

النتائج والمناقشة

تم الحصول على30 عزلة من 70 عينة ادرار شخصت مبدئيا كبكتريا *E.coli*،و شخصت البكتريا اعتمادا على صفاتها الزرعية والمجهرية للخلايا البكتيرية حيث اعطت مظهرا Metallic green sheen على وسط (EMB) وبشكل مستعمرات دائرية ملساء بلون وردي على وسط MacConky agar وفحصت تحت المجهر وكانت سالبة لصبغة كرام.والفحوصات البايوكيميائية باستخدام نظام Api 20 E.عند زرع عزلات بكتيريا *E.coli*على وسط Congo Red Agar (CRA)وبعد حضن لمدة 24 ساعة وبدرجة حرارة 37°م،ظهرتباين في انتاج العزلات للاغشية الحيويةbiofilmوتتفق النتائج مع[14].لوحظ تلون المستعمرات بلون اسود blackcoloniesوبنسبة (90) % دلالة على انتاجية الاغشية الحيوية وظهرت مستعمرات بلون ورديcoloniespink اواحمر redcolonies دلالة على عدم انتاجيتها للاغشية الحيوية و بنسبة (10) % كما مبين في الجدول (1) والشكل(1)(A,B).

جدول-1:نتاج الاغشية الحيوية biofilm من *Escherichia coli* على وسطCongo Red Agar (CRA)

انتاج الاغشية الحيوية	عددالعزلات	النسبة المئوية(%)
منتجة للاغشية الحيوية Positive (black colonies)	27	(90)%
غير منتجة negativecolonies)(red or pink	3	(10)%

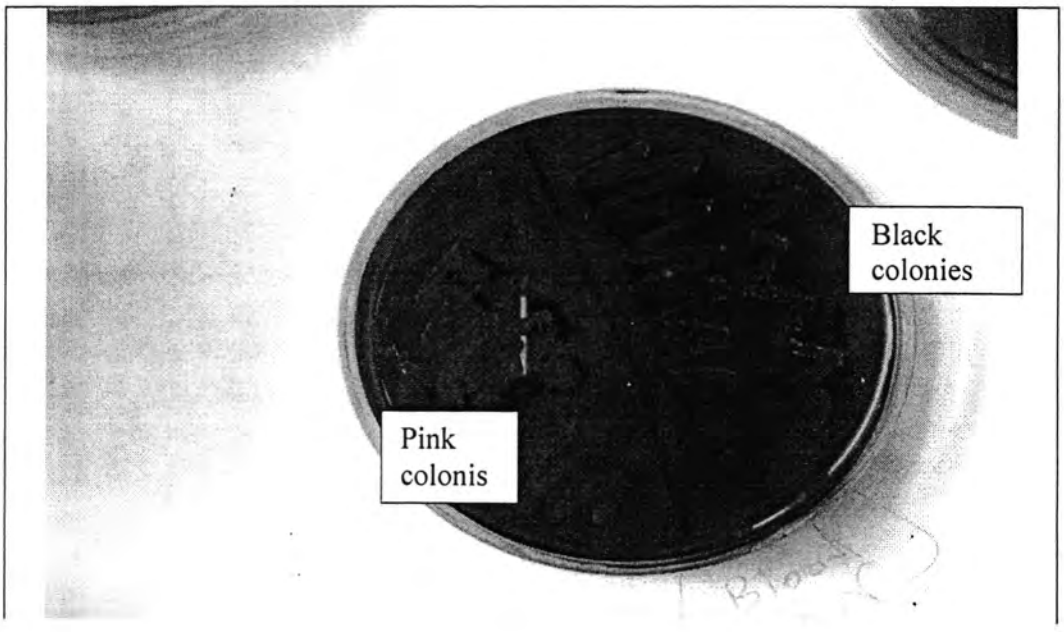

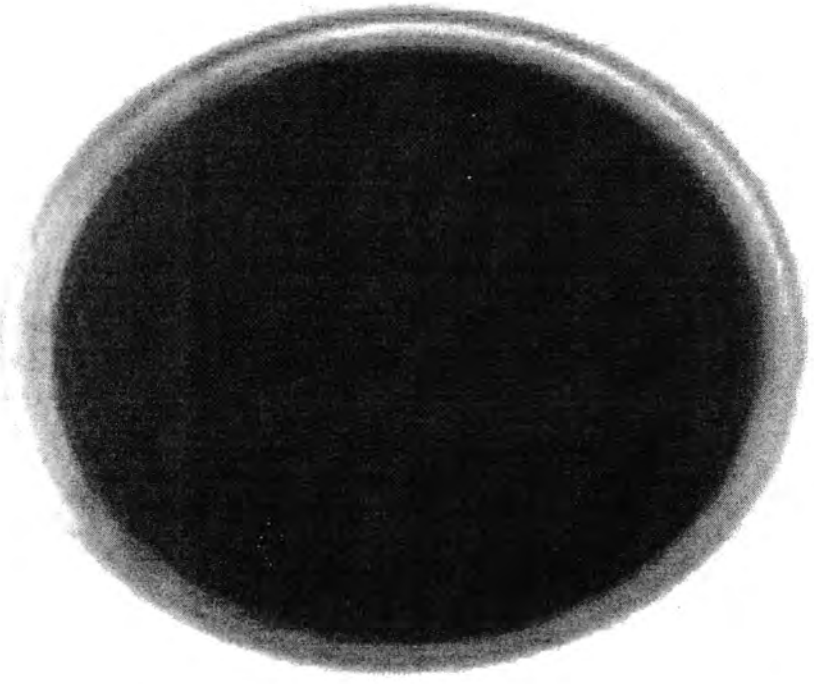

شكل-1:
A: العزلات المنتجة للاغشية الحيوية بلون أسود وغير منتجة بلون وردي على وسط Congo Red Agar (CRA)
B: صورة توضح السيطرة controlوسط Congo Red Agar (CRA)

اختبر التأثير التثبيطي للعسل اتجاه عزلات*E.coli*المنتجة للأغشية الحيوية Biofilm المعزولة محلياً والتي ضمت (30)عزلة وبتراكيز بلغت (25 ، 50 ، 75 و100)%، باستخدام طريقة الحفر بالاكار، اظهرت النتائج الاختبار الحساسية بكتريا *coli. E* للعسل خارج الجسم الحي invitro، وكانت جميع العزلات حساسة للعسل بتركيز100% اذ كان تركيزا مثبطا لنمو العزلات قيد الدراسة وتتفق نتائجنا مع ما ذكره (9). اما التراكيز الاخرى (75,50,25)%فقد تباينت حساسية بكتريا*E.coli*للعسل كما موضح في الجدول(2)،اعطت العزلة *E.coli 6b*اعلى قطرا تثبيطا لنموها وبلغ mm(36) وكانتاكثر حساسية لتركيز العسل 100%وكانت اقطار التثبيط عند التركيز**75%** و **50%**و**25%**هي (30) و(29) و(28)mm على التوالي كما موضح في الشكل (2)، اما العزلتان4 *E.coli*، *E.coli 2b*فقد اعطتا اقل قطرا تثبيطاوبلغ (10)mmعند التركيز25% اما اقطار التثبيط للعزلة4 *E.coli*بلغتعند التراكيز للعسل**100%** و**75%**و**50%** وكانت (33) و(26) و(25) mmعلى التواليكما موضح في الشكل (3)، اما العزلة*E.coli 2b* فبلغت اقطار التثبيط عند التراكيز للعسل **100%** و**75%** و**50%**وكانت (31) و(20) و(17) mm على التوالي كما موضح في الشكل (4).

جدول-2: اقطار تثبيط العزلات المحلية تحت تأثير تراكيز العسل المختلفة

Bacterial isolates	100%honey	75% honey	50% honey	25% honey
	Zone of inhibition (mm)			
E.coli 6b	36	30	29	28
E.coli 5	35	34	30	30
E. coli 8	35	30	28	25
E.coli 15	35	27	25	23
E.coli 12	35	31	30	25
E. coli 5b	34	30	30	30
E.coli 2	34	25	25	20
E.coli 22	34	30	20	14
E.coli 13	33	25	20	12
E.coli 4	33	26	25	10
E.coli 8	32	22	25	0
E.coli 6	32	25	25	15
E.coli24	32	27	20	20
E.coli 2b	31	20	17	10
E.coli 10b	31	25	22	0
E.coli 9	31	24	20	0
E.coli 1	30	30	28	25
E.coli 16	30	25	23	22
E.coli 26	30	30	20	15
E.coli 12b	30	30	24	0
E.coli 11	30	28	27	21
E.coli 7	20	19	15	12
E.coli 17	20	16	0	0
E.coli 30	20	19	0	0
E.coli 10	25	0	0	0
E.coli 14	15	0	0	0

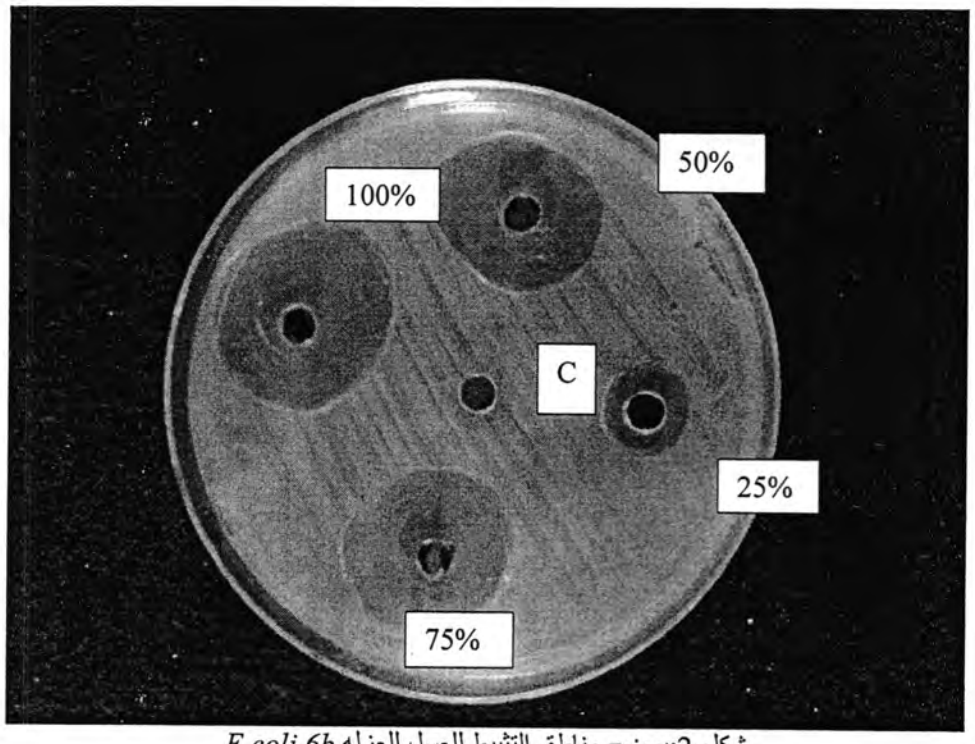

شكل-2:يوضح مناطق التثبيط للعسل للعزله *E.coli 6b*

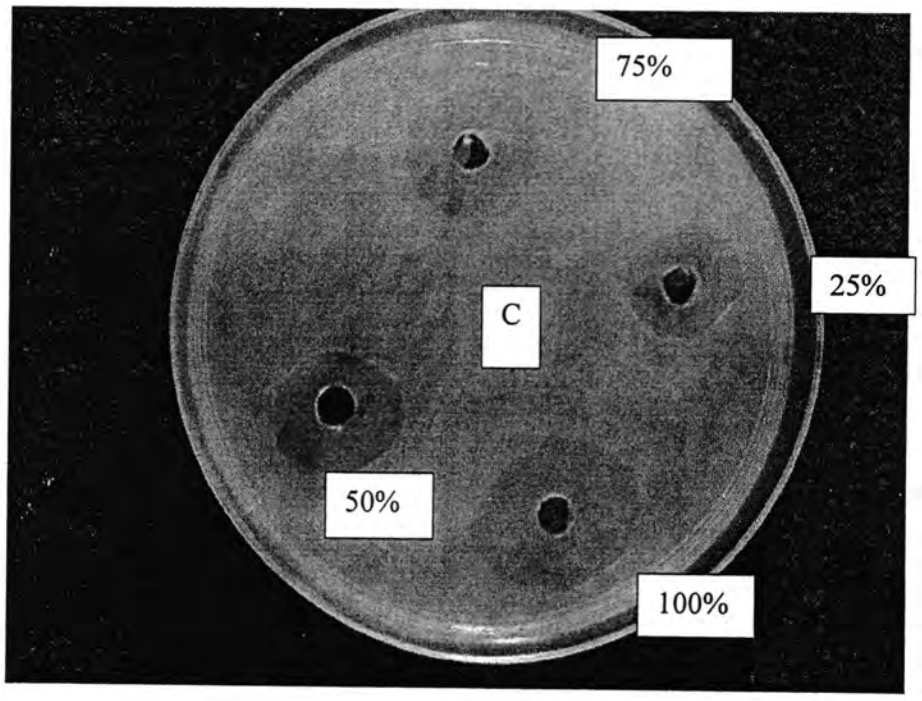

شكل-3:يوضح مناطق التثبيط للعسل للعزله *E.coli4*

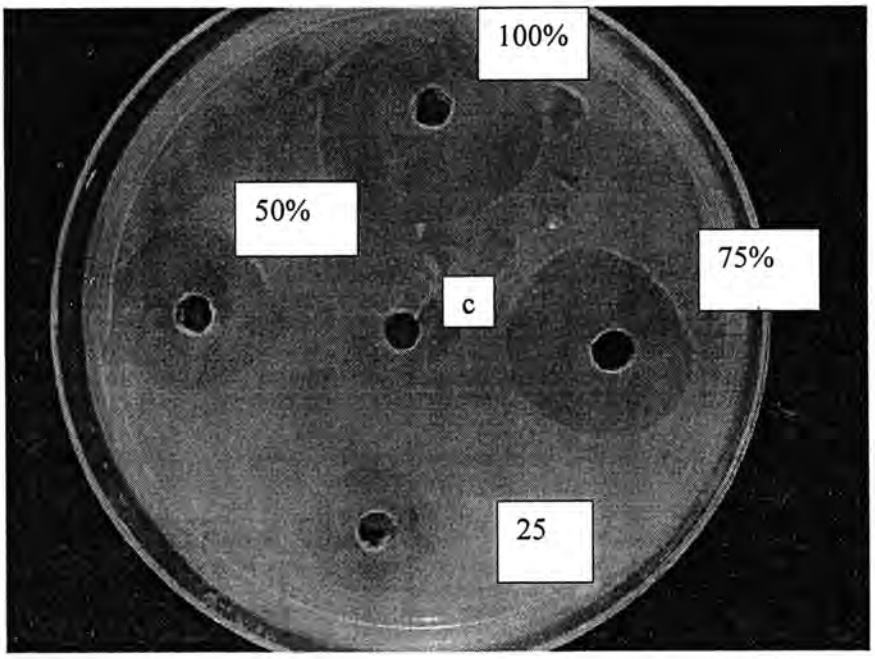

شكل-4:يوضح مناطق التثبيط للعسل للعزله *E.coli2b*

نستنتج من ذلك أنه كلما زاد تركيز العسل فأن ذلك يكون مؤثرا في نمو البكتريا من خلال تثبيط نموها،بشكل عام المكونات الرئيسية للعسل هي سكر الفواكه ، الكلوكوز والماء . غير أن العسل يحتوي على مجموعة واسعة من الفيتامينات والمعادن مثل (الكالسيوم ، البوتاسيوم ، الصوديوم ، الفسفور ، المنغنيز) كما أن العسل يكون غنياً أيضا بالأحماض الأمينية الأساسية . إضافة إلى مكونات أخرى من العسل تشمل الأصباغ مثل (carotion ، xanthophylls ، anthocyanin ، tannin) فضلا عن العديد من الأنزيمات القيمة مثل (catalase ، oxidase ، diastase ، amylase) حيث إن إنزيم أوكسيديز يحفز تكوين بيروكسيد الهيدروجين الذي يساعد على تحقيق الاستقرار في العسل ضد الميكروبات .بشكل عام تكون النسبة المؤية لهذه المكونات هي (18 – 20) % ماء و 54.1 سكريات و 21.7 معادن أما النسبة المتبقية فهي المكونات الأخرىَ من العسل اما السكر العادي يحتوي على السكروز فقط ولا يحتوي على المواد المذكوره اعلاه[15] .

ويمكن أن يكون العسل هو مضاد الحيوي الجديد كما يمكن أن يكون العسل سلاحاً فعالاً في كسر دفاعات الميكروبات ونموها إذ إن البكتريا تتضاعف بما يكفي لتشكيل الغشاء الحيوي وتكون أقل حساسية لمضادات الحيوية والمطهراتفي حين بين[16] .أن استخدام العسل ادى الى الحفاظ على مخزون مضادات الحيوية من خلال تأثير العسل المستخدم على نمو البكتريا وتشكيل الغشاء الحيوي في اصابات الجروح وذلك من خلال اختراق هذه المواد القاتلة للحياة في العسل للسلالات البكتيرية المسببة لالتهابات . وذكر[8]أن العسل الذي هو نتاج طبيعي غير سام وغير مكلف هو فعال في قتل الجرثومة من خلال عمله كأداة فعالة ضد مقاومة الجراثيم لمضادات الحيوية حيث يعمل كمضادات للجراثيم الموضعية وتفكيك الاغشية الحيوية التي تشكلها والسماح لمضادات الحيوية التي كانت تقاومها هذه البكتريا بالقضاء عليها. كما أن العسل لا تعرف له آثار جانبية ضارة . تأثير العسل المضاد للبكتريا وغيرها من الفوائدالصحية فأن العسل يعزز الجهاز المناعي عن طريق تنشيط الخلايا اللمفاوية وبالتالي تقليل الالتهابات وتنشيط نمو الخلايا بالنظر لاحتواء العسل على النسبة العاليه من السكريات تتراوح بين 70% - 80% من سكر الكلوكوز و سكر الفركتوز من جهة ووجود مادة البوتاسيوم من جهه ثانيه فان العسل يعمل على قتل الجراثيم ،حيث تعمل

السكريات ومادة البوتاسيوم على امتصاص الماء من اجسام هذه الجراثيم فتموت والسكر العادي لايحوي على هذه المواد[17]. يكمن النشاط المضاد البكتيري للعسل في خصائصه الكيمياءالفيزيائية مثلاً محتواه العالي من مخلفات السكر وارتفاع الضغط الازموزي واللزوجة وانخفاض الـ PH والمحتوى المائي (aw) وانخفاض المحتوى البروتيني وبيروكسيد الهيدروجين [18][19]، كذلك اوضح كل من[18][20]ان النشاط المضاد البكتيري الى المواد الكيميائية الخاصة في العسل، طبيعة هذه المواد وميكانيكية عملهاغيرمفهومة تماما حتى من خلال كروموتوغرافي الطبقة الرقيقةThin LayerChromatography(TLC) والترحيل الكهربائي بالهلام بولي اكرمايد Polyacrylamide Gel Electrophoresis (PAGE) وكروموتوغرافي High Performance Liquid Chromatography (HPLC). اما[22,21] فقد اثبتوا وجود الاحماض الدهنيةfatty acids والدهون lipids وانزيم الاميليز amylases وحامض ascorbic acids في العسل الطبيعي،واشارت تقاريرالى ان العسل يحتوي علىlysozyme ومعروف انه مضاد بكتيري جيد [23]. وان المضاد البكتيري flavonoid pinocembrin موجود في العسل [24] .

درست حساسية عزلات بكتريا *Escherichia coli*تجاه (5) مضاداتٍ حيويةلمعرفة نوع الاستجابة من خلال قياس قطر منطقة التثبيط ومقارنة النتائج مع ما ورد في[25]. وبذلك اظهرت النتائج تباينا واضحا في مدى استجابة العزلات قيد الدراسة للمضادات الحيوية المستعملة كما موضح في الشكل(5) والشكل(6) . وأشارت نتائج دراستنا الحالية الى ان العزلات ابدت مقاومةعالية للمضادampicillin وبنسبة (100)% على التوالي. وكانت حساسة لكل من المضاداتGentamicin وCiprofloxacin وamoxicillinوNorfloxacin بنسبة (40)(35)(30) (20)% وهذه النتائج تتفق مع[26] .

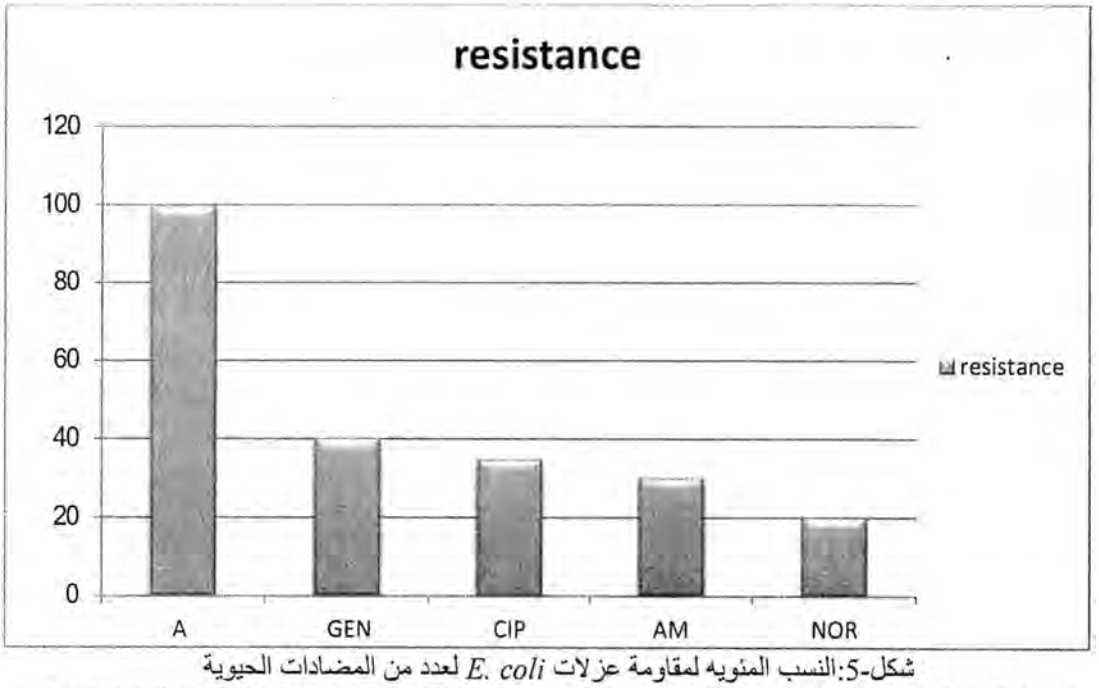

شكل-5:النسب المئويه لمقاومة عزلات *E. coli* لعدد من المضادات الحيوية

A : mpicillin,GEN:Gentamicin,CIP:Ciprofloxacin,AM:Amoxicillin,NOR:Norfloxacin

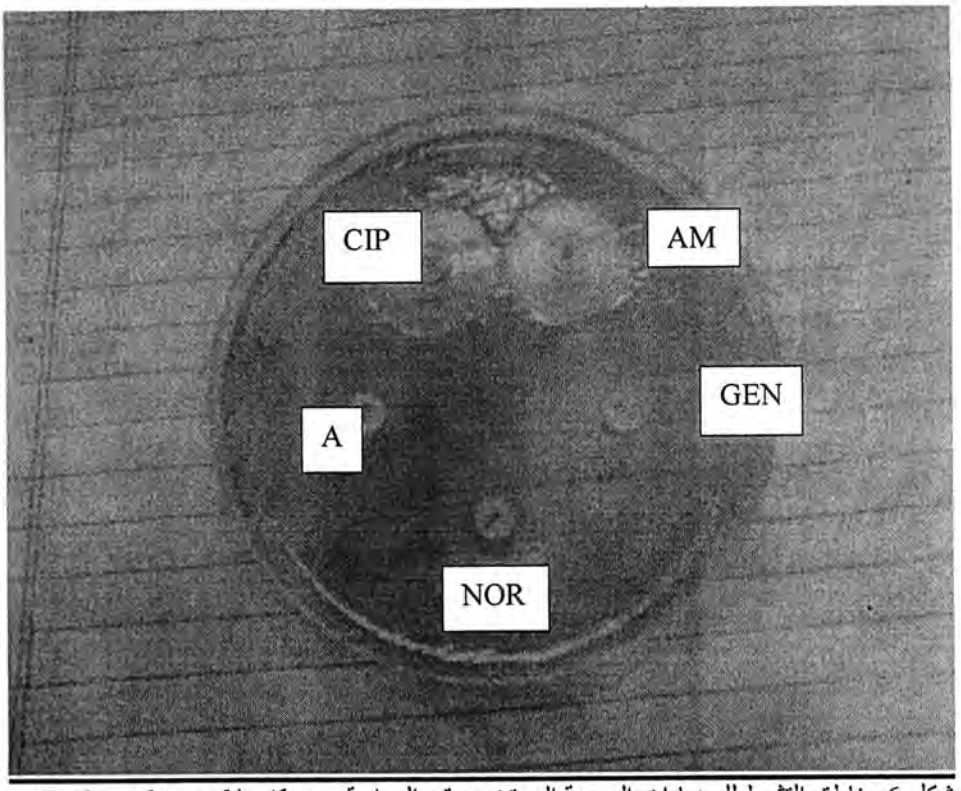

شكل-6:مناطق التثبيط للمضادات الحيوية المستخدمه قيد الدراسة ضد بكتريا*Escherichia coli*

المصادر

[1] Donlan , R. M. and Costerton , J. W.Biofilms : survival mechanisms of clinically relevant microorganisms. Clin .microbial .Rev.15 : 167 – 193.(2002)

[2] kimura,S. ; Tateda , K. ; Ishii ,Y. ; Horikawa ,M . ; Miyairi, S. ; Gotoh ,N . ; Ishiguro, M. and Yamaguchi , K. :*Pseudomonas aeruginosa* Las quorum Sensing autoinducer Suppresses growth and biofilm production in *Legionella species* . J .Microbiology . (155) . 1934 – 1939..(2009)

[3] Hall – Stoodley , L . ; Costerton , J.W. and Stoodley , P . : Bacterial boifilms : from the natural world to infections disease . Nat . Rev. microbial . 2(2) : 95 – 108.(2004)

[4] Philip S. S andMichael J. F .:Physioloical heterogeneity in bioflims . J. Nature Reviews Microbiology .6 :199-210.(2008)

[5] Karatan , E. and Watnick ,P.S, :Regulatory networks and materials that build and break bacterial biofilms . microbial .Mol .Biol .Rev . 73 (2) :310 - 47 .(2009).

[6] Hoffman , L.R. ; Argenio, D. A. , ; MacCoss , M. J. ; Zhang , Z. ; Jones , R.A. and Miller , S. I. : Aminoglycoside antibiotics induce bacterial biofilm formation .Nature 436 (7054) : 1171 – 5 .(2005)

[7] Cucarella , C . ; Tormo ,M. A. ; Ubed , C. ; Trotonda , M .P. ; Monzon , M. ; Peris , C. ; Amorena , B. ;Lasa , I . andPenades , J.R. : Role of biofilm – Associated protein Bap in the pathogensis of Bovin*Staphylococcusaureas* infect. Immun. 72 (4) : 2158 – 2177.(2004).

[8] Permissions , and Reprints . Effectiveness of honey on *Staphylococcusaureas* and *Pseudomonasaeruginosa*biofilm . J. otohns .doi :10 . 1016.(2009)

*[9]*Osho, Aand Bello, O.O.: Antimicrobial effect of honey produced by on some common human pathogens Apismellifera . ASIAN J. EXP. BIOL.vol 1 (4) : 875-880.(2010).

[10] Okhiria , O.A. ; Henriques , A.F.M. ; Burton , N.F. ; Peters, A. and Cooper , R.A.:Heney modulates biofilms of *Pseudomonasaeruginosa*atime and dose dependent manner . Journal of Apiproducat and Apimedical 1(1) 6 – 10 .(2009)

[11] Forbes, B.A. ;Sahm, D.F. and Weissfeld, A.S..Baily and Scott's .Diagnostic microbiology .12thed .Mosby Elsevire .p:371 – 378 .(2007)

[12] Freeman, D.J;Falkiner,F.R. andKeane, C.T. .:New method for detecting slime production by coagulase negative *Staphylococci.* J. Clin. Pathol., 42: 872-874.(1989).

[13] Adebolu, .T.T.. Effect of natural honey on local isolates of diarrheacausing bacteria in southwestern Nigeria . African Journal of Biotechnology Vol. 4 (10): 1172-1174.(2005)

[14] Murugan,S;Devi,P.U. and John,P.N.. Antimicrobial Susceptibility Pattern of Biofilm Producing *Escherichia coli* of Urinary Tract Infections. Current Research in Bacteriology, 4: 73-80.(2011)

[15] Sabine adamczyk ; Regina Lazaro ; Consuelo Perez arquillue ; pilarConchello and Antonio Herrera . (2005) .Evaluation of Residues of Essential Oil Components in Honey after Different Anti – VarroaTreatments.J. Agricultural and food Chemistry .53(26) . P.10085– 10090

[16] Patricia Merckoll; Tom YsteinJonassen ; Marie Elisabeth Vad ; Stig L. JeanssonandKjetil , K. Melby . (2009) Bacteria biofilm andhoney : A study of the effects of honey on planktonic and biofilm – embedded chronic wound bacteria , Scandinavian Journal of infections Diseases . 41(5) 341 – 347

[17] Adamczyk,S.;Lazaro,R.;Arquillue,C.P.; Conchello,P. and Herrera,A. .. Evaluation of Residues of Essential Oil Components in Honey after Different Anti – VarroaTreatments .J . Agricultural and food Chemistry .53 (26) : 10085 – 10090.(2005)

[18] ابو شاور، احمد (2003) . موسوعة تربية النحل ، الطبعة الاولى ، دار اسامة االنشر والتوزيع –عمان –الاردن .

[19] Bergman,A. ;Yanai, J. andWeiss, J. : Acceleration of wound healing by topical application of honey:An animal model.Am. J. Surg., 145: 374-376 .(1983)

[20] Oka, H.;Ihai, Y. and Kawamura, N. :Improvement of chemical analysis of antibiotics: Simultaneous analysis of 7 tetracyclines in honey. J. Chromatogr.,400: 253-261.(1987).

[21] Mohrig,W. and Messner, R. :Lysozymalsantibacteriellesagensimhonig und bienengift. ActaBiologicaMedicaGermanica, 21: 85-95.(1968).

[22] Bogdanov, S. :Characterisation of antibacterial substances in honey. LebensmittelWissenschaftundTechnologie, 17: 74-76.(1984).

[23] Bogdanov, S.: Determination of Pinocembrin in honey using HPLC. J.Apicul. Res., 28: 55-57.(1989).

[24] Mogessie, A. :The in vitro antibacterial activity of "Tazmar mar" honeyproduced by stingless bee. Ethopian J. of Health Dev. 8(1):109-117.(1994).

[25] CLSI . .Performance standerds for Antimicrobial Disks Susceptibility test . V.29 (3).(2009).

[26] AL-Alak , S.K. A. Molécular Study of Adherence Factors in UropathogenicEscherichia coliRelated toFluoroquinolones Resistance .MSC .Thesis . College of Science . University of Al-Mustansiriyah.

قياس مستويات الرادون في مادة الاسمنت بأستخدام كاشف الاثر النووي العضوي LR-115

دنيا فاضل طلب[1] ،امل ساجت صبر[2] ،ابراهيم كيطان قياض[3]
[1]الجامعة المستنصرية – كلية العلوم
[3،1]وزارة العلوم والتكنولوجيا – دائرة بحوث المواد
تاريخ تقديم البحث 2013/9/30 - تاريخ قبول البحث 2014/1/21

ABSTRACT

This research aims to determine the radon concentrations in different samples for cement material using the track detector LR-115. Where in the induction etching time and the relevant etching time were evaluated, 30 min and 100 min respectively, more over the etching track factors were calculated such as($V_B, V_T, V, \eta, \theta_c$)according to optimum etching conditions(normality 2.5 N and the temperature of etchant solution 60°C) .The obtained results were showed that the detector have efficiency above 50% towards alpha particles, furthermore it was found that the radon concentrations was varied between the local and exported samples.

Keywords:Detector,LR-115,radon gas, etching solution

الخلاصة

يهدف البحث الى تحديد تراكيز الرادون في عينات مختلفة من مادة الاسمنت بأستخدام كاشف الاثر LR-115،حيث تم تحديد الزمن التمهيدي للقشط (30 دقيقة)وزمن القشط المناسب (100دقيقة) كما تم حساب عوامل الاثر المقشوط ($\theta_c, V_B, V_T, V, \eta$) وفق ظروف القشط المثلى (عيارية 2.5Nودرجة حرارة المحلول القاشط 60°C) وقد تبين ان الكاشف يمتلك كفاءة اعلى من 50% تجاه جسيمات الفا كما اتضح من الدراسة ان تراكيز الرادون تتفاوت بين العينات المحلية والمستوردة.

المقدمة

إن الاهتمام بموضوع مخاطر غاز الرادون تزايد في السنوات الاخيرة حيث ان الجزء الاكبر من الخلفية الاشعاعية الطبيعية الواصلة للانسان تأتي من الرادون ووليداته وحسب التحديد الذي وضعته المنظمة الدولية العلمية لتأثير الاشعاع الذري (UNSCEAR) حيث بينت ان الرادون المتواجد في البيئة يشكل حوالي % 53 من تعرضات الانسان للاشعاع الطبيعي، [1,2].

غاز الرادون غاز عديم اللون،شديد السمية كما انه خامل كيميائيا وغير مشحون بشحنة كهربائية وهو غاز نشط اشعاعيا يتحلل تلقائيا وينتج وليدات مشعة تسمى نواتج الرادون (وليدات الرادون radon progeny)وتلتصق هذه النواتج بذرات الغبار الموجود في الجو حيث تدخل إلى جسم الإنسان أثناء التنفس. وهذه الجسيمات لها قابلية على الالتصاق بجدران الرئتين وعندما تتحلل إلى عناصر أخرى فإنها تسبب تأين الخلايا الحية نتيجة اطلاقها اشعاعات مؤينة (كونها باعثة لجسيمة الفا) مسببة سرطان الرئتين[3,4].

ينبعث غاز الرادون من الصخور ثم ينطلق من خلال التصدعات والشقوق الصخرية وعبر مسامات التربة لينتشر في الهواء عند سطح الأرض أو يتراكم في الأماكن المغلقة كالمنازل والمباني العامة. وتعد التربة الناتجة عن تعرية الصخور الجرانيتية والبركانية الحمضية مصدراً هاماً للرادون؛ لأنها تحتوي على معظم عناصر السلاسل الإشعاعية الطبيعية، ونظراً لكون الصخور والتربة هي المكونات الأولية والأساسية لمواد البناء مثل الأسمنت والخرسانة وأحجار البناء، فإن مواد البناء هذه يمكن أن تحتوي على نسب متفاوتة من العناصر المشعة كاليورانيوم والثوريوم، وبالتالي فهي تؤثر في تركيز غاز الرادون داخل المنازل وربما تمثل مصدرا مستمرا للرادون في المباني[5,6].

ونظرا لأهمية هذا الموضوع وخطورته فقد ظهرت عدة تقنيات للكشف وقياس النشاط الاشعاعي له وان من اكثر هذه التقنيات شيوعا واستخداما في الوقت الحاضر هي كواشف الاثر النووي للحالة الصلبة والمعروفة اختصارا (SSNTDs)والتي تعرف على انها مواد عازلة كهربائيا تتراوح مقاومتها النوعية بين (10^6-10^{20})ohm.cm حيث تتولد فيهامسارات ضيقة

لضرر الاشعاع تسمى الاثار المستترة latent tracks وذلك عند مرور الجسيمات المشحونة من خلالها[2,7].

الجانب النظري

1-اظهار الاثر :

ان مرور الجسيمات المؤينة خلال المواد العازلة يعمل على تكوين مسارات ضيقة من التلف بحدود Å(30-100)تسمى الاثار المستترة ويمكن ملاحظة هذه الاثار باستخدام المجهر الالكتروني النافذ TEM وبقوة تكبير عالية جدا ولكن طريقة الملاحظة تلك غير مناسبة لاسباب عدة منها ان المجهر الالكتروني يتطلب ان تكون العينات المراد فحصها على شكل شرائح رقيقة جدا مما يجعل هذه التقنية غير ممكنة للابحاث العلمية كما ان الاثار ليست مستقرة تماما عند ملاحظتها بالمجهر الالكتروني النافذ، ولذلك استخدمت تقنية القشط الكيميائي على نطاق واسع لتكبير الاثار المستترة والتي تلاحظ فيما بعد بالمجهر الالكتروني حيث تستخدم في تقنية القشط الكيميائي المحاليل الكيميائية لاظهار الاثر تسمى بالمحاليل القاشطة etchant solutions اذ تعمل هذه المحاليل على تحلل مناطق الضرر بسرعة اكبر بكثير من المناطق غير المتضررة ،حيث تختلف هذه المحاليل باختلاف نوع الكاشف من حيث كونه عضوي او لاعضوي فعلى سبيل المثال غالبا ماتستخدم المحاليل الهيدروكسيدية القلوية للفلزات في عملية القشط مثل هيدروكسيد الصوديوم وهيدروكسيد البوتاسيوم وهيدروكسيد الليثيوم اما في الكواشف اللاعضوية فغالبا ماتستخدم المحاليل الحامضية مثل المحلول المائي لحامض الهيدروفلوريك HF وهناك عدد من العوامل المؤثرة على عملية القشط الكيميائي هي[4,5,6].

ا- نوع وتركيب المحلول القاشط.
ب- زمن القشط.
ج- درجة حرارة المحلول القاشط.
د-تركيز المحلول القاشط.

2- خصائص كاشف الأثر النووي العضوي LR-115 :-

ان الصيغة الجزيئية العامة لكواشف نترات السيليلوز هي $(C_6H_8O_9N_2)$ وهذه الكواشف يدخل في تركيبها النيتروجين بالاضافة الى الكاربون والهيدروجين بنسب معينة ، حيث ان الكاشف LR-115 هو احد انواع كواشف نترات السيليلوز ذو كثافة ($1.48\ g/cm^3$) والمنتج من قبل شركتي kodakpathe France وDaicell Japan وهو على نوعين[8]:

LR-115 نوع I ذوسمك 6µm .
LR-115 نوعII ذوسمك12µm .

يتكون كاشف LR-115 عموما من طبقتين احدهما حساسة للاشعاع وهي طبقة نترات السيليلوز ذات اللون الاحمر الغامق وتستند على طبقة من البوليستر غير حساسة للاشعاع وان الجزء الحساس للاشعاع يكون مواجها لمصدر التشعيع اثناء عملية التشعيع .وبالامكان التعرف على الجزء الحساس من خلال خدش كلا الوجهين اذ ان الجزء غير الحساس لايتأثر بينما يتضح اثر الخدش بالجزء الحساس . ان كاشف LR-115 يعد حساسا للنيوترونات وجسيمات الفا وشظايا الانشطار وبدرجات متفاوتة كما انه يستخدم في قيا س مستويات الرادون ووليداته سواء في التربة او الهواء اوالماء[10,9].

الجانب العملي

1-عملية القشط الكيميائي ومشاهدة الاثار مجهريا:

تمت عملية القشط الكيميائي بأستخدام محلول هيدروكسيد الصوديوم NaOH ووفق المعادلة التالية[8].:

$$W=N*(V/1000)*Weq \quad .....(1)$$

حيث ان:

N – يمثل العيارية ، V – يمثل حجم الماء المقطر ، وانWeq- يمثل لوزن المكافئ لهيدروكسيد الصوديوم(40) .

تتم عملية القشط بتعليق الكاشف داخل محلول القشط ويتم اغلاق الدورق لمنع حصول عملية التبخر مما يؤثر على تركيز المحلول القاشط بعدها يوضع الدورق في حمام مائي يحتوي على محرار لقياس درجة حرارة المحلول وبعد كل فترة قشط يتم رفع الكاشف وغسله بالماء المقطر و تجفيفه و من ثم وزنه بالميزان الحساس (نوع الميزان المستخدم Mettler AE163).

في حساب كثافة الاثار وقياس اقطارها تم استخدام المجهر الضوئي نوع Olympus حيث يتكون من ثلاث عدسات الاولى عدسة شيئية ذات تكبير (50X) وعدستين عينيتين احدهما لقياس كثافة الاثار والاخرى لقياس قطر الاثر وكلاهما بقوة تكبير (10X) وبالتالي تكون محصلة قوة تكبير المجهر (500X).

2- تحديد الزمن المناسب للقشط والزمن التمهيدي للقشط:

يعرف الزمن المناسب للقشط:بأنه الفترة الممتدة من بداية القشط الى ان تصبح كثافة الاثار ثابتة حيث يبدأ الزمن المناسب للقشط واستمرار القشط بعد ذلك يؤدي الى تداخل الاثار وتناقصها،اما،الزمن التمهيدي للقشط فهو الزمن المحصور بين بداية القشط واول ظهور للاثار في الكاشف [9] .

3-حساب بعض متغيرات الاثر المقشوط:

أ- حساب معدل القشط العام V_B:

معدل القشط العام هو السرعة التي تقشط بها كمية المادة من السطح اثناء عملية القشط الكيميائي ويمكن حساب قيمتهامن المعادلة التالية[7]:

$$V_B=1/2A\rho\ (|\Delta M/\Delta t|\ ) \quad \ldots\ldots\ldots\ldots\ldots\ldots (2)$$

حيث ان ρ: تمثل كثافة الكاشف ($1.48\ g/cm^3$)

A : تمثل مساحة الكاشف ($1cm^2$)

$|\Delta M/\Delta t|$: تمثل ميل العلاقة البيانية بين كتلة الكاشف وزمن القشط

ب-قياس معدل القشط على طول الاثر V_T:

معدل القشط على طول الاثر هوسرعة تحلل مادة الكاشف على طول الاثر وتحسب من المعادلة التالية[10,9]:

$$V_T = V_B\left[(1+(\frac{V_D}{2V_B})^2)/\ (1-(\frac{V_D}{2V_B})^2)\right] \ldots\ldots\ldots\ldots (3)$$

V_D: تمثل معدل قشط الاثر وتحسب من $(\frac{\Delta D}{\Delta t})$ والتي تمثل ميل العلاقة البيانية بين قطر الاثر وزمن القشط

ت-قياس معدل القشط النسبي V:

معدل القشط هو النسبة بين سرعة قشط الاثر الى سرعة قشط سطح الكاشف وتحسب من المعادلة [11]:

$$V = \frac{V_T}{V_B} \ldots\ldots\ldots\ldots (4)$$

ث-حساب قيمة الزاوية الحرجة θ_C :

هي اقل زاوية يمكن عندها اظهار الاثر المستتر بالمحاليل القاشطة وتحسب من المعادلة][12:

$$\theta_C = \sin^{-1}\frac{V_B}{V_T} \ldots\ldots\ldots\ldots (5)$$

ج-إيجاد كفاءة المحلول القاشطη:

كفاءة المحلول هي نسبة عدد الاثار التي تم اظهارها بعملية القشط الكيميائي الى عدد مسارات التلف الاشعاعي المستتر عبر وحدة المساحة للسطح الاصلي للكاشف وتحسب كفاءة المحلول القاشط من المعادلة التالية[8]:

$$\eta = 1 - \sin\frac{V_B}{V_T} \dots\dots\dots (6)$$

حيث يوضح الجدول رقم (1) يوضح قيم عوامل الاثر المقشوط عند عيارية2.5Nودرجة حرارة $60\ ^{\circ}C$.

جدول- 1 : بعض عوامل الاثر المقشوط للكاشف

متغيرات الاثر المقشوط	الرمز	القيمة
معدل القشط العام	V_B	1.76
معدل القشط على طول الاثر	V_T	3.43
معدل القشط النسبي	V	1.94
الزاوية الحرجة	θ_c	30.87
كفاءة القشط	η	0.94

4- مناقشة قياسات تراكيز الرادون في مادة الاسمنت :

تم استخدام كاشف من نوع LR-115 لقياس تراكيز الرادون في عينات من مادة الاسمنت المحلي والمستورد حيث وضعت العينات داخل حاوية صغيرة كما موضحة بالشكل(1) بعد ان تم وزن العينة ثم وضع الكاشف فوقها (من جهة نترات السيللوز الحساسة للاشعاع) مع مراعاة وضع مرشح ورقي لمنع دخول جسيمات الفا الصادرة عن الثورون (Rn^{220})وبقيت لمدة ثلاثة اشهر متتالية والجدول رقم (2) يبين كثافات الاثار وتراكيز الرادون في عينات مختلفة من مادة الاسمنت .

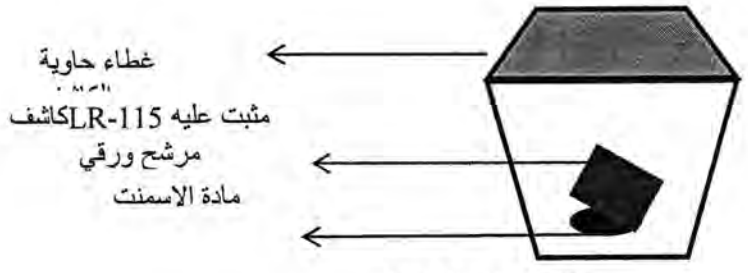

شكل-1: حاوية الكاشف

يتضح من الجدول رقم (2) ان تراكيز الرادون في مادة اسمنت الكوفة اقل منها في كل من مادتي اسمنت السليمانية والسمنت الايراني وقد يعود ذلك الى كون المادتين الاخيرتين من مناشئ تربة جبلية متشابهة في مستويات اليورانيوم.الشكل(2) يوضح آثار جسيمات الفا الصادرة من الرادون المسجلة على كاشف LR-115.

جدول- 2: كثافة الاثار وتراكيز الرادون في مادة الاسمنت المحلي والمستورد

رمز العينة	كثافة الاثار($track/mm^2$)	تراكيز الرادون(Bq/m^3)
KC1(كوفة)	81	14.51
KC2 (كوفة)	73	13,08
KC3(كوفة)	67	12.007
KC4(كوفة)	69	12.36
KC5(كوفة)	91	16.30
KC6(كوفة)	88	15.77
KC7 (كوفة)	83	14.87
KC8(كوفة)	75	13.44
KC9(كوفة)	77	13.79
KC10(كوفة)	72	12.90
KC11(كوفة)	83	14.87
KC12 (كوفة)	90	16.13
KC13(كوفة)	71	12.72
KC14(كوفة)	64	11.46
KC15(كوفة)	82	14.69
SC16(سليمانية)	102	18.27
SC17(سليمانية)	100	17.92
SC18(سليمانية)	89	15.94
SC19(سليمانية)	97	17.38
SC20(سليمانية)	105	18.81
SC21(سليمانية)	97	17.38
SC22(سليمانية)	95	17.02
SC23(سليمانية)	103	18.45
SC24(سليمانية)	101	18.10
SC25(سليمانية)	100	17.92
SC26(سليمانية)	97	17.38
SC27(سليمانية)	107	19.17
SC28(سليمانية)	99	17.74
SC29(سليمانية)	94	16.84
SC30(سليمانية)	91	16.30
SC31(سليمانية)	103	18.45
IC32(ايراني)	105	18,81
IC33(ايراني)	101	18.10
IC 34(ايراني)	99	17.74
IC35 (ايراني)	111	19.89
IC 36 (ايراني)	119	21.32
IC37(ايراني)	99	17.74
IC38(ايراني)	108	19.35
IC 39(ايراني)	101	18.10
IC 40 (ايراني)	106	18.99
IC 41 (ايراني)	98	17.56
IC 42 (ايراني)	106	18.99
IC 43 (ايراني)	103	18.45
IC 44 (ايراني)	98	17.56
IC 45 (ايراني)	102	18.27
IC 46 (ايراني)	113	20.25
IC 47 (ايراني)	116	20.78
IC 48 (ايراني)	105	18.81

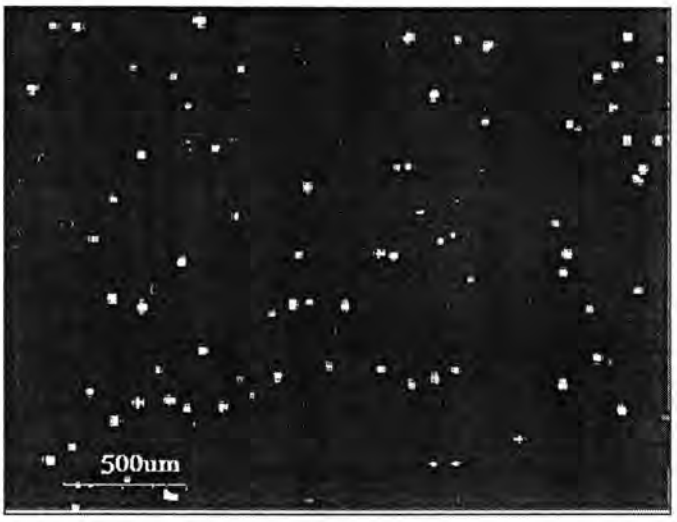

الشكل- 2 : آثارجسيمات الفا على كاشف LR-115

5- فحص النماذج القياسية (معايرة الكاشف):

اجريت عملية وضع النماذج القياسية في غرفة تحتوي على مصدر الراديوم المشع نشاطه الاشعاعي 5μci ابعاد هذه الحاوية $(95x\ 78x\ 62)cm^3$ حيث وضعت كواشف LR-115 داخل حاوية خاصة ووزعت بأبعاد متساوية عن المصدر المشع حيث تم تشعيع الكواشف لفترات زمنية مختلفة بدءا من اسبوع للكاشف الاول وانتهاءا بشهرين للكاشف الاخير وقد حسبت كثافة الاثار للعينات القياسية بعد اجراء عملية القشط الكيميائي لها وعد الاثار عليها ومن خلالها يمكننا حساب تراكيز الرادون للعينات الموضوعة لقياس تراكيز الرادون في عينات مادة الاسمنت ووفق المعادلة التالية:

$$\frac{\text{كثافة الاثار المجهولة } (T_X)}{\text{كثافة الاثار القياسية } (T_S)} = \frac{\text{التعرض للرادون للعينات مجهولة التراكيز } (E_X)}{\text{التعرض للرادون للعينات القياسية } (E_S)}$$

وبما اننا حسبنا ميل العلاقة البيانية بين كثافة الاثار والتعرض للرادون للنماذج القياسية كما موضح في الشكل (2) وقيمته(0.093) اي ان:

$$Slope = \frac{T_X}{E_X} \dots\dots\dots (7)$$

$$E_X = \frac{T_X}{slope} \dots\dots\dots\dots (8)$$

أما حساب تراكيز الرادون C_X فيكون من المعادلة:

$$C_X = \frac{E_X}{t} \dots\dots\dots\dots\dots (9)$$

حيث إن t تمثل الفترة الزمنية الكلية للنماذج المعرضة للرادون في مادة الاسمنت ومدتها شهرين متتاليين.

حيث يبين الشكل(3) العلاقة البيانية بين كثافة اثار النماذج القياسية T_Sومدة التعرض للرادون وهي علاقة خطية اي بقسمة قيم كثافات اثار النماذج المجهولة التراكيزT_X(الكواشف الموضوعة بتماس مع عينات الاسمنت) على قيمة الميل فسنحصل على تراكيز الرادون في عينات الاسمنت المنتخبة.

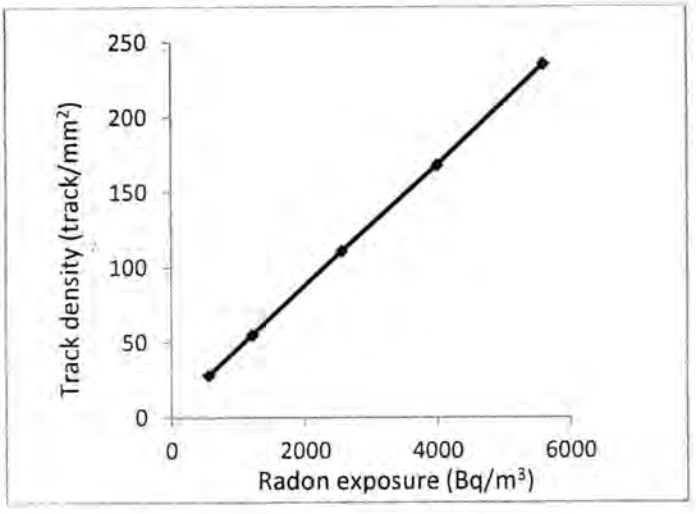

الشكل- 3 : العلاقة الخطية بين كثافة الاثار والتعرض للرادون

6- مناقشة تغير عوامل الاثر المقشوط مع زمن القشط:

تمت دراسة تغير كلا من كثافة الاثار واقطار الاثار بدلالة زمن القشط حيث تم قشط قسم من العينات بفترات زمنية مختلفة لتحديد الزمن التمهيدي للقشط وزمن القشط المناسب وحساب كل من قيم $V_B, V_T, V, \theta_C, \eta$

ا-تغير كثافة الآثار مع تغير زمن القشط:

إن الشكل (4) يمثل العلاقة بين كثافة الاثار مع زمن القشط ويتضح من الشكل ان الزمن المناسب للقشط (100min) حيث تسجل كثافة الاثار اعلى نسبة لها وبعد هذا الزمن تبدأ كثافة الاثار بالتناقص تدريجيا حيث ان الزمن الذي تبدأ فيه الاثار بالظهور هو 30min وهو الزمن التمهيدي للقشط.

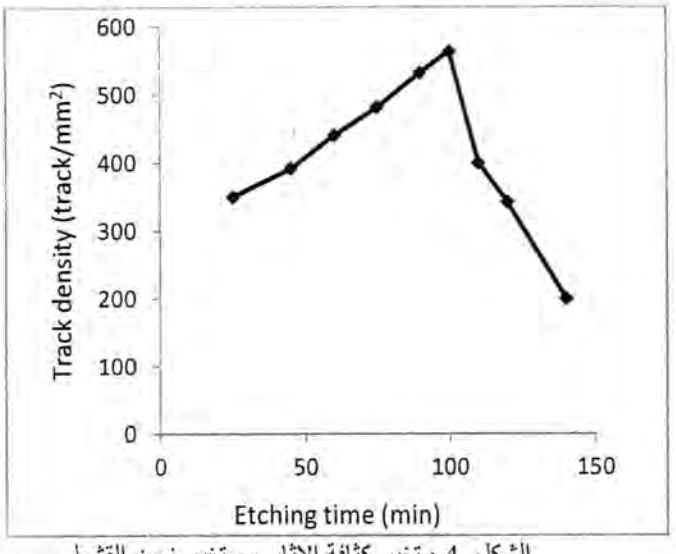

الشكل 4 : تغير كثافة الاثار مع تغير زمن القشط

ب- تغير وزن الكاشف مع زمن القشط:

يلاحظ من الشكل (5) ان وزن الكاشف يقل تدريجيا مع زيادة زمن القشط وهذا يعود الى ازالة سمك المنطقة المتضررة (h)بالاشعاع بفعل المحلول القاشط بسرعة كبيرة مع تزايد زمن القشط وذلك وفق العلاقة:[9].

$$D=2V_B.t=2h \quad \ldots\ldots\ldots\ldots(10)$$

حيث ان:

D: يمثل قطر الاثر المقشوط ، h :يمثل سمك الطبقة المزالة من مادة الكاشف بعد القشط

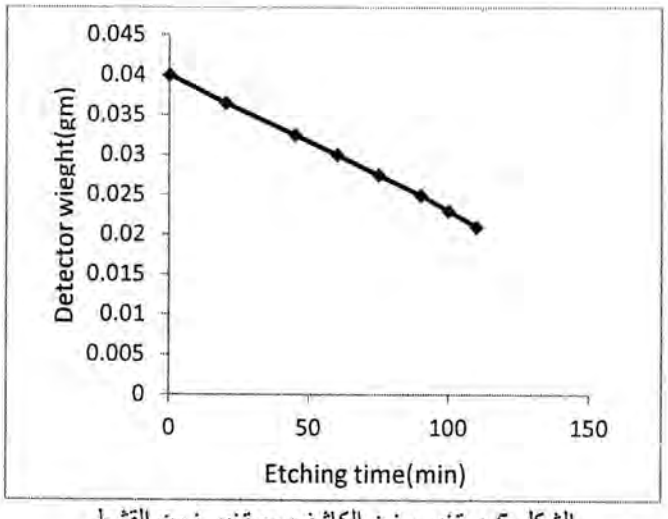

الشكل 5 : تغير وزن الكاشف مع تغير زمن القشط

ت-تغير أقطارالآثار مع تغير زمن القشط:

عند البدء بعملية القشط يلاحظ ان اقطار الاثار تزداد زيادة تدريجية مع زيادة زمن القشط وان الاستمرار بعملية القشط يجعل الاقطار تكبر كثيرا ويحدث تداخل كبير جدا بينها مما يسبب عدم امكانية رؤية الاثار وصعوبة قياس اقطارها والشكل (6) يوضح العلاقة بين زمن القشط واقطار الاثار .

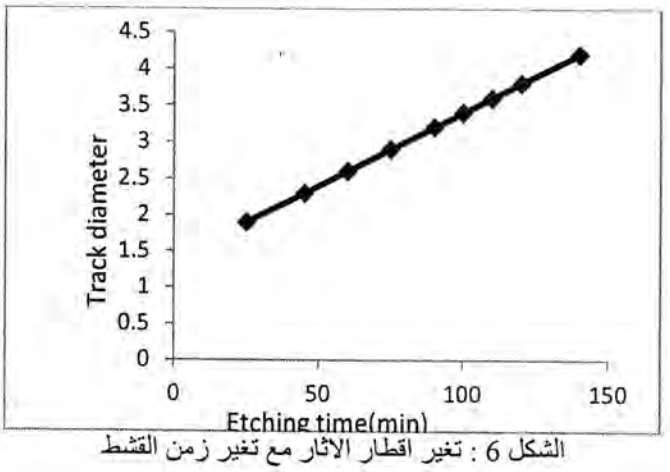

الشكل 6 : تغير اقطار الاثار مع تغير زمن القشط

الاستنتاجات

1- ان زمن القشط التمهيدي لكاشف LR-115 هو 30 دقيقة والزمن المناسب للقشط هو 100دقيقة عند ظروف قشط مثلى (عيارية 2.5N ودرجة حرارة المحلول 60°C).
2- يتضح من خلال الدراسة ان تراكيز الرادون مرتفعة في مادة الاسمنت الايراني اكثر من العينات المحلية

المصادر

[1] Kenawy,M.A.,Sayyah,T.A.,Ahmed MorsyA., HegazyT. M. and Said A.F.,(2004),Measurement of Radon Concentration Inside Uranium Exploration Mines Egypt UsingSSNTDS"VII Radiation Physics and Protection Conference, Ismailia-Egypt,November27-30.

[2] Yip C.W.Y., Nikezic D., Ho J.P.Y., Yu K.N.,(2006),ChemicalEtching Characteristics for Cellulose Nitrate,Materials Chemistry and Physics,Vol.95,PP. 307–312.

[3] Jelle,B. P.,(2012), Development of model for radon concentrations in indoor air , Science Total Environment, Vol.416, PP.343-350.

[4] Singh,B.P.,Pandit,B.,Bhardwaj V.,(2010),Study of radium and radon exhalation rate in some solid samples using SSNTDS, India Journal pure and applied physics ,Vol.48,pp.493-495

[5] Veloso B., Nogueira J.R., and Cardoso M.F.,(2012), Lung cancer and indoor radon exposure in the north Portugal , Cancer epidemiology, Vol.36 PP.(27-32).

[6] Varshney R.,MahurA.K.,andSonkawade R.G.,(2010) Evalution and analysis of Ra-226 ,Th-232,K-40 and radon exhalation rate in various grey cement , Indian Journal of Applied Physics,Vol.48,PP.473-477.

[7] Ho J.P.Y., Yip C.W.Y., Nikezic1 D., Yu K.N.,(2003) ,Differentiation Between Tracks and Damages in SSNTD Under the Atomic Force Microscope "Radiation Measurements" Vol. 36 ,PP. 155 –159.

[8] Dragoslav Nikezi and Carmen Baixeras,(1996) ,Radon, Radon Progeny and Equilibrium Factor Determination Using an LR115 Detector ,Radiation Measurements,Vol. 26, No. 2, PP. 203-213.

[9] Durrani S.A., Bull P.B., (1987), Nuclear Track Detection Principles Methods and Applications, University of Birmingham, U.K., PP.27-35.

[10] Catalug of Kodak pathe Company, (1986), France.

[11] Arias H., Palacios D., Sajó-Bohus L., Viloria T. , (2005), Alternative Procedure for LR- 115 Chemical Etching and Alpha Tracks Counting, Radiation Measurements,Vol.40,No. 2–6, PP.357-362 .

[12] Asaad H. Ismail, (2009), Determination of Critical Angle for Track Revelation for Different CR-39 Nuclear Track Detector Materials, J.ZankoySulaimani Vol.12,No.1,PP 109-118,part A.

دراسة تأثير العوامل الجوية على راحة الإنسان في مدينة كركوك

جودت هدايت محمد أحمد
جامعة كركوك – كلية العلوم – قسم الفيزياء
تاريخ تقديم البحث 2013/10/3 - تاريخ قبول البحث 2014/3/16

ABSTRACT

The study effect of atmospheric parameters on the comfort of the human consider one of the most important studies in atmospheric science, such different atmospheric factors affect on the comfort or discomfort of human as well as affect on human health and his ability on work.

This research aims to explain the relationship between atmospheric parameters represented by (Temperature, Relative Humidity and Wind Speed) and the comfort of human in the city of Kirkuk by using data from Iraqi General for meteorology and seismologic observation for period ranged (1971 to 2007), in addition to applying equation of Temperature – Humidity Index (THI) and equation of Wind Chill Index (K).

The results appears that the months of Summer season (June, July, August) are discomfort months for human because the increasing of temperature, howeve through the use of heating devices and wear heavy , and the months of Winter season (December , January , February) are also discomfort months for human because the decreasing of temperature , however through the use of air conditioning to avoid the high temperature, while the months of Spring season (March , April , May) and the months of Autumn season (September , October , November) are variable between comfort and discomfort for human .

الخلاصة

تُعد دراسة تأثير العوامل الجوية على راحة الإنسان من إحدى الدراسات المهمة في مجال علوم الجو ، إذ تؤثر عناصر الجو المختلفة في شعور الإنسان بالراحة أو الضيق وبالتالي تؤثر في صحة الإنسان وقدرته على العمل . يهدف هذا البحث إلى توضيح العلاقة بين العوامل الجوية المتمثلة بكل من (درجة الحرارة ، الرطوبة النسبية ، سرعة الرياح) وراحة الإنسان في مدينة كركوك وذلك من خلال الإستعانة ببيانات الهيئة العامة للأنواء الجوية العراقية والرصد الزلزالي للفترة الممتدة من (1971–2007) إضافة إلى تطبيق معادلة دليل درجة الحرارة – الرطوبة Temperature – Humidity Index (THI) ومعادلة دليل تبريد الرياح (Wind Chill Index K).

لقد أظهرت النتائج بأن أشهر فصل الصيف (حزيران ، تموز ، آب) تكون فيها الأجواء غير ملائمة للراحة وذلك بسبب الإرتفاع في درجات الحرارة ، إلا من خلال إستخدام وسائل التدفئة وإرتداء الملابس الثقيلة ، كما أن أشهر فصل الشتاء (كانون الأول ، كانون الثاني ، شباط) تكون فيها الأجواء غير ملائمة للراحة أيضا وذلك بسبب الإنخفاض في درجات الحرارة ، إلا من خلال إستخدام وسائل التكييف لتفادي إرتفاع درجة الحرارة ، بينما تتباين أجواء الراحة ما بين مريحة وغير مريحة في أشهر فصل الربيع (أذار ، نيسان ، مايس) ، وأشهر فصل الخريف (أيلول ، تشرين الأول ، تشرين الثاني) .

المقدمة

تتباين العوامل الجوية في العراق من مكان إلى آخر ومن فصل إلى آخر بل حتى ضمن الفصل الواحد مما جعل منه مناخا يتميز بالتذبذب وعدم الثبات في كل مناطق البلد ونتيجة لذلك فإن شعور الإنسان بالراحة المثالية يتباين أيضا وفقا لتباين العوامل الجوية والتي هي الأساس في شعور الإنسان بالراحة أو عدمها [**1**].

وعليه جاء هذا البحث ليبين تأثير العوامل الجوية والمتمثلة بكل من (**درجة الحرارة** ، **الرطوبة النسبية** ، **سرعة الرياح**) وذلك للعلاقة القوية بين هذه العوامل وإستجابة الجسم البشري وبالتالي توضيح الدور الذي تلعبه هذه العوامل في تحديد ملائمة الجو للناس أو عدمه .

الجانب النظري :

إن العوامل التي تؤثر في شعور الإنسان بالراحة والضيق مختلفة والوسيلة التي يمكن استخدامها لقياس الشعور بالراحة مختلفة أيضا ، والمعروف ان الإنسان يشعر بالراحة في ظل ظروف جوية معينة إذا كانت تلك الظروف تتناسب مع درجة حرارة جسمه وهي (37 درجة مئوية) فالإنسان يعيش في وسط يتبادل معه الطاقة بمختلف الوسائل ، والجسم يحاول دائما أن يولد طاقة داخلية عن طريق تحويل الغذاء إلى طاقة وعن طريق الحركة ليتناسب مع التقلبات الجوية إما إذا ما فاقت التقلبات المناخية قدرة الجسم على التعادل معها فان الإنسان يبدأ في الشعور بالضيق والإنزعاج واذا تكرر الأمر كثيرا فقد يصاب بضربة الشمس إذا كان الجو حارا أوالتجمد إذا بلغت درجة الحرارة حدا متدنيا من الانخفاض وأهم وسائل تبادل الطاقة بين الإنسان والجو هي الإشعاع والحمل والتوصيل [2].

لا يشعر الإنسان بدرجة الحرارة التي تسجلها محارير الحرارة العادية والمجردة بل أن شعوره بها يقترن بالرطوبة بالجو وبسرعة الرياح فإذا كان الإنسان يستطيع أن يتحمل ارتفاع درجة الحرارة إلى مدى معين فان قوة احتماله تقل كثيرا إذا اقترن ارتفاع درجة الحرارة بارتفاع مماثل في الرطوبة النسبية كما يتضاعف تأثيره كثيرا بانخفاض درجة الحرارة في المناطق الباردة إذا اقترن برياح سريعة [3].

يمكن تعريف الراحة الفسيولوجية أو الراحة الحرارية كما يعبر عنها أحيانا بكونها (الظروف التي تكون فيها الأجهزة المسؤولة عن تنظيم حرارة الجسم عند أدنى مستوى من الفعالية وتحصل هذه الحالة عندما يتمكن الجسم من فقدان كمية من الحرارة إلى المحيط الخارجي مساوية لتلك الكمية المتولدة من الفعاليات الحيوية بحيث تحافظ على درجة الحرارة ثابتة) [4].

لقد طوّر بعض علماء المناخ مقاييس (معايير ، معادلات) خاصة لقياس مدى تضايق الإنسان من الطقس لعل من أبرزها ، معادلة دليل درجة الحرارة – الرطوبة Temperature – Humidity Index (**THI**) ، ومعادلة دليل تبريد الرياح (**K**) Wind Chill Index ، وفيما يأتي شرح موجز لكل منهما .

1- معادلة دليل درجة الحرارة – الرطوبة Temperature – Humidity Index (**THI**)

ويعتبر هذا الدليل معياراً مناسباً لوصف إحساس الناس بالجو الحار ، من سمات هذا القانون انه استخدم عنصرين في التعبير عن راحة الإنسان وهما الحرارة والرطوبة ، بحيث يوضح لنا الدليل أن في حالة ارتفاع الرطوبة يشعر الإنسان بان درجة الحرارة هي أعلى من الحرارة المسجلة ، لتشبع الجو بالرطوبة مما يؤدي إلى توقف عملية التبخر من الجسم [5].

لم يأخذ الدليل بنظر الاعتبار تأثير الإشعاع الشمسي وسرعة الرياح ، وبعبارة أخرى أن الشعور بالراحة في درجة حرارة ورطوبة معينة يختلف تماماً مع اختلاف سرعة الرياح في موقع ما ، أي أن الرياح في سرعتها المختلفة تقلل أو تزيد من الشعور بتأثير الحرارة والرطوبة معاً ، أن ابسط دليل على ذلك هو أن العراقيين عموماً يميلون إلى الاكتفاء بالمراوح في شهر نيسان ، ولكنهم لا يكتفون بها مع تزايد درجات الحرارة في اشهر الصيف بل يدعمونها باستخدام مبردات الهواء أو المكيفات وهذا يفسر لنا أن الشعور بالحر يرتفع عند زيادة حركة الهواء داخل الغرف ما لم يكن مضموناً بنوع أخر من تكييف الهواء [5].

إن الصيغة العامة لمعادلة دليل درجة الحرارة – الرطوبة (THI) تعطى بالعلاقة الآتية :[6].

$$THI = T - 0.55 \times (1 - 0.01 \times Rh) \times (T - 14) \ldots (1)$$

حيث أن :

THI: دليل الحرارة – الرطوبة .

T: درجة حرارة الهواء (درجة مئوية) .

Rh: الرطوبة النسبية (%) .

إن المعادلة رقم (1) يمكن تفسيرها على أساس ناتج دليل درجة الحرارة – الرطوبة (**THI**) ، والجدول (1) يوضح مراتب وأصناف الراحة ورموزها المستخدمة حسب المعادلة رقم (1) [5].

جدول-1: مراتب وأصناف الراحة ورموزها المستخدمة على أساس ناتج دليل درجة الحرارة – الرطوبةTHI 5

مرتبة الراحة	الصنف	الرمز	THI
غير المريحة الباردة	شديد البرودة	C-	11.9 فأقل
	الأكثر برودة	C*	14-12
	البارد	C	14.9-14.1
المثالية	المثالي	P	16-15
	المثالي	P*	18-16.1
	المثالي	P-	20-18.1
غير المريحة الدافئة	الدافئ	H	23-20.1
	الحار	H*	25-23.1
	شديد الحرارة	H-	25.1 فأكثر

ونظرا لعدم كفاية إستخدام معادلة دليل درجة الحرارة – الرطوبة (**THI**) في تقدير راحة الإنسان نظرا لكون الزياح لها تأثير في زيادة أو إنخفاض درجات الحرارة وحسب فصول السنة وبالتالي تأثيرها في تهيئة أجواء مثالية لراحة الإنسان لذلك كان من الضروري إستخدام معادلة دليل تبريد الرياح (**K**) Wind Chill Index [7].

2- معادلة دليل تبريد الرياح (**K**) Wind Chill Index :

إذا أعتبر جسم البشر عبارة عن ماكنة حرارية تحرر الطاقة بصورة مستمرة فإن أي شيء يؤثر على فقدان الحرارة من الجسم سوف يؤثر بدوره على طبيعة الإحساس الحراري لجسمه وبالتالي يؤثر على راحته [**8**].

يمكن التنبؤ عن إحساس البشر بالحر والبرد من خلال حساب دليل تبريد الرياح Wind Chill Index (**K**) الذي يعرّف على أنه (قياس كمية الحرارة التي يمكن للجو إمتصاصها خلال الثانية الواحدة من السطح المكشوف مثل الوجه واليدين) [**8**].

يمكن تقدير قدرة التبريد للجو (**K**) من خلال المعادلة رقم (**2**) وكالآتي [**8**] **:-**

$$K = (11.622 \times \sqrt{V} + 12.14 - 1.1622 \times V) \times (33 - T) \ldots (2)$$

حيث أن :

K: قوة تبريد الرياح.

V: سرعة الرياح (متر / ثانية).

T: درجة حرارة الهواء (درجة مئوية).

إن المعادلة رقم (2) يمكن تفسيرها على أساس ناتج قدرة التبريد للجو (K) ، والجدول (2) يوضّح مراتب وأصناف الراحة ورموزها المستخدمة حسب المعادلة رقم (2) [5].

جدول-2: مراتب وأصناف الراحة ورموزها المستخدمة على أساس ناتج قدرة التبريد للجو (K)[5]

مرتبة الراحة	الصنف	الرمز	THI
غير المريحة الدافئة	شديد الحرارة	H-	أقل من الصفر
	الحار	H*	49-0
	الدافئ	H	99-50
المثالية	المثالي	P	199-100
	المثالي	P*	299-200
	المثالي	P-	399-300
غير المريحة الباردة	البارد	C	499-400
	شديد البرودة	C*	599-500
	برد قارص	C-	600-فأكثر

مكان الدراسة والبيانات المستخدمة :

لقد تم في هذا البحث إستخدام البيانات التي شملت العوامل الجوية المتمثلة بكل من (**درجة الحرارة ، الرطوبة النسبية ، سرعة الرياح**) في محطة كركوك المناخية والتي تقع على إرتفاع (331 م) عن مستوى سطح البحر ، وعلى خط طول (″44°24) ودائرة عرض (″35°28) ، و للمدة من (**1971 – 2007**) والموضحة في الجدول (**3**) والتي تم الحصول عليها من الهيئة العامة للأنواء الجوية والرصد الزلزالي في بغداد.

جدول-3: درجات الحرارة و الرطوبة النسبية و سرعة الرياح المسجلة في محطة كركوك المناخية للمدة من (1971- 2007) [9]

أشهر السنة / العوامل الجوية	كانون الثاني	شباط	آذار	نيسان	مايس	حزيران	تموز	آب	أيلول	تشرين الأول	تشرين الثاني	كانون الأول
درجة الحرارة (درجة مئوية)	9	11	14.6	20.3	27.3	33	36	35.4	31.3	24.8	16.3	11
الرطوبة النسبية (%)	71.3	66.1	58.3	51.4	34.1	23.4	21.7	23	25.6	36.5	56.3	70
سرعة الرياح (متر / ثانية)	1.16	1.54	1.67	1.88	2.05	1.92	1.88	1.77	1.39	1.39	1.2	1.03

النتائج والمناقشة

تم في الجانب العملي من البحث تطبيق كل من المعادلة رقم (**1**) ، والتي تمثل معادلة دليل درجة الحرارة – الرطوبة (**THI**) Temperature – Humidity Index ، والمعادلة رقم (**2**) والتي تمثل معادلة دليل تبريد الرياح (**K**) Wind Chill Index ، من خلال الإستفادة من البيانات المذكورة في الجدول رقم (**3**) والذي يتضمن درجات الحرارة والرطوبة النسبية وسرعة الرياح المسجلة في محطة كركوك المناخية للمدة من (**1971-2007**) والتي تم الحصول عليها من الهيئة العامة للأنواء الجوية والرصد الزلزالي في بغداد ، وكانت النتائج المستخرجة على النحو التالي :

1- مؤشرات الراحة في مدينة كركوك حسب معادلة دليل درجة الحرارة – الرطوبة (**THI**) :

تم حساب قيم (**THI**) في مدينة كركوك من خلال تعويض قيم كل من درجات الحرارة والرطوبة النسبية في المعادلة رقم (**1**) بعد أن تم تقسيم السنة إلى أربع فصول بإعتبار فصل الشتاء يشمل أشهر (كانون الأول ، كانون الثاني ، شباط) ، وفصل الربيع يشمل أشهر (أذار ، نيسان ، مايس) ، وفصل الصيف يشمل أشهر (حزيران ، تموز ، آب) ، وفصل الخريف يشمل أشهر (أيلول ، تشرين الأول ، تشرين الثاني) ووضعت القيم المحسوبة في الجدول رقم (**4**) الموضح أدناه :

جدول -4: قيم دليل درجة الحرارة – الرطوبة (THI) في مدينة كركوك للمدة من (1971- 2007)

الفصول	الشتاء			الربيع			الصيف			الخريف		
الأشهر	كانون الأول	كانون الثاني	شباط	آذار	نيسان	مايس	حزيران	تموز	آب	ايلول	تشرين الأول	تشرين الثاني
قيم(THI)	11.5	9.79	11.6	14.5	18.6	22.5	25	26.5	26.3	24.2	21	15.7
مرتبة وصنف الراحة	غير مريح شديد البرودة	غير مريح شديد البرودة	غير مريح شديد البرودة	غير مريح بارد	مثالي	غير مريح دافئ	غير مريح حار	غير مريح شديد الحرارة	غير مريح شديد الحرار ة	غير مريح حار	غير مريح دافئ	مثالي
رمز مؤشر الراحة	C-	C-	C-	C	P-	H	H*	H-	H-	H*	H	P

من خلال الجدول رقم (4) الذي يبين قيم دليل درجة الحرارة – الرطوبة (THI) في مدينة كركوك للمدة من (1971- 2007) ، يلاحظ أن أشهر فصل الشتاء تكون غير مريحة وشديدة البرودة وعليه فإنها تكون غير مثالية لراحة الإنسان إلا من خلال إستخدام وسائل التدفئة وإرتداء الملابس الثقيلة ، في حين أن أشهر فصل الربيع تكون غير مريحة باردة في بداية الفصل ويكون شهر نيسان هو الشهر المثالي الوحيد وذلك لأن درجة الحرارة تبدأ بالإرتفاع من نهاية شهر نيسان إلى أن يكون الفصل غير مريحا دافئا عند إنتهائه .

أما أشهر فصل الصيف فتكون عموما غير مريحة حارة إلى شديدة الحرارة وعليه فإنها تكون غير مثالية لراحة الإنسان إلا من خلال إستخدام وسائل التكييف لتفادي إرتفاع درجة الحرارة ، التي تقل تدريجيا مع إقتراب أشهر فصل الخريف الذي يكون شهر تشرين الثاني هو الشهر المثالي الوحيد وذلك لأن درجة الحرارة تبدأ بالإنخفاض من نهاية شهر تشرين الثاني.

2- مؤشرات الراحة في مدينة كركوك حسب معادلة دليل تبريد الرياح Wind Chill Index (K) :

تم حساب قيم (K) في مدينة كركوك من خلال تعويض قيم كل من درجات الحرارة وسرع الرياح في المعادلة رقم (2) ووضعت القيم المحسوبة في الجدول رقم (5) الموضح أدناه :

جدول-5: قيم دليل تبريد الرياح (K) في مدينة كركوك للمدة من (1971- 2007)

الفصول	الشتاء			الربيع			الصيف			الخريف		
الأشهر	كانون الأول	كانون الثاني	شباط	أذار	نيسان	مايس	حزيران	تموز	آب	أيلول	تشرين الأول	تشرين الثاني
قيم(K)	500.2	559.4	545	464	328.8	150.5	0	-77.7	-61.3	41.19	198.7	392.1
مرتبة وصنف الراحة	غير مريح شديد البرودة	غير مريح شديد البرودة	غير مريح شديد البرودة	غير مريح بارد	مثالي	مثالي	غير مريح حار	غير مريح شديد الحرارة	غير مريح شديد الحرارة	غير مريح حار	مثالي	مثالي
رمز مؤشر الراحة	C*	C*	C*	C	P-	P	H*	H-	H-	H*	P	P-

من خلال الجدول رقم (5) الذي يبين قيم دليل تبريد الرياح (K) في مدينة كركوك للمدة من (1971- 2007) ، يمكن ملاحظة الأمور الآتية :

1- يكون للرياح تأثير في عدم شعور الإنسان بالراحة في أشهر فصل الشتاء والتي تكون غير مريحة وشديدة البرودة .

2- يبقى تأثير الرياح في عدم شعور الإنسان بالراحة مستمرا في بداية أشهر فصل الربيع والمتمثل بشهر أذار ، بينما يعد شهرا نيسان ومايس من الأشهر المثالية ، أي أن الإنسان يشعر بالراحة فيهما عند هبوب رياح خفيفة التي يطلق عليها مصطلح (النسيم) .

3- يكون للرياح تأثير في عدم شعور الإنسان بالراحة في أشهر فصل الصيف والتي تكون غير مريحة وشديدة الحرارة .

4- يبقى تأثير الرياح في عدم شعور الإنسان بالراحة مستمرا في بداية أشهر فصل الخريف والمتمثل بشهر أيلول ، بينما يعد شهرا تشرين الأول وتشرين الثاني من الأشهر المثالية ، أي أن الإنسان يشعر بالراحة فيهما.

وكما ذكرنا سابقا بأنه لا يمكن إعطاء مؤشرات راحة مثالية في تقدير راحة الإنسان من خلال إستخدام معادلة دليل درجة الحرارة – الرطوبة (THI) فقط وذلك لكون الرياح لها تأثير في زيادة أو إنخفاض درجات الحرارة وحسب فصول السنة وبالتالي تأثيرها في تهيئة أجواء مثالية لراحة الإنسان لذلك كان من الضروري دمج مؤشرات الراحة حسب قيم (THI) الموضحة في الجدول رقم (4) مع مؤشرات الراحة حسب قيم (K) الموضحة في الجدول رقم (5) ووضعت في جدول رقم (6) لغرض تحديد أشهر الراحة المثالية خلال فصول السنة المختلفة في مدينة كركوك للمدة من (1971- 2007) وكما موضح أدناه :

جدول-6: أشهر الراحة المثالية خلال فصول السنة المختلفة في مدينة كركوك للمدة من (1971- 2007) إعتمادا على دمج مؤشرات الراحة حسب قيم كل (THI) و (K)

الفصول	الشتاء			الربيع			الصيف			الخريف		
الأشهر	كانون الأول	كانون الثاني	شباط	آذار	نيسان	مايس	حزيران	تموز	آب	أيلول	تشرين الأول	تشرين الثاني
رمز مؤشر الراحة	C* C-	C* C-	C* C-	C C	P-P-	P H	H* H*	H- H-	H- H-	H* H*	P H	P- P-

من خلال جدول رقم (6) الذي يبين أشهر الراحة المثالية خلال فصول السنة المختلفة في مدينة كركوك للمدة من (1971- 2007) إعتمادا على جمع قيم (THI) و (K) تم ملاحظة الأمور الآتية:

1- إن أشهر فصل الشتاء تمتاز بكونها غير مريحة وشديدة البرودة بسبب الإنخفاض في درجات الحرارة ، لذلك فإن معظم مناطق مدينة كركوك تحتاج إلى التدفئة للحصول على راحة مثالية .

2- بداية أشهر فصل الربيع والمتمثل بشهر أذار يكون غير مريحا وباردا ، ويعد شهر نيسان من الأشهر المثالية لمعظم مناطق مدينة كركوك ، فيما يتباين شهر مايس بين الدافئ والمثالي .

3- إن أشهر فصل الصيف تمتاز بكونها غير مريحة بين الحارة في شهر حزيران وشديدة الحرارة في شهري تموز وآب بسبب الإرتفاع في درجات الحرارة ، لذلك فإن معظم مناطق مدينة كركوك تحتاج إلى التبريد للحصول على راحة مثالية .

4- بداية أشهر فصل الخريف والمتمثل بشهر أيلول يكون غير مريحا وحارا ، فيما يتباين شهر تشرين الأول بين الحار والمثالي ، ويعد شهر تشرين الثاني من الأشهر المثالية لمعظم مناطق مدينة كركوك .

الإستنتاجات

من خلال الأمور التي تم ذكرها في متن البحث ، تم التوصل إلى الإستنتاجات الآتية :

1- إن التباين في العوامل الجوية (درجة الحرارة ، الرطوبة النسبية ، سرعة الرياح) خلال أشهر وفصول السنة ، أدى إلى تباين شعور الإنسان بالراحة من فصل إلى آخر .

2- سيادة الاجواء غير المريحة خلال أشهر فصل الصيف (حزيران ، تموز ، آب) وبداية فصل الخريف والمتمثل بشهر (أيلول) نتيجة لإرتفاع درجات الحرارة ، وخلال أشهر فصل الشتاء (كانون الأول ، كانون الثاني ، شباط) وبداية فصل الربيع والمتمثل بشهر (أذار) نتيجة لإنخفاض درجات الحرارة .

3- سيادة الاجواء المريحة خلال شهري (نيسان ، تشرين الثاني) .

4- تباين أجواء الراحة بين الحارة والمثالية خلال شهري (مايس ، تشرين الأول) .

المصادر

[1] الركابي ، ناصر والي ، التباين المكاني والزماني لأقاليم الراحة المثالية في محافظة ديالى ، مجلة القادسية للعلوم الإنسانية ، المجلد الحادي عشر ، العددان 1-2 ، 2008 .

[2] شحاذة ، نعمان ، المناخ العملي ، الجامعة الأردنية ، مطبعة النور النموذجية ، الأردن ، 1983 .

[3] الراوي ، عادل سعيد ، إمكانيات العراق السياحية ، مجلة الجمعية العراقية ، العدد 26 ، 1991 .

[4] الشلش ، علي حسين ، المناخ وأشهر الحد الأقصى للراحة وكفاءة العمل في العراق ، مجلة كلية التربية ، جامعة البصرة ، العدد 3 ، 1980 .
[5] الراوي ، عادل سعيد ، قصي السامرائي ، المناخ التطبيقي ، مطبعة دار الحكمة ، بغداد ، 1990 .
[6] شرف ، عبد العزيز طريح ، مناخ الكويت ، مؤسسة الثقافة الجامعية الإسكندرية ، 1980 .
[7] الياسري ، إنعام عبد الصاحب محسن ، أثر المناخ على راحة الإنسان في محافظة القادسية ، مجلة أوروك ، المجلد الثالث ، العدد الثاني ، 2010 .
[8] الجبوري ، منعم حكيم خلف ، سناء عباس عبد الجبار ، تجارب عملية في الرصد والتحليل والتنبؤ الجوي ، مؤسسة مصر مرتضى للكتاب العراقي ، بغداد ، 2009 .
[9] الهيئة العامة للأنواء الجوية العراقية والرصد الزلزالي ، درجات الحرارة ، والرطوبة النسبية ، وسرعة الرياح ، للفترة من (1971 – 2007) ، قسم المناخ .
[10] الهيئة العامة للأنواء الجوية العراقية والرصد الزلزالي ، أطلس مناخ العراق للفترة (1961–1990)، بغداد ، 1994 .

تاثير المولدات الكهربائيـــة على درجات حرارة مدينة بغداد في شهر حزيران

نعمة محسن القتلاوي و علاء نجم عبد
قسم علوم الجو/ كلية العلوم/ الجامعة المستنصرية
تاريخ تقديم البحث 2013/10/9 - تاريخ قبول البحث 2014/3/16

ABSTRACT

The electric generators phenomenon has spread widely in Iraq, and especially between the streets of Baghdad. The number of electric generators officially registered in 2012 provincial council Baghdad more than 12,500. It does burn about 42 million liters of gas burned in the atmosphere in every month . Was obtained on the number of generators of electricity in each neighborhood of the municipalities of the city of Baghdad from the Ministry of Oil.Then we determine the shape of the bubble gases for each type of aerobic ten types of generators of electricity through readings of temperature and distance from header generated. There are two kind of electric generators are the open which be more damage for environment and the closed it is called friendly for environment. were calculated the additional in temperature from electric generators on each neighborhood which number 69 spread over 14 municipalities, then calculated the temperature additions to each municipality of Baghdad city in one day, we found that the greatest heat in the municipality of Al-Mansour 5.34C, Followed the addition of the Municipality Rusafa 3.57 , then Municipality of karrada 3.56 C, all generators will added to the atmosphere of the city of Baghdad about 30.87 C.

الخلاصة

انتشرت ظاهرة المولدات الكهربائية في العراق بشكل واسع ، وبالأخص بين شوارع مدينة بغداد . وبلغ عددها 12521 مولدة كهربائية مسجلة رسمياً في مجلس محافظة بغداد لعام 2012 ،وهي تقوم بحرق حوالي 42 مليون لتر من الغاز في الجو في كل شهر .تم الحصول على أعداد المولدات الكهرباء في كل حي سكني من بلديات مدينة بغداد من وزارة النفط. ثم تم تحديد شكل الفقاعة الحراري الهوائية لكل نوع من الانواع العشرة للمولدات الكهرباء من خلال قراءات لدرجات الحرارة وعلى مسافات من رأس المولدة. هناك نوعين من المولدات وهي المولدات المفتوحة وتكون اكثر ضرراً على البيئة والنوع الثاني المغلقة وتسمى بالصديقة للبيئة. حسبت الاضافة في درجات الحرارة من المولدات الكهربائية في كل حي سكني والتي عددها 69 موزعة على 14 بلدية ، ثم استخرجت الاضافة في درجات الحرارة لكل بلدية في مدينة بغداد في اليوم الواحد. ووجد بان اعظم تسخين في بلدية المنصور 5.34 C^o ، تليها بلدية الرصافة بإضافة 3.57 C^o ، ثم بلدية الكرادة 3.56 C^o،وهكذا تكون الاضافة لجميع المولدات على اجواء مدينة بغداد بـ 30.87 C^o

المقدمة

مدينة بغداد مقسمة إلى قاطعين أستناداً الى قسم المعلومات الجغرافية لأمانة بغداد لعام 2013، القاطع الاول الرصافة ويقسم الى ثمانية دوائر بلدية، وتشتمل على 228 محلة سكنية. والقاطع الثاني الكرخ ويقسم الى ستة دوائر بلدية ، وتشتمل على 221 محلة سكنية. الجدول رقم (1) يبين التقسيمات الادارية لمدينة بغداد، واسماء البلديات التابعة له، واسماء الاحياء السكنية ومساحة البلدية مقدرة بالمتر المربع[1] . في الفترة الأخيرة انتشرت ظاهرة المولدات الكهربائية في العراق بشكل واسع، وبالأخص بين شوارع مدينة بغداد، وبلغ العدد 12521 مولدة كهربائية مسجلة رسمياً في عام 2012 في مجلس محافظة بغداد و انَ أثنان واربعون مليون لتر الكاز يحرق في أجواء مدينة بغداد في كل شهر جراء تشغيل هذه المولدات الكهربائية[2][3]. وهنالك نوعين من المولدات الاولى مغلقة من الجوانب ولها مدخنة ترتفع الى الاعلى وتسمى صديقة البيئة، والنوع الثاني من المولدات مفتوحة من جميع الجوانب وهي تساهم بشكل كبير في تلوث البيئة، ويلحظ من الاحصائيات بان اعداد المولدات النوع الثاني أكثر بكثير من المولدات النوع الاول صديقة البيئة وهذا يعطي انطباع بعدم اخذ معايير العلمية والمحددات بيئية بنظر الاعتبار عند الاستيراد. وقد تم حصر عشرة أنواع رئيسة تعمل في بغداد نسبة الى طاقتها الكهربائية وكما سياتي ذكرها في متن البحث. تم الحصول على بيانات دقيقة عن مساحة كل حي لمدينة بغداد كما

في الجدول رقم(1). علماً بان هنالك مولدات صـــغيرة لم تســجل في وزارة النفط العراقية، والتي تستخدم في البيوت والمحلات التجارية. الشكل رقم(1) يبين أعداد المولدات الكهربائية في الاحياء السكنية لمدينة بغداد.

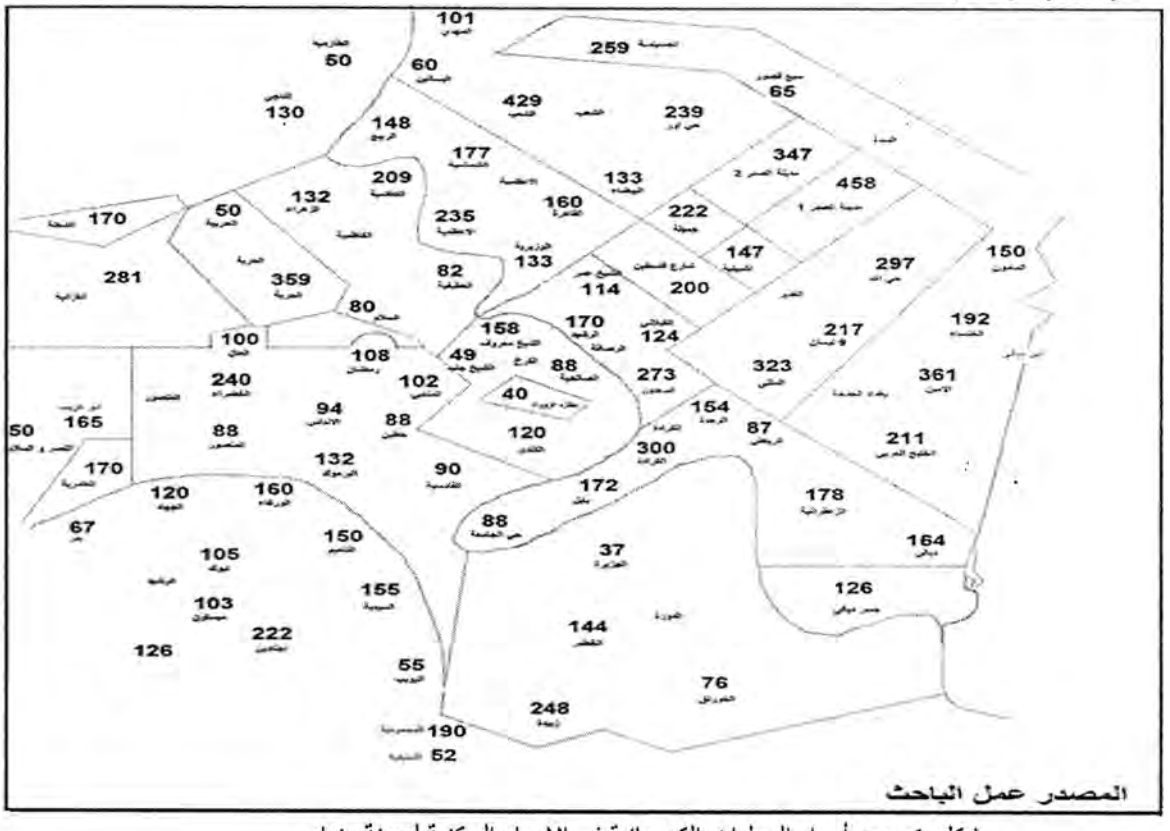

شكل-1: يبين أعداد المولدات الكهربائية في الاحياء السكنية لمدينة بغداد

جدول-1: يبين التقسيمات الادارية لمدينة بغداد [1]

ت	جانب	البلدية	المناطق	المساحة m^2
1	الرصافة	الرصافة	السعدون/الرشيد/الكيلاني/الشيخ عمر/شارع فلسطين	23787791
2		الاعظمية	الاعظمية/الشماسية/الربيع/الوزيرية/القاهرة	27266343
3		الشعب	البيضاء/اور/الشعب/المهدي/البساتين	39829844
4		الصدر الأولى	اشبيلية/مدينة الصدر الأولى	16640778
5		الصدر الثانية	جميلة/مدينة الصدر الثانية	14436101
6		الغدير	المثنى/اكد/9 نيسان	41895086
7		بغداد الجديدة	الخليج العربي/الامين/الخنساء/المأمون	52418743
8		الكرادة	الوحدة/الرياض/ديالى/الكرادة/الجامعة/بابل/ الزعفرانية	57870572
9	الكرخ	الكاظمية	السلام/الزهراء/الكاظمية/العطيفية	16303547
10		الكرخ	الشيخ معروف/الصالحية/الشيخ جنيد/الزوراء/الكندي	23224570
11		الشعلة	الحرية/الحربية/الشعلة	34163942
12		المنصور	اليرموك/حطين/العامرية/المنصور/الاندلس/ المتنبي/رمضان/الخضراء/العدل/القادسية/ الغزالية	64269676
13		الرشيد	الوركاء/التأميم/السيدية/اجنادين/البويب/ميسلون /تبوك/الجهاد/بدر	67550820
14		الدورة	الخضر/الجزيرة/الخورنق/زبيدة	33397634

المواد و طرائق العمل

السجلات الرسمية تصنف المولدات الكهربائية الى عشرة أنواع مختلفة استنادا الى طاقتها الكهربائية، وكما يلي:[1000 KV ، 500 KV، 450 KV، 400 KV، 350 KV، 300 KV، 250 KV، 200KV، 150 KV، 60 KV] . ولهذا اختيرت عشرة مولدات للدراسة واخذت القياسات عليها وكل نموذج يمثل أحدى الانواع المختلفة العشرة والمذكورة أعلاه، ولغرض تحديد شكل الفقاعة الحرارية المنبعثة من المولدة الكهربائية، تم اعتماد الآلية التالية: أولاً تحديد المحور الرئيس(المواجهة لخط انتشار الرياح) ، وذلك من خلال قياس درجات الحرارة أبتدأ من الفتحة الساخنة للراديتر والى أن تتساوى درجة الحرارة الغيمة الحرارية مع درجة حرارة الجو، في بعض المولدات أمتد المحور الرئيس للفقاعة 12 متر، ثانياً تحديد محيط الفقاعة، وذلك من خلال آخذ قياسات درجات الحرارة بخطوط عمودية على المجور الرئيس من الجهتين اليمين واليسار وعلى أبعاد [1 متر ، 2 متر ، 3 متر ، 4 متر ، والى انتهاء المحور الرئيسي] كما موضح في الشكل رقم (2) الذي يبين الآلية التي اعتمدت لتحديد أشكال الفقاعات الحرارية الهوائية، والى أن تتساوى درجة حرارة الغيمة الحرارية مع درجة حرارة الجو، وقد ظهرت أغلب اشكال الفقاعات ذات أشكال بيضوية. لاحظ الشكل رقم (2) الذي يبين الية العمل لقياس اشكال الفقاعات الحرارية الهوائية.

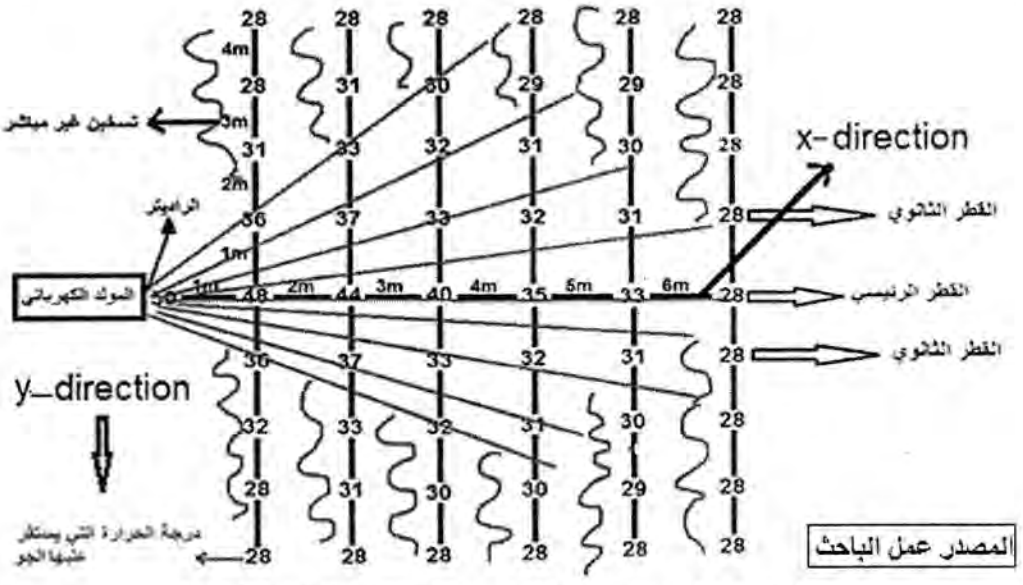

شكل-2: الية العمل المستخدمة لقياس اشكال الفقاعة الحرارية الهوائية

النتائج والمناقشة

الشكل رقم (3) يبين نتائج قياسات تحديد أشكال الفقاعات الحراريـــة المنبعثة للنماذج العشرة للمولدات الكهربائية. ويتضـــح من الشـــكل بان أكبر فقاعة حرارية تشـــكلها المولدة ذات الســـعة الكهربائيـة 500 KV ، بمساحة 94 متر مربع. أما مساحة الفقاعة الحرارية المتشكلة من المولدة ذات الســـعة الكهربائية 1000 KV فهي55 متر مربع ، والملفت للانتباه ان المولدة 500 KV مفتوحة، وطاقتها أقل ولكن مع الاسف فان هذا النوع من المولدات هي الاكثر انتشاراً في الاحياء السكنية لمدينة بغداد وعددها 979 مولـدة ، في حين ان المولدة ذات السعة الكهربائية 1000 KV ، المغلقة والصـــديقة للبيئة يبلغ عددها 246، وهنا يوثق البحث هذا التناقض دليل على قصـــور الوعي البيئي للمسؤولين عند الاستيراد.

تم حســـاب مقدار درجات الحرارة المضـــافة من المولدات في كل حي ســـكني تم ذكره الشـــكل رقم(4)، بالاعتماد على أعداد المولدات ومساحات الاحياء السكنية والمبينـــة في الجدول رقم(2)، وقد اعتمدت مساحة كل حي سكني[3] في بغداد، والجدول رقم (2) يوضح نتائج الحسابات درجة الحرارة للفقاعة الحرارية الواحدة، ودرجات الحرارة الكلية لمجموع الفقاعات الحرارية لكل نوع من المولدات في شهر حزيران وفي كل أحياء مدينة بغداد. بينما يوضح الجدول رقم (3) درجـــة الحرارة المضـــافة ومســـاحة الفقاعة الحرارية الكلية للبلديات الرئيســـية لمدينة بغداد نتيجة تشـــغيل المولدات الكهربائية.

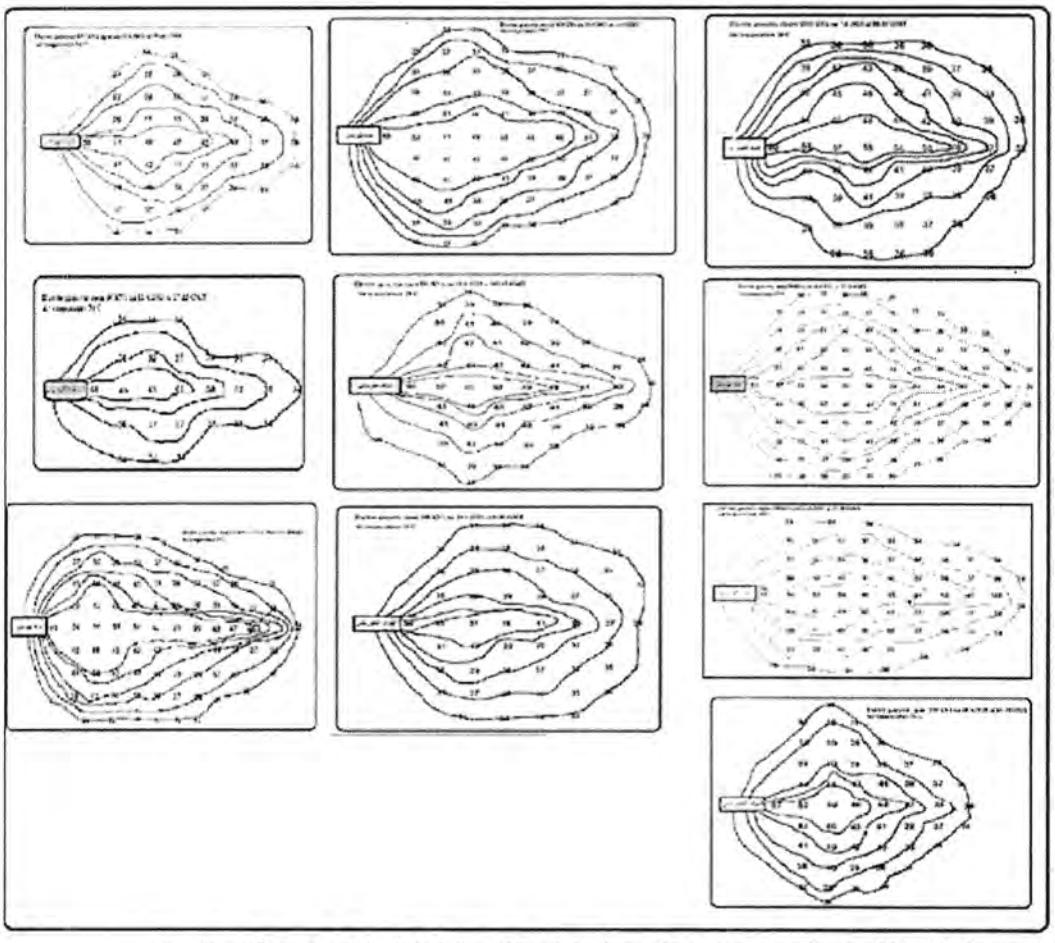

شكل-3: اشكال الفقاعات الحرارية المنبعثة من المولدات الكهربائية العشرة المستخدمة في البحث

جدول-2: مساحات الفقاعات الحرارية و اعداد المولدات

ت	Kv	عدد المولدات	مساحة الفقاعة m^2	مساحة الفقاعة الكلية m^2	الفرق بين درجة حرارة المولد والمحيط C°
1	1000	246	55	13530	24
2	500	979	94	92026	26
3	400	710	68	48280	23
4	450	219	64	14016	23
5	300	1511	50	75550	21
6	350	1340	44	58960	21
7	200	1741	47	81827	25
8	250	2590	76	196840	25
9	150	2644	40	105760	21
10	60	541	21	11361	14
المجموع		12521			

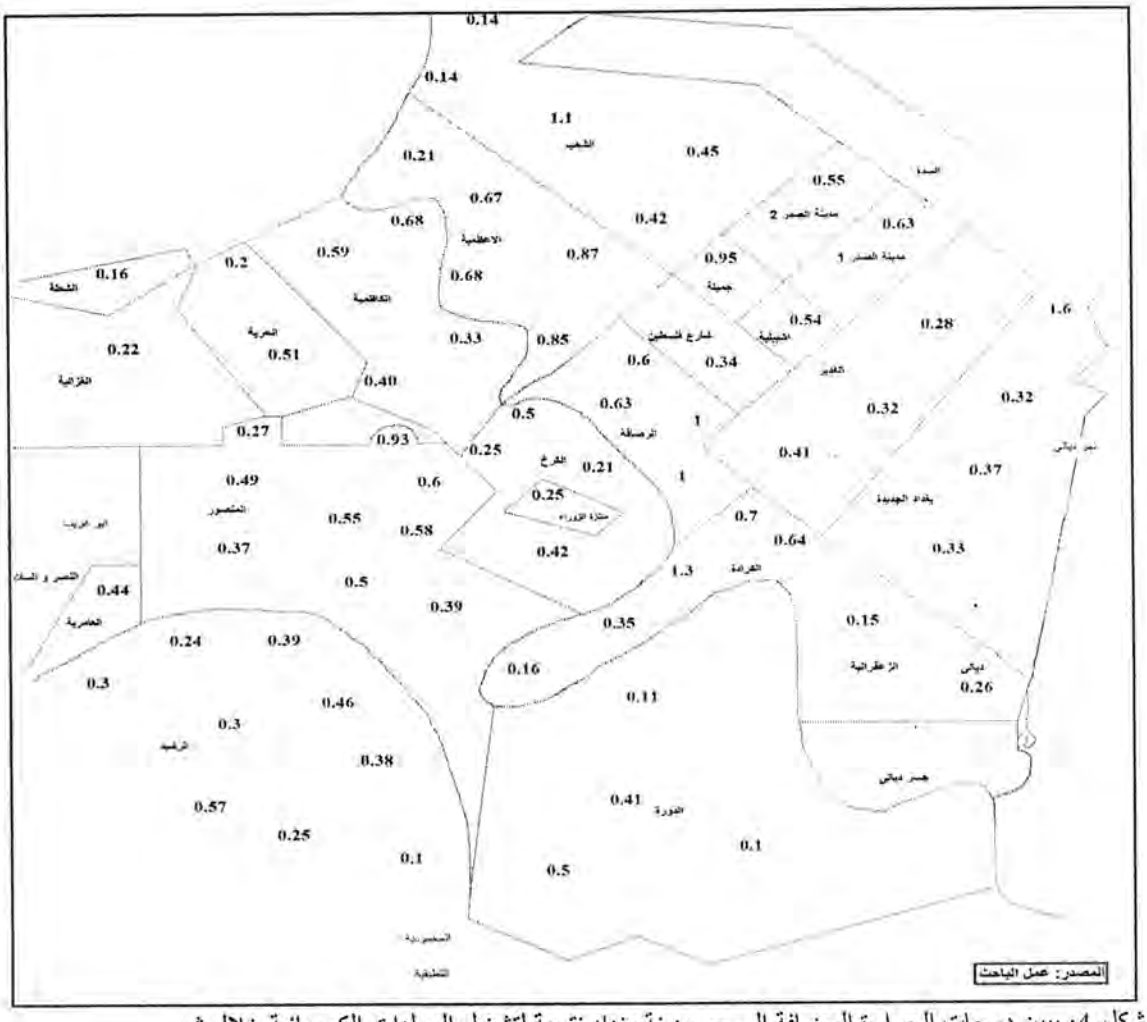

شكل-4: يبين درجات الحرارة المضافة الى جو مدينة بغداد نتيجة لتشغيل المولدات الكهربائية خلال شهر حزيران

الاستنتاجات

يبين البحث ان بلدية المنصور تضم اكثر عدد من المولدات بواقع 1493 مولدة، ثم تاتي بلدية الكرادة بـــــ 1143 مولدة ، ثم بلدية الرشيد بعدد 1137 مولدة ، في حين اقل من المولدات تكون في بلدية الكاظمية بـــــــ 503 مولدة، في حين يبين البحث بأن أكثر أضافة في درجات الحرارة كانت في بلدية المنصور بـــــ 5.34 درجة سيليزية، ثم تليها الاضافة في درجات الحرارة بلدية الرصـافة بإضـافة 3.57، وتاتي بلدية الكرادة 3.56، وفي حال جمع الاضـافات من كل البلديات التابعة لمحافظة بغداد يكون الناتج 30.87 درجة سيليزية في شهر حزيران.

ملاحظة :ان الرقم الكلي للإضـافة الحرارية في الجدول(3) و البالغ $30.87\ C^{o}$ لا يضـاف الى درجة حرارة مدينة بغداد وانما يمثل معدل الاضـافة لدرجة الحرارة للأحياء السكنية لمدينة بغداد والموجودة في الشكل رقم (4).

المصادر

[1] امانة بغداد، قسم المعلومات الجغرافية 2013 (1)
[2] هيئة توزيع بغداد . الشركة العامة لتوزيع المشتقات النفطية التابعة لوزارة النفط العراقية، 2013.(2)
[3] مجلس محافظة بغداد / لجنة النفط والطاقة 2013(3)

اختبار نظرية جابمان لطبقة F_2الايونوسفيرية فوق مدينة بغداد

دينا طارق كامل و عوني ادوار عبد الاحد
قسم علوم الجو / كلية العلوم /الجامعة المستنصرية
تاريخ تقديم البحث 2013/9/1 - تاريخ قبول البحث 2014/3/16

ABSTRACT

In this research Chapman theory for ionization production in upper atmosphere (Ionosphere) have been tested at Baghdad city (Lat. 33.3° N, Long. 44.4°E) the height between (250-400) km in the ionosphere is called F_2-layer which has chosen to test by using hourly critical frequencies from ionosonde type (I.P.S.42) which locted at AL. Batanee station at Al-Jadiryha for years (1989, 1990, 1991, 1994). Results of this research have found from the monthly critical frequencies and Zenith angle of Baghdad city. That F_2 Layer didn't follow this theory as well as during day time and at high solar activity. and during winter seasone. While this Layer may be follow this theory at night time.

الخلاصة

في هذا البحث تم اختبار نظرية جابمان للإنتاج الأيوني في الغلاف الجوي العلوي (الايونوسفير) لمدينة بغداد (دائرة عرض 33.3° شمالا ، خط طول 44.4° شرقاً) وعلى ارتفاع ما بين (250-400) كم وتحديداً في طبقة - F_2 والتي اختيرت ليتم اختبارها باستخدام البيانات الساعية للترددات الحرجة من جـــهاز الايونوسوند من نوع (I.P.S. 42) الواقع في محطة البتاني في الجادرية للســنوات (1989, 1990, 1991, 1994) ومن نتائج البحث وجد من قيم المعدلات الشهرية للترددات الحرجة وزاوية السمت المقاسة لمدينة بغداد بان طبقة - F_2 لا تتبع هذه النظرية كذلك الحال خلال النهار وخلال فترة النشاط الشمسي العالي وخلال فصل الشتاء في حين ان هذه الطبقة من الممكن ان تتبع نظرية جابمان ليلاً.

المقدمة

الايونوسفير هو ذلك الجزء العلوي من الغلاف الجوي للأرض الذي يمتد من ارتفاع حوالي(60) كم الى حوالي (1000) كم فوق سطح الأرض ويمتاز بأحتوائة على أيونات وألكترونات حرة وبأعداد كافية بحيث يمكن ان تؤثر على انتقال الموجات الراديوية [1] ويقسم الأيونوسفير الى عدة طبقات اعتمادا على الكثافة الألكترونية وأرتفاع كل طبقة منها عن سطح الأرض وهي طبقة D وطبقة E وطبقة Es وطبقة F التي تنقسم خلال النهار الى طبقتين هما F_2 , F_1 وتتميز هذه الطبقة بكونها ذات كثافة ألكترونية أعلى من بقية الطبقات التي تحتها حيث تبلغ كثافتها الألكترونية (10^5-10^6) الكترون لكل سنتمتر مكعب ويبلغ ارتفاعها بين (120– 400)كم فوق سطح الارض وتسمى بطبقة ابلتون Appleton Layer وتعد الأشعة (EUV) بأطوال موجية (10-100)نانومتر مسؤولة عن تأين ذرات الأوكسجين O_2 وهي الطبقة الوحيدة التي تبقى متأينة بصورة دائمية ليلا ونهارا ولجميع فصول السنة لهذا تعتبر مهمة جدا في الاتصالات [2] ويتراوح ارتفاع طبقة (F) بين (120–250)كم وتعد هذه الطبقة مسؤولة عن انعكاس معظم الموجات الراديوية(HF) والموجات القصيرة (SW) لاتصالات الراديو ولمسافات طويلة وتعد طبقة F_1 اكثر فاعلية في عكس الإشارات الراديوية وخصوصا خلال النهار أما خلال الليل فترجع لتنظم مرة ثانية إلى طبقة (F_2) مكونة طبقة واحده هي طبقة F وتمتاز أيضا باحتوائها على أيونات ذرية وجزيئية موجبة منها (No^+, O_2^+, O^+).

طبقة F_2 - F_2- Layer

تمثل طبقة F_2 الجزء العلوي من طبقة F وهي طبقة عشوائية شاذة وتكون على شكل سحب من الايونات ذات كثافة الكترونية عالية نسبيا وتظهر شذوذا وهذا الشذوذ يكون على نوعين هما .

1. الشذوذ اليومي ويشير الى حقيقة ان اكبر كثافة الكترونية لطبقة (F_2) تحدث عادة في أوقات غير تلك التي تظهر عند الظهر بالتوقيت المحلي وبشكل نموذجي من الساعة 13:00 الى 15:00 بالتوقيت المحلي .

2. الشذوذ الفصلي ويحدث في مناطق خطوط العرض الوسطى ويتمثل هذا الشذوذ من خلال كون الكثافة الإلكترونية لطبقة (F_2) في وقت الظهر وخلال فصل الشتاء تزيد عن تلك التي في فصل الصيف [3] . والسبب في ذلك يعزى الى انه في خطوط العرض المتوسطة يتميز الإنتاج الأيوني خلال النهار في طبقة (F_2) بكونه اكبر في فصل الصيف وذلك بسبب ان الشمس تكون تقريبا عمودية . لذلك يوجد تغير فصلي في نسب الجزيئات والذرات المتعادلة في الجو وتزداد عملية الخسائر الكيميائية في التأين في فصل الصيف وتصبح كبيرة . وبالنتيجة في الصيف تزداد الخسائر الأيونية في اثناء زيادة الإنتاج الإلكتروني ، فمجمل هاتين العمليتين ينخفض صاف التأين في طبقة (F_2) في فصل الصيف .وهذا الشذوذ يسمى بالشذوذ الشتوي وتمتاز هذه الطبقة (F_2) باحتوائها على ايونات ذرية موجبة اهما O^+ الذي يعد الايون السائد في هذه الطبقة [4] [5] .

2 - الجزء النظري

نظرية جابمان

تمثل نظرية جابمان التي وضعت في بداية القرن الماضي نقطة البداية التي تركت بصمة مميزة في تفسير سلوك الايونوسفير وفهمه وتعتمد هذه النظرية التي وضعها العالم سدني جابمان (1931) على افتراضات مبسطة [1] تطبق على طبقات الايونوسفير والتي تتغير مع الزمن وجوهر هذه الافتراضات هو كالأتي.

1. يعد الغلاف الجوي (exponential) اي كثافته تقل سريعا مع الارتفاع بمركبة غازية واحدة مع ارتفاع قياسي ثابت
2. افقيا لايوجد تغير عوامل الغلاف الجوي (plane Stratification)
3. امتصاص الاشعاع الشمسي يتناسب مع تركيز جسيمات الغاز
4. معامل الامتصاص ثابت اي ان الاشعاع المؤين (احادي الطول الموجي)

وبالاعتماد على هذه الفرضيات توصل الى معادلة لحساب معدل انتاج الايونات (q)في منطقة الأيونوسفير

$$\frac{q}{qm_0} = \exp\left(1 - z - Sec e^{-z}\right) \qquad (1)$$

حيث أن :

$$Z = \frac{h - h_m}{H}$$

ويسمى بالارتفاع المختزل (Reduced height)

qm_0 تمثل اكبر معدل للأنتاج الألكتروني على ارتفاع h_{m0} عندما تكون الشمس عمودية على الرأس .

1. .شكل المنحني للعلاقة وعلى الأرتفاعات العالية جدا عندما تكون قيمة Z كبيرة

$$q = qm_0 \exp(-e^{-z}) \qquad (2)$$

2. عندما تكون قيمة z صغيرة

$$q = qm_0 \exp(-\sec e^{-z}) \qquad (3)$$

3. الارتفاع المختزل عند حدوث اكبر معدل للأنتاج عندما تكون الشمس عمودية :

$$Z_m = \text{Ln sec } \chi \qquad (4)$$

من المعادلتين (2) و (4) ينتج

$$q_m = qm_0 \cos \chi \qquad (5)$$

حيث ان
q_m هو اكبر معدل للأنتاج
qm_0 هو اكبر معدل للأنتاج عندما تكون الشمس عمودية

4. ان المعادلتين (4) و (5) تعتبر المقياس لكمية انتاج الأيونات في طبقات الايونوسفير ويمكن الدلالة منها اذا كانت هذه الطبقات تخضع لقانون جابمان ام لا .

المواد وطرائق العمل

استخدم في هذا البحث بيانات ساعية للترددات الحرجة Critical frequancies لطبقة F_2 وطبقة F_1 الايونوسفيرية ويعرف التردد الحرج f_o (بأنها على تردد ممكن ان تعكسه الطبقة) أذ تم استخدام هذه البيانات الساعية لاختبار تبعية طبقة F_2 الايونوسفيرية فوق مدينة بغداد لنظرية جابمان Chapman Theoryاو عدمها جرى خلال هذا البحث حساب قيم المعدلات الشهرية للترددات الحرجة وتم ذلك بالاستعانة ببرنامج Excel وبرنامجSigmaplote وجرى ايضا حساب(F_n) الـ Normalization function (معامل التقويم) وذلك بقسمة قيمة التردد الحرج للساعة 12:00 UT ليوم 15من الشهر ولكل شهر على قيمه اعلى تردد حرج لشهري (حزيران او تموز) بعد اختيار الأعلى من بينهما ومن ثم حساب (F_n) لكل شهر من أشهر سنوات البحث ولا يفوتنا ذكر ان قيمه F_n تتغير من سنة إلى اخرى وذلك حسب تغير الدورة الشمسية. ويمكن حساب F_n وكما يلي حسب المعادلة التالية

$$F_n = \frac{f}{f_o} \qquad (A)$$

f: معدل الترددات الحرجة للساعة 12:00 ظهرا
f_o: اعلى تردد حرج للساعة 00 : 12ظهرا لشهري (حزيران أو تموز)

جرى خلال هذا البحث فرز قيم المعدلات الشهرية للترددات الحرجة خلال فترة النشاط الشمسي العالي كما تم فرز قيم المعدلات الليلية والنهارية للبيانات المتوفرة اما قيم زاوية السمت (*Zenith angal*) لبغداد فقد تم حسابها في البحث ببرنامج (*SunMotion*) لتقدير قيمها الشهريه [6] ورسمت العلاقات وكانت النتائج كما يلي.

اختبار المعدلات الشهرية لطبقة F_2

لاختبار هذه الطبقة الايونوسفيرية. تم استخراج القيم الشهرية للترددات الحرجة وجرى حساب(F_n) للقيم الشهرية ومن ثم رسمت العلاقة بين F_n و COS χ وكما في الشكل (1) اذ يوضح الـ (Fit line) علاقة عكسية وكان معامل الانحدار Regression Coefficient R=0.35 والذي يعطي المعادلة الموضحة في الجدول رقم (1). والذي يقودنا الى الاستنتاج بان طبقة (F_2) الايونوسفيريه فوق مدينة بغداد لا تتبع في تأينها نظرية جابمان

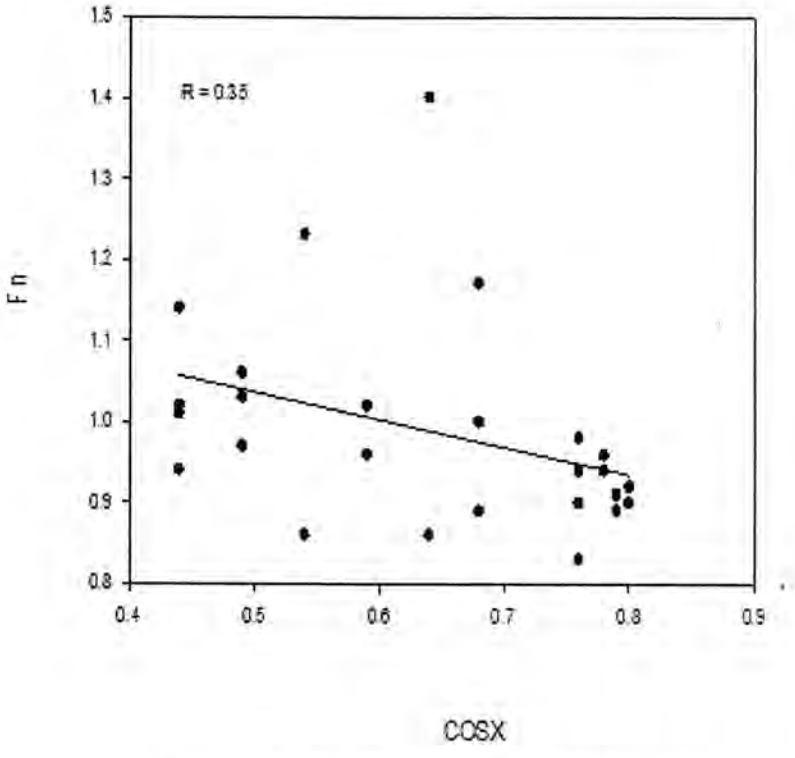

شكل-1: يبين العلاقة بين Fn و χ Cos لطبقة F_2الأيونوسفيرية

جدول - 1: يوضح معادلة الخط المستقيم وقيمة معامل الانحدار للطبقة F_2

الطبقة	معادلة الخط المستقيم	R	SE
F_2	N=1.206 - 0.338*COSχ	0.35	0.11

اختبار نظريه جابمان Chapman Theory في حالة النشاط الشمسي العالي

في هذا الجزء الاختباري من البحث تم تقسيم الأشهر الى قسمين.الأشهر التي يكون فيها عدد البقع الشمسيه (Sun spots number (SSN (60) بقعة شمسية فما دون اعتبرنها أشهر ذات نشاط شمسي واطئ اما الأشهر التي يكون فيها عدد البقع الشمسية اكثر من (60) بقعة شمسية فتعتبر اشهر ذات نشاط شمسي عالي وتم ذلك بالاستعانة بجداول عدد البقع الشمسية الشهري SUNSPOT NUMBER MONTHLY MEAN AMERICAN [7] للسنوات المدروسة ولكون الفترة المدروسة خلال هذا البحث كانت واقعة ضمن فترة النشاط الشمسي العالي اي ضمن فترة الصعود للدورة الشمسية 22 اي ان عدد البقع الشمسية اكثر من (60) بقعة شمسية اذ تراوحت أعداد البقع الشمسية بين (109.9- 217. 5) بقعه شمسية لذا تم اختبار هذه الطبقة خلال فترة النشاط الشمسي العالي ورسمت العلاقة بين F_n للأشهر ذات النشاط العالي و COSχ ومن الشكل التالي رقم (2) يتبين نوع العلاقة حيث كانت علاقة عكسية و كان معامل الانحدار R = 0.48 ويعطي المعادل الموضحة في جدول رقم (2)

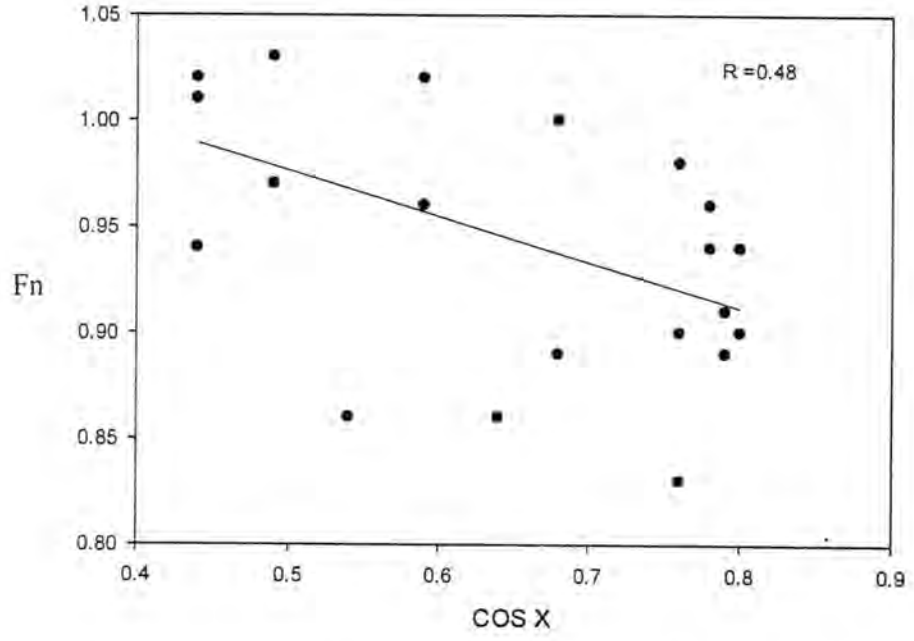

شكل -2: : يبين العلاقة بين$COS\chi$ وFn لطبقة F_2 في حالة النشاط الشمسي العالي للسنوات , 1991 , 1990 , 1989

ومن الرسم نستنتج أنه ليس للنشاط الشمسي العالي تأثير على عدم تبعيته طبقة F_2الايونوسفيرية فوق مدينة بغداد لنظرية جابمان.

جدول -2: يوضح معادله الخط المستقيم وقيم معامل الانحدار للطبقة F_2 حالة النشاط الشمسي العالي

الطبقة	معادلة الخط المستقيم في حالة النشاط الشمسي العالي	R	SE
F_2	N=1.08 – 0.21 *(COS χ)	0.48	0.05

اختبار اشهر الشتاء لطبقة – F_2

في هذه الفقرة تم عزل اشهر الشتاء للطبقة F_2عن بقية الاشهر للتحقق من سلوك هذه الطبقة الايونوسفيريه فوق مدينة بغداد شتاءاً ورسمت العلاقة ما بين قيم Fnو قيم $COS\chi$ من الخط المستقيم المرسوم في الشكل (3) نلاحظ بأن العلاقة عكسية قوية اذ كان معامل الانحدار 0.78 =Rالموضحة معادلتة في جدول رقم (3) ومن الرسم نستدل بأن هنالك شذوذاً شتوياً واضحاً لهذه الطبقة الايونوسفيرية عن نظرية جابمان لاشهر الشتاء للطبقة F_2

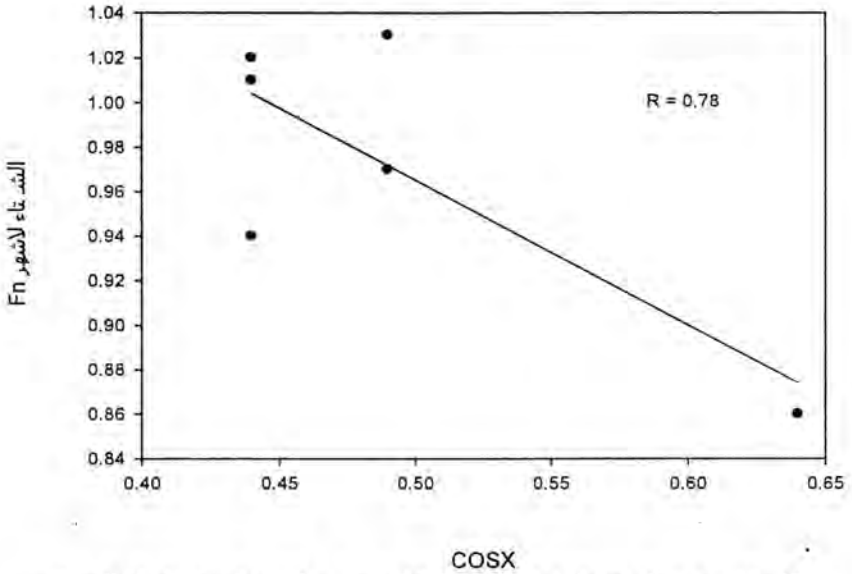

شكل-3: يوضح الشذوذ الشتوي لطبقةF_2 الايونوسفيريةعن نظريه جابمان للسنوات 1989 ,1990 , 1991

جدول-3: يوضح معادلة الخط المستقيم وقيم معامل الانحدار لأشهر الشتاء لطبقة F_2

الطبقة	معادلة الخط المستقيم	R	SE
F2	N= 1.29-0.65*(COSχ)	0.78	0.40

اختبار المعدلات الليلية لطبقة F

في حالة طبقة F تم فرز قيم المعدلات الليلية لهذه الطبقة بعدها رسمت العلاقة بين F_n للمعدلات الليلية مع COS χ كما في الشكل التالي نستنتج ومن الخط المستقيم المرسوم بين القيم ان العلاقة طردية قوية إذ كان R=0.84 ويعطي المعادلة في الجدول رقم (4) . مما يقودنا الى اعتبار ان طبقة F ليلا تتبع نظريه جابمان.

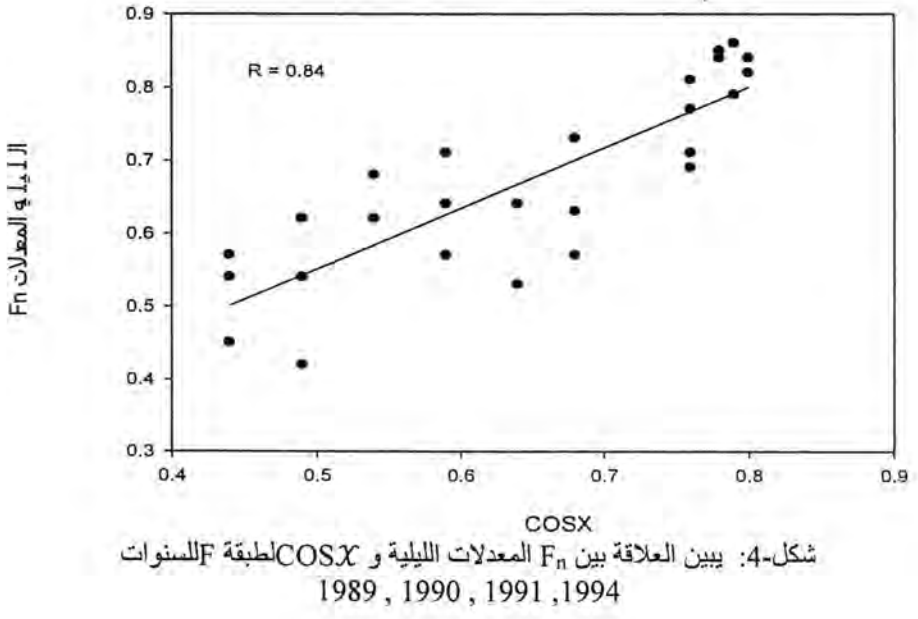

شكل-4: يبين العلاقة بين F_n المعدلات الليلية و COSχلطبقة Fللسنوات 1989 , 1990 , 1991 ,1994

جدول -4: يوضح معادلة الخط المستقيم و قيم معامل الانحدار للمعدلات الليلية لطبقة F_2الايونوسفيرية .

الطبقة	المعادلة في حالة المعدلات الليلية	R	SE
F_2	N=0.13+0.83*(COSX)	0.84	0.07

اختبار المعدلات النهارية لطبقة F_2

بعد فرز قيم المعدلات النهارية لطبقة F_2 رسمت العلاقة بين F_n النهاري مع $COS\chi$ وظهرت العلاقة كما في الشكل (5) وتبدو علاقة عكسية ضعيفة حيث كان معـــامل الانحدار R= 0.30 كما موضحة معادلتة في الجدول رقم (5) على الرغم من أن معامل الانحدار ضعيف الا انه يمكن الاستدلال على ان طبقة F_2 نهارا لا تتبع نظرية جابمان.

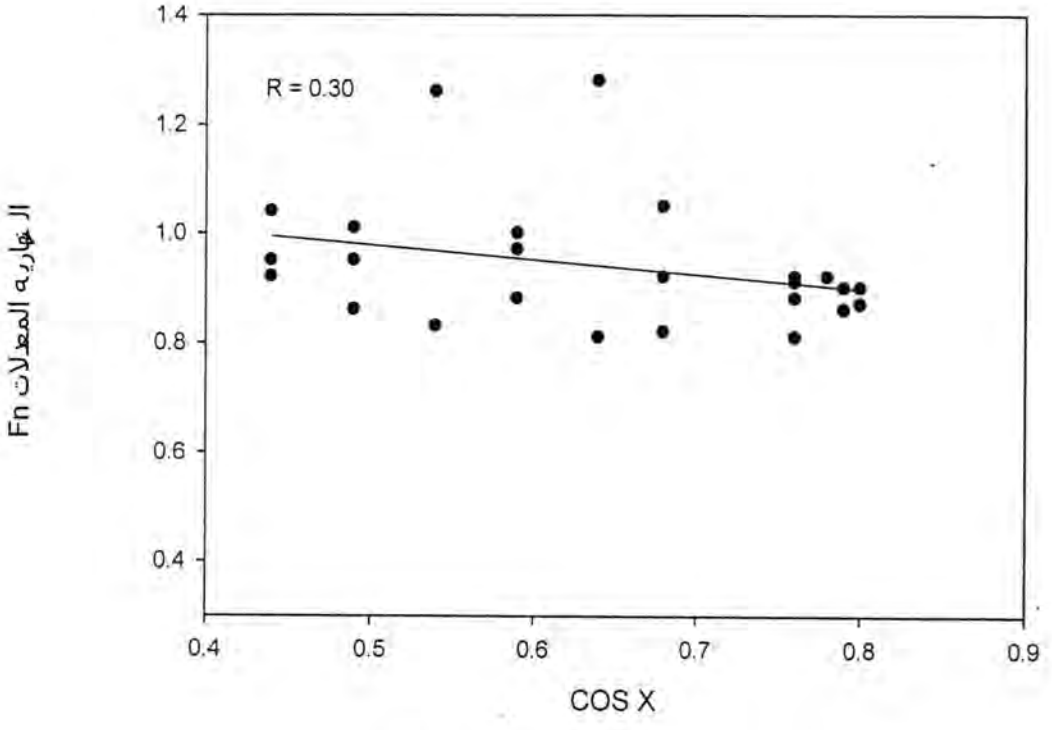

شكل -5: يبين العلاقة بين Fn المعدلات النهارية و $COS\ \chi$ لطبقة F_2.
1989 , 1990 , 1991 ,1994

جدول -5: يوضح معادلة الخط المستقيم و قيم معامل الانحدار للمعدلات الليلية لطبقة F_2 الايونوسفيرية .

الطبقة	المعادلة في حالة المعدلات النهاريه	R	SE
F_2	N=1.11-0.27*(COSX)	0.30	0.11

الاستنتاجات

1. وجد من النتائج ومن خلال العلاقة بين قيم المعدلات الشهرية للترددات الحرجة وزاوية السمت للطبقةF_2 فوق مدينة بغداد بأن العلاقة عكسية بينهما اي ان طبقة F_2 الايونوسفيرية لا تتبع نظرية جابمان

2. كما وجد من خلال البحث ان طبقة F_2 لاتتبع هذه النظرية خلال فترة النشاط الشمسي العالي
3. وخلال اشهر الشتاء فأن طبقة F_2 اظهرت شذوذاً واضحاً عن هذه النظرية
4. ومن اختبار قيم المعدلات الليلية والنهارية للترددات الحرجة للطبقةF وجد بأن هذه الطبقة تشذ عن نظرية جابمان نهارا وتتبعها ليلا

المصادر

1. Hunsucker R. D and Hargreaves J. K , (2003) ., " The highe – latitude ionosphere and its effects on radio propagation " ,Cambridge University press .
2. Philipe ,L. Fandmarray ,J.M.(1975). "Chemistry of the atmosphere" .academic press New Zealand, p.p (5-12)
3. Jursa , Adolph S ., ed ., (1985) Hand book of Geophysics and the Space environment , Air Forc Geophysics Lab , Hansome AF 13 , MA.
4. رعد عزيز اسحاق , (1984) : " دراسة التغيرات اليومية والفصلية لطبقات الايونوسفير فوق بغداد وتأثرها بالنشاط الشمسي ". رسالة ماجستير مقدمة الى قسم الفيزياء في كلية العلوم – جامعة – بغداد .
5. Forster , P .R .S . Freckleton and K .P shine 1997 "Onaspects of the concept of radiative forcing climate", Dyn ., 13 , 547 – 560
6. Iqbal , M., (1983). "An Introduction to Solar Radiation " Academic Press New York .
7. http://Spaceweather .com /glossary/ imags /Zurich . gif
8. Recommendation and Reports of (1986) 5 – 2 , p.p (1 – 12) , Geneva , Vol . VR Rep